

Changes in corneal thickness in
keratoconic eyes with variation in scleral
contact lens central clearance

by

Kirsten Sara Carter

A thesis
presented to the University of Waterloo
in fulfillment of the
thesis requirement for the degree of
Master of Science
in
Vision Science

Waterloo, Ontario, Canada, 2021

©Kirsten Sara Carter 2021

AUTHOR'S DECLARATION

I hereby declare that I am the sole author of this thesis. This is a true copy of the thesis, including any required final revisions, as accepted by my examiners.

I understand that my thesis may be made electronically available to the public.

Abstract

Purpose: There has been a resurgence of scleral lens wear, particularly for patients with corneal ectasia, such as keratoconus. This method of lens correction provides good visual acuity for these individuals and is often a clinically sought-after lens modality where others fail. The scleral lens vaults the ocular surface over a fluid reservoir, which provides additional comfort and neutralization of irregular astigmatism. The height of this fluid reservoir is often referred to as the central corneal clearance of the scleral lens. The long-term ocular physiological effects of scleral lens wear have not been definitively established. It is hypothesized that there is a low-grade level of corneal edema secondary to corneal hypoxia due to the barrier of the lens and fluid reservoir. There is an unanswered clinical question of “how much is too much?” with regards to central corneal clearance, in terms of limiting the amount of oxygen reaching the eye. This question has primarily been explored in the healthy rather than keratoconic population, as well as over a shorter period of wear, typically eight hours. The purpose of this study was to investigate the longer-term effects of scleral lens wear on a keratoconic population and explore differences in the effect on corneal physiology between two lenses of different targeted central clearances.

Methods: Two pairs of scleral lenses of targeted central clearances of 150 (low clearance) and 250 μm (high clearance) were fit on eight male participants with keratoconus, aged 31.6 (\pm 6.6) years. Each pair of lenses was worn for a 3-week period. At baseline and follow-up, central and paracentral corneal thickness was measured in the horizontal, vertical, and two oblique meridians at 8mm chord lengths. Total corneal thickness measurements were taken with the Oculus Pentacam® HR (OCULUS, Wetzlar, Germany) and the Spectralis® OCT (Heidelberg Engineering, Heidelberg, Germany), along with epithelial thickness measurements with the Spectralis® OCT.

Results: Scleral lens wear with both the low and high clearance lens consistently resulted in a statistically significant increase in corneal thickness from baseline. There were statistically significant

increases in corneal thickness when comparing follow-up measurements from the low to high clearance lens measured with both instruments for the vertical meridian (Spectralis OD $p=0.003$, OS $p=0.01$; Pentacam OD $p=0.014$, OS $p<0.001$). In other cases, the Pentacam® showed a significant increase in corneal thickness from the low to high clearance lens for the horizontal (OS $p<0.001$) and oblique meridian involving the inferior temporal-superior nasal regions (OD $p=0.006$). For the oblique meridian involving the superior temporal-inferior nasal regions, both the Spectralis® and Pentacam® HR measured a significant difference between lenses for left eye data (Spectralis OS $p=0.002$; Pentacam OS $p<0.001$), but neither detected a significant difference between lenses for the right eye (Spectralis OD $p=0.484$; Pentacam OD $p=0.436$). For corneal epithelial thickness measurements, there were significant differences only noted in the left eye, oblique meridian (superior temporal-inferior nasal) when comparing the low to high clearance lens follow-ups (increase in epithelial thickness, $p=0.007$), and the baseline to low clearance lens follow-up visit (decrease in epithelial thickness, $p=0.014$). These results were inconsistent and minimally significant. Individual patterns with corneal thickness difference mapping revealed patterns of both diffuse and sectoral swelling, with a general preference for the nasal side when measured with the Spectralis®, and on the temporal side with the Pentacam®. Patterns of corneal swelling did not appear to be associated with the individual's disease stage. Other individual differences were noted and described. Associations were sometimes noted between central total corneal swelling and decreases in visual acuity; locations of total corneal and corneal epithelial swelling; and total corneal swelling and position of lens decentration, however, links between these factors were not consistently observed. Bulbar hyperemia appeared to increase descriptively with scleral lens wear. Subjective comfort varied descriptively in lenses of varying central corneal clearance, with less comfort noted while wearing the higher clearance lens.

Conclusion: A 3-week period of scleral lens wear in the keratoconic population has been shown to induce low-grade corneal edema, regardless of whether low or high targeted central lens clearance has been fit. A higher targeted level of central corneal clearance may induce greater swelling, that is possibly location-dependent in this population. Individuals with keratoconus can exhibit distinctive patterns of corneal swelling in response to scleral lens wear, which may be independent of their disease stage, and should be considered in addition to the general effect of scleral lens wear in this population.

Acknowledgements

I would like to firstly thank my immediate and extended family for their support and love throughout this process. I could not have done this without you. Mom and Dad, you have done so much for me to help me achieve this goal, and I cannot thank you enough. Jake, you kept me laughing throughout, which was so important.

My supervisor, Dr. Denise Hileeto, and committee members Dr. Natalie Hutchings and Dr. Marc Schulze provided unwavering support to me throughout, especially during difficult and changing circumstances. Thank you, Denise for stepping up as my principal supervisor, for prioritizing your role in my supervision, and your enduring kindness and support. Thank you, Nat for your unmatched expertise in statistical analysis, and for guiding me throughout this portion of my project. I would also like to thank you for giving your time and assistance in generating the corneal thickness difference maps from my data, which were an integral part of this work, as well as additional tables in the Results chapter. Marc, your excellent feedback, and willingness to answer questions at a moment's notice were highly appreciated. Thank you to my whole committee for your enduring compassion and assistance – I am so grateful to have worked with all of you.

Much of my work was completed in the Clinics at the University of Waterloo. Individuals who helped my work to run smoothly included Ann Girling and Sabrina Jassal (Contact Lens Clinic), and Janice Mesenbrink and Angela Hare (Ocular Health Clinic) – you are all wonderful, thank you. Thank you as well to Dr. Nadine Furtado, Head of the Ocular Disease and Imaging Service for allowing me to utilize imaging instruments in your clinic for my study. To the Optometric Technicians and imaging staff coordinating use of this instrument with me, Justina Eguavoen and Anthony Nwokoro, thank you for your flexibility, and kindness. Thank you to the Ocular Disease and Glaucoma Resident, Dr. Rachel Amaral for your time and assistance to confirm imaging details – I greatly appreciated this.

I would also like to thank those from The University of Waterloo School of Optometry and Vision Science. Graduate coordinators (Stephanie Forsyth, Holly Forsyth, and Emily O'Connor) and graduate officers (Drs. Kristine Dalton, Jeff Hovis, Paul Murphy, Vivian Choh, Ben Thompson, and Daphne McCulloch) were greatly helpful for any questions I had during my time as a graduate student. The support of the GIVS community of fellow graduate students was also integral. Thank you to Chris Mathers and Ryan Baltare for your expertise in all things technical. A big thank-you to Dr. Vivian Choh for your assistance, especially with navigating logistics during data collection, and

for your mentorship over the years. Thank you to Vanessa Risser, Melissa Graham, and Georgia Graves for your help with the financial side of the study logistics. Fellow graduate students providing their expertise in imaging and image-processing, who gave me great advice should also be acknowledged: in particular, Amitojdeep Brar and Sourya Sengupta – thank you. New friends during my graduate degree kept motivated and in good spirits with our daily Skype work sessions – Stephanie and Brianna, I am grateful for your support and company.

Whenever I had a question about an imaging instrument, or about the scleral lenses used in my study, individuals employed by manufacturers of these products were readily available to help however they could. A special thank you to Mika Hague and Maggie Walsh (Alden Optical/Bausch + Lomb Specialty Vision Products), Annie Kwan (Innova – Heidelberg Supplier), Stacy-Lee Annis (Innova), and Chris O’Flaherty (OCULUS) for your consultation and willingness to help.

My wonderful friends from childhood and optometry years provided incredible encouragement and friendship along the way. Mariah, Drs. Kara Jones, Lacey Haines, Catherine Wright, Jess Skillen, and Jenny Chang – love to you all!

This research has been funded by an Independent Research Grant from Bausch + Lomb, with additional funding from The Canadian Optometric Education Trust Fund (COETF). Additional financial support for student salary was provided by the NSERC CGS M Award, and student awards from the University of Waterloo.

Dedication

This thesis is dedicated to Dr. Gina Sorbara. Thank you for everything you have taught me, and for always believing in me. I could always count on your unwavering support. Your expertise, kindness and friendship were such valuable gifts that I will always treasure. I am so fortunate to have had you in my life as a mentor and friend. I will continue to do my best to make you proud and honour your memory.

Table of Contents

AUTHOR'S DECLARATION	ii
Abstract	iii
Acknowledgements	vi
Dedication	viii
Table of Contents	ix
List of Figures	xiii
List of Tables	xvi
Chapter 1 Literature Review on Hypoxia, Scleral Lenses, and Keratoconus.....	1
1.1 Corneal Hypoxia.....	1
1.1.1 Physiological Mechanism.....	1
1.1.2 Hypoxia with Contact Lens Wear	4
1.1.3 Other Physiological Ocular Manifestations of Contact Lens-Induced Hypoxia	6
1.2 Scleral Lenses.....	8
1.2.1 Description of Scleral Lenses	8
1.2.2 Indications for Scleral Lens Wear	10
1.2.3 Complications of Scleral Lens Wear	11
1.3 Keratoconus.....	15
1.3.1 General Overview.....	15
1.3.2 Demographics.....	16
1.3.3 Biochemistry and Histopathology	17
1.3.4 Clinical Presentation and Diagnosis	21
1.3.5 Management	31
1.3.6 Biomechanics and Corneal Edema.....	42
Chapter 2 Study Rationale.....	45
2.1 Study Background	45
2.2 Study Motivation.....	47
2.3 Study Hypotheses	48
2.4 Study Purpose and Objectives	49
Chapter 3 Methods and Study Design.....	51
3.1 Scleral Lens Fitting Terms	51
3.2 Methods and Materials	53

3.2.1 Participant Recruitment.....	53
3.2.2 Study Materials	54
3.2.3 Study Procedure	61
3.3 Demographics and Study Lens Parameters.....	72
3.3.1 Participant Demographics	72
3.3.2 Study Lens Parameters and Fitting Characteristics.....	74
Chapter 4 Analysis Procedures	77
4.1 Region Selection for Spectralis® Data Analysis	77
4.2 Image Selection and Corneal Thickness Measurements.....	78
4.2.1 Pentacam® HR Total Corneal Thickness	78
4.2.2 Spectralis® Total Corneal and Corneal Epithelial Thickness.....	79
4.3 Refractive Index Correction.....	86
4.4 Image Orientation Modification.....	88
4.4.1 Spectralis® Image Orientation Modification.....	88
4.4.2 Pentacam® HR Image Orientation Modification.....	91
4.5 Correcting for Image Magnification for Lens-On Images	91
4.6 Investigation into Correction Factor for Differing Lens Central Thicknesses.....	96
Chapter 5 Study Results.....	101
5.1 Detailed Description of Disease Stage and Surgical History by Eye.....	101
5.2 Descriptive Statistics of Corneal Thickness Data	101
5.3 Initial Repeated-Measures ANOVA and Subsequent Paired Samples t-Tests.....	110
5.3.1 Total Corneal Thickness: Parametric RMANOVAs.....	110
5.3.2 Corneal Epithelial Thickness: Non-Parametric RMANOVAs and Paired Samples Wilcoxon Testing.....	114
5.4 Illustration of Regional Changes in Corneal Thickness.....	117
5.4.1 Group Analysis: Estimated Marginal Means of Pentacam® Corneal Thickness.....	117
5.4.2 Group Analysis: Descriptive Percent Changes in Corneal Thickness	122
5.4.3 Individual and Subcategory Analysis: Corneal Thickness Difference Mapping	123
5.5 Additional Parameters Relating to Lens Fit and Ocular Health.....	148
5.5.1 Central Corneal Clearance	148
5.5.2 High and Low Contrast Visual Acuity.....	149
5.5.3 Subjective Comfort	151

5.5.4 Lens Centration	153
5.5.5 Ocular Health Parameters	154
Chapter 6 Discussion	157
6.1 Group Analysis Interpretation	157
6.1.1 Total Corneal Thickness	157
6.1.2 Corneal Epithelial Thickness	165
6.2 Subcategory and Individual Exploratory Analysis Interpretation	166
6.2.1 Total Corneal Thickness Analysis	167
6.2.2 Corneal Epithelial Thickness Analysis	183
6.3 Lens Fit and Ocular Health	184
6.3.1 Central Corneal Clearance	184
6.3.2 High and Low Contrast Visual Acuity	185
6.3.3 Subjective Comfort Results	185
6.3.4 Lens Centration	186
6.3.5 Ocular Health Parameters	186
6.4 Comparison to Findings of Michaud et al.	187
6.5 Study Limitations	189
Chapter 7 Conclusions and Future Work	191
7.1 Conclusions	191
7.1.1 Corneal Thickness Changes	191
7.1.2 Individual Differences	191
7.1.3 Association of Total Corneal Thickness Changes and Varying Lens Clearance with Other Factors	192
7.2 Future Work	193
Letters of Copyright Permission	195
Figure 1-2	195
Figure 1-3	202
Figure 1-4	209
Figure 1-5A-B	217
Figure 1-5C	221
Figure 1-7	228
Figure 3-1	233

Figure 3-8.....	236
Appendix B.....	238
Figure 4-7.....	240
Appendix A Ocular Symptom Questionnaire.....	245
Appendix B Oculus Pentacam® Cornea Sclera Profile Scleral Fitting Guide. © Image provided courtesy of Oculus. ²⁶⁰	248
Appendix C Personal Communication, Annie Kwan, Technical and Clinical Support Representative, Innova-Heidelberg Supplier, 23 February 2021.....	249
Appendix D Personal Communication, Annie Kwan, Technical and Clinical Support Representative, Innova-Heidelberg Supplier, 4 March 2021.....	250
Appendix E Descriptive Statistics: Total Corneal Thickness Measurements.....	251
Appendix F Descriptive Statistics: Corneal Epithelial Thickness Measurements.....	267
Appendix G High and Low Contrast Visual Acuity.....	278
Appendix H Subjective Comfort Results.....	282
Appendix I Assessment of Lens Centration.....	284
Appendix J Bulbar and Limbal Hyperemia Grading by Oculus K5®M.....	286
Appendix K Corneal Fluorescein Staining Results.....	288
References.....	290

List of Figures

Figure 1-1: The five established layers of the cornea in cross-sectional diagrammatic form.....	1
Figure 1-2: Diagrammatic representation of anaerobic lactate generation	4
Figure 1-3: Schematic diagram of a scleral lens	9
Figure 1-4: Diagram of a round (left) vs oval (right) cone.	21
Figure 1-5: Clinical signs of keratoconus	24
Figure 1-6: An example of tomographic data.....	27
Figure 1-7: A lens-on fluorescein image of a corneal GP lens	37
Figure 2-1: Fatt equation modified to consider each barrier to oxygen independently.....	45
Figure 3-1: Ocular sagittal height	52
Figure 3-2: Oculus Pentacam® HR anterior segment tomographer.....	56
Figure 3-3: Spectralis® OCT at UWSOVS.....	58
Figure 3-4: The Visante™ OCT instrument at UWSOVS.....	58
Figure 3-5: The Oculus K5® topographer at UWSOVS.....	60
Figure 3-6: Study flow outlining the order of study visits.	63
Figure 3-7: Sample display of the Pentacam® HR CSP report.	64
Figure 3-8: Zenlens™ full diagnostic set parameters.....	66
Figure 3-9: Image of scleral lens insertion.....	67
Figure 3-10: Sample of a poorly segmented image from the Visante™ Global Pachymetry Map.	70
Figure 4-1: Example of a central Spectralis® OCT B-Scan.....	79
Figure 4-2: Measurement positions marked on a Spectralis® OCT B-Scan	82
Figure 4-3: An example of a binarized image with the anterior corneal boundary marked.....	84
Figure 4-4: An example of two images taken within the same imaging session, appearing to have different magnification subjectively.....	92
Figure 4-5: Magnification equation	93
Figure 4-6: Rearrangement of magnification equation to solve for CCC_t	93
Figure 4-7: Plots demonstrating baseline and settled central corneal clearances	94
Figure 4-8: Density plot outlining the distribution of magnification factors.....	95
Figure 4-9: Theoretical per cent increase in corneal thickness per Dk/t unit	99
Figure 5-1: Density plots of corneal thickness at the location 4mm temporal to centre.	103
Figure 5-2: Density plots of corneal thickness at the location 3mm temporal to centre.	103
Figure 5-3: Density plots of corneal thickness at the location 2mm temporal to centre.	104
Figure 5-4: Density plots of corneal thickness at the location 1mm temporal to centre.	104
Figure 5-5: Density plots of corneal thickness at the central location.....	105
Figure 5-6: Density plots of corneal thickness at the location 1mm nasal to centre.....	105
Figure 5-7: Density plots of corneal thickness at the location 2mm nasal to centre.....	106
Figure 5-8: Density plots of corneal thickness at the location 3mm nasal to centre.....	106
Figure 5-9: Density plots of corneal thickness at the location 4mm nasal to centre.....	107
Figure 5-10: Estimated Marginal Means - Pentacam® OD Horizontal (T-N) Meridian.....	118
Figure 5-11: Estimated Marginal Means - Pentacam® OS Horizontal (T-N) Meridian	118
Figure 5-12: Estimated Marginal Means - Pentacam® OD Vertical (I-S) Meridian.....	119

Figure 5-13: Estimated Marginal Means - Pentacam® OS Vertical (I-S) Meridian	119
Figure 5-14: Estimated Marginal Means - Pentacam® OD Oblique (IT-SN) Meridian	120
Figure 5-15: Estimated Marginal Means - Pentacam® OS Oblique (IT-SN) Meridian	120
Figure 5-16: Estimated Marginal Means - Pentacam® OD Oblique (ST-IN)	121
Figure 5-17: Estimated Marginal Means - Pentacam® OS Oblique (ST-IN).....	121
Figure 5-18: Difference maps of total corneal thickness subtracting baseline from follow-up values for Participant 02-KC, as measured by the Spectralis®	124
Figure 5-19: Difference maps of total corneal thickness subtracting baseline from follow-up values for Participant 04-KC, as measured by the Spectralis®	125
Figure 5-20: Difference maps of total corneal thickness subtracting baseline from follow-up values for Participant 07-KC, as measured by the Spectralis®	126
Figure 5-21: Difference maps of total corneal thickness subtracting baseline from follow-up values for Participant 09-KC, as measured by the Spectralis®	127
Figure 5-22: Difference maps of total corneal thickness subtracting baseline from follow-up values for Participant 11-KC, as measured by the Spectralis®	128
Figure 5-23: Difference maps of total corneal thickness subtracting baseline from follow-up values for Participant 13-KC, as measured by the Spectralis®	129
Figure 5-24: Difference maps of total corneal thickness subtracting baseline from follow-up values for Participant 14-KC, as measured by the Spectralis®	130
Figure 5-25: Difference maps of total corneal thickness subtracting baseline from follow-up values for Participant 15-KC, as measured by the Spectralis®	131
Figure 5-26: Difference maps of total corneal thickness subtracting baseline from follow-up values for Participant 02-KC, as measured by the Pentacam® HR.....	132
Figure 5-27: Difference maps of total corneal thickness subtracting baseline from follow-up values for Participant 04-KC, as measured by the Pentacam® HR.....	133
Figure 5-28: Difference maps of total corneal thickness subtracting baseline from follow-up values for Participant 07-KC, as measured by the Pentacam® HR.....	134
Figure 5-29: Difference maps of total corneal thickness subtracting baseline from follow-up values for Participant 09-KC, as measured by the Pentacam® HR.....	135
Figure 5-30: Difference maps of total corneal thickness subtracting baseline from follow-up values for Participant 11-KC, as measured by the Pentacam® HR.....	136
Figure 5-31: Difference maps of total corneal thickness subtracting baseline from follow-up values for Participant 13-KC, as measured by the Pentacam® HR.....	137
Figure 5-32: Difference maps of total corneal thickness subtracting baseline from follow-up values for Participant 14-KC, as measured by the Pentacam® HR.....	138
Figure 5-33: Difference maps of total corneal thickness subtracting baseline from follow-up values for Participant 15-KC, as measured by the Pentacam® HR.....	139
Figure 5-34: Difference maps of corneal epithelial thickness subtracting baseline from follow-up values for Participant 02-KC, as measured by the Spectralis®	140
Figure 5-35: Difference maps of corneal epithelial thickness subtracting baseline from follow-up values for Participant 04-KC, as measured by the Spectralis®	141

Figure 5-36: Difference maps of corneal epithelial thickness subtracting baseline from follow-up values for Participant 07-KC, as measured by the Spectralis®	142
Figure 5-37: Difference maps of corneal epithelial thickness subtracting baseline from follow-up values for Participant 09-KC, as measured by the Spectralis®	143
Figure 5-38: Difference maps of corneal epithelial thickness subtracting baseline from follow-up values for Participant 11-KC, as measured by the Spectralis®	144
Figure 5-39: Difference maps of corneal epithelial thickness subtracting baseline from follow-up values for Participant 13-KC, as measured by the Spectralis®	145
Figure 5-40: Difference maps of corneal epithelial thickness subtracting baseline from follow-up values for Participant 14-KC, as measured by the Spectralis®	146
Figure 5-41: Difference maps of corneal epithelial thickness subtracting baseline from follow-up values for Participant 15-KC, as measured by the Spectralis®	147

List of Tables

Table 1-1: Amsler-Krumeich staging of keratoconus.....	32
Table 3-1: Average and maximum keratometry values, and minimum corneal thickness values for each eye and participant.....	73
Table 3-2: Summary of study lens parameters.....	76
Table 4-1: Descriptive summary of corneal thickness changes	77
Table 4-2: Results of tangent measurements for each image at each location	85
Table 4-3: Scan direction for right and left eye for the Spectralis®	90
Table 5-1: Summary of eyes used for final analysis.....	101
Table 5-2: Paired t-testing and Bayesian analysis results between baselines for total corneal thickness measurements.	108
Table 5-3: Paired t-testing and Bayesian analysis results between results obtained at both baseline visits for corneal epithelial thickness measurements.....	109
Table 5-4: RMANOVA results for condition (baseline average, LC follow-up, HC follow-up) for total corneal thickness.	110
Table 5-5: Results of specific paired t-tests for total corneal thickness measurements.....	112
Table 5-6: Descriptive values for each condition for total corneal thickness.....	113
Table 5-7: Friedman RMANOVA for corneal epithelial thickness measured by the Spectralis®.	114
Table 5-8: Results of specific paired t-tests for corneal epithelial thickness measurements.....	115
Table 5-9: Descriptive values used for statistical analysis for corneal epithelial thickness.....	116
Table 5-10: Percent change in total corneal thickness from baseline to low clearance	122
Table 5-11: Percent change in total corneal thickness from baseline to high clearance	123
Table 5-12: Summary table of individual clearances measured for all participants for each lens. ...	148
Table 5-13: Group summary and descriptive statistics for central corneal clearances.....	149
Table 5-14: Summary of changes in high contrast visual acuity.....	149
Table 5-15: Summary of changes in low contrast visual acuity	150
Table 5-16: Summary of clarity and comfort values and change from baseline to follow-up for the low clearance lens.....	151
Table 5-17: Summary of clarity and comfort values and change from baseline to follow-up for the high clearance lens.....	152
Table 5-18: Lens preference	153
Table 5-19: Summary of directions of decentration for all participants.	154
Table 5-20: Mean and standard deviation of bulbar and limbal hyperemia	155
Table 5-21: Summary of corneal fluorescein staining using the BHVI scale.....	156
Table 6-1: Direction of decentration for each eye, sorted by Amsler-Krumeich disease stage.	177
Table 6-2: Settled direction of decentration for each eye, sorted by lens clearance.....	179

Chapter 1

Literature Review on Hypoxia, Scleral Lenses, and Keratoconus

1.1 Corneal Hypoxia

1.1.1 Physiological Mechanism

The cornea is a dome-shaped structure with unique architecture which covers the pupil and iris and allows light to enter the eye. As part of the visual system, the primary attributes of the cornea are its transparency and refractive power, both required for light to be adequately transmitted and converged onto the retina. The cornea serves as a significant contributor to the latter function, providing approximately two-thirds of the visual system's refractive power.¹ The cornea is comprised of five main layers, which are, anteriorly to posteriorly: the epithelium, Bowman's layer, the stroma, Descemet's membrane, and the endothelium (see Figure 1-1). Because of its distinctive properties, the posterior-most aspect of the corneal stroma has recently been described as a possible sixth pre-Descemet's membrane layer.² The stroma comprises the majority of the thickness of the cornea and is the tissue layer whose structural state corneal transparency mostly depends on.

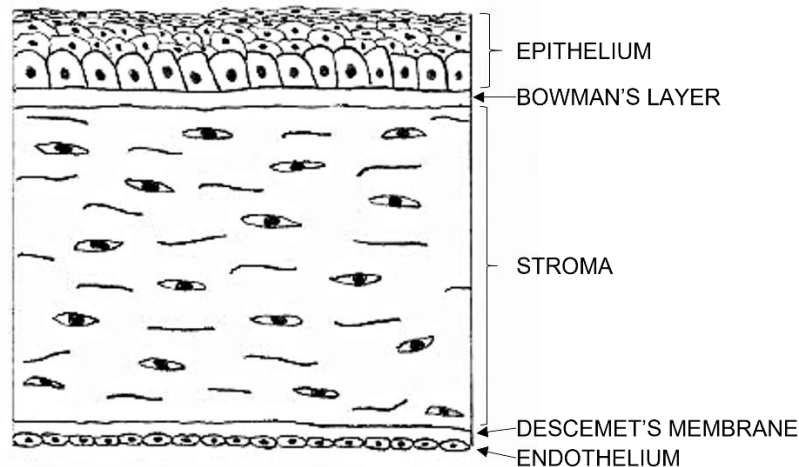


Figure 1-1: The five established layers of the cornea in cross-sectional diagrammatic form.

Corneal properties and functions are maintained through the specific arrangement of collagen fibrils in the corneal stroma. The collagen fibrils, bound together by a predominantly proteoglycan matrix and supported by keratocytes, are arranged into bundles, referred to as lamellae.^{1,3} The homogeneous size and precise equal spacing of less than one wavelength of visible light between collagen fibrils promote optimal light transmission, with light scattering being negligible. If this particular arrangement is disrupted, the cornea will lose its transparency. This negative consequence of architectural disturbance is characteristic for many pathological conditions, the most common being corneal swelling of various etiology, in which increasing degrees of stromal hydration are associated with a progressive decrease in corneal transparency.

In its homeostatic state, the corneal stroma maintains a water content of 78%.¹ The corneal stroma is hydrophilic in nature, due to its high concentration of proteoglycans. To prevent an influx of water which would disrupt this tissue's structure, both the corneal epithelium and endothelium serve as protection. The epithelium and endothelium are physical tissue barriers to passive transport of water through to the stroma, but also carry out active cellular processes to maintain this state. Both tissue layers are host to ion-exchange pumps, through which the controlled concentration of all ions drive the entrance and exit of water to and from the stroma via active transport.

The epithelium's most significant role in the maintenance of corneal homeostasis is to form a physical barrier both to fluid and pathogen entrance into the corneal stroma.¹ It is structurally comprised of 5-7 cell layers of three cell types: basal, wing, and squamous cells. The key structural factor that allows the epithelium to function as a sound semipermeable barrier are the tight junctions, or *zonula occludens* between the exterior squamous cell membranes.⁴ All cell layers are also interconnected via gap junctions. Of lesser influence than that of the endothelium, the epithelium also allows for ion transport in maintenance of stromal deturgescence.¹ Epithelial squamous cells are host to many ion exchangers and co-transporters which require biochemical energy in the form of

adenosine triphosphate (ATP). Along with passive transport of ions down their chemical gradient, these active processes manifest as a net result of sodium ions entering the stroma from the tear film, propelling chloride ions from the stroma to the tears, resulting in water being osmotically driven out of the cornea to the tears.

The endothelium, composed of a single, non-regenerating layer of polygonal cells is considered to be a more permeable barrier to water and ions compared to that of the epithelium.¹ Across the endothelium, water and solute passively flow through cells and between cell junctions (*macula occludens*).⁴⁻⁶ Corneal swelling is then counteracted through the exchange and cotransport of sodium and other ions, to a greater extent out of the stroma to the aqueous humour, where water osmotically follows.⁷ These active metabolic processes necessary for preserving the corneal stroma's structure also require biochemical energy in the form of adenosine triphosphate (ATP).

The generation of ATP is achieved through cellular metabolism, which is most effectively carried out aerobically when an adequate supply of oxygen is available. In this aspect, the corneal epithelium is roughly ten times more metabolically efficient than the stroma.^{1,8} If oxygen availability is reduced, the cornea must divert to anaerobic methods of metabolism, yielding lactate as a by-product. Lactate accumulates greatly in the epithelium, passively enters the stroma, and then draws water into both the epithelium and stroma, causing an edematous response in both tissues (see Figure 1-2).⁹

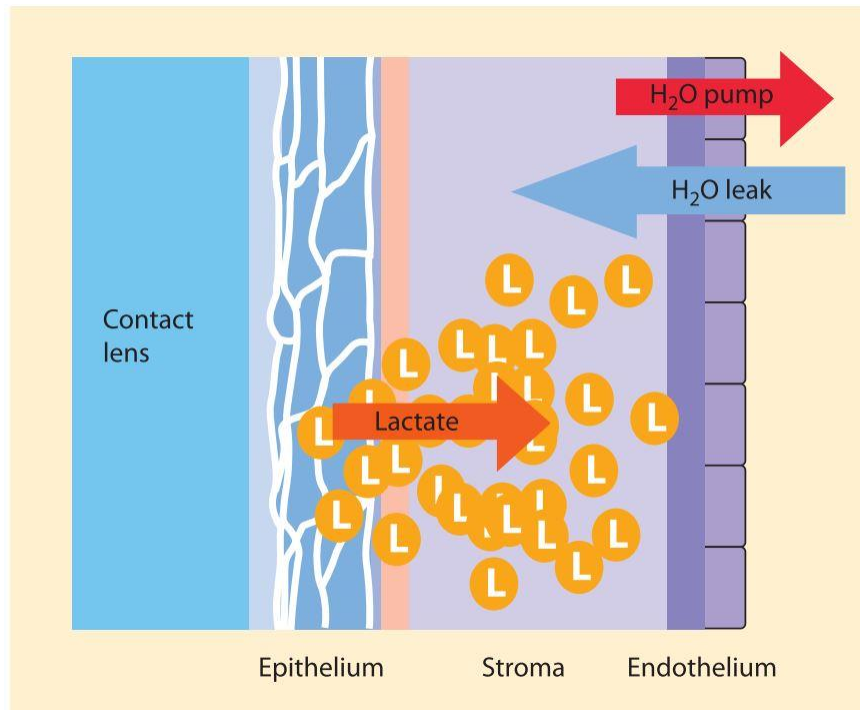


Figure 1-2: Diagrammatic representation of anaerobic lactate generation and subsequent influx of water, causing corneal edema. Figure is reproduced with permission from Efron, 2012.¹⁰

Because the cornea lacks its own vascular supply, oxygen must be delivered to it in an open-eye environment from the atmosphere via the tears, the aqueous humour, and the limbal vascular supply, the majority being supplied by the former (155 mmHg).^{1,11-15} In a closed-eye environment, the tarsal conjunctival vessels are the major source of oxygen, but provide a lower amount (55 mmHg). As a result, during sleep, the eye experiences a state of relative hypoxia. Another practical example of a barrier to corneal oxygen availability at its primary source in an open-eye environment is contact lens wear, which has been proven to interfere with the cornea's access to oxygen.¹⁶⁻²²

1.1.2 Hypoxia with Contact Lens Wear

The ability of a contact lens material to allow oxygen to pass through it is most often communicated as the oxygen permeability parameter known as the Dk, or, specific to a particular lens, oxygen transmissibility (Dk/t). The lens material itself has its own Dk (oxygen permeability) that does not

depend on the lens' physical form or its surface properties.²³ More descriptive in this aspect is the Dk/t, or oxygen transmissibility of the contact lens, which takes into account the thickness of the lens, by dividing the Dk by this property (in mm), and multiplying it by 10. This is significant because the amount of oxygen that reaches the ocular surface depends not only on the permeability of the material, but also on how much material it must pass through. The units of Dk are $[10^{-11} \text{ cm}^2 \times \text{mL O}_2]/[\text{sec} \times \text{mL} \times \text{mmHg}]$, and of Dk/t are $[10^{-9} \text{ cm}^2 \times \text{mL O}_2]/[\text{sec} \times \text{mL} \times \text{mmHg}]$. To avoid hypoxic complications during daily soft contact lens wear, it was first determined by Holden and Mertz that the ocular surface requires a lens of minimum central Dk/t of 24 units to prevent hypoxia-induced corneal edema,¹⁸ and later postulated to be 35 units centrally when considering the prevention of total corneal anoxia, versus prevention of hypoxia in the basal epithelial cells (23 units).²¹ More recently, it has been proposed that the minimum lens Dk/t parameters to prevent corneal edema are 19.8 units centrally, and 32.6 units peripherally, since it has also been discovered that central corneal swelling behaves differently from that in the periphery during hypoxic stress.^{22,24}

In the early days of contact lenses when corneal oxygen requirements were not known, contact lens materials included glass and polymethyl methacrylate (PMMA), both of which have a Dk of 0.²⁵ After ocular hypoxic complications were observed with these low Dk materials, contact lenses began to be manufactured from materials with a higher oxygen permeability, such as acrylate polymeric combinations of silicone acrylates and other chemicals in rigid materials, and hydrogel polymers in soft materials, later incorporating silicone as well.

Hypoxia with contact lens wear may result in corneal edema, depending on the oxygen transmissibility (Dk/t) of the lens, and the conditions under which the lens is worn²⁶. An increase in total corneal thickness has been used as a surrogate measure for corneal edema, especially when it occurs at low levels.^{17,18} Many studies have shown that the total cornea swells as a result of hypoxia in response to both daily and extended wear of soft contact lenses, centrally and peripherally, with

various methods of measurement.^{16,19,22,27,28} In studies where acute corneal swelling secondary to hypoxia in a closed-eye environment have been studied, the greatest extent of edema occurs in the corneal stroma when measured by light backscatter,²⁹ and directly by thickness.³⁰ Some studies have claimed that epithelial swelling during hypoxia is not significant,^{31,32} while others have noted a significant amount of epithelial edema.^{30,33,34}

The extent of hypoxia-related swelling was previously thought to be greater posteriorly due to the mechanical resilience of the epithelium.³⁵⁻³⁷ More recently, hypoxia-related corneal swelling was reported to be greater in the anterior stroma and epithelium compared to that of the posterior cornea, measured with optical coherence tomography (OCT).³⁰ Conversely, with long-term extended wear of contact lenses of lower oxygen transmissibility, chronic effects on the cornea include reduction in both epithelial and stromal thickness centrally³⁸⁻⁴⁰ and in the midperipheral and peripheral cornea.⁴⁰ In subjects with varied wear schedules, long-term total corneal thinning was noted both centrally and peripherally.⁴¹ This has been noted in both rigid and soft lens materials.^{38,39} Epithelial thinning occurs to an even greater extent in soft lenses when the Dk of the lens is low,^{39,40} presumably due to structural damage as a result of chronic hypoxia.²⁶ The relationship and interaction between the hypoxia-induced corneal changes, which might be temporary and reversible, and the permanent changes in corneal thickness with lens wear are complex and dependent on multiple factors with highly variable influence.

1.1.3 Other Physiological Ocular Manifestations of Contact Lens-Induced Hypoxia

In addition to corneal edema, corneal hypoxia results in changes to the characteristics of the corneal epithelium. Epithelial cells experience lactic acid accumulation, which can compromise the integrity of the cells, leading to functional decompensation.¹⁰ This damage has been observed clinically as diffuse superficial punctate keratitis (SPK), visible with fluorescein staining.⁴² It has been proven that contact-lens related hypoxia also results in damage and downregulation to the *zonula occludens* of

corneal epithelial cells, largely responsible for this tissue layer's function as a tight barrier, along with loss of squamous epithelial cells themselves.^{43,44} The weakening of these attachments compromises the epithelial barrier integrity, and also manifests as corneal staining.²⁶

When the ocular surface experiences a metabolically hypoxic environment, the concentration of chemical mediators in the ocular interstitial fluid are increased, causing arterioles of the conjunctiva to dilate in response, to promote blood flow to ocular tissues.^{10,45} It is suspected that in the limbal vasculature, endothelial release of nitrous oxide may cause vasodilation, resulting in increased limbal hyperemia in a hypoxic event, although this has not been proven.⁴⁶ There is a stronger association between hypoxia and increased limbal redness,⁴⁷ in comparison to hypoxia and conjunctival redness,^{45,48} although both phenomena in theory should occur due to vascular autoregulation.⁴⁹ Increased blood flow to the conjunctiva and limbus manifest as redness, or hyperemia, and both can be observed and graded clinically.

Although both corneal fluorescein staining and limbal and conjunctival hyperemia have been established as signs of hypoxia, both clinical signs are non-specific and can be associated with ocular surface insult, as in ocular surface disease or contact lens wear.

Other ocular consequences of clinically significant corneal hypoxia include stromal striae and folds, epithelial microcysts, corneal neovascularization, endothelial polymegathism, and significant fluid influx into the corneal stroma, which disrupts the regularly spaced collagen lamellae.^{1,9,10,23} This is believed to create an optical effect wherein localized fluid spaces which are no longer occupied homogeneously by collagen fibrils exhibit a decrease in transparency, and are visible as linear "striae". It has been proposed that striae appear when the cornea swells to more than 5% of its original thickness.^{10,23} Further corneal edema, on the order of 10% or greater may result in stromal folds, which are thought to be due to the alteration in shape from a smooth curve to having more localized

bending or “buckling” in the posterior stroma and Descemet’s membrane as a result of the stress from corneal swelling. In very extreme cases of edema, haze or corneal clouding may occur, where there is a significant reduction of transparency due to diffuse loss of homogeneity in the arrangement of collagen fibrils. Other factors, such as an excess of lactic acid production during hypoxia, or the mechanical compression of a contact lens on already-present blood vessels to yield greater lactic acid, may also play a role.^{50,51}

Chronic hypoxia upregulates the expression of VEGF (vascular endothelial growth factor), an important chemical mediator which promotes new blood vessel growth – neovascularization of the cornea.^{10,23} Neovascularization can negatively affect both the structural integrity of the cornea as well as the candidacy for corneal transplantation.

1.2 Scleral Lenses

1.2.1 Description of Scleral Lenses

Scleral contact lenses are large-diameter rigid contact lenses composed of gas-permeable materials, which vault over the ocular surface with a fluid layer between lens and eye, and land on the sclera.⁵² The use of a firmly confined liquid reservoir to optically correct corneal refractive error was theorized upon by Leonardo da Vinci in 1508, however, the invention of scleral lenses was not reported on for many years later.^{53,54} In fact, the first published use of a contact lens was a scleral lens, by Adolf Fick in 1888.⁵³ Other early researchers, Eugene Kalt and August Müller, independently developed scleral lenses around this time, apparently without awareness of one another’s discoveries. However, at the time, these lenses were comprised of glass materials and later PMMA, both not permeable to oxygen, and fell out of favour for a number of years.^{23,55}

Scleral lenses can typically range in size from 15 to 25mm,⁵⁵ and depending on size and its relation to the patient’s ocular surface anatomy, previous convention established that a lens was termed as

either a corneo-scleral or scleral lens, which may include mini-sclerals and large sclerals.⁵² The Scleral Lens Education Society has since established universal terminology and categories to describe different scleral lenses, as well as the fit of a scleral lens.⁵⁶ This report has termed all lenses landing on the conjunctiva to be considered scleral lenses, regardless of their sizes. A scleral lens is comprised of three zones (see Figure 1-3); the central optical zone (Figure 1-3A), the midperipheral transition zone (Figure 1-3B) and the peripheral landing zone (Figure 1-3C).

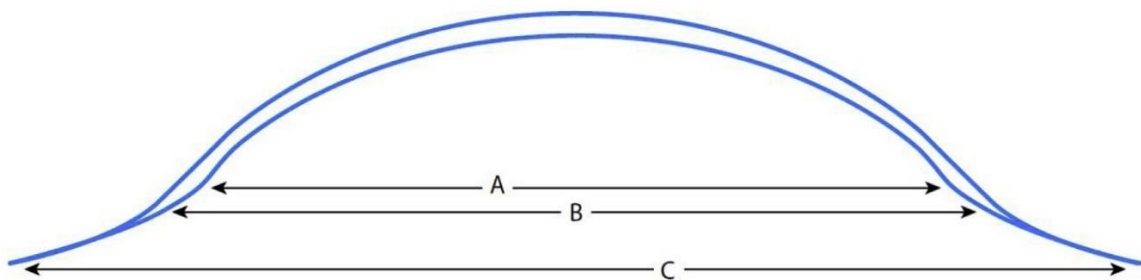


Figure 1-3: Schematic diagram of a scleral lens depicting A: optical zone, B: transition zone, and C: landing zone. Reproduced with permission from Michaud et al, 2020.⁵⁶

On the eye, the central optical zone (A) will typically align with the cornea, the midperipheral transition zone (B) with the limbus, and the peripheral landing zone (C) with the sclera, which should be the only area on the ocular surface with which the lens makes contact.⁵²

The fluid layer between the lens and cornea can be quantified and measured, and is referred to as the “clearance” or “tear reservoir height”,^{52,55} and in the above mentioned report, has been established officially as the fluid reservoir.^{1 56} The clearance is clinically measured centrally as the central corneal clearance (CCC), and over the highest point of corneal elevation if this is different from the centre (as in cases of corneal ectasia^{57,58}) as well as over the limbus. Clearance can be estimated by the clinician at the biomicroscope using the optic section technique angling the slit beam on a 45-^{52,58} or 60-degree angle,⁵⁹ or with OCT.⁵⁹ It has been shown that biomicroscopic estimation of

¹ The fluid reservoir will also be referred to as “clearance” throughout this thesis.

this parameter at a 60-degree angle tends to overestimate the amount of clearance, compared to that of anterior segment OCT, likely because the cross section is being observed obliquely, rather than orthogonal to the surface, as with OCT.⁵⁹ This parameter is significant to assess when fitting scleral lenses. Excessive clearance may limit the amount of oxygen that reaches the cornea,^{11,60,61} but minimal clearance may result in lens touch, which is not desired as this may be abrasive to the corneal epithelium and result in erosions and scarring.^{23,62,63}

A scleral lens must be applied concave side up, with fluid – usually preservative-free saline – in the lens bowl. This is done with the patient holding their head parallel to the ground, so that the fluid does not spill out of the lens bowl upon insertion. As the lens is worn, the amount of clearance between the lens and the ocular surface is not static; in fact, the lens will “settle” towards the eye due to the landing zone of the lens gradually sinking into the conjunctiva, resulting in a reduction in the amount of clearance.^{52,64–66} For this reason, careful measurements of ocular surface biometry and consideration of the desired amount of clearance for prediction of ideal lens parameters (along with subsequent calculation including compensation for settling) are necessary to facilitate selection of the optimal initial diagnostic scleral lens during the fitting process.^{67,68} Additionally, if fluid is lost upon insertion or the lens fit is not ideal, air bubbles may form in the post-lens tear reservoir, which can cause desiccation of the ocular surface.⁵¹

1.2.2 Indications for Scleral Lens Wear

There are many indications for scleral lens wear, including but not limited to corneal ectasia, post corneal transplant, high corneal astigmatism or refractive error, corneal scarring, corneal dystrophies and degenerations, ocular surface disease, aphakia, myopia, and ptosis.^{69–72} Of these, the largest population of scleral lens wearers are those with corneal ectasia, specifically keratoconus. The first report of a scleral lens being used for an individual with keratoconus was by Panas in 1888, shortly after the first scleral lens was reported upon by Adolf Fick.^{53,54} The use of scleral lenses for visual

correction in cases of an irregular corneal shape is useful because the fluid within the lens bowl optically counteracts irregular astigmatism and aberrations by physically filling in the space between the irregular cornea and the optically regular scleral lens surface.

Additionally, due to the sealed nature of the lens fit, there is a maintenance of the hydrostatic pressure of the fluid reservoir, stabilizing the lens and minimizing movement.⁶⁹ The relatively immobile nature of the lens provides good visual stability, particularly in eyes with a higher amount of aberrations,⁵⁵ as in keratoconus.^{23,73-75} This is also the case in patients who have had corneal transplants, where high, often irregular astigmatism, as well as increased higher-order aberrations are often present.⁷⁰ In the case of ocular surface disease, the lens and fluid layer provide protection and lubrication to the ocular surface.^{71,72,76}

1.2.3 Complications of Scleral Lens Wear

Comparable to the wear of other lens types, complications that can result from scleral lens wear may be of hypoxic, mechanical, infectious, or inflammatory origin.⁵⁷ Currently, the long term impacts that scleral lens wear has on the physiology of the cornea and limbus are being explored, but have not been definitively established, due to the recent resurgence of this lens modality. Known complications with scleral lens use will be briefly outlined.

Relative hypoxia with subsequent corneal edema, limbal and conjunctival hyperemia, and hypoxia-induced corneal staining are a few of the possible complications of prolonged scleral lens wear. There are two barriers to oxygen delivery from the atmosphere to the cornea in scleral lens wear, that is, the lens itself, and the post-lens fluid reservoir. In addition to these barriers, modern scleral lenses are also known to promote little tear exchange due to the nature of the lens fit, where further oxygenation would typically occur.^{51,57,60,61} The combination of these aspects limit the routes for oxygen delivery to the cornea through both the lens and the post-lens fluid reservoir, possibly resulting in corneal

edema, as well as an increase in limbal and conjunctival hyperemia and corneal staining due to hypoxia.^{10,47} Scleral lens wear has been shown to induce a subclinical amount of total corneal edema secondary to hypoxia,⁷⁷⁻⁸⁴ which may be associated with changes in the depth of the fluid reservoir, or central corneal clearance.^{77,79-81,84,85} This will be discussed in greater detail in Chapter 2.

Contact lens-induced hypoxia has been associated with increases in epithelial thickness acutely in a closed-eye environment,^{30,34} and a decrease in thickness chronically.^{38,40} With scleral lens wear, epithelial thickness changes were not found to be outside of the normal level of diurnal fluctuation.^{33,83,84} In contrast, observed hypoxia-induced changes in the corneal stroma with scleral lens wear were quite significant and not attributable to diurnal variation in healthy patients. In other words, corneal edema as a result of scleral lens wear has been postulated to be largely due to stromal, rather than epithelial edema. Other possible yet nonspecific epithelial changes as a result of hypoxia with scleral lens wear include epithelial bullae and microcysts,⁵¹ and, more recently, transient endothelial bleb formation.⁸⁶ Neovascularization, another classic sign of direct hypoxia is also possible with scleral lens wear, but its occurrence in this case is theorized to be more likely primarily due to lens fit issues. For example, this may occur in a tight lens fit, which may hinder blood flow and result in increased lactic acid production,¹⁰ or additionally in cases of chronic conjunctival prolapse,⁸⁷ which will be discussed in greater detail below.

Other complications of scleral lens wear may be the result of the lens fit and are therefore more mechanical in nature. It is known that the topography of the sclera is asymmetric,^{88,89} sometimes leading to a less than ideal fitting relationship between the landing zone of a spherical scleral lens and the sclera.^{51,57} As a result, uneven weight distribution of the lens may occur and consequentially induce compression across the landing zone, or even impingement of tissue and vasculature, both of which apply pressure to the conjunctival tissue and blood vessels in certain regions.⁹⁰ Specifically, compression describes an increased pressure of the lens on the ocular surface across the lens landing

zone, where impingement refers to increased pressure concentrated at the lens edge. An interruption of blood flow can result in these locations, clinically noted as “blanching”, in the case of both compression and impingement.²³ In the opposite case, the landing zone of the edge may be lifted relative to the ocular surface, which may contribute to bubble formation, and, if persistent, may result in corneal staining due to desiccation, along with debris accumulation underneath the lens.⁵² This is suboptimal for both ocular surface health, and patient comfort. In order to mitigate these complications, scleral lenses can often be ordered with a toric periphery applied, where different peripheral curves are specified in order to optimally align with the ocular surface, or an overall flatter landing zone if these complications are noted circumferentially.

Other mechanical complications that may occur as a result of negative pressure in the fluid behind the lens include conjunctival prolapse, or hooding, and lens “seal-off”.^{23,51,57} Briefly, the former involves the movement of conjunctival tissue towards the peripheral cornea, in some cases making prolonged contact with the cornea, which may chronically result in corneal scarring and vascularization.⁸⁷ Generally, conjunctival prolapse is not considered to be an adverse event, so long as it is reversible after lens removal, indicating that conjunctival-corneal adherence is not occurring. Clinically, decreasing the limbal clearance of the scleral lens, or applying a toric periphery may prevent this complication. Lens seal-off occurs when the lens is strongly suctioned onto the eye, which limits the exchange of tears from the tear film to the fluid reservoir and vice versa, which may have implications in corneal hypoxia, and cause retention of metabolic waste products in the fluid reservoir. Additionally, this is not comfortable for the patient, notably during removal of the lens. This characteristic of scleral lens fitting has been suggested to result in increased intraocular pressure, due to fluid pressure forces on the ocular surface, but this has not been definitively established, in part due to the difficulty of measuring intraocular pressure with a scleral lens applied.⁹¹

Depending on the fit of the lens and ocular surface elevation, corneal bearing or touch may be encountered, where the lens does not completely vault the cornea. Mechanical corneal staining and discomfort may result, as well as epithelial bullae and microcysts, and chronic epithelial breakdown.^{23,51} This can occur over the corneal apex, in particular, the pathological cone area in keratoconus, and at the limbus.⁵⁷ Ocular surface epithelial cells, in particular limbal stem cells, play a key role in corneal health and regeneration.⁹² Thus, when fitting scleral lenses, lens parameters should be chosen to minimize touch at the ocular surface, and if this cannot be avoided, these areas should be carefully monitored to ensure that there are no adverse ocular health outcomes for the patient.

In some cases, mid-day fogging or reservoir debris accumulation has been noted with scleral lens wear.^{23,51,57} There is not thought to be a single cause for this phenomenon, but it has been observed more frequently in those with ocular surface disease, as well as atopic disease. Other suspected causes include a suboptimal lens fit, in particular a high lens clearance, a tight lens fit, or conversely, excessive edge lift. There are various types of fogging that have been observed, including mucus debris, “diluted milk” fogging, and lipid debris, all of which have a distinct appearance. If the cause of the debris is modifiable by adjusting the lens fit, this complication may be mitigated. However, if this is not possible, other options that may be trialed in order to minimize this include substitution for a more viscous solution for scleral lens application, or removal and re-application of lenses throughout the day.

Although rare, infectious complications can occur with scleral lens wear. In a great number of these reported cases, the individual had ocular surface disease, or was taking corticosteroids, which in theory would reduce the mechanical epithelial and chemical immune response to infection.⁵⁷ If microorganisms are present on the lens or in solution, the limited tear exchange and sealed nature of the tear reservoir in a scleral lens fit can create a stagnant environment for an infection to occur.⁹³ Inflammatory events are also possible with scleral lens wear. Scleral lens wear involves the lens, on

which deposits may accumulate, the cleaning and conditioning solution, and the tear reservoir behind the lens, which may contain metabolic waste, exotoxins and other debris.^{23,51} These elements are all potential irritants to the ocular surface, and have the capability of causing hypersensitivity or sterile inflammatory events, such as giant papillary conjunctivitis, or corneal infiltrates. Similar logic as previously discussed for infectious events with respect to the sealed nature of the lens fit applies here – non-infectious irritants may remain in the relatively inert fluid reservoir due to minimal tear exchange and continue to aggravate the ocular surface. Additionally, the nature of the interaction of the lens and the ocular surface due to the lens fit may result in irritation or inflammation. To reduce the likelihood of both infectious and inflammatory complications, prudent and aggressive disinfection of lenses is recommended, and in some cases for inflammatory events, lens parameter modification may be of preventative value.

1.3 Keratoconus

1.3.1 General Overview

Keratoconus is a progressive, degenerative corneal dystrophy, wherein corneal ectasia manifests as irregular astigmatism.^{23,94,95} Ectasia is a term used clinically to describe corneal pathology where the corneal shape deviates from that of the average population. Individuals with keratoconus often experience vision distortion and loss as a result of corneal ectasia, which varies according to disease severity, and in many cases cannot be corrected with conventional spectacles and contact lenses.

Keratoconus is bilateral but often asymmetric in its presentation, most commonly presenting and accelerating in youth, then stabilizing around the fourth decade.^{23,94} There has not been a sole etiology established for keratoconus, however various factors including eye rubbing, atopy, genetics, connective tissue disorders, Down Syndrome, and oxidative stress are associated with this condition. Although initially thought to be a non-inflammatory disease process, there is increasing evidence that

this condition has certain attributes that are inflammatory in nature.^{96,97} Clinical signs that may prompt a practitioner to investigate or diagnose keratoconus include, but are not limited to, corneal scarring and stromal thinning, Fleischer's ring, Vogt's striae, or even simply in early stages, reduced vision that cannot be corrected to 20/20 in the absence of other causes.^{63,98,99} Clinically indicated testing for the management and diagnosis of individuals with keratoconus may include topography and tomography to measure corneal pachymetry,² curvature and elevation individually or simultaneously via diagnosis and progression indices, as well as OCT to measure total and epithelial corneal thickness and visualize morphological abnormalities.¹⁰⁰⁻¹⁰³

1.3.2 Demographics

The incidence of keratoconus has been reported to range from 50-230 individuals per 100 000,^{94,99} with some studies citing rates as low as 1.4 per 100 000¹⁰⁴ and 2 per 100 000,¹⁰⁵ and as high as 600 per 100 000,¹⁰⁶ all three of these studies having been performed in predominantly Caucasian populations in the United States and Finland. The prevalence of this disease is reported to be approximately 54.5 per 100 000 in an American population,¹⁰⁵ and 28.7¹⁰⁷ – 28.8¹⁰⁴ per 100 000 in European Caucasian populations. A more recent study from The Netherlands has suggested an annual incidence of 13.3 individuals per 100 000 and a prevalence of 265 per 100 000.¹⁰⁸ The diverse range in these figures may be due to varying diagnostic criteria for this condition among practitioners in different areas, and changing technology to enhance diagnosis, depending on where and when the study was conducted.^{94,99} It was previously thought that keratoconus has no predilection for ethnicity, but more recent studies carried out in the United Kingdom have reported a much higher incidence in the South Asian population compared to Caucasians, particularly those of Northern Pakistani origin, reporting a four to nine fold increase in incidence when comparing these two ethnic groups.^{107,109,110}

² Throughout this work, pachymetry does not refer to the use of a physical pachymeter unless otherwise specified. Instead, this term is used interchangeably with corneal thickness.

There is not a consensus on whether keratoconus is more prevalent in males^{107,111,112} versus females^{94,98} as various findings have been reported for both cases, where other investigators claim that both sexes are affected equally.^{99,105}

1.3.3 Biochemistry and Histopathology

In the disease process of keratoconus, all corneal layers may eventually be affected, however it has been long believed to originate with changes to the corneal epithelium.^{23,94,99,113} A classic “triad” of prominent effects have been observed in the pathological process, including corneal stromal thinning, breaks in Bowman’s layer, and the accumulation of iron in the basal epithelial cells of the cornea around the base of the cone, which may be observed clinically as a Fleischer ring (shown in Figure 1-5A, where clinical signs of keratoconus are detailed in a later section).^{23,94,99} Early in the disease process, the structural integrity of the basal epithelial cells are thought to deteriorate, with ensuing damage to their basement membrane and sometimes epithelial or stromal invasion into Bowman’s membrane.¹¹⁴ In some cases, a thickening of material below basal epithelial cells is observed, forming a membrane-like structure,^{99,113} containing unidentified “particles”, which have also been observed on the surface of Bowman’s membrane.^{94,99} These particles have been proposed to contain the enzyme collagenase, an enzyme which degrades collagen and contributes to the initial architectural distortion of the stroma, ultimately resulting in thinning and anterior protrusion.^{94,115} Other epithelial cellular changes observed *in vivo* include altered morphology of epithelial cells at the cone apex, including elongation of superficial cells arranged in a whorl-like configuration, and folding of basal cells, which demonstrate high reflectivity.^{116–120} Increasingly elongated, or spindle-shaped superficial cells have been primarily noted in severe cases of keratoconus.^{116,119–121} There is not an agreement in the literature on whether these cells are greater in size, resulting in a lower cell density compared to eyes without keratoconus,¹¹⁶ or if cell size and density do not differ between these two populations.¹²² In severe cases, wing epithelial cells have been noted to be larger than in control eyes.^{119–121,123} Most

of these same studies determined basal cell density to be lower in KC due to larger cell size, and a more abnormal appearance, particularly in cases of severe disease¹¹⁹⁻¹²¹ Conversely, other researchers found basal cell density to be significantly higher in eyes with keratoconus compared to controls.^{120,122}

Further, epithelial thickness has been reported to vary greatly centrally in vivo and in vitro^{119,120} as well as ex vivo¹²⁴ more so than peripherally, which has been attributed to cellular polymegathism, rather than an increase in cellular propagation.¹¹³ In these studies, the proximity of the pathological cone region of the cornea to the centre was not specified for patients and samples analyzed. However, the cone region in keratoconus more often involves the central and paracentral cornea, in contrast to the periphery. Qualitative cellular morphology,^{117,118} as well as decreased variability in measured epithelial thickness¹¹³ in the peripheral cornea outside of the cone area has been observed to be more representative of a normal cornea. Others have noted specifically corneal epithelial thinning to be a very common histopathologic finding in eyes with keratoconus in ex vivo sections involving the cone¹²⁵, and also reported as a general finding where the cone location was not specified with respect to the epithelial thinning.^{114,119}

Due to the close association between the epithelium and Bowman's layer, the latter providing support and a means of attachment to the anterior stroma for the former, it is easily foreseeable that locations of epithelial irregularity would correlate to compromise of Bowman's layer.¹¹³ In keeping with this, it has been observed that in-vitro, there was a thinning or loss of Bowman's layer more so centrally than peripherally, where the disease process primarily occurs.¹¹³ More recently, it has been proposed that damage to Bowman's layer is more pathologically complex than straightforward rupturing and breaks, noting the complete absence of this structure in some locations.^{113,118,126} Other observations have included hyperreflectivity adjacent to Bowman's layer,¹¹⁷ as well as the apparent bifurcation of this structure.^{119,120} In the peripheral cornea outside of the typically severely diseased

area, investigators have observed distinct processes from the stroma infiltrating Bowman's layer, which may indicate early steps of the pathological mechanism, as this was noted outside of the severely diseased area.^{118,120,127}

As previously noted, the corneal stroma is composed of collagen fibrils bundled into lamellae, bound together by a proteoglycan matrix, both secreted by keratocytes.¹ In the keratoconic cornea, there are different amounts and characteristics of these substances, in particular in the "cone" area.⁹⁴ Type I collagen, which is the most ubiquitous of all collagen types present in the cornea, makes up the majority of the stroma's lamellar structure. Studies that have quantified these proteins with transmission electron microscopy have shown that between normal and keratoconic corneas, there is no difference between the thickness of the lamellae,¹²⁸ and between these two groups, spacing between lamellae has been confirmed to be similar through X-ray diffraction.¹²⁹ Another study has disputed these findings, claiming that collagen fibril diameter may be decreased in keratoconus, and additionally that collagen fibrils are more densely packed in keratoconic corneas.¹³⁰ Biochemical studies that have attempted to quantify the amount of collagen have not universally reported that the keratoconic cornea has lower quantities compared to the normal cornea.¹¹⁸ Some investigators have reported less collagen¹²⁸ and total protein in general in the keratoconic cornea,^{131,132} while others report the opposite,¹³⁰ specifically, a technically greater amount of Type I collagen in keratoconic corneae, however this was not a significant difference.^{118,133} Similarly, others reported no differences in collagen composition between the keratoconic and normal cornea, with the exception of a greater amount of type III collagen over areas of scarring.^{118,134,135} Scarring has also been proposed to be a result of compaction of stromal fibres, occurring in similar locations to where epithelial breaks and thinning have been noted, suggesting that these epithelial changes occur prior to further stromal remodeling.^{114,125} Other researchers have claimed a variable presentation of collagen composition across keratoconic corneas in terms of collagen amount, as they found this parameter to vary across

individuals with this disease.^{131,136} Keratocyte density has been reported to be decreased in keratoconic eyes compared to non-keratoconic eyes in the case of previous contact lens wear, but in this study, there was not a significant difference between diseased and non-diseased eyes who did not wear contact lenses.¹³⁷ In addition, keratocyte morphology has been reported to differ qualitatively between keratoconic and healthy eyes.¹¹⁷ More recent evidence of cells that were markedly histologically distinct from keratocytes have been noted in the anterior stroma of the keratoconic cornea, which investigators suspected were either highly differentiated keratocytes, or cells of a different origin.^{113,117} These cells did not have inflammatory cellular characteristics but were hypothesized to play a role in the pathological loss of corneal tissue, due to the observation of their close association with keratocytes, as well as large amounts of adjacent stromal cellular debris. There is evidence that the extracellular matrix component of the stroma in a keratoconic cornea is of lesser volume than that of a normal cornea,¹²⁹ however, this is not unanimously agreed upon in the literature.⁹⁴ Countering this finding, other studies have reported a significantly greater amount of glycosaminoglycans and proteoglycans in the keratoconic cornea compared to the normal cornea.^{130,136} These extracellular matrix components have also been reported to have modified expression and distribution in keratoconic corneas compared to those of normal individuals.^{126,136,138}

Descemet's membrane may be affected in keratoconus, in some cases exhibiting structural folds.^{118,126,139} The development of corneal hydrops, a complication of keratoconus (further detailed in Section 1.3.4.3), occurs when Descemet's membrane breaks and subsequently detaches from the endothelium, and then will assume a "scroll" or "ridge"- like state.^{99,140}

The corneal endothelium in general is often unaffected in keratoconus, however, there have been descriptions of cellular pleomorphism, in particular cellular elongation as well as the presence of dark intracellular structures.^{99,118} Additionally, when Descemet's membrane is affected in corneal hydrops, adjacent endothelial cells have been observed to be damaged.^{113,141}

1.3.4 Clinical Presentation and Diagnosis

1.3.4.1 Introduction

Clinically, keratoconus may present with both qualitative and quantitative signs, with or without visual symptoms.^{94,99} In its early stages, patients may initially have corneal morphological changes detectable on slit lamp biomicroscopy, or show refractive changes due to ectasia.²³ Corneal ectasia occurs at the pathological “cone” area, the location of which can vary^{142,143} and result in structural damage to the cornea,^{98,114,125,142} hindering its role as a key transparent refractive interface for the visual system. As keratoconus advances, visual consequences often become more perceptible to the patient,^{73–75,144–148} although typically they are more severe in one eye over the other, especially in the early stages.^{149,150}

1.3.4.2 Cone Types

Anterior segment ocular health findings in keratoconus often will be present in the diseased or ectatic part of the cornea, (the “cone”). The cone location varies across patients, and two distinct clinical subtypes exist, the round, or nipple cone, and the oval, or sagging, cone (see Figure 1-4).^{99,142,143}

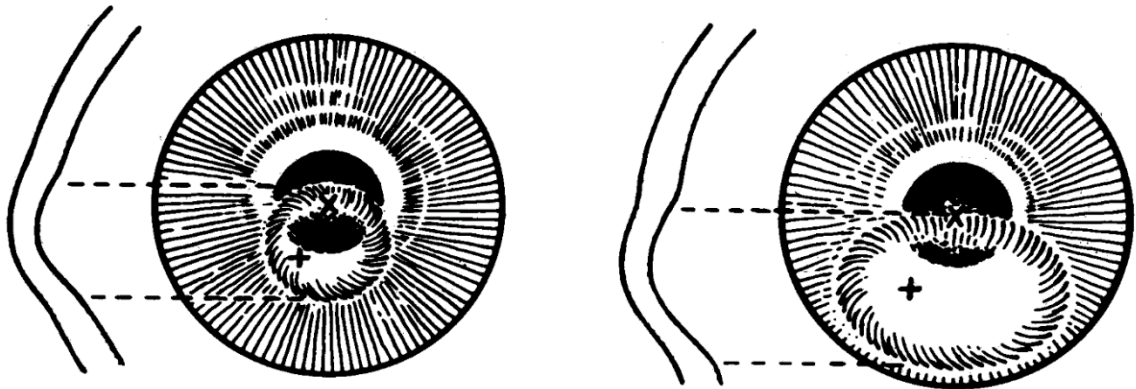


Figure 1-4: Diagram of a round (left) vs oval (right) cone. In this image, the “x” represents the visual axis, and the “+” the cone apex. Reproduced with permission from Perry et al, 1980.¹⁴³

Typically, the round cone is more centred in location, that is, the conical apex is closer to the visual axis, generally located just inferior nasally. Conversely, the oval cone is more often located further inferior temporally, with its apex further from the visual axis. Comparatively, the round cone is smaller in diameter than the oval cone.⁹⁴ To the best of current knowledge, patients have not been noted to exhibit both cone types, either over time, or between eyes. Further, histopathologic differences have been noted between these two clinical subtypes. For example, oval cones have been noted to have significantly more, as well as, larger breaks in Bowman's membrane, and possibly more frequent damage to Descemet's, paralleling a higher occurrence of corneal hydrops and corneal scarring, compared to round cones.¹²⁵

1.3.4.3 Qualitative Signs

Qualitatively, a clinician can identify signs of keratoconus during slit-lamp biomicroscopy. Naturally, with keratoconus being an ectatic disorder, stromal thinning at the corneal apex is often evident on examination, optimally viewed using an optic section biomicroscopic technique.^{23,94,99,142} The rapid change in curvature resulting in paracentral steepening of the cornea and may also be appreciable on slit-lamp biomicroscopy, due to the protrusion of the cone. This parallels the histopathological observation in keratoconus of stromal thinning,^{114,118} which is more often appreciated clinically in more advanced stages of keratoconus.

As previously mentioned in 1.3.3, in the pathological process of keratoconus, the basal epithelial cells become infiltrated with iron, specifically an iron storage complex referred to as hemosiderin.^{23,94,99} The source of this compound is postulated to be that of the tear film pooling in areas of corneal pathological variation,¹⁵¹ and the deposition, referred to as "Fleischer's ring", can either completely or incompletely encircle the base of the cone (Figure 1-5A).^{98,152} Under white light, Fleischer's ring has been observed to have an olive-green to yellow-brown hue, but is also feasibly visualized as a dark ring when illuminated with a cobalt-blue filter on slit-lamp biomicroscopy.

As the cornea becomes structurally thinner in keratoconus, but the intraocular pressure continues to exhibit outward force, there is strain placed on the thinner cornea, which is also weaker. As a result, the cone protrudes outwards, and it is believed that the pressure on the posterior corneal stroma both places strain on and disrupts the regular orientation pattern of collagen lamellae.^{23,98,142} This is thought to be the most likely cause for Vogt's striae, shown in Figure 1-5B, which are vertical or oblique stress lines in the posterior stroma and Descemet's membrane.^{94,99} This strain may also lead to breaks in Bowman's membrane which may be occupied by either collagen or epithelial cells.¹¹⁴ This could be noted clinically as anterior linear scars at the conical apex.¹²⁵ When scarring occurs in the corneal stroma, it is hypothesized to be a result of stromal collagen fibres becoming more densely packed in later stages of the disease (Figure 1-5C).

At times, in advanced cases of keratoconus, Descemet's membrane and the corneal endothelium weaken. If breaks form in these barriers to the anterior chamber, the aqueous humour can then enter the cornea in the form of corneal hydrops, resulting in corneal edema.^{23,94,98,99} This process is incredibly painful and visually debilitating for the patient. Acutely, the corneal stroma will appear opacified due to corneal edema, and conjunctival hyperemia may also be present. However, corneal edema as a result of hydrops will resolve steadily with time, typically over weeks to months. Despite the hydrops being resorbed as the cornea heals, their occurrence will often leave behind structural corneal damage and often scarring.

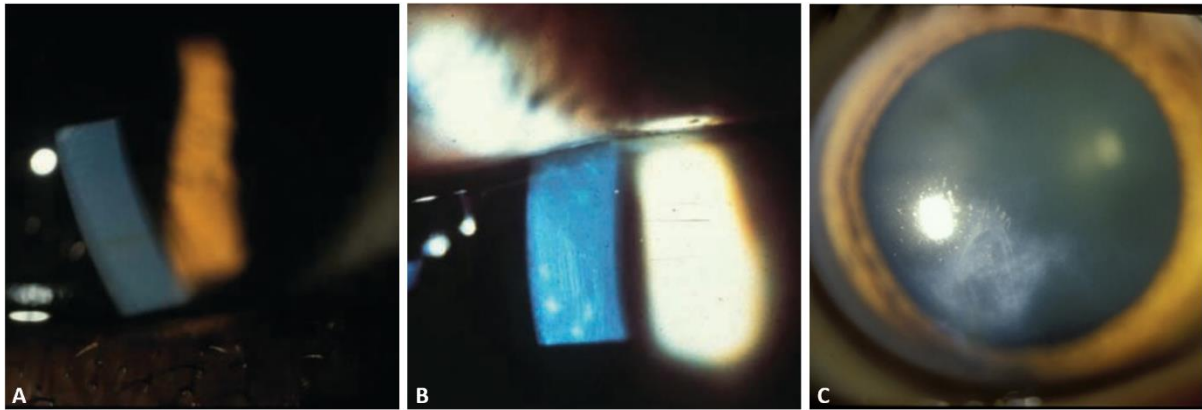


Figure 1-5: Clinical signs of keratoconus, A: Fleischer’s ring, B: Vogt’s striae, C: Apical scarring. Adapted by Kirsten Carter, with permission of [Wolters Kluwer Health, Inc], from [Clinical Manual of Contact Lenses, Bennett and Henry, 4th edition, Elsevier, 2015]; permission conveyed through Copyright Clearance Center, Inc.²³ (1-5A, 1-5B) and Wagner et al, 2007¹¹² (1-5C) with permission.

Outside of the biomicroscope, qualitative signs of keratoconus that may alert a clinician to the presence of this condition include a “scissor-like” light reflex on retinoscopy, and the “Charleux oil-droplet” or circular reflex with an encircling darker annulus on direct ophthalmoscopy or retinoscopy.^{23,94,99,142} Additionally, mires that are irregular in appearance on keratometry, particularly in the central or inferior location may serve as additional signs. Another supplementary pathological finding, which is clinically noted in advanced cases, often after other signs have already indicated the diagnosis, is Munson’s sign. Munson’s sign can be described as the deformation of the lower eyelid on downgaze, as the keratoconic cornea forces it into an angular shape.⁹⁸

1.3.4.4 Quantitative Signs

There are also quantitative factors that can aid a clinician in diagnosing keratoconus. As mentioned, disease progression is tied to increasing corneal thinning and steepening, and therefore astigmatism.^{23,94,99} This structural change is asymmetric, yielding nonorthogonal corneal astigmatism, and often increased myopia which cannot be corrected by conventional spectacles and contact lenses.

Despite this being irregular astigmatism, increased regular astigmatism can be noted in the attempt to measure this clinical parameter, as in topographic measurements such as keratometry, and in refractive measurements, such as retinoscopy, auto-refraction, and subjective refraction, all of which become more difficult with disease progression.¹⁵³ What may alert a clinician to suspect keratoconus includes large amounts of astigmatism at an oblique axis, as well as this astigmatism fluctuating in its amount or direction (particularly from with-the-rule to oblique) over time. That said, these clinical methods of measurement of regular astigmatism are not reliable measures of irregular astigmatism and disease progression, but may change rapidly in the progression of keratoconus, and thus may draw the clinician's attention to its presence. Accompanying this may be decreased best-corrected visual acuity, another non-specific quantitative indicator of this disease process, which is sometimes the first clinical sign.^{98,147} Other ancillary measurements that may be of value include contrast sensitivity, low contrast visual acuity, and aberrometry. Individuals with keratoconus have reduced contrast sensitivity^{74,144,145,154} and low contrast visual acuity, particularly in cases of corneal scarring,^{146,148} as well as a greater amount of higher-order aberrations,^{74,75} in particular, coma.⁷³ While these signs may provide clues, they are not diagnostic of keratoconus, as the clinical standards for this are corneal topography and tomography – quantitative methods that can be used both for diagnosis and management/monitoring of keratoconus.

1.3.4.5 Corneal Topography and Tomography in Diagnosis and Screening

Corneal topography, also referred to as videokeratography, in its detection of the anterior corneal surface, can provide elevation and curvature measurements and model local variation in these measurements in the form of topographic maps.²³ Many topographic instruments employ the optical concepts of a Placido disk, which involves the projection of concentric rings onto the ocular surface, and the analysis of how the rings are reflected to gain topographic information about the cornea.⁹⁹ The first study to report on the existence of forme fruste keratoconus detectable only by corneal

topography, published by Marc Amsler in 1938, involved the use of a photographic Placido disk.¹⁵⁵ In anterior segment tomography, both the anterior and posterior corneal surfaces are detected during imaging, and measurements of both surfaces can be carried out to obtain further diagnostic information, including corneal thickness, in cases of suspected ectasia.¹⁵⁶ Examples of this technology are Scheimpflug imaging and optical coherence tomography (OCT). In brief, Scheimpflug imaging is useful when imaging a non-planar object, such as the cornea, as this method uses an optical technique wherein the lens plane is tilted in order for the film and focal plane to be intersected, rendering the anterior and posterior cornea in sharp focus.^{157,158} The Oculus Pentacam® HR uses this principle to take rotational cross-sectional images of the cornea with a visible blue light source, from which elevation, curvature, and pachymetric measurements (along with much more information) can be extracted.¹⁵⁹ In contrast, OCT instruments can generate tomographic images with location and reflective information obtained via interferometry with an infrared laser light source (e.g. Heidelberg Spectralis® OCT).^{160,161} With the Spectralis® device, manual pachymetric measurements can be made with the instrument software or in adjunct software with exported images, as no automatic image measurements are made.

With both topography and tomography obtained in an automated manner, instruments take data pertaining to one or both surfaces and plot it as a colour-coded map to aid the clinician in visualizing relative changes in parameters measured (see Figure 1-6).²³ With these maps, the cone can be well delineated, as the cone apex and local steepening are well-marked.

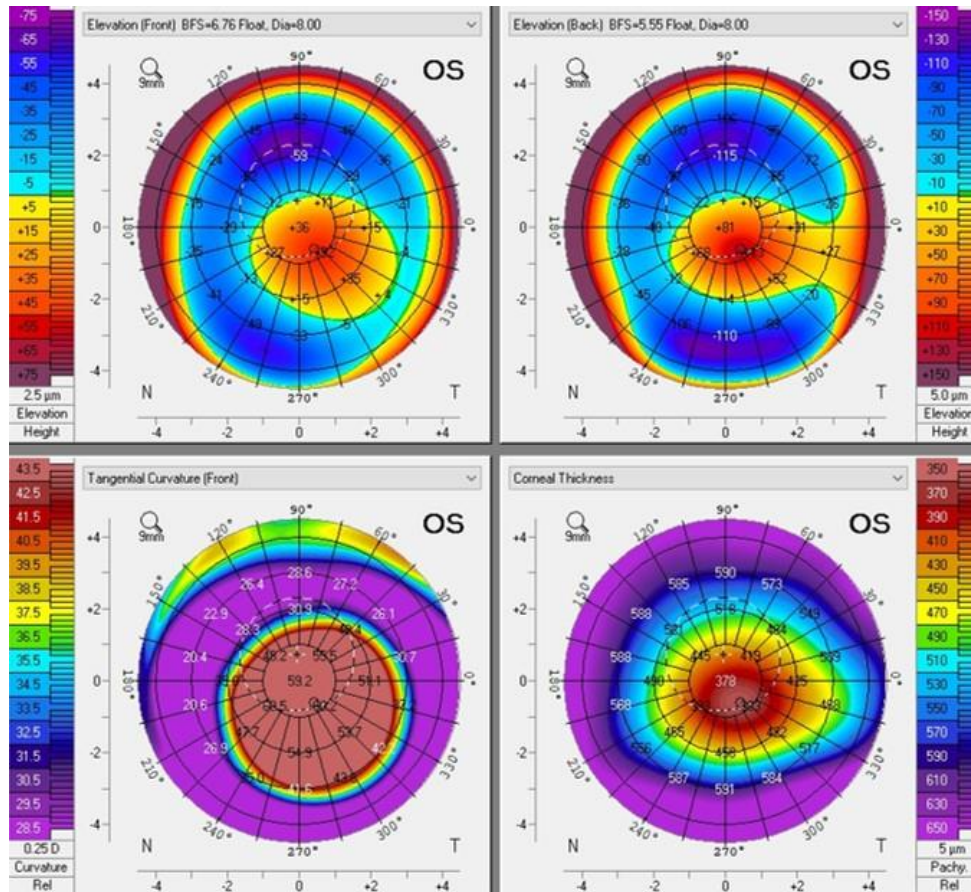


Figure 1-6: An example of tomographic data taken with the Oculus Pentacam® HR tomographer displayed as colour maps of a patient with advanced keratoconus.

Many researchers have proposed methods using topographic indices to screen for and diagnose keratoconus,^{162,163} and specifically, to discriminate normal eyes from keratoconus suspects and early cases of keratoconus.¹⁶⁴ A method using topographic parameters relating to the size and location of the diseased area, or cone, to identify keratoconus has also been described.¹⁶⁵ Aberrometry may also be helpful in these cases.¹⁶⁶ Detecting keratoconus may also be done with tomographers, such as with Scheimpflug imaging, which is frequently employed by clinicians.^{100,156,167,168}

In terms of diagnosing keratoconus with the assistance of topography versus tomography, many experts feel that tomography is optimal, as it is important to note ectatic changes of both the anterior

and posterior corneal surface, as well as pachymetric data across the cornea.⁹⁵ While other clinical instruments are capable of measuring central pachymetry, this has been determined to have low value in diagnosing keratoconus, compared to other parameters. In particular, a panel of experts have released a consensus that the following criteria must be met to diagnose keratoconus:⁹⁵

- 1) Abnormal posterior elevation
- 2) Abnormal corneal thickness distribution
- 3) Clinical noninflammatory thinning

Parameters relating to the posterior cornea are important to note not only with diagnosis, but monitoring for progression as well, discussed further in Section 1.3.5.2.⁹⁵ A specific diagnostic tool which allows the clinician to evaluate the consensus criteria is the “Belin-Ambrósio Enhanced Ectasia Display”, an analysis feature built into the software of the Oculus Pentacam®.^{100,158} On this display, elevation and pachymetry data are presented in a manner to aid the clinician in determining the likelihood that the individual has a corneal ectatic disorder. Firstly, elevation is re-calculated using an “enhanced reference surface” method, where the best-fit sphere is re-calculated to exclude the elevation of the 4mm circular area where the corneal thinnest point is the centre (i.e., the area most likely to correspond to the cone). This is done to avoid underestimation of pronounced elevation changes in this area of the cornea which may be otherwise overlooked using the standard best-fit sphere method. After this, elevation of the front and back surface is displayed with colour maps, showing elevation both based on the standard reference sphere, as well as based on the enhanced reference surface excluding the ectatic region. Colour plots for both the front and back surface showing the difference in microns between the standard best-fit sphere and enhanced reference surface are also displayed. The greater the difference between these two maps, the more likely it is

that an individual has corneal ectasia, as it has been shown that in normal eyes the two methods of elevation measurement yield very similar results. Pachymetric data is also displayed and plotted in this display, with thickness data taken in concentric circles about the thinnest point of the cornea displayed as a colour map. Plots from these circles of the average thickness and percent change in thickness are displayed for the individual, as well as where their data falls relative to the normative population. As individuals with keratoconus typically have a sharper increase in these parameters, along with thinner corneas overall, this tool aids the clinician in their diagnosis of an individual with keratoconus, particularly in early cases. In addition to this, the distance of the thinnest point of the cornea from the apex is displayed, where in keratoconic eyes, this distance between these two locations has been measured to be significantly greater than in normal eyes.

1.3.4.6 Differential Diagnosis of Keratoconus from Related Ectasias

There are varied clinical presentations of corneal ectasia which are recognized as distinct ectatic disorders from keratoconus;⁹⁵ however they are believed to be of similar etiology and disease process, in particular because all presentations have been noted in individual families.^{23,94} The primary distinction between these disorders and keratoconus is the location of the cornea that is altered.²³ While the pathological area in keratoconus located more centrally or paracentrally, pellucid marginal degeneration results in more peripheral corneal ectasia, located approximately 1-2mm from the limbus.^{94,99} Above the diseased area, typically the central cornea, a non-pathological thickness is noted in pellucid marginal degeneration. To differentiate between keratoconus and pellucid marginal degeneration, corneal topography is helpful in addition to slit-lamp biomicroscopy, particularly in less advanced cases. In pellucid marginal degeneration, there is a classic “butterfly” or “kissing doves” appearance due to the presence of high against-the-rule astigmatism and central vertical flattening.¹⁶⁹ Keratoglobus, true to its name, is a disorder wherein the corneal ectasia assumes a globe-like shape, rather than a cone (as in keratoconus). The thinning is more diffuse and peripheral in nature compared

to keratoconus, and can reach the limbus, however it does not progress as quickly as keratoconus.^{23,94,99} In both pellucid marginal degeneration and keratoglobus, corneal scarring is observed less frequently in comparison to keratoconus, however corneal perforation is more common in keratoglobus, while it is uncommon in keratoconus.^{94,99} Terrien's marginal degeneration and posterior polymorphous corneal dystrophy could sometimes present other possible differential diagnostic entities, since in some instances these conditions can lead to a keratoconic-like steep cornea.

1.3.4.7 Symptoms

Depending on the disease stage of keratoconus, symptoms may vary.⁹⁹ In general, as the disease progresses, an individual with keratoconus will often experience a decline in visual function. The asymmetrical thinning and local steepening of the cornea yields irregular corneal astigmatism, which optically can manifest as blur, shadowing and haloing of images, distortion, as well as monocular polyopia.^{23,94,98} Individuals with keratoconus may also report glare, irritation, photophobia and asthenopia.¹⁴⁸ Structural pathological changes, including corneal scarring present in keratoconus, compromises corneal transparency, reducing the amount of light that can transmit this structure to focus on the retina.^{74,170}

Structural corneal damage either from corneal scarring or other pathological changes in keratoconus⁷⁴ can increase ocular light scatter, reducing the quality of the retinal image.¹⁷⁰ Irregular astigmatism and other structural changes together often result in reduced vision perceptible to both the patient, and measurable by the clinician. Specifically, and as previously mentioned, this may translate to decreased best-corrected high contrast visual acuity,^{23,98,99,147} low contrast visual acuity, particularly in keratoconic scarred eyes,^{146,148} and decreased contrast sensitivity^{74,144,145,154} in these patients, compared to those without keratoconus. It should be noted that the patient may perceive a decline in their vision prior to manifesting a decrease in high contrast best-corrected visual acuity,

which may be detectable by these ancillary tests.^{94,145,154} Acutely, in the case of corneal hydrops, patients are symptomatic for both pain and an even further decline in their vision⁹⁹ due to corneal damage and ensuing edema and later scarring, respectively.^{23,94}

1.3.5 Management

1.3.5.1 Staging

To optimally manage and monitor patients with keratoconus clinically, it is helpful to classify their disease stage, or severity. The most universally accepted classification system for disease severity of keratoconus is the Amsler-Krumeich classification, which assigns disease to Stages 1-4, depending on the refractive and structural criteria, which are mostly quantitative, that are met (Table 1-1).^{99,149,171}

This system, however antiquated, is inclusive of topographic diagnostic characteristics, particularly in the subclinical or “forme fruste” stage (Stage 1), where other clinical signs are absent, although specific and up-to-date quantitative parameters, particularly tomographic parameters, are not included.¹⁵⁵ With technological improvements in corneal topography and tomography, it has been proposed that it would be prudent to establish a more specific set of criteria to account for measurements from these modalities, in order to enhance diagnosis.^{95,156}

Table 1-1: Amsler-Krumeich staging of keratoconus, adapted by Kirsten Carter from Krumeich et al, 1998.¹⁷¹

Stage	Clinical Criteria
1	Eccentric corneal steepening Induced myopia and/or astigmatism ≤ 5 D Corneal radii ≤ 48 D Vogt's striae, no scars (Typical corneal topography)
2	Induced myopia and/or astigmatism >5 to ≤ 8 D Corneal radii ≤ 53 D No central scars Corneal thickness: minimally ≥ 400 μm
3	Induced myopia and/or astigmatism >8 to ≤ 10 D Corneal radii >53 D No central scars Corneal thickness: 200 – 400 μm
4	Refraction not measurable Corneal radii >55 D Central scars, perforation Corneal thickness: minimally ≥ 200 μm

Various objective methods to stage keratoconus have been proposed since the Amsler-Krumeich classification, some supplementing or comparing to the already existing system with the addition of Scheimpflug tomographic parameters.^{167,168} Other proposed staging methods have been based solely on keratometry,^{142,143} topographic parameters and indices alone^{163,166} or in conjunction with clinical signs.^{164,172} Staging based purely on structural observation with OCT imaging has also been proposed

in the literature.¹⁷³ Despite this, there has not been sufficient scientific validation, nor a consensus, for a potential replacement of the Amsler-Krumeich classification system.¹⁵⁶

The clinically observable biomicroscopic signs discussed in Section 1.3.4.3 and displayed in Figure 1-5 may aid a clinician in assessing disease severity. Changes in these signs may also help the clinician to qualitatively monitor disease progression over time. Briefly, in forme fruste, or early keratoconus, frank clinical signs are often absent, and can be present bilaterally, or unilaterally in a patient with more clinically recognizable keratoconus in the fellow eye.^{94,99,149,150} In early keratoconus, or Stages 1-2 of the Amsler-Krumeich classification, there is significantly less epithelial and stromal scarring, as well as less breaks in Bowman's layer and Descemet's membrane folds.¹¹⁴ It is in these cases where identification of other potential signs which can be present in this stage, including irregular keratometry mires, the "Charleux oil droplet" sign on direct ophthalmoscopy, and a retinoscopic "scissor-like" reflex may be helpful to a clinician. In moderate to advanced keratoconus, clinically recognizable stromal thinning, conical protrusion, Fleischer's ring, Vogt's striae, and apical corneal scarring may be present,^{23,98,174} although Fleischer's ring may also be present in early cases.⁹⁸ In advanced cases, corneal hydrops may develop, and Munson's sign may also be present.^{23,98,99} This however is a general overview of the stage at which a clinician is more likely to note these clinical signs, and staging based on clinical signs alone is variable across individuals, due to its qualitative nature.

1.3.5.2 Monitoring for Disease Progression

For many years, the clinical progression of ectasia itself did not have a universally agreed upon definition.¹⁵⁶ A panel of experts, previously referred to in Section 1.3.4.5, recently established ectasia progression to embody at least two of the following characteristics:⁹⁵

- 1) Progressive steepening of the anterior corneal surface
- 2) Progressive steepening of the posterior corneal surface
- 3) Progressive thinning and/or an increase in the rate of corneal thickness change from the periphery to the thinnest point

Evidently, for monitoring an ectatic condition, as well as diagnosing it as previously discussed, information about the posterior corneal surface and total corneal thickness is paramount, as carried out in tomography.⁹⁵ Even so, in many studies, particularly clinical trials involving corneal collagen cross-linking surgery, progression is defined by a change in keratometric or refractive status,^{175,176} or this in conjunction with changes in visual acuity and topographic change in the cone area,¹⁷⁷ within a fixed time period. Topographic indices previously mentioned to detect and stage keratoconus may potentially aid in determining progression.¹⁷⁸ However, as stated, it is considered most prudent to have information about the anterior and posterior cornea, as outlined in the above criteria. In the literature, establishing progression using Scheimpflug imaging with the Oculus Pentacam® has been reported, where three parameters, which are corneal thickness at the thinnest point, and anterior and posterior radius of curvature, have been shown to be very strong determinants for progression.¹⁵⁶ This instrument's software also has an analysis feature referred to the "ABCD Progression Display", which factors these three parameters in conjunction with distance best-corrected visual acuity to assist a clinician on their judgement of whether progression has occurred or not.¹⁷⁹ Despite these multiple guidelines and methods, there has not yet been sufficient validation or standardization for any to be considered a clinical gold standard.⁹⁶ It should also be noted that these methods are instrument-dependent and are not interchangeable with one another to monitor progression in a single patient.^{179,180} Similar to staging, increased or the appearance of new clinical signs may hint towards progression, such as reduced best-corrected visual acuity, although this may not always represent true

change, or it may be unchanged when there is in fact, progression.⁹⁵ Analogous to staging, biomicroscopic changes may also provide insight, however this is also a coarse qualitative method, and therefore not established to determine progression.

1.3.5.3 Management Options

There is no cure for keratoconus, nor a treatment to reverse the disease in the host cornea. Surgical options do exist with the objective to slow the progression of the disease process or replace the cornea with that of donor tissue. It has been reported that in most cases, approximately 10-25%^{23,99,105,174,181-184} or up to 36%¹⁸⁵ of individuals with keratoconus eventually need a corneal transplant. In terms of visual rehabilitation, patients may be content with conventional spectacle or contact lens therapy in mild cases, however as the disease progresses, specialty contact lens correction is often required for optimal visual function.^{23,94,99,186} While these management options can improve visual outcomes for patients with keratoconus, none of them will reverse progression or cure the disease.

1.3.5.3.1 Non-Surgical Refractive Correction

1.3.5.3.1.1 Conventional Methods

Keratoconus may result in no discernible to only mild visual loss in a patient with forme fruste or mild forms of keratoconus.⁹⁹ In these cases, a patient may be content with best possible correction of regular astigmatism, either in the form of spectacles or soft contact lenses.^{23,183,186} Approximately 16% of individuals with keratoconus will use spectacles for correction,¹⁸⁷ however as the disease progresses, these patients may find that frequent updates to their prescriptions are required, and at a certain point, these methods may no longer provide acceptable visual correction to the patient, especially in cases of anisometropia and increasing irregular astigmatism and aberrations.⁹⁴ Conventional soft contact lenses may partially neutralize irregular

astigmatism, and may be an option for those who cannot tolerate rigid contact lenses.¹⁸⁸ Often, adjunctive spectacle correction is required with this to correct the remaining refractive astigmatism as much as possible.¹⁸⁹

1.3.5.3.1.2 Specialty Contact Lenses

The most optimal form of correction for eyes with keratoconus, particularly in the more moderate to advanced stages, are corneal gas-permeable (GP) contact lenses.^{23,183} By maintaining a rigid spherical surface at the anterior plane of the ocular refraction system, a great amount of irregular astigmatism and aberrations caused by the irregular anterior cornea can be neutralized via the tear film, having a refractive index close to the cornea, and the optically smooth lens surface.^{74,190} However, posterior corneal irregularities are unfortunately not accounted for, and visual performance, particularly contrast thresholds, may still be suboptimal despite improvements in measured visual acuity.¹⁴⁴ Corneal GP lens correction is generally the first method of specialty lens correction clinically employed in keratoconus, as these lenses can provide the patient with excellent vision, and are physiologically safe to wear when fit adequately.⁹⁹ Contrary to early thinking of fitting these lenses to intentionally bear on the apex of the cone, which induced and exacerbated apical scarring and other undesirable effects,⁶² or the apical clearance method where there is a risk of increased lens-to-cornea adhesion and seal-off in the periphery,¹⁹¹ these lenses should be fit with the 3-point touch philosophy.¹⁸⁶ This refers to having a very light amount of touch centrally, clearance in the paracentral area, light bearing in the midperiphery, and an adequate amount of peripheral clearance.^{23,191} This fitting method allows for even weight distribution across the cornea,¹⁸⁸ for the lens to move adequately to promote exchange of oxygen from the atmosphere and tears to the

cornea without inducing mechanical damage such that it is not bearing on the cornea. An example of a lens fit exhibiting the characteristics of a 3-point touch fit is displayed in Figure 1-7. Some practitioners recommend employing a balance between the 3-point touch and apical clearance methods while avoiding peripheral seal-off and lens adhesion, so that apical bearing and its ensuing complications are avoided.^{183,191}

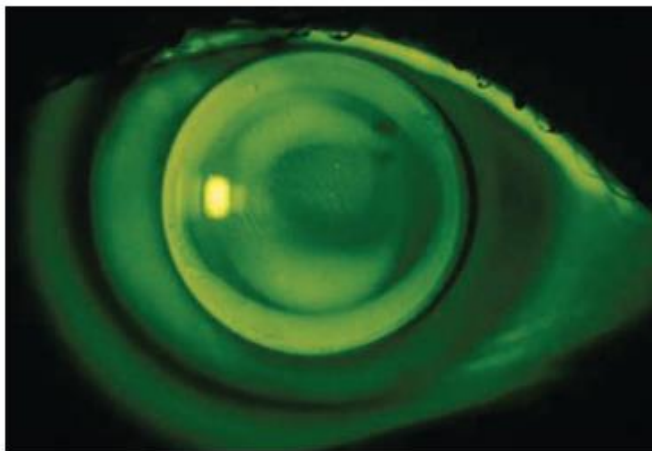


Figure 1-7: A lens-on fluorescein image of a corneal GP lens exhibiting the "3-point touch" fitting philosophy. Of note, there is a light touch centrally, clearance paracentrally, light midperipheral bearing, and an adequate amount of peripheral edge clearance. Republished with permission of [Wolters Kluwer Health, Inc], from [Clinical Manual of Contact Lenses, Bennett and Henry, 4th edition, Elsevier, 2015]; permission conveyed through Copyright Clearance Center, Inc.²³

In cases where there is discomfort or intolerance with GP lenses alone, but the optical correction of this lens is still desired, there are fitting methods available incorporating the comfort of a soft contact lens. The first option described is quite simply fitting a soft contact lens underneath the GP lens, referred to as a "piggyback" lens system, or "hard-soft combination lenses".^{23,94,183,188,192} Due to the fact that in this case, there are two obstacles to oxygen transmission to the cornea, it is important that both lenses

have a high oxygen transmissibility, and that the cornea is closely monitored for signs of hypoxia.¹⁹³ The role of the soft lens in this case is not to provide optical correction, as generally a low plus-powered lens is recommended, and thus its purpose is to provide increased comfort for the patient and protection of the cornea, so that the GP lens is not adjacent to the ocular surface but can still provide the patient with optimal optical correction. A similar idea to this is that of a hybrid contact lens. These lenses have a GP lens at their centre for optical correction but are surrounded by a soft lens material “skirt” in the periphery.⁹⁹ The idea behind these lenses is primarily increased comfort for the patient, by avoiding ocular surface contact with the edge of the rigid lens, having the main point of lens contact with the eye being the soft contact lens skirt. The fit of these lenses should be carefully monitored, so to avoid possible complications such as lens tightening months after an acceptable fit is achieved, and corneal edema.¹⁹⁴

Scleral lenses, another speciality lens option in keratoconus, were discussed in detail in Section 1.2, along with their indication in keratoconus and other ectatic disorders and complications.

Despite conventional soft lenses not playing a great role in refractive correction in keratoconus, there are specialty versions of soft lenses that are available and may work well for some patients.^{23,195} These lenses are custom lathe-cut for ectatic corneae and can come in both silicone hydrogel and hydrogel materials. Some have optics incorporated into the lens for aberration control as well. Often if required, individual curves can be modified depending on the fit of the lens. Typically, these lenses will perform better on eyes with centred cones, with topography that is

relatively symmetrical in the periphery, as it will tend to yield a more optimal fit in these eyes.

1.3.5.3.2 Surgical Options

The most invasive, and in earlier years most commonly implemented method of surgical management of keratoconus is a full-thickness corneal transplant.^{23,94,196} This is known as penetrating keratoplasty (PKP), and is often performed as a last-resort option in advanced stages of keratoconus.¹⁹⁷ In most cases, PKP is considered when contact lenses can no longer be properly fit or are no longer tolerated, or structural damage from disease progression, such as extensive scarring, is reducing visual acuity.^{99,182,187} This is the longest standing and still universally accepted surgical procedure for keratoconus, and is still performed today, due to its generally excellent outcomes and high success rates, many reports being in the range of 85.4-100%.^{23,94,99,184,196-198} However, due to the exposed nature of this surgery, complications include intraoperative infection and choroidal hemorrhages. Postoperatively, endothelial cell loss as well as graft rejection are likely to occur in the years following surgery and may also occur soon after surgery in rare cases. After surgery is performed, the individual is monitored closely for signs of graft rejection and are placed on long-term topical steroids to reduce the likelihood of this.¹⁹⁹ Due to the nature of the graft suturing, it is common for the individual to have postoperative astigmatism, which still will often require specialty contact lens, or in some cases spectacle correction.

With the risk of possible complications with PKP, advances in technology and medicine have permitted for the development of modified versions of this procedure, for example, deep anterior lamellar keratoplasty (DALK). DALK involves the excision of all corneal layers excepting Descemet's membrane and the corneal endothelium in the host cornea,^{23,196,198,199} commonly performed via the Anwar "big bubble" technique, where air is used to enable this separation.²⁰⁰ This procedure is being done more frequently, as there is a lower risk of graft rejection often encountered

in a full thickness transplant (PKP), as the host maintains their own endothelial cells,²⁰¹ and has a lower risk of intraoperative complications compared to PKP, due to the closed nature of DALK. Some have found graft longevity to be better for PKP than for DALK,¹⁹⁹ however there is significantly less long-term endothelial cell loss in DALK compared to PKP.¹⁹⁶ DALK presents its own set of complications, including perforations in Descemet's membrane,²⁰¹ as well as reduced visual acuity in some cases,¹⁹⁹ which may be due to losses of transparency inducing light scattering where the host meets the donor tissue.¹⁹⁸ Other studies have noted visual acuity and other measures of visual function to be comparable between groups who had PKP and DALK.^{196,198} Prior DALK is not a contraindication for PKP, meaning subsequent PKP can still be done in eyes where DALK has not been successful.

In more recent years, other surgical management options for earlier stages of the disease which may be considered before a patient requires the need for a corneal transplant, have emerged. These techniques, such as intrastromal corneal ring segment implantation and corneal collagen cross-linking, involve altering the corneal shape and attempting to slow the progression of disease.²³ Briefly, intrastromal corneal ring segments are composed of PMMA material, and are inserted into the corneal stroma using a tunnelling method either mechanically^{202,203} or now more commonly, via femtosecond laser, which is thought to reduce postsurgical complications including improper relocation and extrusion of segments, and corneal melting.²⁰⁴ Ideally, this surgery is performed in mild-moderate stages of keratoconus.^{203,205} The primary aim of this surgery includes manipulating the irregular conically shaped tissue into a more regular profile for refractive purposes in order to improve visual outcomes, which was why it was originally developed for correction of myopia. There is also suggestion that intracorneal ring segments may slow the progression of keratoconus, due to the reallocation of corneal strain on collagen lamellae through the change in corneal shape.

Corneal collagen cross-linking (CXL), one of the more novel surgical management options for keratoconus, is a procedure that promotes additional cross-links, or attachments, between collagen lamellae of the cornea, to increase resiliency.^{23,206-211} The goal of CXL is to slow the progression of corneal ectasia, through the increased biomechanical strength provided by additional molecular cross-links within the tissue, stabilizing the cornea.^{212,213} Secondary outcomes which have been noted include improvement of visual acuity and function, diminishing of refractive error, as well as flattening of corneal shape in areas of steep curvature. There are two forms of this procedure, “epithelium-off” and “epithelium-on”, the former being more commonly performed to promote maximal riboflavin permeation, in particular following The Dresden Protocol.²⁰⁷

The procedure is generally performed in the following manner: once the cornea has been anaesthetized, the central epithelium is removed, commonly with a scalpel, rotating brush, or alcohol solution.^{23,206-213} Following this, the corneal stroma is saturated with riboflavin solution, serving as a photosensitizer for the chemical reaction of collagen cross-linking. Then, the tissue is irradiated with ultraviolet-A light, which induces the formation of cross-links between collagen fibrils, specifically, reactive oxygen species are produced by riboflavin upon irradiation, and covalent chemical bonds are formed at multiple chemical levels involving both collagen and proteoglycans. Healing involves the regeneration of the corneal epithelium, typically under the protection of a bandage contact lens, placed after surgery. Topical antibiotics and corticosteroids are also commonly instilled and prescribed, to protect against infection due to the loss of the normally protective epithelial barrier.

Various contraindications have been presented in the literature and are clinically employed. The most consistent of these refers to the candidate’s total corneal thickness, which should not be less than 400 μm ,^{23,207,211-213} not inclusive of the corneal epithelium.^{209,210} Due to the possibility of reactivation of ocular herpes simplex infection, clinicians may consider previous ocular herpes simplex a contraindication, or prescribe oral antivirals prophylactically prior to surgery. Other suggested

contraindications include severe ocular surface disease, history of incisional refractive surgery, pregnancy/nursing, and systemic collagen vascular disorders. CXL has become widely considered to be the standard of care especially where progression has been clinically noted,²¹⁰ and in cases where progression is likely, particularly in young patients, and where other corneal surgeries have been done.⁹⁵ It however should be noted that a relatively recent Cochrane review performed in 2015 deemed the quality of evidence for CXL in the treatment of keratoconus to be insufficient, primarily due to inadequate study design.²¹⁴ However, ongoing clinical trials are being widely conducted to establish high quality evidence for this management option in keratoconus.¹⁷⁶

1.3.6 Biomechanics and Corneal Edema

Without question, the keratoconic cornea is mechanically weaker than the normal cornea, particularly over the cone area.^{94,99,124,215} Quantification of the cornea's biomechanical strength can be achieved through measurement of both corneal hysteresis (CH) and defining the corneal resistance factor (CRF). Specifically, hysteresis can be measured by determining the difference between two pressures, firstly, the amount of pressure required to applanate the cornea, and the pressure exhibited by the cornea during its recovery at a fixed time after the first pulse.^{216,217} This process described is the way in which the Ocular Response Analyzer (ORA) (Reichert, Inc., Buffalo, NY) measures corneal hysteresis in a clinical manner. Also measured by this instrument, CRF is a proprietary parameter calculated which is said to reflect the elasticity of the cornea. Studies done measuring these parameters have shown that in eyes with keratoconus, the CH²¹⁶ and CRF are decreased compared to eyes without keratoconus.^{96,215,218,219}

The orientation of collagen fibrils in the keratoconic cornea is of a more random organization, compared to the normal cornea,^{124,220} and fewer cross-links are present between fibrils.^{219,221} This phenomenon, in conjunction with pathological modifications to the extracellular matrix and a decline in corneal volume yield a denser, thinner and less resilient corneal stroma.^{124,219,222} This is theorized to

biomechanically result in a lower Young's modulus, or an "increased ease of extensibility".²¹⁹ It has been suggested that in both the normal and keratoconic cornea, the most resilient part of this tissue is anterior, as it is "locked" at the epithelium, relative to its more posterior counterparts.^{30,34,223} When corneal edema induced by hypoxia with soft contact lens wear was directly compared between eyes with and without keratoconus, an observation of greater change in anterior corneal curvature in keratoconic eyes compared to those without suggests that the anterior cornea is not as robust and thus more affected by corneal edema in this disease population.³⁷ This same study noted a lesser absolute degree of corneal swelling centrally in those with keratoconus compared to those without, but a similar amount in the midperipheral and peripheral regions. This configuration of edema was paralleled by Weissman in 1994, where frank corneal edema, induced by a PMMA scleral contact lens, was found to exhibit a "ring-shaped" pattern, observed with biomicroscopy.²²⁴ This finding was said to be "atypical" as it was not observed with scleral lens wear in eyes without keratoconus, yet this area of greatest swelling did seem to coincide with the thickest region of the contact lens, where oxygen delivery would be diminished.

As previously mentioned, in keratoconus, the cornea may exhibit scarring as the disease progresses, or the cornea may be treated with CXL, both of which have aims to increase the strength of the cornea. It is known that in regions of corneal apical scarring, the degree of nonorthogonal spatial disorganization of collagen fibrils is greater than for other areas of the cornea,²²⁰ compromising its tensile and mechanical strength.^{225,226} To the best of my current knowledge, *in-vivo* measurement of CH and CRF in scarred eyes with keratoconus has not been reported on. Post CXL, studies have reported that there was not a significant change in hysteresis or CRF one-year post surgery,²²⁷⁻²³⁰ however an increase in these parameters was noted initially after the procedure, indicating initial post-surgical increased mechanical strength. It is possible that corneal strength is not increased long-term after this procedure, or these methods of measurements are possibly not the most sensitive measure of this

parameter, as initial change from pre- to immediately post-surgery was often measured to be around 1 unit.^{219,229,230} Theoretically, if an injurious process, such as scarring, decreases the strength of the cornea, this should result in a greater degree of edema in response to hypoxia, which may be seen regionally, where the process occurs. The opposite would be true in the case of increased corneal strength, which has been theoretically but not experimentally established with CXL.

When addressing the physiological effects of scleral lens wear on the keratoconic cornea, it is crucial to be mindful all aspects which may influence corneal behaviour, including its unique biomechanics due to pathology, or previous surgery.

Chapter 2

Study Rationale

2.1 Study Background

Scleral lenses have made a relatively recent resurgence in the last two decades, particularly in the refractive correction for individuals with keratoconus.^{23,55} It has been long established that scleral lens wear will induce corneal edema, especially when lenses of lower oxygen permeabilities are used, and when lens centre thicknesses are increased considerably, especially in lower-Dk materials as opposed to high-Dk materials.^{11,60,231,232} Modern scleral lens materials have much higher oxygen permeabilities than those that classically induced corneal edema due to hypoxia,^{25,55,233,234} however, the risk of hypoxia still remains.⁶¹ Rather than having the only barrier to atmospheric oxygen being an approximately 3µm-thick tear film,^{235,236} the ocular surface is separated from its typical open-eye environment by an, on average, 50-400 µm-thick fluid reservoir (Dk = 80²²⁴), and a conventional scleral lens with a central thickness between 250-350 µm (Dk 100-200).⁶¹

In 2012, Michaud et al.⁶¹ published a theoretical paper predicting the oxygen delivery to the ocular surface through a typical scleral lens environment. These calculations were based on the assumption that the lens and fluid reservoir can be treated as “resistors in series”, as suggested by Fatt,²³⁷ and later, Weissman.¹⁹³ This resulted in the modification of the original Fatt equation to calculate total Dk/t of a scleral lens system:⁶¹

$$\frac{Dk}{t_{SL}} = \frac{1}{\left(\frac{t_1}{Dk_1}\right) + \left(\frac{t_2}{Dk_2}\right)} = \frac{1}{\left(\frac{t_{SL}}{Dk_{SL}}\right) + \left(\frac{t_{FR}}{Dk_{FR}}\right)}$$

Figure 2-1: Fatt equation modified to consider each barrier to oxygen independently, the scleral lens (SL) and fluid reservoir (FR), where t=thickness, and Dk=the oxygen permeability of these entities. Equation is from Michaud,⁶¹ modified from Fatt²³⁷ and Weissman,¹⁹³ with added subscripts specific to this study.

Different combinations of central corneal clearances, lens permeabilities, and lens thicknesses were considered in these calculations.⁶¹ From these calculations, the authors' recommendation in order to reduce corneal edema due to hypoxia was to use a scleral lens whose central thickness did not exceed 250 microns, composed of a material with the highest Dk possible (>150), with a central clearance no greater than 200 microns. These calculations assumed that a Dk/t of less than 24 units centrally, and 35 units peripherally would induce corneal edema secondary to hypoxia, according to prior thresholds established in the literature.^{18,21} Further theoretical models have been published since, many recommending similar clinical guidelines specifically,⁷⁷ and more generally,^{238,239} whereas other model recommendation has emphasized minimizing overall Dk/t rather than advising on specific central clearances.⁸⁰

Since Michaud et al., 2012,⁶¹ many researchers have clinically investigated this question as well, primarily in eyes without ocular pathology. There has been a mixed consensus on whether scleral lens wear alone will⁷⁷⁻⁸⁴ or will not²⁴⁰ result in statistically significant corneal edema due to hypoxia, however more evidence indicates that edema does occur than the contrary. More recent studies have been done on the hypoxic effects of varying post lens fluid reservoir, or corneal clearance, in short-term scleral lens wear of higher Dk materials on the corneae of healthy individuals,^{77,79-81,85,240,241} for which there is also no unanimous agreement. In all of the above studies, levels of edema measured have not been clinically significant,^{51,77-80,83-85,240} meaning, they have not exceeded the 4-4.5% swelling that has been reported to occur overnight,^{27,242} with the exception of one study, where measured edema was 5.1%.⁸² Other studies have investigated how the modification of scleral lens permeability influences corneal edema due to hypoxia, and it seems to be most likely that, for high Dk materials, oxygen delivery is more dependent on the oxygen transmissibility of the fluid reservoir, rather than the transmissibility of the lens itself.^{84,232,239} Further, oxygen tension at the ocular surface has been directly measured to be less in the instance of increased central corneal clearance.²⁴¹ It is

likely that there is a critical post lens tear film thickness at which one would expect to observe a greater degree of corneal edema secondary to hypoxia, but a single value or range has not been definitively determined.

2.2 Study Motivation

Aforementioned studies have investigated the effect of both scleral lens wear and central corneal clearance on corneal edema, however they have all been carried out in eyes without ocular pathology, and for a short-term wear time (typically 3, 5, or 8 hours of wear on one day).^{77-85,240} There is a lack of literature on the hypoxic effects of scleral lens wear and central clearance over a longer term of wear, as well as in with keratoconus or other corneal ectasia. Additionally, most of these studies have investigated only central corneal pachymetry,^{77,79-82,240} rather than paracentral changes in corneal thickness. Further detail on how the peripheral cornea remote from the centre responds to hypoxia in a healthy cornea with scleral lens wear in addition to studies published^{78,83-85} would be valuable to further establish how the entire cornea behaves in this environment.

To the best of current knowledge, only four studies have been done investigating scleral lens wear in eyes with keratoconus, most failing to satisfy all of the above criteria²⁴³⁻²⁴⁵ with the exception of one study, where limbal clearance was varied, rather than central corneal clearance.²⁴⁶ Only one of these studies has examined varying central clearance in a controlled manner in this population.²⁴⁴ From these few studies, there is no agreement on whether scleral lens wear induces an edematous effect in the short²⁴⁴ or long term,^{243,246} or a thinning effect, particularly in the diseased region of the cornea,²⁴⁵ in eyes with keratoconus. In addition to this, the pathological region of keratoconus might be remote from the central cornea,^{95,99,142,143} and so investigation into the effects of scleral lenses on the paracentral cornea is of interest, which has only been carried out in two studies thus far and with no unanimous defined conclusions.^{245,246}

This need for further investigation into the optimal level of central clearance in scleral lens wear for this population is significant, as scleral lenses are considered to be principally indicated for use in individuals with keratoconus and other corneal ectasias compared to individuals without this disease,⁵⁵ and studies performed on eyes without pathology cannot be generalized for this population, as corneal biomechanical properties differ between these two groups.^{96,245}

The proposed study will investigate varying central corneal clearance of scleral lenses over a longer term of wear in eyes with keratoconus to provide insight into an optimal amount of clearance for reducing clinically significant corneal edema, centrally and paracentrally. This will contribute to the quantification of a limit of central corneal clearance with scleral lenses in optometric clinical research, which will provide practitioners with further insight into the effect of their potential clinical decisions when fitting scleral lenses.

2.3 Study Hypotheses

In eyes without ocular pathology, scleral contact lens wear is associated with low levels of corneal hypoxia manifesting as an increase in total corneal thickness due to edema, due to the presence of the lens and fluid reservoir. These findings may be extrapolated with caution to mild cases of keratoconus but may not hold in moderate to advanced cases of keratoconus.

Eyes with keratoconus exhibit distinct biomechanical properties due to pathological structural alterations, as well as a generally thinner cornea. Due to decreased resiliency, and a theorized “increased ease of extensibility”,²¹⁹ edema may be expected in keratoconic eyes, particularly in the diseased area. However, in cases of previous corneal collagen crosslinking, levels of edema may be lessened due to increased compensatory strength, if this has occurred long-term. It is hypothesized that scleral lens wear alone, as well as a relatively higher central clearance will induce hypoxia and thus possibly relatively more pronounced total corneal edema will be noted after lens wear when

compared to a lower clearance, and when compared to baseline pachymetry in eyes with keratoconus. However, the degree of edema may be more pronounced in the diseased area with or without scarring due to stromal fibril disorganization, and less pronounced or equal than others in cases of previous cross-linking surgery, due to possible, but not definitively determined, increased biomechanical strength.

On the contrary, the degree of corneal edema might be highly unpredictable in keratoconus, since it might lack regular distribution and might affect to a lesser degree the areas most affected by keratoconic changes. These areas characteristically have highly compact architecture¹²⁴ and would be less prone to swelling in comparison to the less affected more peripheral areas with more regular, thicker, and looser stroma, which would be more susceptible to swelling. It is reasonable to also expect that the hypoxia-induced changes, due to the reducing gradient of architectural abnormalities from centre to periphery, would be more pronounced in the more peripheral areas.

Corneal edema due to scleral lens wear is suggested to be primarily due to stromal rather than epithelial swelling when studied in healthy eyes,^{83,84} as this has not been studied in this population and so it is hypothesized that epithelial edema will occur, however it may not be statistically significant.

2.4 Study Purpose and Objectives

With the increasing use of scleral lenses by eyecare practitioners, particularly for patients with keratoconus and other ectasias, there is a need to gain more knowledge about the longer-term physiological effects of these lenses in this population. The purpose of this study is to investigate hypoxic effects of varying central clearance in scleral lens wear, as well as scleral lens wear alone in eyes with keratoconus. For each participant, two scleral lens designs of differing central clearances

will be worn for three weeks to reveal differences in corneal edema as an objective physiological marker of hypoxia.

The primary objective of this study will be to detect the presence of corneal edema in scleral lens wear, a surrogate quantification of hypoxia, measured by the Spectralis® OCT and Oculus Pentacam® HR, and changes in this parameter for lenses of different central clearances in eyes with keratoconus. In addition to this, individual patterns of corneal swelling and how they relate to individual characteristics such as cone apex location, disease stage, and history of CXL, will be explored. Additional parameters relating to scleral lens fit, including ocular health, subjective comfort, and high and low contrast visual acuity, will also be reported on. In fulfilment of these objectives, the overarching aim of this study is to contribute to the knowledge base of optometry and vision science to assist clinicians in the determination of an optimal quantitative range in central clearance to minimize corneal edema secondary to hypoxia in scleral lens wear in an at-risk population. This study will also provide greater insight into how individuals in this disease population respond to scleral lens wear, and how this may relate to their own characteristics, as well as the fit of the scleral lens.

Chapter 3

Methods and Study Design

3.1 Scleral Lens Fitting Terms

The anatomy of a scleral lens was previously introduced. For further description of scleral lens fitting, additional terminology must be defined. The nature of a scleral lens fit involves the lens vaulting the cornea over a fluid reservoir.⁵² The amount of apical or central clearance is influenced by lens settling, introduced in Chapter 1, which may range from approximately 63 to 200 μm over an 8-hour period of lens wear.^{52,64,66,244} Central clearance is also dependent on the relationship between the ocular surface sagittal height and the sagittal depth of the lens.

A measurement of the ocular surface sagittal height at a particular chord length can be taken by drawing the chord on a cross-sectional image of the anterior segment, and then at the midpoint of the chord, placing a perpendicular line from the chord to the anterior boundary of the ocular surface. The length of this line will be the sagittal height of the ocular surface at that specific chord length. Similarly, for a scleral lens, the sagittal depth (SD) is the perpendicular distance from the midpoint of the chord length equal to the overall diameter of the lens, to the apex of the lens. Both the ocular sagittal height and the sagittal depth of a scleral lens is modelled below diagrammatically in Figure 3-1.

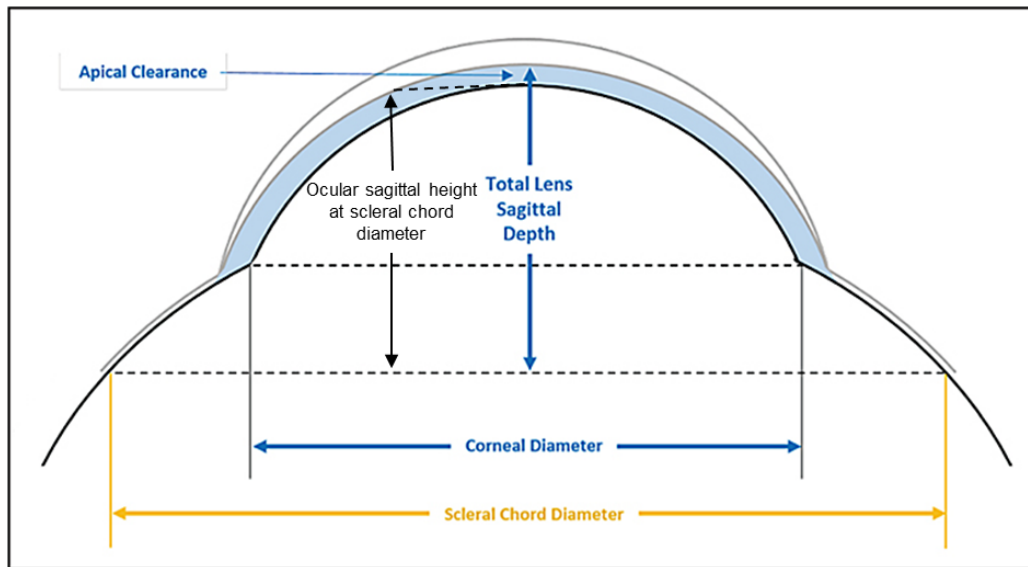


Figure 3-1: Ocular sagittal height, how it relates to scleral lens sagittal depth, and how both relate to the apical, or central, clearance. Modified from Hall, 2015²⁴⁷, with permission.

Another parameter to be defined is the limbal clearance of a scleral lens. This refers to the amount of clearance between the lens and the cornea at the transition, or limbal zone (see Figure 1-3B). It is possible to increase and decrease this amount from standard lens parameters to achieve optimal limbal clearance. To protect limbal stem cell health, both limbal bearing and excessive limbal clearance should be avoided.⁵² The ideal level of limbal clearance varies in the literature, but in general may range from 50-100 μm .^{52,248}

It is known that the sclera is anatomically asymmetric across quadrants, and that scleral shape varies across individuals,²⁴⁹ particularly between those with and without keratoconus.^{250,251} For this reason, when fitting scleral lenses, one can customize the curvature of the peripheral landing zone (see Figure 1-3C), where the lens contacts the sclera. Relative to the standard peripheral curve of the lens being fit, the practitioner may wish to flatten or steepen these curves to obtain an optimal lens-to-sclera relationship, where compression, or conversely, edge lift will be avoided, respectively.

Horizontal and vertical curves can be modified, and in many cases, quadrant-specific designs of

peripheral curves are possible. For the Zenlens™, which was fit in this study, this parameter is referred to as the advanced peripheral system (APS).

3.2 Methods and Materials

3.2.1 Participant Recruitment

3.2.1.1 Informed Consent

Participant recruitment primarily took place through the contact of eligible patients with keratoconus who received eye care at the University of Waterloo School of Optometry and Vision Science (UWSOVS) Contact Lens Clinic. These individuals had given consent to be contacted for research purposes and were reached by the study investigator through telephone or e-mail, or in-person.

Advertisements for the study were also posted in the clinic with contact information included for recruitment. After the participant read the Information and Consent letter, the investigator discussed the project and answered participant's questions regarding the study procedures and any potential risks associated with the study. Informed consent was then given by the participant prior to the study. Recruitment protocols were carried out in accordance with the tenets of the Declaration of Helsinki and were approved by the Office of Research Ethics (ORE #31201) at the University of Waterloo.

3.2.1.2 Inclusion and Exclusion Criteria

To be eligible for this study, participants must have been diagnosed with keratoconus in at least one eye and had to have been at least 18 years of age with full legal capacity to volunteer, at the time of the study commencement. Participants were excluded if they were using any topical medications affecting ocular health and had any ocular pathology or severe insufficiency of lacrimal secretion (severe dry eyes) that would affect the wearing of contact lenses. Additionally, patients with any of the following conditions were also excluded from the study: known allergy or sensitivity to diagnostic pharmaceuticals or products used in the study, any persistent, clinically significant corneal or

conjunctival staining using sodium fluorescein dye, any clinically significant lid or conjunctival abnormalities and any active neovascularization. Participants who had undergone previous penetrating keratoplasty, or who were participating in any other type of eye related clinical or research study were also excluded. Participants were screened for their eligibility to ensure that they met all inclusion criteria, and that none of the exclusion criteria applied to them.

3.2.1.3 COVID-19 Pandemic and Study Impact

It should be noted that recruitment and the resultant number of participants who completed this study was greatly affected by the coronavirus disease (COVID-19) pandemic. The spread of this novel strain of the coronavirus shut down all in-person activity in Southwestern Ontario in March of 2020, and as of 20 March 2020, all in-person research activity at the University of Waterloo School of Optometry and Vision Science ceased. At that point in time, eight participants had completed this study. Due to the uncertainty of the future effects of the pandemic on research activity, and to the benefit and safety of everybody involved, it was determined that this thesis project had already gathered sufficient data and would be completed based on the data already collected. The time frames and participant numbers of the study were adjusted to reflect the changed circumstances and the in-person study visits were discontinued earlier than originally planned.

3.2.2 Study Materials

3.2.2.1 Zenlens™ Scleral Lens

The Zenlens™, manufactured by Alden Optical (Lancaster, NY, USA) is a commercially available, Health Canada-approved (license #96602) scleral lens, indicated for both a range of ocular surface shapes as well as ocular surface disease.²⁵² This lens is available in Boston XO® (Dk=100), the material used for this study, and Boston XO₂® (Dk=141).²⁵² Lenses with diameters of 16.0 and 17.0 mm and any sagittal depth between 3200 and 6700 in 10 µm steps can be ordered and custom

made.²⁵² The lens profile is available in both a prolate (used for this study) and oblate shape.²⁵² A quadrant-specific, toric advanced peripheral system (APS) allows customization of the peripheral curves to optimally match the ocular scleral shape.²⁵² Additionally, central sagittal depth can be modified without consequential alteration of other lens parameters due to the *Smart Curve*TM technology, which strongly influenced the decision to select this lens for use in this study.²⁵²

3.2.2.2 Scheimpflug Anterior Segment Tomography: Oculus Pentacam® HR

The optical principles of Scheimpflug imaging with the Oculus Pentacam® HR (OCULUS, Wetzlar, Germany) were briefly detailed in Chapter 1, section 1.3.4.5 (see Figure 3-2). Using rotating Scheimpflug photography, the Pentacam® HR automatically and non-invasively takes rotational cross-sectional images of the cornea with a visible blue LED light source (475 nm, UV-free), from which information such as elevation, curvature, and pachymetric measurements can be extracted.¹⁵⁷⁻

¹⁵⁹ This instrument is capable of taking 100 images, generated from up to 25,000 elevation points, and 138,000 data points, in 2 seconds.¹⁵⁷⁻¹⁵⁹ This elevation data (relative to a best-fit sphere) is assembled into a 3D model of the anterior segment, which is used to indirectly determine other parameters such as corneal thickness and curvature.¹⁵⁸ For example, corneal thickness is determined via the subtraction of the posterior surface from anterior surface elevation measurements. Two cameras are used, one rotating Scheimpflug camera to acquire anterior segment elevation data, and the other, a stationary camera, to measure pupil size and identify any eye movement, which is automatically corrected for by the software.^{157,158}

In conjunction with its standard software, the Pentacam® HR has an additional module – the Cornea Scleral Profile (CSP) Report. This software automatically and non-invasively takes 50 radial images of the anterior segment in 5 different zones.²⁵³ These zones are the central, nasal, temporal, superior and inferior cornea, all while the individual being imaged maintains a straight-forward gaze.²⁵³ Once these scans are carried out, all 250 images (50 images in each of the 5 zones) are integrated into a

composite representative corneoscleral profile of up to 18mm in diameter.²⁵³ Parameters acquired include those obtained for a central corneal Pentacam® scan (just described), and in particular for scleral lens fitting, a corneal horizontal white-to-white (HWTW) measurement, in addition to parameters unique to the CSP software including bulbar slope angle measurements and sagittal height at the flat and steep meridians for a given “Ring Diameter”, or sagittal height which can be customized by the user.²⁵³

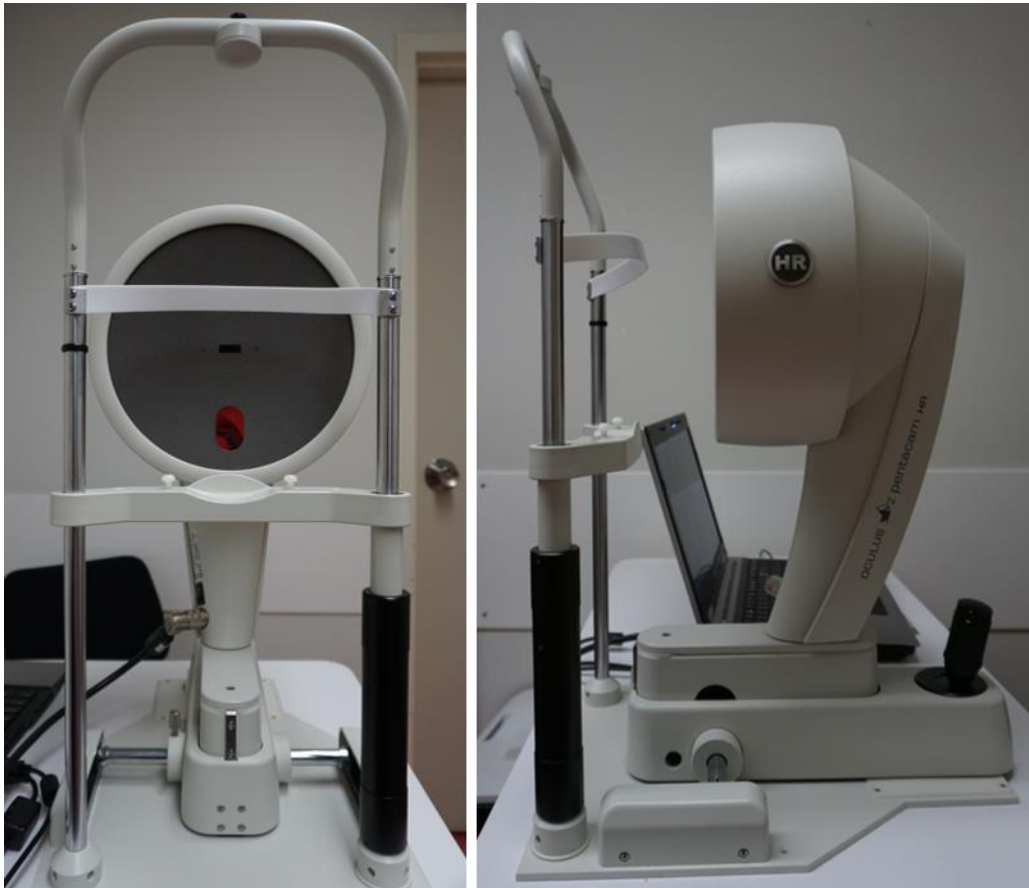


Figure 3-2: Oculus Pentacam® HR anterior segment tomographer used for this study.

3.2.2.3 Anterior Segment Optical Coherence Tomography: Spectralis® and Visante™ OCT

Like Scheimpflug imaging, optical coherence tomography (OCT) is a method of anterior segment imaging where the anterior and posterior surfaces of the ocular surface are detected, however, it uses a different optical principle. In brief, OCT is an ophthalmic clinical application of the Michaelson interferometer, in particular, low-coherence interferometry.^{160,254} In very general terms, an infrared laser light source is divided into two paths, one in the “reference arm”, where a mirror at the end of the path reflects the signal back to the detector, and the other in the “sample arm” which is sent towards the tissue being imaged, and transmitted through and reflected back in a way that is unique to that tissue.^{160,254} Both reflections are merged, and detected by a device, such as a camera or photodiode.¹⁶⁰ This information, representative of a small area of the tissue, is then used to generate a one-dimensional A-scan, which, together with other A-scans at adjacent locations in a single plane will comprise a singular two-dimensional B-scan.^{160,254} Similarly, multiple B-scans, or cross-sectional scans in the same plane at adjacent locations can be assembled to represent a three-dimensional volumetric representation of the tissue being imaged. The first published use of OCT in 1991 involved visualizing the posterior segment of the eye,¹⁶⁰ but not long after, in 1994, it was further developed to be capable of imaging the anterior segment as well.²⁵⁵

In this study, two clinical OCT instruments were used, the Spectralis® OCT with its Anterior Segment Module (Heidelberg Engineering, Heidelberg, Germany), displayed in Figure 3-3, and the Visante™ OCT (Carl Zeiss Meditec, Dublin, CA), in Figure 3-4. The Spectralis® uses a spectral-domain OCT system, where the Visante™ OCT uses a time-domain design, to acquire cross-sectional images of the anterior segment.



Figure 3-3: Spectralis® OCT at UWSOVS with the anterior segment objective lens (left) and a demonstration of the use of the anterior segment imaging module to acquire an image (right).



Figure 3-4: The Visante™ OCT instrument at UWSOVS.

Both instruments have the capability of imaging the cornea, sclera, anterior chamber angles, and iris. Light sources for both instruments are super-luminescent light emitting diodes, with an average wavelength of 870 nm in the Spectralis® OCT and 1310 nm for the Visante™ OCT. The Spectralis® has a respective axial and lateral resolution of 7 x 30 μm optically and 3.9 x 11 μm digitally in the imaging mode that was used for this study, and a maximum scan rate of 40 000 A-scans per

second.¹⁶¹ The resolution of the Visante™ OCT is 18 μm axially and 60 μm in the transverse plane.²⁵⁶ The maximum imaging dimensions that each instrument is capable of are up to 1.9mm deep in tissue and 16mm wide for the Spectralis®, and up to 6mm deep and 16mm wide for the Visante™.^{161,256} For both instruments, different imaging settings, such as high resolution modes and different scan dimensions are possible for the user to employ. The Visante™ OCT software can generate a “Global Pachymetry Map” where corneal thickness measurements are generated and displayed from multiple acquired B-scans, whereas automatic corneal thickness measurements are not available with the Spectralis® OCT software, Heidelberg Eye Explorer (HEYEX). In both the Visante™ and Spectralis® (HEYEX) software, it is possible to measure ocular structures manually with built-in caliper and angle tools.^{161,254}

3.2.2.4 Anterior Segment Imaging: Oculus Keratograph® 5M

The Oculus Keratograph® 5M, or K5® (OCULUS, Wetzlar, Germany) is primarily a corneal topographer which uses Placido-disk imaging, which was previously detailed in Chapter 1, section 1.3.4.5. Along with keratometry measurements, this instrument is also capable of additional external imaging of the ocular surface via its built-in digital CCD camera, which are useful parameters for contact lens fitting as well as ocular health and dry eye assessments.²⁵⁷



Figure 3-5: The Oculus K5® topographer at UWSOVS.

For this study, additional features of the K5® including the R-Scan to objectively grade bulbar and limbal hyperemia, as well as fluorescein imaging to document corneal staining were used.²⁵⁷

Specifically, for the R-Scan, the ocular surface is evenly illuminated with Placido rings, and an enface image of the ocular surface is taken with the camera. Then, the software calculates the ratio between the percentage area of blood vessels, relative to the rest of the region analyzed to produce a score from 0.0 to 4.0 (as the maximum ratio is 40%).²⁵⁸ This scale is referred to as the JENVIS scale,²⁵⁷ which has been clinically validated.²⁵⁹ Fluorescein imaging with the K5® involves the use of a blue light emitting diode to illuminate the ocular surface, specifically with a wavelength of 465 nm.²⁵⁷ The built-in camera then takes an image of the ocular surface, and with the aid of yellow filters in the observation beam path, a simulated fluorescein-image is generated.²⁵⁷

3.2.3 Study Procedure

Data gathered in this study included total corneal thickness (Pentacam® HR, Visante™ OCT, Spectralis® OCT), epithelial corneal thickness (Spectralis® OCT), ocular health parameters (biomicroscopic examination with fluorescein staining, K5® R-Scan), high and low contrast Snellen distance visual acuity, and subjective measures of visual clarity, comfort, and dryness with lens wear (Ocular Symptom Questionnaire with responses based on an interval scale, see Appendix A).

There were 5 anticipated study visits, the first being a screening visit (Visit 0-0) that also included a contact lens fitting assessment for the eligible participants. Prior to the first baseline and delivery visit (Visit 1-1) for the first pair of scleral lenses, a minimum wash-out period of no habitual lens wear of 48 hours was carried out, if possible, for the participant. At that visit (Visit 1-1), baseline ocular parameters were measured, and the first pair of lenses were delivered to the participant. If the comfort, fit, and vision were acceptable, the participant was given the lenses to wear for 3 weeks \pm 3 days for 6-12 hours/day, 5-7 days/week (minimum-maximum range). If the comfort, fit, and vision were not acceptable, lenses were re-ordered accordingly, and a second delivery visit was carried out (Visit 1-1 x 2). After three weeks of lens wear, a follow-up visit took place (Visit 1-2), where the same parameters were measured, and comfort, lens fit, and vision were again assessed. The baseline delivery and follow-up visits were repeated for the second pair of lenses after a minimum 48-hour wash-out period (Visits 2-1 and 2-2, respectively). Please see below for a detailed outline of the scheduled collection of outcome variable data at each visit:

1) Screening/Fitting Visit (0-0)

- a. Screening for inclusion/exclusion criteria (Information and Consent Letter)
- b. Anterior segment imaging to assist in determining optimal initial diagnostic scleral lens (Pentacam® HR CSP 5 x 50)
- c. Screening for inclusion/exclusion criteria (biomicroscopy)

- d. Baseline keratometry/auto-refraction with ARK-1s (NIDEK CO., Gamagori, Aichi, Japan)
- e. Trialling scleral lenses on eye using diagnostic set, allow lens settling for 20 minutes
- f. Assess lens fit (biomicroscopy, Spectralis®) and over-refraction

LENSES ARE ORDERED, 48 HOUR WASH-OUT

2) Delivery Visit 1 (1-1)

- a. Participant arrives wearing no lenses, parameters measured include:
 - i. Habitual ocular comfort (Subjective Questionnaire)
 - ii. Corneal thickness (Spectralis®, Pentacam® HR (25 picture/1 second), Visante™ Global Pachymetry Map)
 - iii. Conjunctival and limbal redness and corneal fluorescein staining (K5®, biomicroscopy)
- b. Study lenses are inserted, parameters measured include:
 - i. HC/LCVA (Snellen notation)
 - ii. Ocular comfort with study lenses (Subjective Questionnaire)

LENSES ARE WORN x 3 WEEKS

3) Follow-up Visit 1 (1-2)

- a. Arrive wearing study lenses, parameters measured include:
 - i. Ocular comfort with study lenses (Subjective Questionnaire)
 - ii. HC/LCVA (Snellen notation)
 - iii. Conjunctival and limbal redness (K5®)
- b. Study lenses are removed, parameters measured include:
 - i. Corneal thickness (Spectralis®, Pentacam® HR, Visante™)
 - ii. Corneal fluorescein staining (biomicroscopy)

LENSES ARE ORDERED, 48 HOUR WASH-OUT

4) Delivery Visit 2 (2-1)

- a. See Delivery Visit 1

LENSES ARE WORN x 3 WEEKS

5) Follow-up Visit 2 (2-2)

- a. See Follow-up Visit 1

Figure 3-6 illustrates the order of study visits in a flow chart.

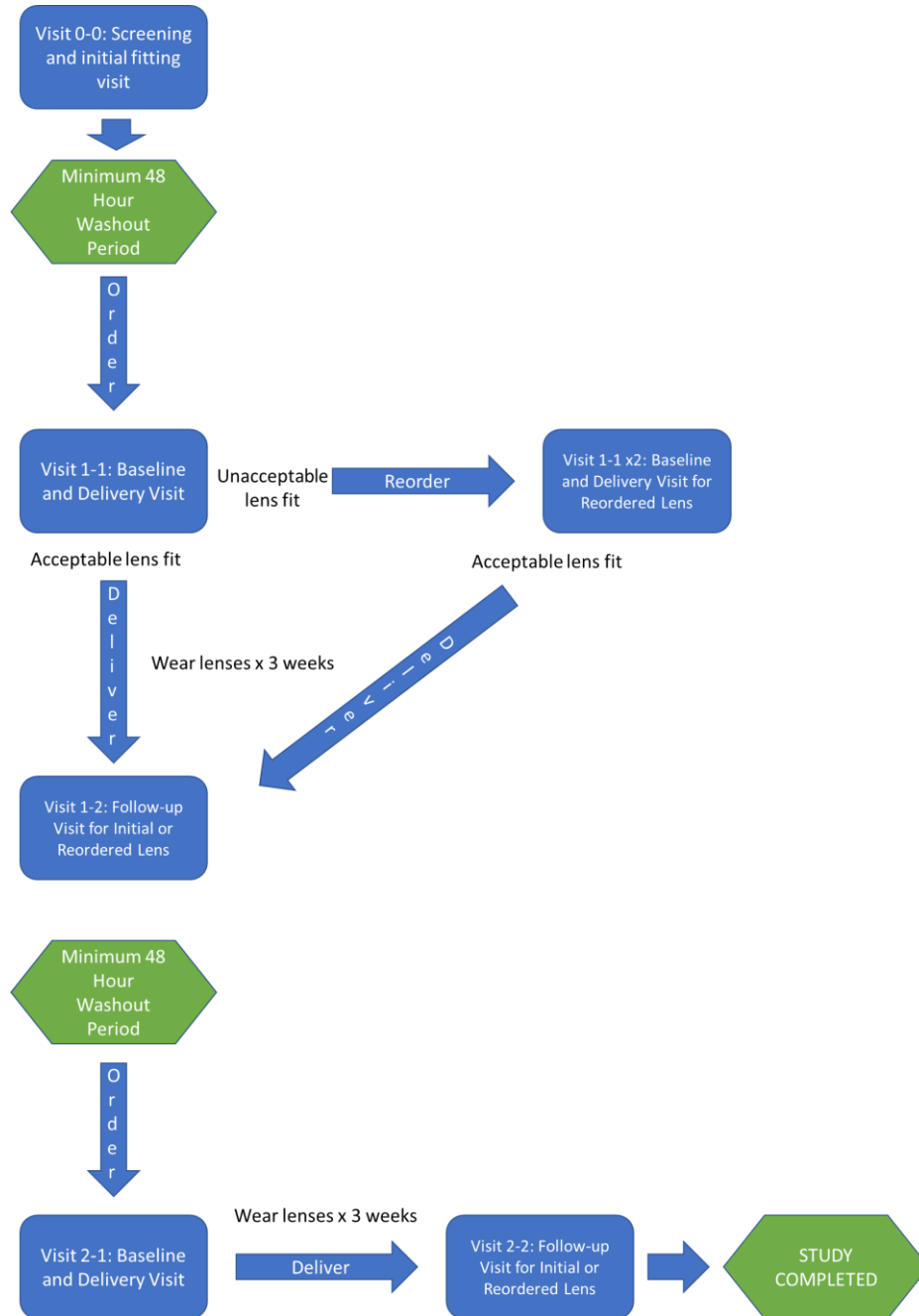


Figure 3-6: Study flow outlining the order of study visits. Note that words in arrows refer to the lenses (e.g., order lens, deliver lens)

3.2.3.1 Imaging with the Oculus Pentacam® HR CSP Software Module at Visit 0-0

To determine which diagnostic lens to trial first, participants were imaged with the Oculus Pentacam® HR CSP Software Module. Images were taken in a closed room in complete darkness. With the participant positioned comfortably and securely, five images were taken of the ocular surface with the instrument. After each image, the Scheimpflug cross-sectional and en-face iris images were examined, and if any of the cross-sectional images were black or missing on the former, or if the eyelid was obstructing the Purkinje images at the visual axis on the latter, the scan data was not used, as per recommendation from a representative employed by the manufacturer. Additionally, in accordance with this, the quality and diagrammatic coverage of each scan was assessed when displayed, and if adequate coverage less than 1mm beyond the cornea was not achieved, the scan was repeated (Chris O’Flaherty, Product Manager, OCULUS, Inc., Personal Communication, 26 August 2019). When this scan was completed, the “CSP Report” was generated (see below Figure 3-7).

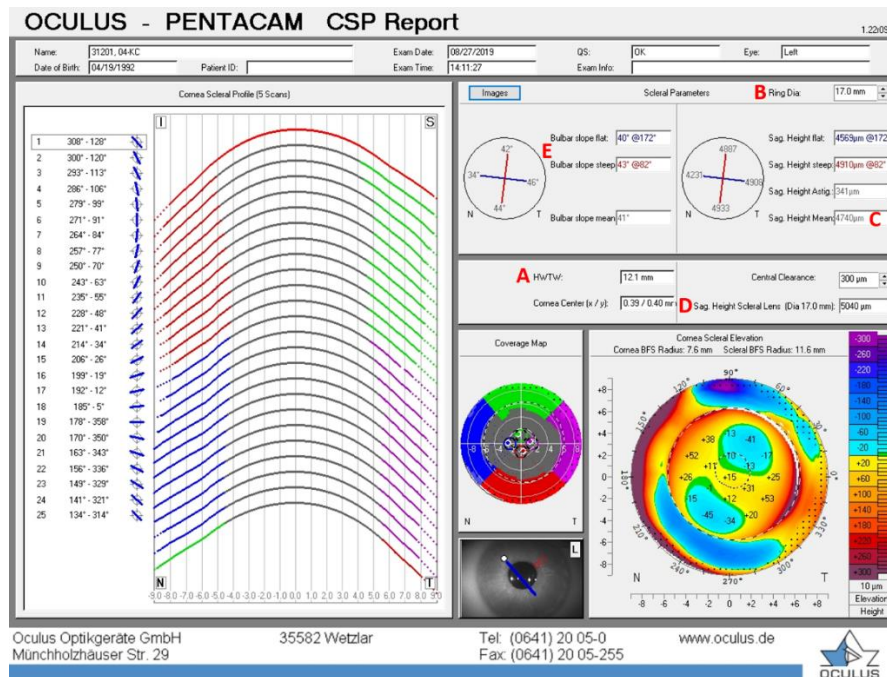


Figure 3-7: Sample display of the Pentacam® HR CSP report. A: Horizontal White-to-White. B: Ring Diameter. C: Mean sagittal height of the ocular surface. D: Calculated lens sagittal depth. E: Bulbar slopes of flat and steep meridians.

Only the diagnostic lenses with a prolate profile were used for this study. In selecting the initial diagnostic Zenlens™ Scleral Lens (see Figure 3-8), scleral lens diameter (16.0 or 17.0 mm, based on HWTW, Figure 3-7A) and corresponding sagittal depth was determined according to the manufacturer's guide for the CSP program when fitting this particular lens (see Appendix B for the manufacturer's guide).²⁶⁰ The chosen scleral lens diameter was then entered in the "Ring Diameter" box on the display (Figure 3-7B) to generate calculated measures at that particular diameter. The amount of central clearance added can be customized, for this study, the recommended addition of 300 µm was used (see Appendix B, step 3). The resultant calculated sagittal depth of the scleral lens (Figure 3-7D) based on ocular sagittal height at the chosen scleral lens diameter (Figure 3-7C) was rounded to the nearest numerical diagnostic lens sagittal depth available, and this lens was trialed first. As an example, for this study, from parameters measured in Figure 3-7, the study investigator would select a lens from the "17mm" diameter row in the prolate section, as the HWTW (Figure 3-7A) is greater than 11.8mm (per Appendix B, step 1). The "Ring Dia" has been adjusted to 17mm in the CSP display for this reason (Figure 3-7B), and the resultant "Sag Height Scleral Lens" at this chord length, as displayed (Figure 3-7D) is 5040 µm. In this case, Z-9 (4900 Sag) is the closest numerically to this value, and so this diagnostic lens would be initially selected. In the CSP report, both the "bulbar slope flat" and "bulbar slope steep" are displayed (Figure 3-7E). These angles were converted to their corresponding APS value per the Zenlens™ CSP guide and were the chosen initial horizontal and vertical parameters for the ordered lenses.

							TORIC PCs	
PROLATE	16MM	Z-1 4200 SAG 8.20 BC	Z-2 4500 SAG 7.60 BC	Z-3 4800 SAG 7.10 BC	Z-4 5100 SAG 6.70 BC	Z-5 5400 SAG 6.40 BC	Z-6 5700 SAG 6.10 BC	ZT-5 5400 SAG 6.40 BC
	17MM	Z-7 4300 SAG 9.20 BC	Z-8 4600 SAG 8.40 BC	Z-9 4900 SAG 7.80 BC	Z-10 5200 SAG 7.30 BC	Z-11 5500 SAG 6.90 BC	Z-12 5800 SAG 6.60 BC	ZT-11 5500 SAG 6.90 BC
OBLATE	16MM	Z-13 4100 SAG 10.00 BC	Z-14 4400 SAG 9.50 BC	Z-15 4700 SAG 9.00 BC	Z-16 5000 SAG 8.50 BC	Z-17 5300 SAG 8.00 BC	Z-18 5600 SAG 7.50 BC	ZT-17 5300 SAG 8.00 BC
	17MM	Z-19 4200 SAG 10.90 BC	Z-20 4500 SAG 10.30 BC	Z-21 4800 SAG 9.70 BC	Z-22 5100 SAG 9.10 BC	Z-23 5400 SAG 8.50 BC	Z-24 5700 SAG 7.90 BC	ZT-23 5400 SAG 8.50 BC

Figure 3-8: Zenlens™ full diagnostic set parameters. Only the prolate design (top two rows in grey and purple) was used for this study. © Images provided courtesy of Bausch + Lomb.²⁵²

3.2.3.2 Scleral Lens Trial: Visit 0-0

Prior to lens cleaning and insertion, the participant was seated in the examination chair, which was elevated to its maximum height. Paper towels were placed across the participant’s lap. As determined by steps outlined in 3.2.3.1, the appropriate initial trial Zenlens™ was selected from the diagnostic kit. After the lens was cleaned thoroughly on both surfaces with Boston Simplus® Multi-Action Solution (Bausch + Lomb, Rochester, NY, USA) and rinsed with *Sensitive Eyes*® Saline Plus Solution (Bausch + Lomb, Rochester, NY, USA), the lens was placed concave-side up on a DMV® plunger (DMV Corporation, Zanesville, OH, USA) and filled with preservative-free saline solution (0.9% sodium chloride injection solution, Addipak® (3mL), Hudson RCI Teleflex, Markham, ON, CA). A fluorescein strip (Diofluor™ strips, Dioptic Pharmaceuticals Inc, Toronto, ON, CA) was then mixed in the saline solution in the lens bowl to aid with the assessment of the lens-to-ocular surface relationship. The participant was asked to lean their torso forward, placing their face parallel to the ground. In this position, the participant was asked to pull down and hold open their inferior eyelid, while the investigator pulled upwards on and held open the participant’s superior eyelid. The lens which had been previously placed on the plunger was then swiftly inserted into the participant’s eye

by the investigator (see Figure 3-9). Immediately following insertion, the investigator used a handheld cobalt blue light to assess for the presence of bubbles behind the lens, which would cause a disruption in the green tear fluid layer behind the lens due to the fluorescein. A demonstration of this process is shown in Figure 3-9.



Figure 3-9: Image of scleral lens insertion as this would be done at the initial fitting visit (0-0).

A spherical over-refraction was carried out to ascertain the appropriate power to order for each scleral lens. Initially and after a minimum of twenty minutes to allow the lens to settle, the lens fit relative to the ocular surface was assessed. At the biomicroscope, central corneal clearance was estimated to ensure that the central fit of the lens was not grossly outside of the target range. Initially, central corneal clearance was assessed at the biomicroscope, and after settling, central corneal clearance was both assessed at the biomicroscope and measured with the Spectralis® OCT. After settling, limbal clearance and the lens-to-sclera relationship was also assessed at the biomicroscope. The characteristics of a desirable lens fit during the trial fitting included a central corneal clearance of 200-300 μm in accordance with clinical recommendation and that of the manufacturer, adequate clearance over the limbus, and proper scleral alignment that did not appear to have significant compression or edge lift.^{52,252,261} If the lens fit was deemed unacceptable, an appropriate alternate diagnostic lens was trialed where possible, and/or modifications were made to the lens parameters ordered. In order to optimize the lens-to-scleral fitting relationship, when ordering the lenses, the

scleral profile of the lens or Advanced Peripheral System (APS) was determined using suggested bulbar slope parameters from the CSP Report (Figure 3-7E), according to the manufacturer's guide (Appendix B, step 4).²⁶⁰

3.2.3.3 Pachymetric OCT and Scheimpflug Imaging: Visits 1-1 – 2-2

Pachymetric imaging was carried out at four sessions, at each of the two baseline visits (1-1 and 2-1) and each of the two follow-up visits (1-2 and 2-2). OCT imaging with both the Spectralis® and Visante™ instruments was carried out, as well as Scheimpflug imaging with Pentacam® HR. For baseline visits, it was ensured that measurements were taken at least 2 hours after waking to circumvent effects of corneal edema secondary to overnight eyelid closure.²⁸ All study visit start times were kept consistent where possible, and within four hours of one another at most to minimize the possibility of diurnal fluctuation in corneal thickness.

3.2.3.3.1 OCT Imaging with Spectralis® and Visante™

The Spectralis® was set for anterior segment imaging according to manufacturer guidelines.¹⁶¹ After participant ID was entered into Heidelberg Eye Explorer (HEYEX) software, the average keratometry measurement of each eye from baseline measurements were entered in the “C-Curve” boxes of the Eye Data Dialog Box. According to the user manual and in correspondence with the manufacturer, values entered in this box did not affect measurements taken on each image (Annie Kwan, Technical and Clinical Support Representative, Innova – Heidelberg Supplier, Personal Communication, 22 July 2019). Then, the instrument was mounted with the anterior segment lens and the position of the focus knob was set to 0mm. Automatic brightness control and high-resolution mode were selected as acquisition parameters. Corneal imaging with the following settings were used: a default Automatic Real Time (ART) setting of 16, and scan parameters of 15° x 1° to provide a volume scan of 8mm x 0.5mm. Each volume scan consisted of 9 B-scans, separated by 69 µm. ART refers to the number of

images being averaged at a particular location to generate the image.¹⁶¹ During imaging, the contralateral eye was patched, and the participant was instructed to fixate on the red light inside of the imaging probe. In conjunction with the use of the bright central specular reflection artefact to position the scan, this was used to ensure that the same part of the cornea was imaged at each session. Scan positioning was aligned with the central specular reflection, which was centred laterally on the imaging display. While the image was being acquired, the participant was instructed to minimize eye fixation movements, but was permitted to blink when needed during imaging. One scan in each orientation of horizontal, vertical, and both oblique meridians, was taken. After acquisition, images were visually inspected to ensure good quality. Specifically, it was confirmed that the refractive correction was completed in the HEYEX software, images were not blurred due to motion, corneal and epithelial boundaries were discernible to the periphery of the image, and that the apical specular reflection was present and centred laterally in the images. If any of the images did not meet these criteria, they were re-taken.

At delivery visits (1-1, 2-1), baseline pachymetric imaging with Spectralis® was carried out prior to any scleral lens insertion. At both follow-up visits (1-2, 2-2), this imaging was carried out immediately after the removal of the scleral lens one eye at a time, which was done in the same room where imaging was taking place.

Following Scheimpflug imaging with the Pentacam® HR (to be detailed in Section 3.2.2.2), additional pachymetric OCT imaging was carried out with the Visante™ OCT (detailed in Section 3.2.2.3) using the Global Pachymetry Map option. Multiple scans were obtained with this instrument. However, in many cases, inaccurate detection of corneal boundaries was noted when segmented images (used to generate the maps) were inspected. For this reason, these data were recorded but not used. An example of one of these cases is shown below in Figure 3-10.

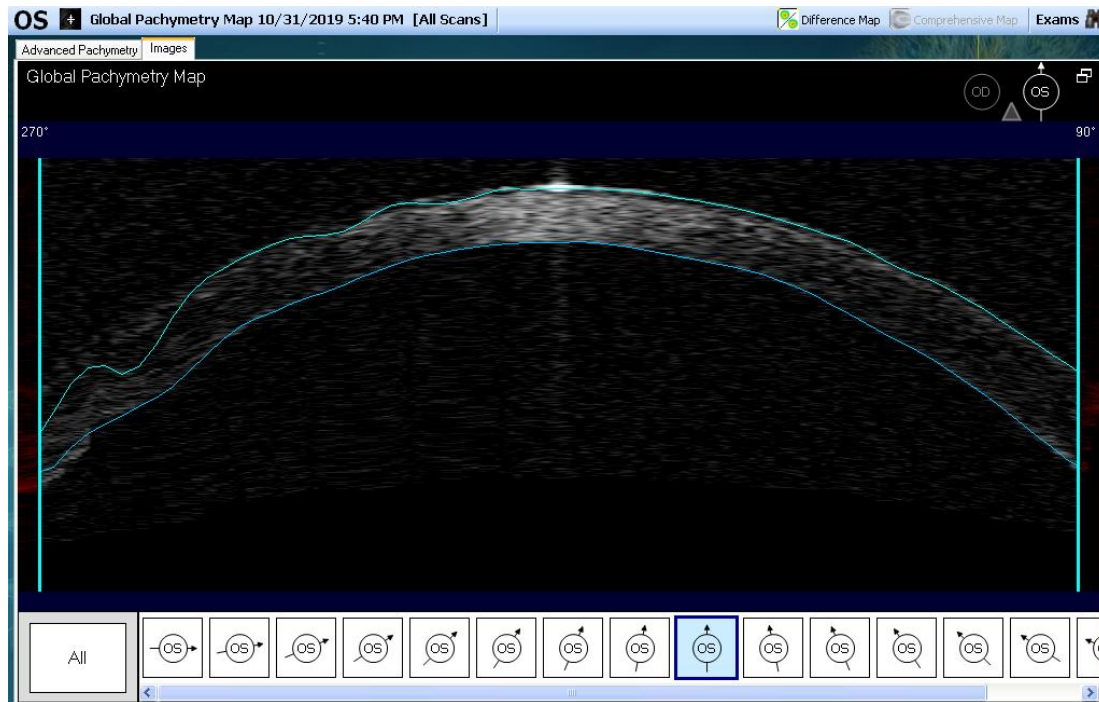


Figure 3-10: Sample of a poorly segmented image from the Visante™ Global Pachymetry Map. Note how the anterior segment boundary at the 270° position has not been properly detected.

3.2.3.3.2 Scheimpflug Imaging with Pentacam® HR

Imaging with the Pentacam® HR was additionally carried out. For this study, the 3D Scan option of 25 pictures/1 second was used to acquire scans generating corneal thickness data. At the delivery visit, Pentacam® HR scans were taken prior to fluorescein instillation. At follow-up visits, these images were taken as soon as possible following image acquisition with the Spectralis® OCT after lens removal. Images were taken in a completely dark room, and participants were encouraged to fixate on the target inside of the instrument and to hold their gaze and only blink once the image had been taken. Only images with a quality rating of “OK” or better were accepted, otherwise another image was taken to achieve this quality rating, if possible. One scan of each eye per subject was analyzed as in previous study, and good repeatability of measurements taken with this instrument has been shown.¹⁰²

3.2.3.4 Assessment of Central Corneal Clearance: Visits 0-0 – 2-2

At all visits, central corneal clearance of the scleral lens was assessed both at the biomicroscope and with the Spectralis® OCT. Briefly, an optic section technique was used to estimate the ratio of the central lens thickness to the fluid reservoir depth to determine the approximate central corneal clearance immediately and after 20 minutes of lens wear. This was also examined at the location of minimum clearance, which often would correlate with the cone apex. Then, after 20 minutes of lens wear, corneal clearance was measured with the Spectralis® OCT. Image acquisition was carried out in the same manner as previously described in detail in 3.2.3.3.1. Initially, volume scans using the same imaging settings as described were attempted, however this was not always possible to obtain due to motion, and difficulty of the instrument in imaging the ocular surface with the barrier of the scleral lens. Instead, line scans were taken at each of the four scan orientations, centred about the central corneal reflex. Corneal imaging with the following settings were used: a default ART setting of 60, and a line scan parameter of 15° to produce a B-scan of 8mm. Measurement of central corneal clearance from these images will be detailed in Chapter 4. At delivery visits (1-1, 1-1 x 2 if applicable, and 2-1), OCT imaging with the scleral lenses on were taken after 20 minutes of lens settling. At both follow-up visits (1-2, 2-2), this imaging was carried out immediately prior to the removal of the scleral lenses, after lenses had been worn for a minimum of 6 hours.

3.2.3.5 Evaluation of Ocular Health and Subjective Parameters: Visits 0-0 – 2-2

Ocular health was assessed at every visit with biomicroscopy, and with the K5® at baseline and follow-up visits. For the K5®, the R-Scan for bulbar and limbal redness classification was carried out at the beginning of both delivery and follow-up visits. If corneal fluorescein staining was present upon biomicroscopic examination, a simulated fluorescein image with the K5® was taken. For both images, the participant was instructed to hold their eye open while the user focused the instrument on

scleral blood vessels (R-Scan) or the cornea (fluorescein imaging) to acquire the image. Images were re-taken if they were of subjective low quality due to motion or poor focus.

Biomicroscopic anterior segment examination with corneal fluorescein instillation was also carried out and recorded, with close attention to the cornea for both clinical signs of keratoconus, and hypoxia (both detailed in Chapter 1). In particular, the presence of Fleischer's ring, Vogt's striae, and apical scarring were noted as keratoconic signs (section 1.3.4.3), as well as clinical signs of hypoxia, specifically, corneal neovascularization, stromal striae and folds, and epithelial microcysts (section 1.1.3).

The first step for all baseline and delivery visits was the administration of the Ocular Symptom Questionnaire to adequately assess subjective comfort without the influence of procedures carried out during the study visit. This questionnaire is attached in Appendix A. High and low contrast distance visual acuity were assessed under half room illumination, which was consistent for all participants. A digital illuminated Snellen system (ProVideo Classic, Innova Systems USA, Inc., Burr Ridge, IL) was used. Habitual visual acuity, as well as visual acuity with scleral lens wear with best-corrected spherical over-refraction, were recorded.

3.3 Demographics and Study Lens Parameters

3.3.1 Participant Demographics

Sixteen male and two female individuals with keratoconus were recruited for this study (36 eyes).

Eight male participants (16 eyes) with keratoconus completed the study. Reasons for study discontinuation included maladaptation to scleral lens wear (3 participants), strong reflex blepharospasm preventing scleral lens insertion (1 participant), unforeseen changes to personal life circumstances (1 participant), failure to maintain the study visit appointment schedule (1 participant),

and inability to complete study visits due to COVID-19 restrictions to in-person research (4 participants).

The average age of participants who completed the study was 31.6 ± 6.6 (range: 23.6-44.9). Based on the Amsler-Krumeich classification, seven eyes had Stage 1 keratoconus, four had Stage 2, one had Stage 3 and four had Stage 4 keratoconus. Automated keratometry readings were used for average keratometry values, and Pentacam® HR total corneal thickness measurements at the thinnest location were used for thinnest pachymetry values (see below Table 3-1, along with maximum keratometry values).

Table 3-1: Average and maximum keratometry values, and minimum corneal thickness values for each eye and participant.

Participant	Eye	Kavg	Kmax	Minimum CT
02-KC	OD	51.00	51.50	467
02-KC	OS	48.25	48.75	499
04-KC	OD	45.75	48.00	484
04-KC	OS	46.25	49.25	483
07-KC	OD	57.50	59.75	364
07-KC	OS	56.50	58.00	359
09-KC	OD	51.75	53.25	507
09-KC	OS	43.25	43.50	589
11-KC	OD	43.00	44.00	474
11-KC	OS	50.50	52.25	434
13-KC	OD	46.00	47.50	510
13-KC	OS	45.25	47.50	524
14-KC	OD	53.50	60.00	400
14-KC	OS	42.50	44.50	492
15-KC	OD	43.50	45.75	566
15-KC	OS	47.00	53.00	557

Seven eyes (44%) had previously undergone CXL at least six months prior to the first baseline study visit, nine eyes (56%) had no history of CXL. Three eyes (19%) had previously worn corneal gas-permeable contact lenses habitually for a period of greater than six months. Six eyes (25.0%) had a history of scleral lens wear, with two eyes (12.5%) having continued to wear them habitually,

however both had discontinued wear at the time of the study. Habitual correction at the initial screening study visit was as follows: none (eight eyes, 50.0%), spectacles (six eyes, 37.5%), and corneal gas-permeable contact lenses (two eyes, 12.5%).

3.3.2 Study Lens Parameters and Fitting Characteristics

Study methods for selecting an initial diagnostic lens has been previously detailed in sections 3.2.3.1 and 3.2.3.2. Briefly, a novel method (Pentacam® HR CSP) of determining the initial appropriate diameter and sagittal depth of each diagnostic lens was used. Lens diameter was based on HWTW and sagittal depth was determined by adding 300 μm to the mean ocular surface sagittal height, per the manufacturer.²⁶⁰ Anterior segment OCT has been historically utilized to determine scleral lens sagittal depth, in particular with the Visante™ OCT.^{67,262} A common clinical method involves determining the ocular surface sagittal height at a 15mm chord parallel to the iris plane on an OCT image of the ocular surface, using methods described in 3.1.^{251,254} To determine the sagittal depth of the initial diagnostic scleral lens, many practitioners will add 300-400 μm to this parameter.^{67,68} Because a recent pilot study had shown that comparison of the two methods (Pentacam® HR CSP and Visante™ OCT at 15mm chord) were statistically, but not clinically significantly different in the determination of the initial diagnostic scleral Zenlens™ in eyes with keratoconus, thus the Pentacam® HR CSP method was used.²⁶³

When ordering lenses, a settled clearance of 150-250 μm was targeted when altering sagittal depth of the low clearance lens, and for the high clearance lens, a target settled clearance of 250-350 μm was used. These ranges were chosen to be on the lower and higher range of a clinically desirable settled clearance of 200-300 μm . Whether the low or high clearance lens was ordered first was randomly determined by a third party with a randomization table, and both the investigator and participant were masked to this order. Only the first pair of lenses were initially ordered in case changes were required. At the first follow-up (1-2), the investigator was temporarily unmasked to

ensure that the settled lens clearance was in the targeted range for that specific lens. If this was not the case, the order of low and high clearance lens delivery was reversed. Specifically, the amount of clearance was measured on Spectralis® images, and the investigator referred to the sagittal depth parameters on both drafted lens orders to determine if the high, or low clearance lens was intended. For example, if this amount of clearance were measured to be 400µm for the intended low clearance lens, this would be exceeding the targeted range of this lens (150-250 µm). So, this lens would be re-assigned as the high clearance lens, and the sagittal depth on the drafted order for the second, newly low clearance lens was modified appropriately prior to submission to the manufacturer. The investigator was again masked for data analysis, as sufficient time had passed between this brief unmasking and later data analysis, which occurred many months after the end of the study.

As mentioned, horizontal and vertical landing zone parameters (APS) of trial lenses ordered after trial fitting were determined using the bulbar slope measurements (Figure 3-7E) taken by the Pentacam® HR CSP software, through the CSP guide (Appendix B, step 4). Although there was the option for a front-toric design if indicated, this was not employed for this study due to introduced variability in lens thickness along the steep and flat meridians. Best-sphere over-refraction over diagnostic trial lenses determined the power of the lenses ordered. The standard central thickness of the Zenlens™ is 0.35mm,²⁵² and could not be altered in cases of low minus or plano powered lenses without altering the thickness profile of the lens (Mika Hague, Product Specialist, Alden Optical/Bausch + Lomb Specialty Vision Products, Personal Communication, 1 November 2019). See Table 3-2 for a summary of all lens parameters for participants who completed the study.

Table 3-2: Summary of study lens parameters for all participants.

Participant	Eye	Lens	Actual Lot #	BC	Pwr	Dia	SD	APS - H	APS - V	LC (µm)	CT (µm)
02-KC	OD	LC	BD536710	7.30	pl	17.00	5150	F3	S6	10	420
02-KC	OD	HC	BC367210	7.30	-0.50	17.00	5250	F3	S6	10	400
02-KC	OS	LC	BD536720	7.30	-1.00	17.00	5100	F1	S8	10	380
02-KC	OS	HC	BC367220	7.30	-1.50	17.00	5200	F1	S8	10	360
04-KC	OD	LC	BD226410	7.80	-1.25	17.00	4900	S4	F2	10	360
04-KC	OD	HC	BB934710	7.80	-1.25	17.00	5000	S4	F2	10	360
04-KC	OS	LC	BD226420	7.80	-0.50	17.00	4920	S2	S1	10	390
04-KC	OS	HC	BC307220	7.80	-0.50	17.00	5020	S2	S1	10	390
07-KC	OD	LC	BC559710	7.30	-3.75	17.00	5200	S6	F5	10	350
07-KC	OD	HC	BB934010	7.30	-3.00	17.00	5300	S6	F6	10	350
07-KC	OS	LC	BC559720	7.30	-3.75	17.00	5200	F3	S7	10	350
07-KC	OS	HC	BB934020	7.30	-3.75	17.00	5300	F3	S7	10	350
09-KC	OD	LC	BD375310	7.30	-2.75	17.00	5280	S2	S10	10	350
09-KC	OD	HC	BC642810	7.30	-2.75	17.00	5380	S2	S10	10	350
09-KC	OS	LC	BD375320	7.30	-3.50	17.00	5120	F2	S10	10	350
09-KC	OS	HC	BC642820	7.30	-3.50	17.00	5220	F2	S10	10	350
11-KC	OD	LC	BD226710	7.80	-2.00	17.00	4800	S5	S1	0	350
11-KC	OD	HC	BB933710	7.80	-1.50	17.00	4900	S5	S1	0	350
11-KC	OS	LC	BD226720	7.80	-0.50	17.00	4850	F2	S3	0	390
11-KC	OS	HC	BB933720	7.80	-1.00	17.00	4950	F2	S3	0	370
13-KC	OD	LC	BC853210	7.80	-3.00	17.00	4950	Std	Std	10	350
13-KC	OD	HC	BB932810	7.80	-2.00	17.00	5050	Std	Std	10	350
13-KC	OS	LC	BC853220	7.80	-1.50	17.00	4900	F1	S8	20	350
13-KC	OS	HC	BB932820	7.80	-3.00	17.00	5000	F1	S8	20	350
14-KC	OD	LC	BD646810	7.30	-5.25	17.00	5200	S4	S4	10	350
14-KC	OD	HC	BC578410	7.30	-5.00	17.00	5300	S4	S4	10	350
14-KC	OS	LC	BD646820	7.30	-5.50	17.00	5100	S3	S8	10	350
14-KC	OS	HC	BC578420	7.30	-5.00	17.00	5200	S3	S8	10	350
15-KC	OD	LC	BC853110	8.40	-1.25	17.00	4760	F4	90: S5 270: S3	10	360
15-KC	OD	HC	BD650910	8.40	-1.50	17.00	4860	F4	90: S5 270: S3	10	360
15-KC	OS	LC	BC578620	8.40	-0.25	17.00	4800	F2	S2	10	390
15-KC	OS	HC	BD650920	8.40	pl	17.00	4900	F2	S2	10	400

Chapter 4

Analysis Procedures

4.1 Region Selection for Spectralis® Data Analysis

As previously described, all total corneal and epithelial thickness measurements taken by the Spectralis® OCT were carried out manually in Fiji, an image processing package of ImageJ.²⁶⁴ Due to the high volume of data required to process whether the horizontal (0-180°), vertical (090-270°), and two oblique (045-225°, 135-315°) meridians were to be analyzed, it was suggested that if there was not a significant change in corneal thickness outside of the typically inferior diseased area of the cornea along the oblique meridians, the superior oblique be excluded from analysis. To investigate this, pachymetry maps taken on the Oculus Pentacam® HR from each visit were examined, and total corneal thickness measurements at a 2mm radius (4mm chord) were recorded and tabulated by location. In each case, the pachymetry difference between baseline and follow-up was calculated, and descriptive statistics were carried out on these differences (displayed in Table 4-1).

Table 4-1: Descriptive summary of corneal thickness changes from baseline to follow-up by location at a 4mm chord, measured by the Oculus Pentacam® HR.

	Location			
	Superior Nasal	Superior Temporal	Inferior Temporal	Inferior Nasal
Average Difference (µm)	8	7	9	11
Standard Deviation	10	9	9	11

Across all regions, it appeared that the average change and standard deviation from baseline were similar. Since there did not appear to be a preference for location for corneal swelling, it was not justified to analyze only the inferior halves of the oblique meridians from the Spectralis® data. Measurements in the eight corneal anatomical locations (nasal, superior nasal, superior, superior temporal, temporal, inferior temporal, inferior, and inferior nasal) were analyzed.

4.2 Image Selection and Corneal Thickness Measurements

4.2.1 Pentacam® HR Total Corneal Thickness

For both the Pentacam® HR and Spectralis® corneal thickness data, measurements were taken along the horizontal, vertical, and two oblique (45°) meridians, at 1mm increments from the centre of the cornea, up to a 4mm radius.

4.2.1.1 Image Selection

As mentioned in Chapter 3, section 3.2.3.3.2, one Pentacam® HR image per eye per session was used for corneal thickness measurements. During study visits, at least three Pentacam® HR images were taken of each eye. The first image chronologically that satisfied the following criteria was used: quality score (QS) of at least “OK”, with maximum coverage was noted on the enface iris image, and with the least amount of segmentation error of anterior and posterior corneal boundaries in the Scheimpflug image display (cross-sectional B-Scan images).

4.2.1.2 Total Corneal Thickness Measurements

Total corneal thickness data collected from the Pentacam® HR corresponding to images chosen were exported as comma-separated values (.csv) file and viewed in Microsoft Excel version 2105 (14026.20246). These files were converted into a readable form using the Text to Columns function, and as a result, a corneal thickness map was displayed, each cell corresponding to an x and y coordinate in 0.1mm increments. A macro was created in Excel to highlight and copy data points corresponding to those analyzed by the Spectralis® for each meridian of interest. Specifically, relative to the centre (0,0), corneal thickness values in 1mm increments up to 4mm from centre were collected in all scan directions. For points along oblique meridians, the Pythagorean theorem was used to calculate these coordinate values, since they lie along a 45° angle. With this same macro, these points were pasted into a separate sheet in tabular form.

4.2.2 Spectralis® Total Corneal and Corneal Epithelial Thickness

4.2.2.1 Image Selection

Spectralis® corneal three-dimensional volume scans were exported as Tag Image File Format (TIFF) files from HEYEX software. Initial B-scans to be used for corneal pachymetric comparison from baseline (1-1) were chosen based on the image within the volume scan with the brightest specular reflection from the undeviated ray at the corneal apex.^{77,80,85,241,244} The goal was to obtain the most centrally located B-scan using this criterion. One B-scan from visit 1-1 was chosen for each of the four scan meridians: horizontal, vertical, and both obliques, specified by the Spectralis® as: 0-180°, 090-270°, 045-225°, 135-315°.

Each of these B-scans along with their respective enface confocal scanning laser ophthalmoscope (cSLO) images with the marked scan position indicated by an arrow, were printed on transparent films (Over Head Projector Film, product code A122, Uinkit: Hartwii Imaging Materials Co. Ltd., Nanjing, China). On all cSLO images, the location of the apical specular reflection was visible in the enface image as a circular reflection. This is visible in the cross-sectional B-scan as the apical specular reflection in the centre of the image. An example of this scan display with cross-sectional B-scan and the enface cSLO image is presented in Figure 4-1.

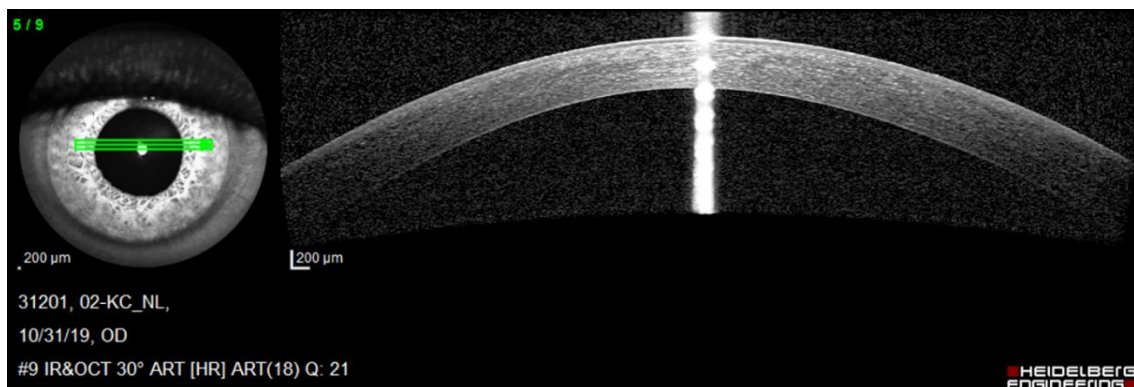


Figure 4-1: Example of a central Spectralis® OCT B-Scan with the apical specular reflection (right) alongside the enface cSLO image (left) indicating the scan position with an arrow, along the horizontal meridian.

For subsequent visits (1-2, 2-1, 2-2), films with the baseline (1-1) scan chosen were used to select the B-scan in the most congruent location to be selected for image analysis and comparison. This was done by overlaying the transparent baseline scan films with prospective images from subsequent study visits on a computer screen displaying the prospective image, using the location of the scan position on the enface cSLO image, and determining the image whose position most optimally matched that of the baseline transparent film with a bracketing technique. Specifically, on the cSLO image, the position of the line indicating the scan location relative to the circular light reflex on the cornea was examined and compared to that of the baseline, and the B-scan whose location was most similar was chosen.

All subsequent steps described in 4.2.2.2 were carried out in Fiji.²⁶⁴

4.2.2.2 Total Corneal and Corneal Epithelial Thickness: Manual Measurements in Fiji

4.2.2.2.1 Centre Determination

Firstly, the scale within the software was set to accurately take measurements in microns in all directions. This was done using the scale bar printed on each image (see Fig 1), attributing 16 pixels to every 200 microns (0.08 pixels/micron). This was initially measured for some of the images, was found to be consistent, and the scale was therefore assumed to be the same for all images. A macro was then created to set the scale as such for every image to increase efficiency and reduce error. The total size of each image was 12 650 x 4 275 μm , of which the B-scan occupied 9 425 x 2 425 μm . For each cross-sectional corneal image, the central position in the lateral plane was determined by inspection. With respect to each image, this was done in the “x” direction, regardless of the orientation of the imaging meridian. This localization was done by way of visual inspection of the bright apical specular reflection, generated by the undeviated ray, which was used to centre the imaging beam on the cornea. In Fiji,²⁶⁴ the central position of this artefact was first estimated with the Line tool, which was placed by inspection and subsequently measured using the Measure function,

and recorded in the Results dialog box. Then, the Rectangle tool was placed at the estimated hyperreflective boundaries of the artefact, measured, and displayed, and the x-coordinate of the centroid of this shape was noted. This coordinate was taken to be the centre of the cross-sectional image, and if this was a sub-pixel value, the centre coordinate was rounded to the nearest pixel in the direction of the initially estimated position with the Line tool. This position was also labelled with a vertical line using the Draw function in the Fiji software.²⁶⁴

4.2.2.2.2 Image Registration

Image registration was initially carried out via a Fiji²⁶⁴ registration plugin called “Align Image by line ROI”²⁶⁵ using the Line tool placed at the centre of each image using the centre determination method described above (4.2.2.2.1). All follow-up and second baseline images were registered to the initial baseline images for each participant, for each eye and meridian. However, in some instances with this method, the output-registered image had markedly decreased image quality in comparison to the original image. Troubleshooting was carried out, and the issue did not seem to resolve, even when it was confirmed that images were translated by full pixel values.²⁶⁶ Instead, an alternative method of image registration was tested and utilized, and is described below.

For each individual participant, if the image had the following conditions: right eye, horizontal meridian, lens 1, visit 1 (OD_H_1-1), this image was taken to be the reference image in terms of positioning in the x-direction for all subsequent images for this participant. For all other images, the central x-coordinate was noted, along with its difference from the x-coordinate of the reference image in the positive (right) or negative (left) direction in the image. The difference between these values, referred to as the translation factor, was noted in a Microsoft Excel spreadsheet. With subsequent images, the Translate function in Fiji²⁶⁴ was used to register these images to the x-position of the reference image, using the translation factor amount and direction (positive or negative sign). When prompted, the amount and direction-specific translation factor described above was entered in the “X

offset” input, with the “Y offset” input set to 0. The Line tool demarcating the centre was then moved to the new centre position, matching that of the reference image.

4.2.2.2.3 Position Marking

Following image registration, each image had all measurement locations at 1 mm, or 1000 μm , increments marked to facilitate the measurement process. On the reference image (OD_H_1-1) for each participant, a macro was recorded, where the Draw function was used to place a vertical line at the predetermined central location (4.2.2.2.1), and four vertical lines spaced 1mm apart as measured in Fiji²⁶⁴ were drawn each to the left and to the right of this position (eight lines in total). To do so, each line was positioned using the Line tool, its proper x-location was confirmed using the Measure function, and then it was subsequently drawn on. Lines were drawn from the top of the image, downwards in the area anterior to the cornea in the axial plane of imaging, but not obstructing, or interfering with the corneal cross-sectional image. Once this was carried out for all locations, the macro was saved, and applied to all other images for that participant. An example output image from this step is shown in Figure 4-2.

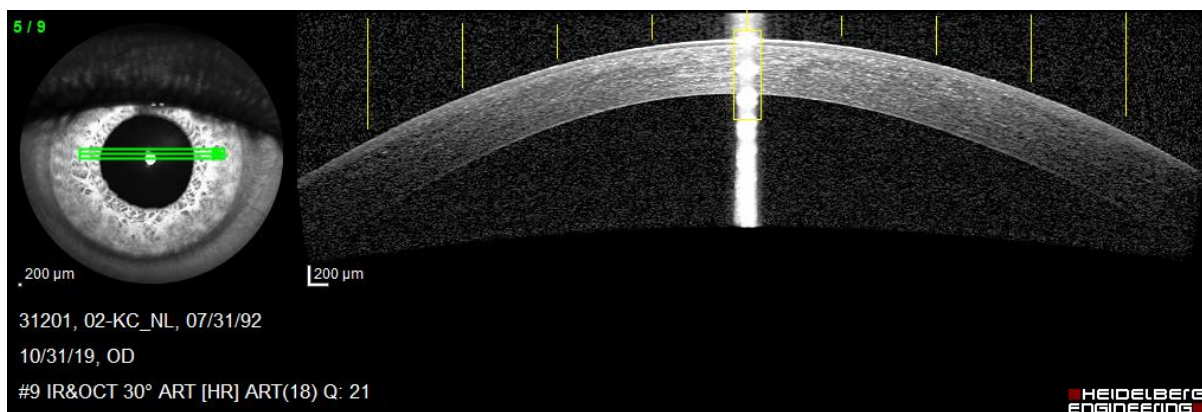


Figure 4-2: Measurement positions marked on a Spectralis® OCT B-Scan for the right eye, horizontal meridian. Positions are marked at 1mm increments from the centre, from 4mm temporal (left) to 4mm nasal (right).

4.2.2.2.4 Development of Segmentation and Corneal Thickness Measurement Method

Initially, various techniques were trialed to determine an automatic or semi-automatic method to segment the anterior and posterior cornea, and posterior epithelium, and subsequently measure total corneal and epithelial thickness by taking linear measurements from appropriate segmented boundaries. Segmentation plugins available in Fiji²⁶⁴ were used on multiple sample images, as well as functions available in the standard ImageJ software, such as Thresholding, and use of the Freehand Selection tool, which among other techniques, were trialed on multiple images. However, these methods were not consistently successful on this set of images to determine both epithelial and total corneal boundaries, and therefore a standardized automatic or semi-automatic method of segmentation could not be determined using these techniques. The process detailed below was therefore employed. This systematic method was largely manual but utilized elements of the image processing software to facilitate the process and optimize precision and accuracy.

4.2.2.2.5 Anterior Corneal Boundary Detection

To maintain consistency for all epithelial and total corneal thickness measurements, the pixel coordinates of the anterior corneal boundary was selected objectively for each measurement position in each image. The image with location markings from steps outlined in 4.2.2.2.3 (as shown in Figure 4-2) was opened in Fiji,²⁶⁴ and the image was binarized to black and white using the Process function. With this image, the cross-section of the cornea was represented by black pixel values on a white background. Then, the image was converted back to an RGB Color format. To select the anterior corneal boundary, the point tool was lined up at the appropriate x-location with the aid of the marked positions (4.2.2.2.3) and translated downward using the arrow keys to where the first anterior corneal black pixel was at this x-location. The coordinates of this pixel location were marked on the image in colour using the Draw function and noted in the Excel spreadsheet. Because the anterior cornea at the central location was obstructed by the apical specular reflection from the undeviated ray, this pixel

location was visually interpolated based on the y position of the row of pixels at the anterior corneal boundary just outside of the specular reflection. An example output image from this step of image processing is displayed below in Figure 4-3.

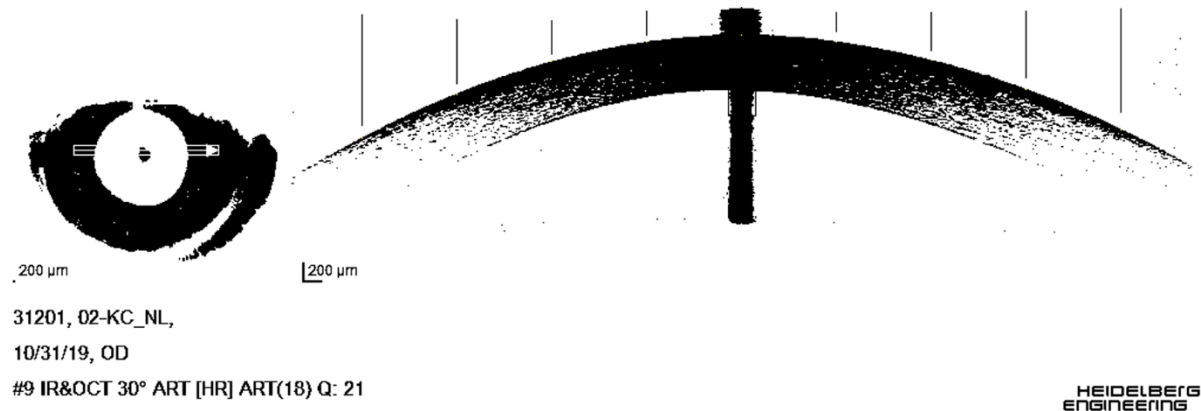


Figure 4-3: An example of a binarized image with the anterior corneal boundary marked at previously determined 1mm increments from the centre, also marked.

If the anterior cornea was not visible at a particular location using this method, particularly at more peripheral points due to signal drop-off, an extra step was taken to determine the anterior cornea objectively. Extraneous details to the left and below the corneal cross section (cSLO image, participant demographics) were outlined with the rectangular Selection tool, then the Process function was used to set these regions to a pixel value of 0 (black). This image with the background essentially subtracted was then binarized, and it was again attempted to determine the anterior corneal boundaries with the same steps as previously detailed. If the anterior corneal boundaries at these points were still not visible, the original image without binarization was examined, and these points were selected by inspection by the user and noted in the Excel spreadsheet.

4.2.2.2.6 Tangent Measurements

Prior to epithelial and total corneal thickness measurements, the angle of measurement - orthogonal to the tangent to the anterior corneal boundary - was predetermined at each location. This was done via visual inspection of the binarized image, where the investigator drew a line tangent to the anterior

corneal boundary point chosen at each measurement location. This was achieved with the Line tool, whose angle was then measured (Measure function) and noted in the Excel spreadsheet. Each line was also drawn on using the Draw function. In the Excel spreadsheet, 90 degrees was added to this value to determine the angle orthogonal to the tangent to establish the direction of measurement at that corneal location. With initial trials, all images for one participant had tangent measurements at each location carried out in this manner, however, this was found to be repeatable across all 4 visits for one imaging condition, that is, for a specific eye and imaging meridian. For example, for participant 02-KC, tangent measurements at each location were consistent across images through sessions 1-1 – 2-2 for the condition of right eye, horizontal meridian (OD_H). This example is illustrated with tangent measurements presented in Table 4-2.

Table 4-2: Results of tangent measurements for each image at each location for one participant in the horizontal meridian, when these measurements were initially done for all images. Measurement angles orthogonal to those below were omitted for brevity.

Participant	Visit	Eye	Direction	Tangent Angle Measurements (°)								
				-4	-3	-2	-1	0	1	2	3	4
02-KC	1_1	OD	H	26.76	21.29	15.15	7.47	-0.09	-7.55	-13.72	-19.63	-25.38
02-KC	1_2	OD	H	24.19	21.24	15.19	8.22	0.06	-7.37	-13.55	-20.12	-26.21
02-KC	2_1	OD	H	24.50	21.54	14.50	7.37	0.33	-7.77	-14.20	-20.50	-25.84
02-KC	2_2	OD	H	27.07	22.35	15.57	7.73	0.18	-7.47	-13.81	-19.82	-26.10

So, instead of taking tangent measurements for all four visits, tangent measurements were taken for the lens 1 baseline visit (1-1) for each meridian and assumed to be consistent for subsequent visits (1-2, 2-1, 2-2) at each location.

4.2.2.2.7 Total Corneal and Corneal Epithelial Thickness Measurements

Firstly, the properly registered image (4.2.2.2.2) with each measurement location marked (4.2.2.2.3) was opened in Fiji,²⁶⁴ with the Excel spreadsheet concurrently open with details for each measurement location (anterior corneal locations and angle orthogonal to tangents determined in 4.2.2.2.5 and 4.2.2.2.6, respectively). Using this information, the line measurement tool was used to

mark the boundaries of the anterior cornea and posterior epithelium to measure epithelial thickness, and then to mark the boundaries of the anterior and posterior cornea to measure total corneal thickness. The line was placed along the appropriate predetermined angle for each location, and once set, the Measure and Draw functions were used. Measurements were displayed in the Results dialog box, with Length corresponding to the thickness of the tissue. After the line was drawn, the Undo function was used to remove the drawn line, in order to observe which pixels had been detected at each border, as a means of quality control for the automatic selection of the anterior corneal location (detailed in 4.2.2.2.5), and non-automatic selection of anterior epithelial and posterior corneal borders by inspection. If these pixel locations were deemed appropriate by visual inspection by the user (i.e., not appearing to over- or underestimate thickness when the image was zoomed out, and not choosing a pixel of inappropriate intensity by inspection when zoomed in), the Undo function was used once again to re-draw the line. If the line position was deemed inappropriate, the measurement details were deleted in the Results dialog box, and the measurement was performed again along with the re-drawing of the line. The line lengths corresponding to epithelial and total corneal thickness were then copied and pasted into the Excel spreadsheet and measurement results were additionally saved as a .csv file. Each marked image was saved for reference. For example, for one condition, epithelial thickness measurements were measured and then marked and saved on one image, and total thickness measurements were obtained, and then marked and saved as a separate image. After epithelial and total corneal thickness measurements were taken and recorded in the Excel spreadsheet for one condition, these data cells had a black background applied when the user was taking these measurements for subsequent study visit thickness values to avoid measurement bias.

4.3 Refractive Index Correction

When measuring central and paracentral corneal pachymetry on exported Spectralis® images of the cornea alone, it was deemed unnecessary to further correct for distortion secondary to refractive

index, per the manufacturer's recommendation. This was ascertained through email correspondence with the manufacturer, via a Clinical and Technical Support Representative (Annie Kwan, Technical and Clinical Support Representative, Innova-Heidelberg Supplier, Personal Communication, 23 February 2021). In brief, when the exported corneal image is generated, it has undergone preprocessing in the Spectralis® HEYEX software, wherein the anterior cornea is segmented, and everything below this boundary is scaled via ray tracing according to the refractive index of the cornea, assumed to be 1.376. Therefore, scale bars on the exported image indicating 200 μm is true to the space anterior to the cornea, as well as the corneal tissue itself. The full response to this question is included in Appendix C. It should be noted that each layer of the cornea has a distinct refractive index, which would induce a small amount of distortion as light passes through each boundary.^{267,268} However, the above assumption has been employed at the recommendation of the manufacturer, as the only reliably automatically segmented layer is the anterior cornea. Accounting for these small variations would be very challenging to carry out manually, as each layer is not consistently discernible across the whole cornea. This would also be beyond the scope of this thesis and would not significantly impact the outcome measurements.

It is known that with OCT images taken of a contact lens, there is distortion due to both the refractive index of the lens, as well as its curvature.^{68,269,270} Thus, when taking measurements of central corneal clearance from Spectralis® images of the scleral lens on the eye, refractive index changes must be properly accounted for, as distortion due to lens curvature will be minimal if the measurement is taken as close as possible to the lens vertex, perpendicular to the ocular surface.²⁶⁹ Since when generating the images, the instrument software assumes a uniform refractive index of 1.376 below the anterior segmented surface, measurements directly taken will not be accurate due to the differing scleral lens refractive index (Boston XO® RI = 1.415),²⁷¹ or the tear film refractive index, which is assumed to be 1.336.^{235,272} Confirmation of a proper correction method for these parameters was

elucidated from the manufacturer through the same Clinical and Technical Support Representative mentioned above (Annie Kwan, Technical and Clinical Support Representative, Innova-Heidelberg Supplier, Personal Communication, 4 March 2021). In summary, the recommendation was to calculate the optical path length by multiplying the measurement taken by the refractive index of the cornea, and then obtain the true physical path length by dividing by the refractive index of the material, which would be either the scleral lens (if measuring lens thickness), or the tear film (if measuring central corneal clearance). This calculation was carried out when determining the central corneal clearance beneath the scleral lens, as well as measuring the centre thickness of the lens. In addition to this, it was stated that to ensure optimal accuracy, these measurements should be taken as close to the apex as possible, and these assumptions for correction can only be done in the vertical direction, presumably due to distortion induced by lens curvature remote from this location.²⁷⁰ Both of these conditions were satisfied when measuring central corneal clearance. The detailed recommendation from the manufacturer is attached in Appendix D.

4.4 Image Orientation Modification

4.4.1 Spectralis® Image Orientation Modification

When total corneal and corneal epithelial thickness measurements were carried out for Spectralis® images, this was consistently done from left to right on the cross-sectional OCT image (B-scan). The Spectralis® scan direction remains the same regardless of the eye being imaged. For example, left to right in the horizontal meridian corresponds to the temporal to nasal direction in the right eye, but conversely corresponds to the nasal to temporal direction in the left eye. To ensure that anatomical regions being analyzed were appropriately compared between eyes, the order of the data was reversed where appropriate. For all data taken from the Pentacam® HR and Spectralis®, the convention chosen was all scan directions determined when imaging the participant's right eye with the

Spectralis®. This means that only left eye measurements had to be reversed to match that of the right eye. For example, the -4 location in the horizontal meridian of the right eye would refer to 4mm temporally but on the left eye, 4mm temporally would originally be the +4mm point. To place all temporal values in the same column for statistical analysis, all positively valued points for the left eye became negative (i.e., the data was reversed using the Sort function with empty cells above numbered consecutively in Excel). The convention meant that negative values on the horizontal meridian would always represent the temporal region, for example. To illustrate this for all scan directions, Table 4-3 below shows the imaging direction for the Spectralis® where arrows represent left-to-right on cross sectional B-scans, and therefore negative to positive positions on original measurements. Instances where reversal of measurements was necessary are shown.

Table 4-3: Scan direction for right and left eye for the Spectralis®. Arrow direction indicates left (L) to right (R) on OCT cross section, and negative to positive positions on original measurements. Images where data was reversed are indicated.

	OD	OS
H	<p style="text-align: center;">Superior</p> <p style="text-align: center;">Inferior</p>	<p style="text-align: center;">REVERSE Superior</p> <p style="text-align: center;">Inferior</p>
V		
IT		<p style="text-align: center;">REVERSE Superior</p>
IN		<p style="text-align: center;">REVERSE Superior</p>

4.4.2 Pentacam® HR Image Orientation Modification

For Pentacam® HR measurements, data was obtained from the instrument using the “Call-All” function available in the instrument software. Total corneal thickness values were extracted from exported .csv files and tabulated accordingly, as previously described in 4.4.1. For the left eye, a second macro was created to invert values where appropriate. Additionally, for both eyes, values in the vertical meridian were reversed due to the nature of how the initial macro copied and pasted the values.

4.5 Correcting for Image Magnification for Lens-On Images

To measure central corneal clearance, Spectralis® images were taken with the lens on, positioned at the brightest area within the apical specular reflection. This process was described in detail in Chapter 3, section 3.2.3.4. It was assumed that this image was taken in the centre of the lens, perpendicular to the ocular surface and thus the measured clearance from the image would be the central corneal clearance, and the thickness of the lens should represent the central thickness, once both were corrected for refractive index, as detailed in 4.3. Centre thickness of each lens was specified by the manufacturer, and verified to be within tolerance²⁷³ once lenses arrived, with a physical thickness gauge (Mitutoyo Absolute, Richdome '87 Ltd. Optics, Devon, UK). When examining the Spectralis® lens-on images, it was noted subjectively that in some cases, the overall magnification of the image appeared to vary across images, specifically for scleral lens thickness as well as the central clearance. Specifically, two images of similar quality, both positioned at the apex would appear to have similar ratios of central thickness of the lens to central clearance within one image, however the measurement of central clearance and central lens thickness (in Fiji²⁶⁴) would both appear to vary across images. An example of this is shown in Figure 4-4.

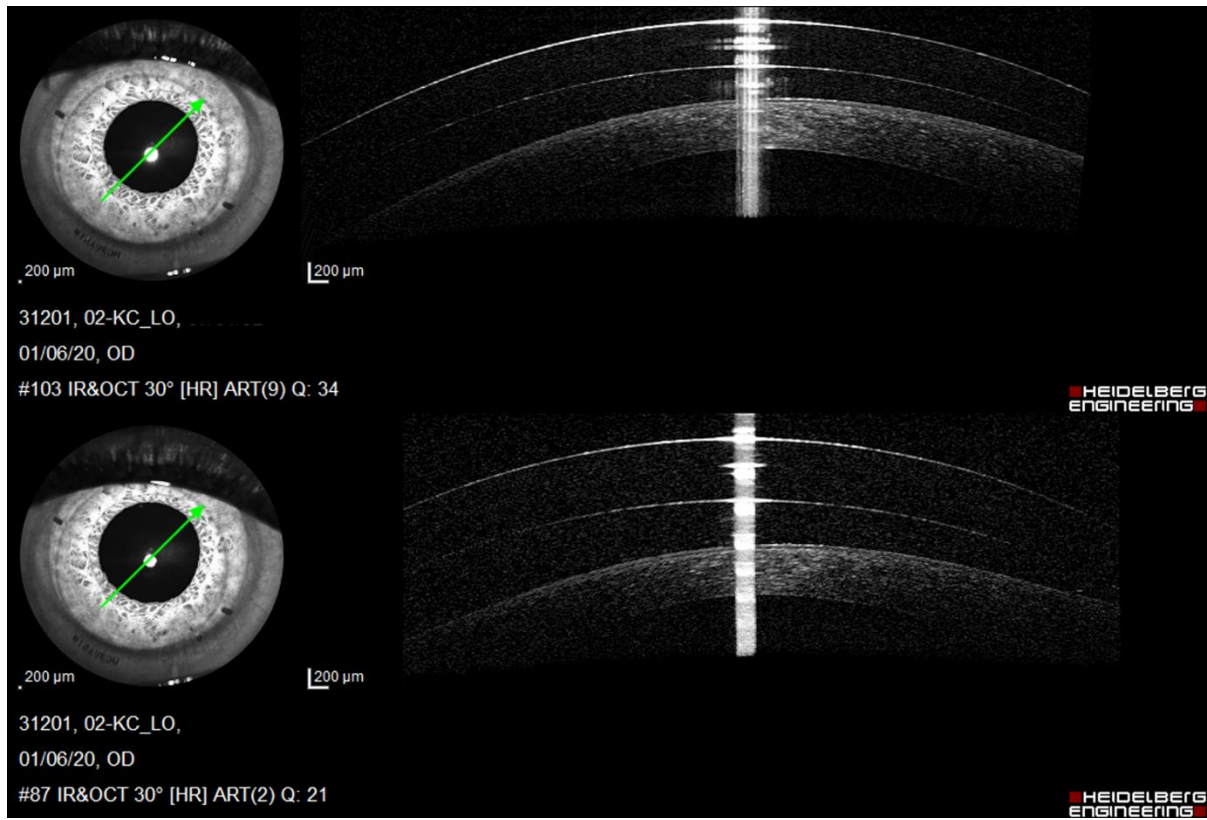


Figure 4-4: An example of two images taken within the same imaging session, appearing to have different magnification subjectively, and confirmed to have differently measured scleral lens central thicknesses and central clearances, but similar ratios of these parameters across images, while corneal thickness appeared to be similar.

To measure the central clearance, the best quality image was chosen, and measurements were taken of both the central clearance and central lens thickness in Fiji,²⁶⁴ using the Line tool. This was after the centre was determined as in 4.2.2.2.1. For measurements of lens thickness, a line was measured and drawn in the centre from the anterior to posterior lens surface. To measure clearance, a line was measured and drawn in the centre from the posterior lens surface to the anterior corneal boundary. Both the central clearance and the lens central thickness were refractive index corrected as described in 4.3. After this correction, it was confirmed that the central thickness did not always match that specified by the manufacturer, and what was physically measured. It was also confirmed that across

images of the same subject within the same imaging session, the ratios of centre thickness to central clearance were consistent. With the assumption that these images were taken in the centre and that the measured lens thickness should match the central thickness specified by the manufacturer, it was very likely that there was some magnification effect during imaging. The magnification equation below (Figure 4-5) was rearranged and used (Figure 4-6) to determine the true central clearance:

$$M = \frac{CT_{OCT}}{CT_t} = \frac{CCC_{OCT}}{CCC_t}$$

Figure 4-5: Magnification equation used where OCT denotes parameters measured by OCT, and t represents the true measurement.

$$CCC_t = \frac{CCC_{OCT}(CT_t)}{CT_{OCT}}$$

Figure 4-6: Rearrangement of magnification equation to solve for CCC_t (actual central corneal clearance)

It appeared that the measured and magnification-corrected central clearances followed similar trends for low and high clearances across participants. This can be visualized in Figure 4-7 below, where this is shown for both baseline and follow-up visits, in graphical form (created with GraphPad Prism 9, version 9.1.1).

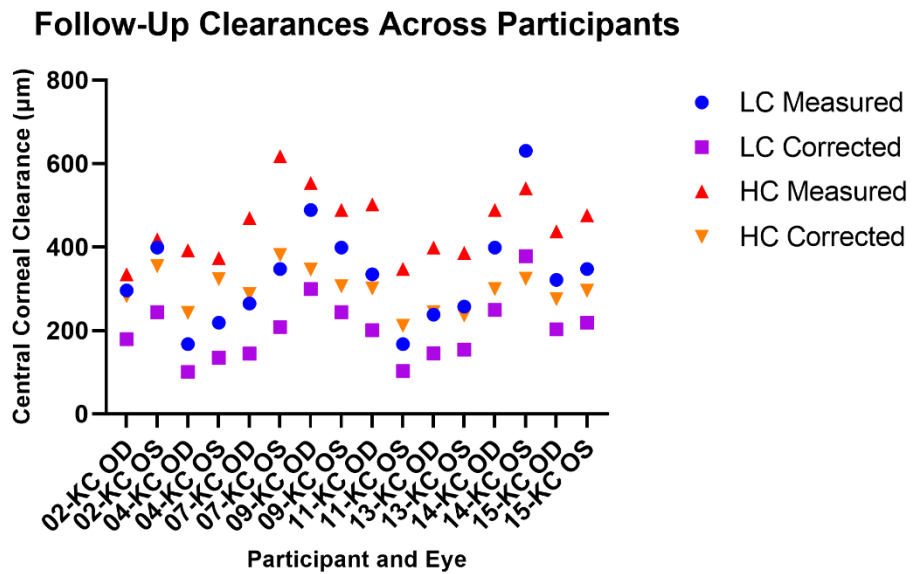
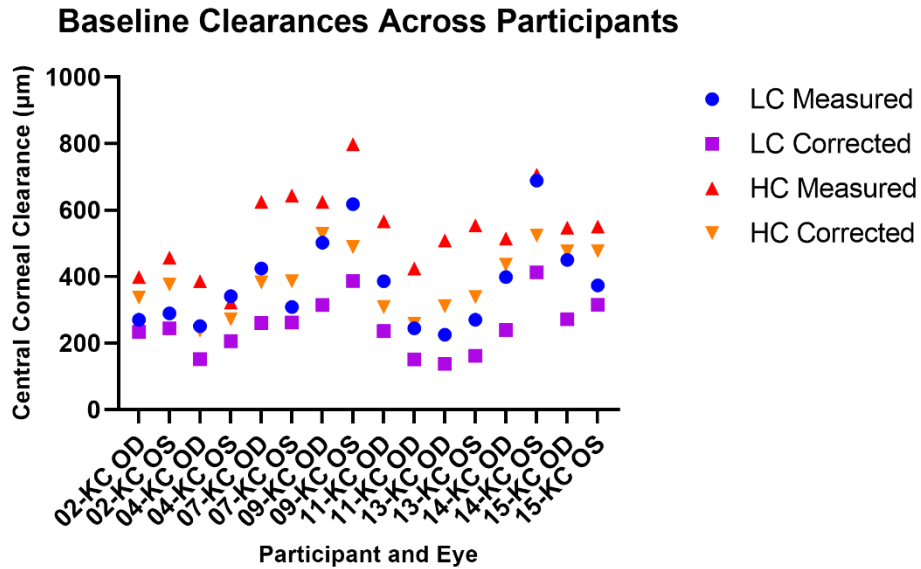


Figure 4-7: Plots demonstrating baseline and settled central corneal clearances (top and bottom graphs, respectively) measured with Spectralis® OCT with refractive index correction applied (measured), and subsequently corrected for magnification (corrected). Low clearance lenses are indicated by LC, and high clearance by HC in the graph legends.

The percent change from corrected clearance to measured clearance was also calculated in each case to reflect the amount of magnification. It seemed that overall, there were two distinct cases of magnification, that is, on average, the percent change was either ~18% or ~63%, the latter being the more frequent case. A density plot of all cases is displayed in Figure 4-8 below to illustrate this:

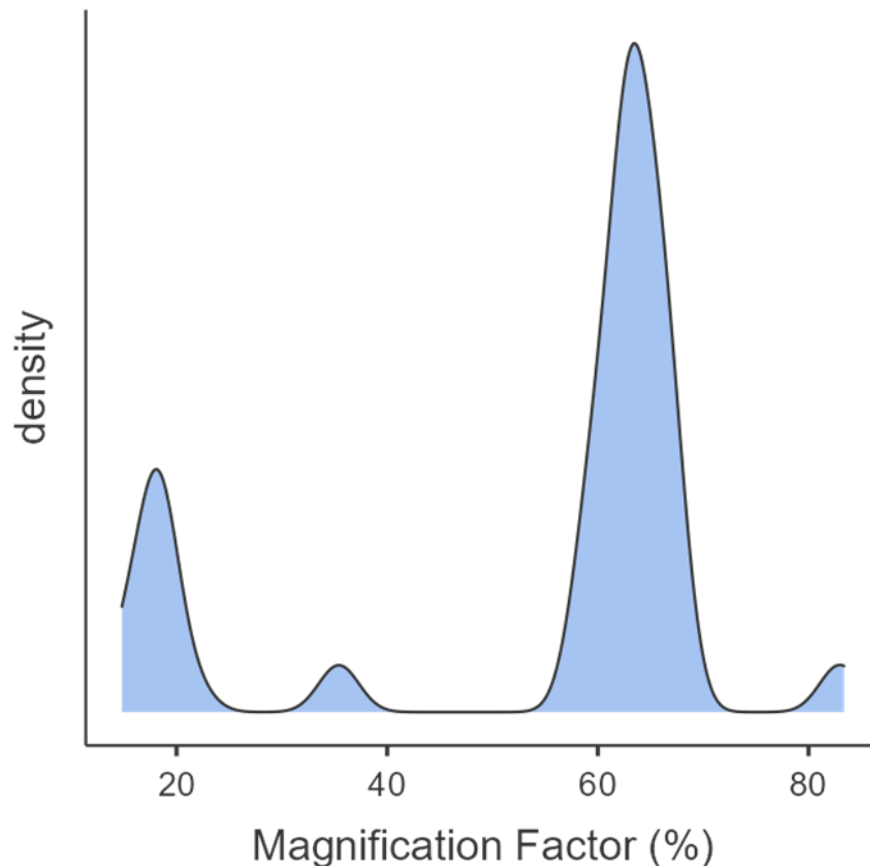


Figure 4-8: Density plot outlining the distribution of magnification factors across scleral lens OCT images.

Using Pearson's Correlation coefficient, centre thickness of the lens was significantly negatively correlated with the magnification factor ($r=-0.355$, $p=0.004$). That is, the lower the central thickness of the lens, the higher the expected magnification. This was true in most, but not all cases.

Additionally, most cases in the ~18% cluster were measurements from the baseline visit, rather than

follow-up, where the central clearance would be relatively higher due to settling. Based on these observations, it can be speculated that one may expect to see a more magnified OCT scleral lens on image in the case of a scleral lens with a relatively thinner central thickness, measured at a follow-up visit, with relatively lower central clearance.

It is possible that assumptions made here were not perfectly met, that is, the image was not taken exactly in the centre, and the imaging beam was not perfectly perpendicular to the ocular surface. Additionally, the sample size of this observation is limited and warrants further investigation on a larger number of individuals. However, since there was a clear difference noted between images, accounting for potential magnification effects was warranted.

4.6 Investigation into Correction Factor for Differing Lens Central Thicknesses

The Zenlens™, manufactured by Alden Optical (Lancaster, NY, USA) used in this study has a standard centre thickness of 0.35mm, or 350µm. As stated, participants were wearing each lens pair for a 3-week period, for a total of 6 weeks for both pairs. For this reason, it was important to correct vision as adequately as possible, with the most optimal spherical power (as discussed in Chapter 3, section 3.2.3.2). In some cases, this resulted in a low minus, plano, or plus powered lens, which due to the optics of the lens, resulted in the central thickness of the lens being greater than 350µm. As discussed in detail in Chapter 2, section 2.1, the oxygen delivery of a scleral lens system is dependent on four factors, those being:

$D_{k_{SL}}$ = oxygen permeability of the scleral lens

t_{SL} = thickness of the scleral lens

$D_{k_{FR}}$ = oxygen permeability of the fluid reservoir

t_{FR} = thickness of the fluid reservoir, or corneal clearance

The alteration of the central thickness of the scleral lens, or t_{SL} in some of the lenses presented a theoretical obstacle in maintaining consistent conditions for oxygen delivery to the ocular surface across all participants. In communication with the manufacturer of the ZenLens™, specifying a centre thickness of 0.35mm was possible in the application of a negative flex control factor, such that the lens would be made intentionally thinner centrally (Mika Hague, Personal Communication, 1 November 2019). However, this was not pursued as it would alter the overall thickness profile of the lens and create inconsistencies in lens designs across participants. Without the negative flex control factor, the maximum deviation from the standard 350µm centre thickness was 70µm, for a lens centre thickness of 420µm.

Previous research carried out by Morgan et al. established predicted central and peripheral thresholds for corneal edema due to hypoxia with soft contact lens wear.²² These thresholds were plotted as a theoretical curve relating overall oxygen transmissibility (Dk/t) at the ocular surface, and its corresponding predicted per cent increase in corneal thickness (see Figure 4-9).²² Using theoretical calculations from Michaud et al., it is possible to predict where each participant's overall Dk/t for both eyes will fall on the theoretical curve, relating this parameter to predicted per cent change in corneal thickness.^{22,61} There was a consideration of using this knowledge to calculate the overall Dk/t of the experimental system (that is, with the manufacturer-reported centre thickness), and then calculate the same parameter but using a centre thickness of 350µm. From here, the theoretical per cent difference in corneal edema could be determined by subtracting the two percentage values. This factor could be applied to the measured corneal thicknesses to correct for the change in oxygen delivery, that is, to calculate what the theoretical corneal thickness would be in the case of lens wear of a lens with a CT of 350µm, in an attempt to account for these differences.

To further investigate the need to consider this correction method, the Dk/t of the scleral lens system was calculated in experimental conditions using the manufacturer-reported centre thickness of the

lens (herein referred to as experimental thickness), and then in the case of a lens with a CT of 350 μ m (herein referred to as standardized thickness). The equation previously mentioned in Chapter 2, section 2.1, to calculate Dk/t of a scleral lens system, from Michaud et al. was used.⁶¹ Central corneal clearance values that had been corrected for refractive index and magnification as previously described in sections 4.3 and 4.5, respectively, were used. In experimental and standardized cases, the average, as well as minimum and maximum Dk/t values were determined, and plotted on the curve from Morgan et al., using Fiji.^{22,264} From this plot, theoretical percent changes in corneal thickness corresponding to these values were determined in both experimental and standardized conditions. When comparing experimental and standardized values, the minimum Dk/t of the system remained unchanged. It was found that there was a minute difference between experimental (18.14 Dk/t units) and standardized (18.56 Dk/t units) values calculated when considering the average, as well as for the maximum Dk/t in these conditions (14.46 Dk/t units for experimental conditions versus 14.82 Dk/t units for standardized). To illustrate this, average values for experimental and standardized conditions are plotted in Figure 4-9 below.

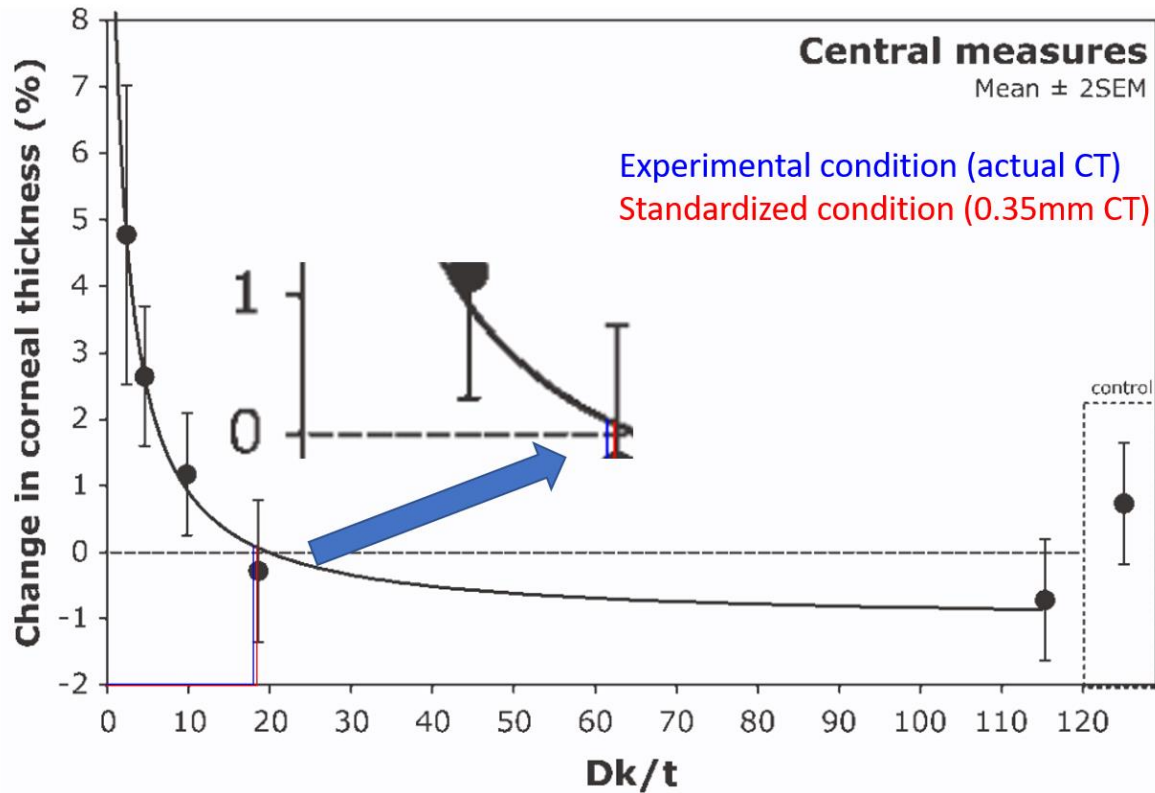


Figure 4-9: Theoretical per cent increase in corneal thickness per Dk/t unit. Average calculated Dk/t values for experimental and standardized conditions are shown to illustrate predicted per cent change and potential correction amount (being the difference in y-values of these two points on the curve). Modified from Morgan et al., 2010²², with permission.

The resultant per cent difference between experimental and standardized averages, illustrated above, or the difference in their y-values on the theoretical curve, is 0.001%. To put this amount into perspective, for a central corneal thickness of 555 μm , this change would translate to an adjustment of 0.5 μm . As previously stated, the resolution when measuring exported images from the Spectralis® OCT is 12.5 μm , which exceeds this amount of change. Further, it is theorized that when scleral lenses of high Dk lens materials are used, which is the case for this study, oxygen delivery is more limited by the tear fluid reservoir and its oxygen transmissibility, rather than the oxygen transmissibility of the scleral lens (which would depend on the central thickness of the lens).^{84,232,239}

In summary, it was decided that a correction factor would not be applied, as the resulting changes would be miniscule. Additionally, theoretical predictions in corneal thickness changes used above are based on data obtained from a study examining hypoxia as a result of soft, rather than scleral, lens wear.²² To the best of current knowledge, an equivalent study based on measurements carried out from scleral lens wear has not been performed. Secondly, this study was carried out in participants without ocular disease, which is not the case for the current study, and it is likely that the keratoconic cornea would manifest edema differently due to physiological and biomechanical deviations from the healthy population. Lastly, corneal thickness measurements were taken with the Oculus Pentacam® in the theoretical study referenced here, which was used in the current study, however, this not necessarily translatable to images taken with the Spectralis® OCT, an instrument employing a different method of extracting corneal thickness measurements.

Chapter 5

Study Results

5.1 Detailed Description of Disease Stage and Surgical History by Eye

As stated in 3.3.1, for final data analysis, sixteen eyes of eight participants were used. Seven eyes had Stage 1 keratoconus, four had Stage 2, one had Stage 3 and four had Stage 4 keratoconus. Seven eyes had a history of cross-linking (CXL), and nine eyes had not. History of CXL as well as disease severity for each eye is specifically detailed below in Table 5-1. These details will be referenced in sections of chapters to follow.

Table 5-1: Summary of eyes used for final analysis, with each eye's disease stage (Amsler-Krumeich (A-K) Classification) and history of cross-linking (CXL) surgery listed.

Participant	Eye	A-K Classification	Hx CXL
02-KC	OD	2	Y
02-KC	OS	2	Y
04-KC	OD	1	Y
04-KC	OS	2	Y
07-KC	OD	4	N
07-KC	OS	4	N
09-KC	OD	3	Y
09-KC	OS	1	N
11-KC	OD	1	N
11-KC	OS	2	N
13-KC	OD	1	N
13-KC	OS	1	N
14-KC	OD	4	N
14-KC	OS	1	N
15-KC	OD	1	Y
15-KC	OS	4	Y

5.2 Descriptive Statistics of Corneal Thickness Data

Corneal thickness data from the Pentacam® HR and Spectralis® was sorted in Microsoft Excel version 2105 (14026.20246) by instrument, tissue type (total corneal or corneal epithelial thickness),

eye (OD or OS), scan orientation (H/V/IT/IN), visit type (baseline or follow-up) and lens type (low clearance or high clearance). Descriptive statistics of epithelial and total corneal thickness were generated for each instrument and eye in every scan orientation, using jamovi 1.8.1.^{274,275} Descriptive statistics for total corneal thickness are tabulated in Appendix E, and for corneal epithelial thickness in Appendix F.

Shapiro-Wilk testing for normality was $p > 0.05$ in all instances for total corneal thickness. However, for epithelial thickness measurements, there were instances where this was not the case, indicating that these data were not normally distributed. Results of statistically significant Shapiro-Wilk testing for epithelial thickness measurements can be found in Appendix F within descriptive statistics tables.

The distributions of total and epithelial thickness for each eye and instrument, divided by visit type and lens type, were generated as part of the descriptive statistical analysis. For these distributions, scan orientations (e.g., horizontal, vertical, etc.) were grouped together to give a broader sense of the tissue thickness distribution. Then, rather than lens type (low versus high clearance), visits were categorized by chronological order (e.g., baseline 1, follow-up 2, etc.). Distributions of separate baseline measurements for each location appeared overall very similar to one another in most cases by inspection. In some cases, a slight shift of the distribution toward greater thickness values was qualitatively noted, and in other cases, a shift towards lower thickness values was noted. To illustrate this, sample density plots of each visit by location of right eye total corneal thickness measurements taken with the Spectralis® are displayed below (Figure 5-1 – Figure 5-9). Baseline distributions are displayed in blue and follow ups are in orange.

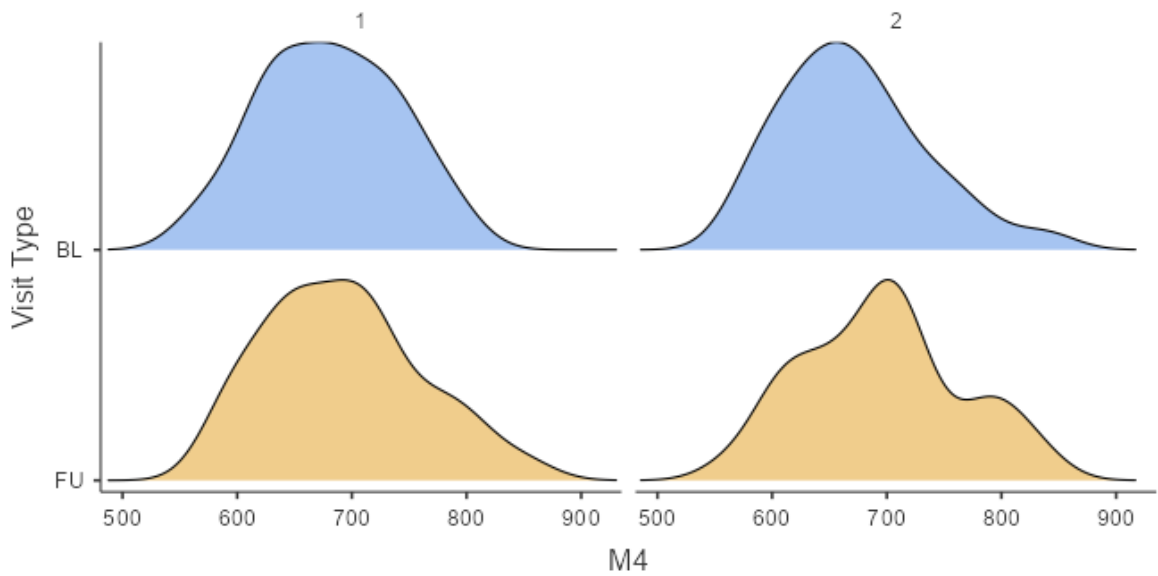


Figure 5-1: Density plots of corneal thickness at the location 4mm temporal to centre. Distributions are grouped by baseline (blue) and follow-up (orange) visits, with measurements from the first chronological pair of visits on the left, and from the second pair on the right. This grouping description applies to Figure 5-1-Figure 5-17.

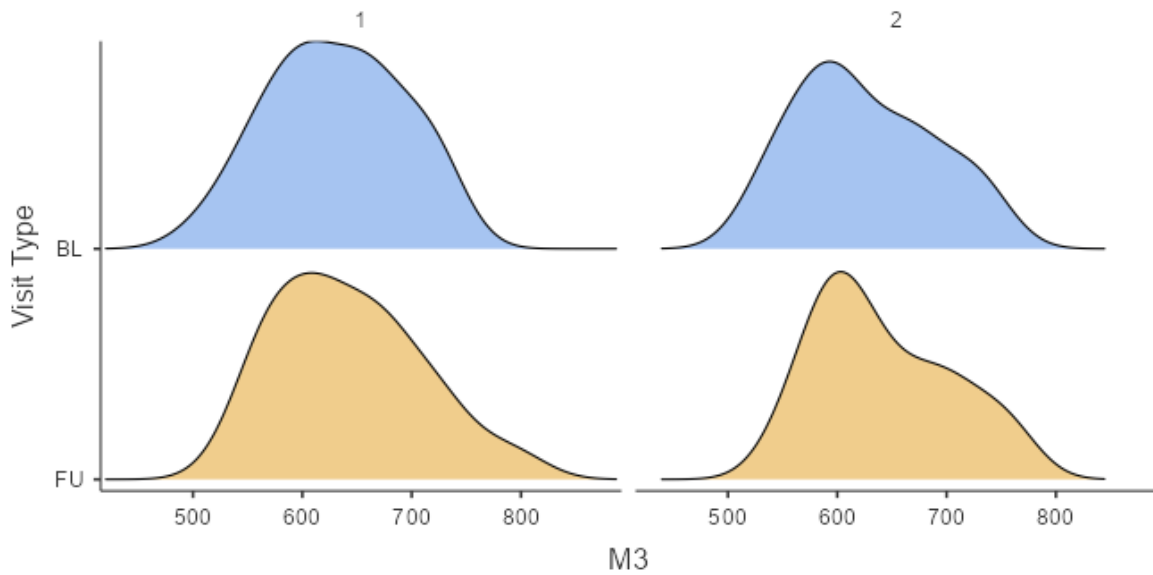


Figure 5-2: Density plots of corneal thickness at the location 3mm temporal to centre.

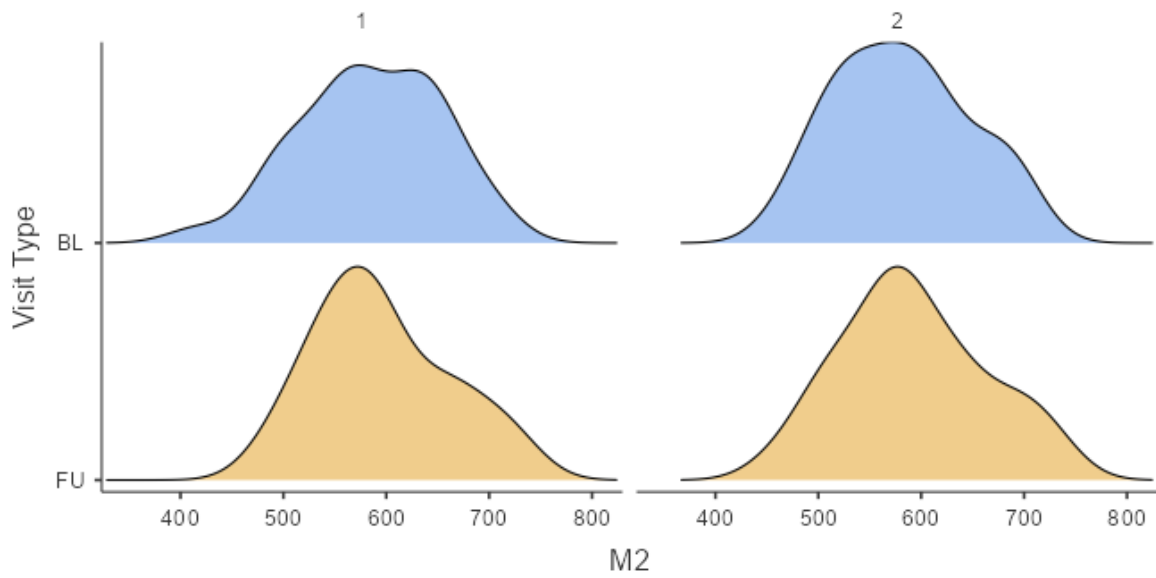


Figure 5-3: Density plots of corneal thickness at the location 2mm temporal to centre.

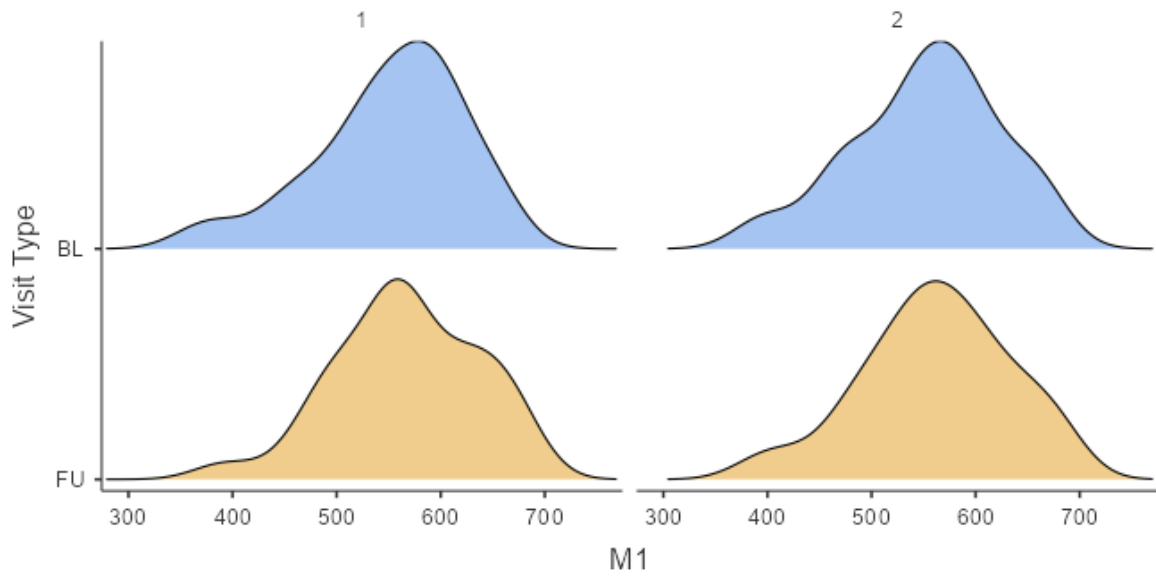


Figure 5-4: Density plots of corneal thickness at the location 1mm temporal to centre.

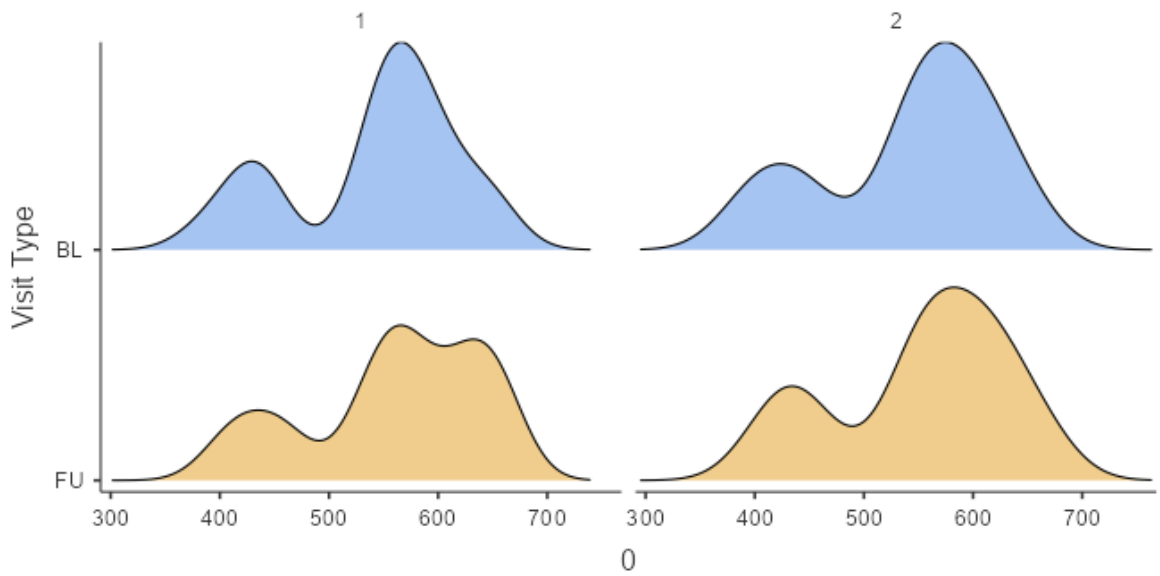


Figure 5-5: Density plots of corneal thickness at the central location.

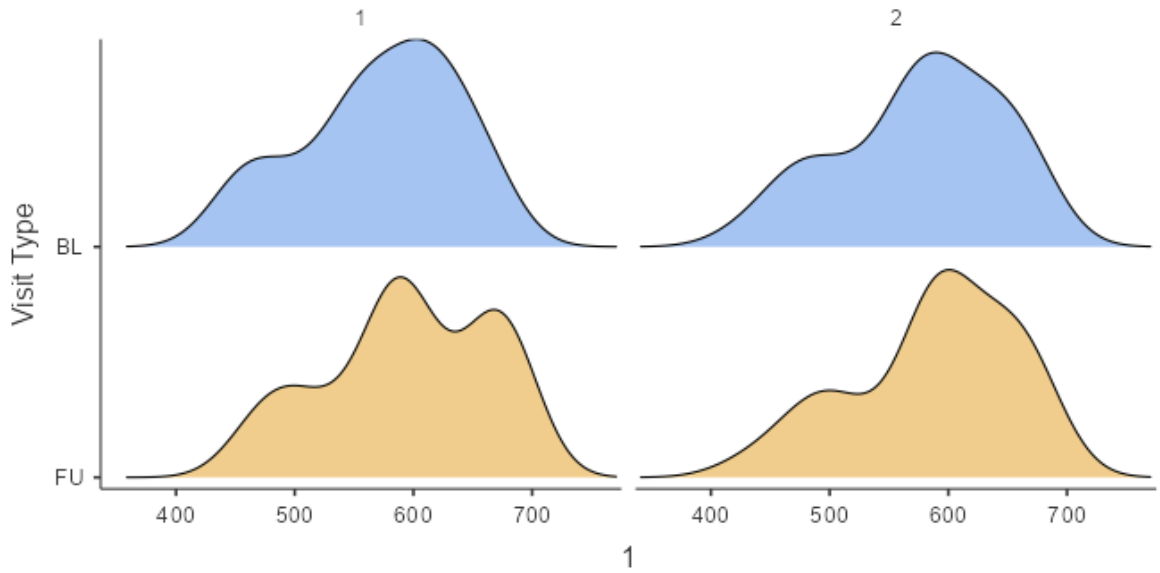


Figure 5-6: Density plots of corneal thickness at the location 1mm nasal to centre.

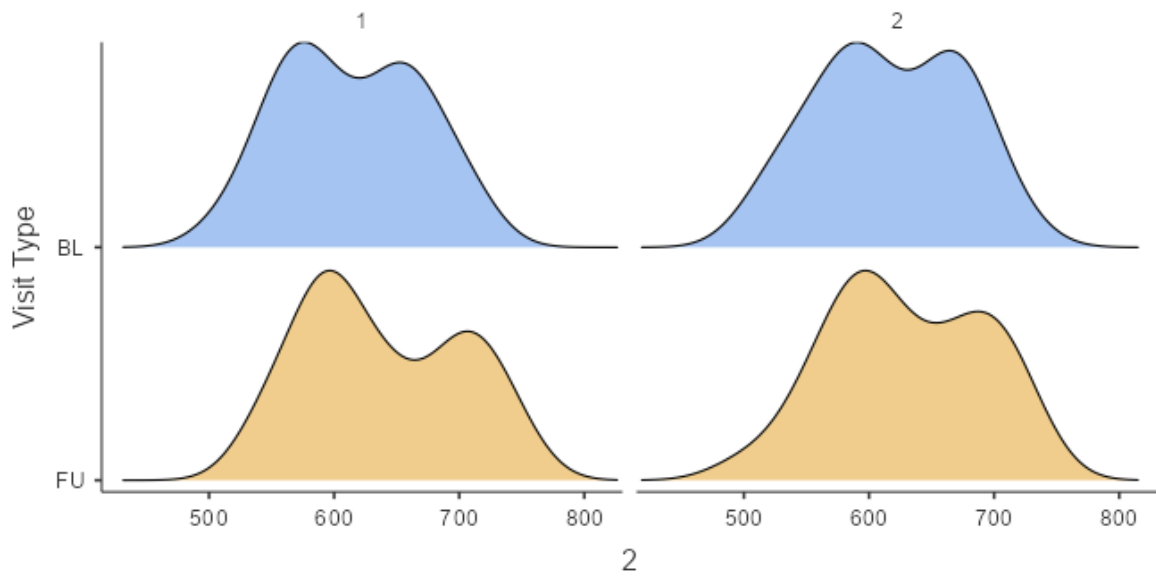


Figure 5-7: Density plots of corneal thickness at the location 2mm nasal to centre.

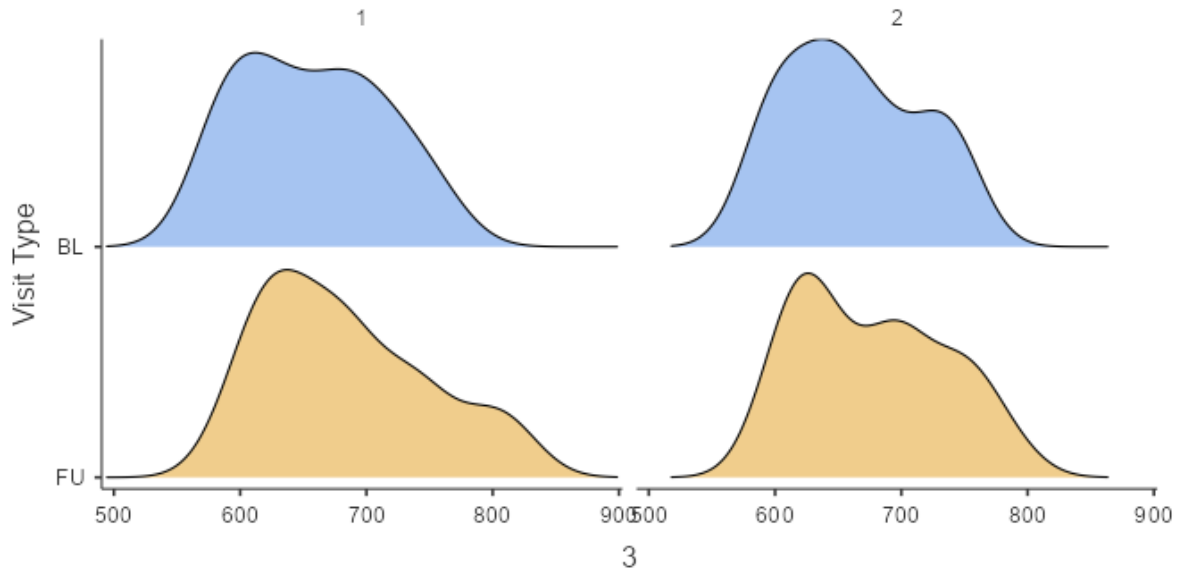


Figure 5-8: Density plots of corneal thickness at the location 3mm nasal to centre.

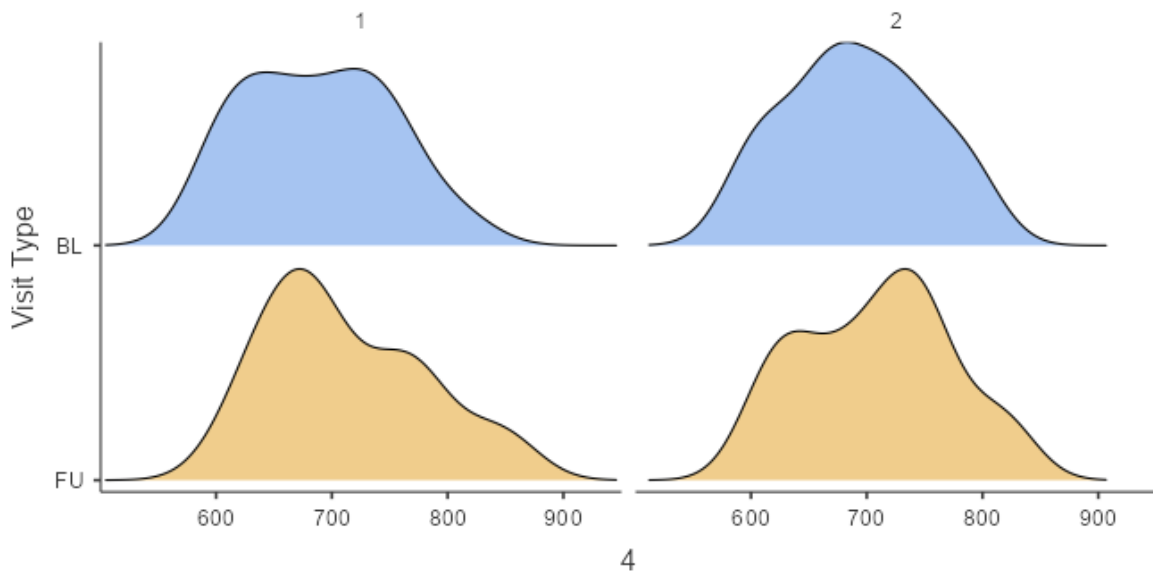


Figure 5-9: Density plots of corneal thickness at the location 4mm nasal to centre.

Quantitative analysis of corneal thickness at each location measured at baseline visits alone with paired t-tests confirmed that in all but one case (Spectralis® total corneal thickness in the left eye, measured at the central location), the difference between baselines was not statistically significant. Specifically, in cases where Shapiro-Wilk normality testing was significant, non-parametric paired t-tests with Wilcoxon signed rank testing were carried out. Initial paired t-test results in jamovi^{274,275} were manually corrected for multiple comparisons with the Holm-Bonferroni method²⁷⁶ in Microsoft Excel. Bayes factor₁₀ was also determined in this analysis.^{277,278} In the majority of cases, this value was less than 1, indicating weak support for the alternative hypothesis that baseline measurements were different from one another. Paired t-testing and Bayesian analysis is displayed in Table 5-2 for total corneal thickness and corneal epithelial thickness measurements in Table 5-3.

Table 5-2: Paired t-testing and Bayesian analysis results between baselines for total corneal thickness measurements. Location analyzed is indicated by a number after the condition, where M represents negative location values. BL1 refers to the first baseline and BL2 is the second. Statistical significance is indicated by an asterisk (*), and non-significant (NS) results of comparisons are indicated after Holm-Bonferroni correction.

Condition and Location	Test Type	Statistic	df	p	Corrected α	Significance	Bayes Factor ₁₀	$\pm\%$	
Spectralis TCT OD Paired Samples t-Test									
BL2_1	BL1_1	Wilcoxon rank	348	31	0.051	-	NS	0.848	5.30E-05
BL2_2	BL1_2	Wilcoxon rank	289	31	0.249	-	NS	0.307	1.69E-04
BL2_3	BL1_3	Wilcoxon rank	306	31	0.260	-	NS	0.402	4.58E-05
BL2_4	BL1_4	Wilcoxon rank	228	27	0.355	-	NS	0.407	2.35E-04
BL2_M3	BL1_M3	Wilcoxon rank	204	31	0.394	-	NS	0.370	7.52E-05
BL2_M4	BL1_M4	Wilcoxon rank	230	31	0.536	-	NS	0.382	6.30E-05
BL2_M2	BL1_M2	Wilcoxon rank	202	31	0.537	-	NS	0.286	2.14E-04
BL2_M1	BL1_M1	Wilcoxon rank	277	31	0.818	-	NS	0.193	6.05E-04
BL2_0	BL1_0	Wilcoxon rank	227	31	0.846	-	NS	0.194	6.02E-04
Spectralis TCT OS Paired Samples t-Test									
BL2_0	BL1_0	Wilcoxon rank	376	30	0.003	0.006	*	13.633	1.16E-08
BL2_3	BL1_3	Wilcoxon rank	333	29	0.013	0.006	NS	4.880	2.76E-08
BL2_2	BL1_2	Wilcoxon rank	305	30	0.021	-	NS	5.411	1.65E-08
BL2_1	BL1_1	Wilcoxon rank	248	30	0.022	-	NS	3.593	1.99E-08
BL2_4	BL1_4	Wilcoxon rank	262	27	0.186	-	NS	0.478	2.54E-04
BL2_M4	BL1_M4	Wilcoxon rank	115	24	0.324	-	NS	0.538	6.71E-07
BL2_M2	BL1_M2	Wilcoxon rank	142	30	0.402	-	NS	0.339	1.48E-05
BL2_M3	BL1_M3	Wilcoxon rank	187	30	0.517	-	NS	0.307	4.17E-05
BL2_M1	BL1_M1	Wilcoxon rank	205	30	0.710	-	NS	0.222	2.17E-04
Pentacam TCT OD Paired Samples t-Test									
BL2_M2	BL1_M2	Wilcoxon rank	353	31	0.041	0.006	NS	1.608	2.18E-08
BL2_M4	BL1_M4	Wilcoxon rank	268	30	0.145	-	NS	0.515	4.46E-05
BL2_M3	BL1_M3	Wilcoxon rank	339	31	0.163	-	NS	0.577	7.46E-06
BL2_M1	BL1_M1	Wilcoxon rank	236	31	0.262	-	NS	0.474	9.11E-06
BL2_0	BL1_0	Wilcoxon rank	174	31	0.512	-	NS	0.207	5.17E-04
BL2_1	BL1_1	Wilcoxon rank	164	31	0.555	-	NS	0.239	3.65E-04
BL2_4	BL1_4	Wilcoxon rank	212	30	0.673	-	NS	0.194	3.32E-04
BL2_2	BL1_2	Wilcoxon rank	192	31	0.962	-	NS	0.189	6.31E-04
BL2_3	BL1_3	Wilcoxon rank	232	31	0.992	-	NS	0.195	5.92E-04
Pentacam TCT OS Paired Samples t-Test									
BL2_3	BL1_3	Wilcoxon rank	344	31	0.023	0.006	NS	2.436	1.74E-08
BL2_4	BL1_4	Wilcoxon rank	345	30	0.058	-	NS	1.046	3.61E-08
BL2_2	BL1_2	Wilcoxon rank	279	31	0.085	-	NS	1.099	7.46E-05
BL2_0	BL1_0	Wilcoxon rank	206	31	0.107	-	NS	0.283	2.22E-04
BL2_M1	BL1_M1	Wilcoxon rank	263	31	0.334	-	NS	0.327	1.31E-04
BL2_1	BL1_1	Wilcoxon rank	264	31	0.529	-	NS	0.259	2.91E-04
BL2_M4	BL1_M4	Wilcoxon rank	278	31	0.808	-	NS	0.196	5.86E-04
BL2_M3	BL1_M3	Wilcoxon rank	276	31	0.837	-	NS	0.189	6.35E-04
BL2_M2	BL1_M2	Wilcoxon rank	210	31	0.891	-	NS	0.190	6.23E-04

Table 5-3: Paired t-testing and Bayesian analysis results between results obtained at both baseline visits for corneal epithelial thickness measurements. BL1 refers to the first chronological baseline and BL2 is the second. Location analyzed is indicated by a number after the condition, where M represents negative location values. Statistical significance is indicated as in Table 5-2 after Holm-Bonferroni correction.

Condition and Location		Test Type	Statistic	df	p	Corrected α	Significance	Bayes Factor ₁₀	$\pm\%$
Spectralis ECT OD Paired Samples t-Test									
BL2_M1	BL1_M1	Wilcoxon rank	310	31	0.015	0.006	NS	4.551	1.21E-08
BL2_M2	BL1_M2	Wilcoxon rank	124	31	0.074	-	NS	1.165	7.80E-05
BL2_3	BL1_3	Wilcoxon rank	306	31	0.133	-	NS	0.965	6.52E-05
BL2_2	BL1_2	Wilcoxon rank	152	31	0.160	-	NS	0.420	3.37E-05
BL2_1	BL1_1	Wilcoxon rank	264	31	0.168	-	NS	0.470	1.02E-05
BL2_0	BL1_0	Wilcoxon rank	165	31	0.217	-	NS	0.365	8.03E-05
BL2_4	BL1_4	Wilcoxon rank	287	31	0.267	-	NS	0.212	4.90E-04
BL2_M3	BL1_M3	Wilcoxon rank	194	30	0.619	-	NS	0.223	2.13E-04
BL2_M4	BL1_M4	Wilcoxon rank	218	31	0.741	-	NS	0.212	4.89E-04
Spectralis ECT OS Paired Samples t-Test									
BL2_M4	BL1_M4	Wilcoxon rank	121	28	0.105	-	NS	0.904	8.14E-08
BL2_1	BL1_1	Wilcoxon rank	151	30	0.241	-	NS	0.441	1.82E-05
BL2_M3	BL1_M3	Wilcoxon rank	180	30	0.424	-	NS	0.323	2.64E-05
BL2_M2	BL1_M2	Wilcoxon rank	215	30	0.540	-	NS	0.194	3.31E-04
BL2_3	BL1_3	Wilcoxon rank	181	30	0.624	-	NS	0.197	3.18E-04
BL2_M1	BL1_M1	Wilcoxon rank	198	30	0.838	-	NS	0.215	2.39E-04
BL2_4	BL1_4	Wilcoxon rank	210	29	0.880	-	NS	0.200	1.15E-04
BL2_0	BL1_0	Wilcoxon rank	109	30	0.896	-	NS	0.241	1.57E-04
BL2_2	BL1_2	Wilcoxon rank	202	30	0.991	-	NS	0.198	3.10E-04

Knowing that corneal thicknesses measured at baseline visits did not vary significantly in all but one case from subjective density plots and statistical analysis, baseline measurements were averaged for initial RMANOVAs, and subsequent paired t-testing detailed in the next section (5.3).

5.3 Initial Repeated-Measures ANOVA and Subsequent Paired Samples t-Tests

Initially, parametric RMANOVAs were carried out on all total corneal thickness data due to its normal distribution in descriptive analysis (5.2), and non-parametric RMANOVAs were performed on all epithelial thickness data due to its non-normal distribution in this analysis.

5.3.1 Total Corneal Thickness: Parametric RMANOVAs

For total corneal thickness data, RMANOVAs in jamovi 1.8.1 were performed.^{274,275,279} Data were arranged by location for this analysis, that is, each corneal location (e.g. 4mm temporal relative to centre) had its own column in the statistical software. Due to the spherical nature of the data presumably due to limited sample size, both between-subjects effect testing (F-statistics and p-values) and sphericity testing were not available within statistical software. To obtain results of RMANOVA within-subject effects testing for condition in the software, no sphericity correction was made. Results of this analysis are displayed below in Table 5-4. From this analysis, there was only one instance of non-significance, for the Spectralis® OS measurements in the inferior temporal meridian.

Table 5-4: RMANOVA results for condition (baseline average, LC follow-up, HC follow-up) for total corneal thickness. Measurements are sorted by scan orientation and eye.

Eye	Scan Orientation	Instrument	Within Subjects Effects - Condition		
			F	p	η^2_p
OD	H	Spectralis	10.540	*0.002	0.637
OS	H	Spectralis	12.931	*<0.001	0.649
OD	V	Spectralis	19.297	*<0.001	0.794
OS	V	Spectralis	7.180	*0.007	0.506
OD	IT	Spectralis	15.855	*0.002	0.799
OS	IT	Spectralis	3.326	0.141	0.625
OD	IN	Spectralis	20.090	*<0.001	0.801
OS	IN	Spectralis	18.570	*<0.001	0.788
OD	H	Pentacam	8.920	*0.003	0.560
OS	H	Pentacam	25.830	*<0.001	0.773
OD	V	Pentacam	9.770	*0.003	0.620
OS	V	Pentacam	15.090	*<0.001	0.715
OD	IT	Pentacam	9.300	*0.003	0.571
OS	IT	Pentacam	8.560	*0.004	0.550
OD	IN	Pentacam	5.600	*0.016	0.444
OS	IN	Pentacam	34.650	*<0.001	0.832

Because data were deemed too spherical to warrant sphericity testing within the statistical software, it was determined that selective paired t-tests with the Holm-Bonferroni correction applied²⁷⁶ would be used to compare between conditions of baseline, low clearance follow-up and high clearance follow-up, in lieu of post-hoc RMANOVA tests. For this testing, data were not split by location. Specifically, all baseline measurements for a particular eye and scan orientation were listed in one column for the baseline visit average measurements, and two other columns for each follow-up. Paired t-tests were performed between measurements from the averaged baseline visits and each individual follow-up visits, and between the low and high clearance follow-up visits. Shapiro-Wilk testing for normality was again carried out, and in cases where data were not normally distributed, paired t-tests with Wilcoxon signed rank testing was carried out. Manual correction of these data in Microsoft Excel using the Holm-Bonferroni method²⁷⁶ was performed. These data for total corneal thickness for both the Spectralis® and Pentacam® HR are displayed below in Table 5-5. Descriptive thickness values used for paired t-testing are shown in Table 5-6. For total corneal thickness, scleral lens wear always yielded a statistically significant increase in corneal thickness compared to baseline, whether it was at the low or high clearance lens follow-up visit. The high clearance lens follow-up corneal thickness was at times, but not consistently statistically significantly greater than the low clearance lens follow-up corneal thickness. However, for the vertical meridian, there was a consistent statistically significantly greater corneal thickness when comparing the high to the low clearance lens follow-up for both the eyes, and for both Pentacam® and Spectralis® measurements. More often, statistically significant differences between the high and low clearance follow-ups were noted with Pentacam®, compared to Spectralis® measurements. Aside from the vertical meridian, significantly greater corneal thickness measurements comparing high to low clearance lens follow-ups were noted for the Pentacam® OS horizontal meridian, the Pentacam® OD inferior temporal meridian, and for the OS inferior nasal meridian for both the Spectralis® and Pentacam®.

Table 5-5: Results of specific paired t-tests for total corneal thickness measurements comparing all locations between baseline, low clearance follow-up, and high clearance follow-up conditions. Statistical significance is indicated as in Table 5-2 after Holm-Bonferroni correction.

Conditions Compared		Test Type	Statistic	df	p	Corrected α	Significance	Test Type	Statistic	df	p	Corrected α	Significance
		Spectralis TCT OD Horizontal Paired Samples t-Test						Pentacam TCT OD Horizontal Paired Samples t-Test					
Baseline	LC Follow-Up	Wilcoxon rank	384	71	<.001	0.017	*	Wilcoxon rank	204	71	<.001	0.017	*
Baseline	HC Follow-Up	Wilcoxon rank	358	70	<.001	0.025	*	Wilcoxon rank	244	71	<.001	0.025	*
LC Follow-Up	HC Follow-Up	Wilcoxon rank	905	70	0.145	-	NS	Wilcoxon rank	830	71	0.078	-	NS
		Spectralis TCT OS Horizontal Paired Samples t-Test						Pentacam TCT OS Horizontal Paired Samples t-Test					
Baseline	LC Follow-Up	Wilcoxon rank	333	71	<.001	0.017	*	Wilcoxon rank	102	71	<.001	0.017	*
Baseline	HC Follow-Up	Wilcoxon rank	525	71	<.001	0.025	*	Wilcoxon rank	46	71	<.001	0.025	*
LC Follow-Up	HC Follow-Up	Wilcoxon rank	1152	71	0.938	-	NS	Wilcoxon rank	621.5	71	<.001	0.050	*
		Spectralis TCT OD Vertical Paired Samples t-Test						Pentacam TCT OD Vertical Paired Samples t-Test					
Baseline	LC Follow-Up	Wilcoxon rank	107	69	<.001	0.017	*	Wilcoxon rank	280	70	<.001	0.017	*
Baseline	HC Follow-Up	Wilcoxon rank	134	70	<.001	0.025	*	Wilcoxon rank	123	70	<.001	0.025	*
LC Follow-Up	HC Follow-Up	Wilcoxon rank	616	68	0.003	0.050	*	Wilcoxon rank	849	70	0.014	0.050	*
		Spectralis TCT OS Vertical Paired Samples t-Test						Pentacam TCT OS Vertical Paired Samples t-Test					
Baseline	LC Follow-Up	Wilcoxon rank	430	71	<.001	0.017	*	Student's t	-9.47	70	<.001	0.017	*
Baseline	HC Follow-Up	Wilcoxon rank	358	71	<.001	0.025	*	Student's t	-11.02	71	<.001	0.025	*
LC Follow-Up	HC Follow-Up	Wilcoxon rank	775	71	0.01	0.050	*	Student's t	-3.75	70	<.001	0.050	*
		Spectralis TCT OD Inferior Temporal Paired Samples t-Test						Pentacam TCT OD Inferior Temporal Paired Samples t-Test					
Baseline	LC Follow-Up	Wilcoxon rank	193	68	<.001	0.017	*	Wilcoxon rank	224	71	<.001	0.017	*
Baseline	HC Follow-Up	Wilcoxon rank	273	70	<.001	0.025	*	Wilcoxon rank	134	71	<.001	0.025	*
LC Follow-Up	HC Follow-Up	Wilcoxon rank	951	68	0.429	-	NS	Wilcoxon rank	747	71	0.006	0.050	*
		Spectralis TCT OS Inferior Temporal Paired Samples t-Test						Pentacam TCT OS Inferior Temporal Paired Samples t-Test					
Baseline	LC Follow-Up	Wilcoxon rank	247	66	<.001	0.017	*	Wilcoxon rank	181	71	<.001	0.017	*
Baseline	HC Follow-Up	Wilcoxon rank	272	65	<.001	0.025	*	Wilcoxon rank	192	71	<.001	0.025	*
LC Follow-Up	HC Follow-Up	Wilcoxon rank	856	64	0.523	-	NS	Wilcoxon rank	911	71	0.077	-	NS
		Spectralis TCT OD Inferior Nasal Paired Samples t-Test						Pentacam TCT OD Inferior Nasal Paired Samples t-Test					
Baseline	LC Follow-Up	Wilcoxon rank	316	69	<.001	0.017	*	Wilcoxon rank	190	71	<.001	0.017	*
Baseline	HC Follow-Up	Wilcoxon rank	299	61	<.001	0.025	*	Wilcoxon rank	355	71	<.001	0.025	*
LC Follow-Up	HC Follow-Up	Wilcoxon rank	686	61	0.484	-	NS	Wilcoxon rank	1045	71	0.436	-	NS
		Spectralis TCT OS Inferior Nasal Paired Samples t-Test						Pentacam TCT OS Inferior Nasal Paired Samples t-Test					
Baseline	LC Follow-Up	Wilcoxon rank	386	70	<.001	0.017	*	Wilcoxon rank	94.5	71	<.001	0.017	*
Baseline	HC Follow-Up	Wilcoxon rank	287	70	<.001	0.025	*	Wilcoxon rank	18	71	<.001	0.025	*
LC Follow-Up	HC Follow-Up	Wilcoxon rank	568	69	0.002	0.050	*	Wilcoxon rank	492.5	71	<.001	0.050	*

Table 5-6: Descriptive values for each condition for total corneal thickness, sorted by meridian, instrument, and eye, used for each paired t-test (results displayed in Table 5-5).

Condition	N	Mean	Median	SD	SE	Condition	N	Mean	Median	SD	SE
Spectralis TCT OD Horizontal Paired Samples t-Test						Pentacam TCT OD Horizontal Paired Samples t-Test					
BL	72	612	617	74.5	8.78	BL	72	567	567	88.8	10.5
LC FU	72	622	623	77.1	9.09	LC FU	72	576	577	90.7	10.7
BL	71	611	616	74.3	8.82	BL	72	567	567	88.8	10.5
HC FU	71	626	628	82.7	9.82	HC FU	72	578	584	93.6	11.0
LC FU	71	621	619	76.8	9.11	LC FU	72	576	577	90.7	10.7
HC FU	71	626	628	82.7	9.82	HC FU	72	578	584	93.6	11.0
Spectralis TCT OS Horizontal Paired Samples t-Test						Pentacam TCT OS Horizontal Paired Samples t-Test					
BL	72	618	615	75.0	8.84	BL	72	580	572	89.1	10.5
LC FU	72	631	628	82.9	9.76	LC FU	72	589	586	89.8	10.6
BL	72	618	615	75.0	8.84	BL	72	580	572	89.1	10.5
HC FU	72	630	628	83.4	9.83	HC FU	72	592	585	93.2	11.0
LC FU	72	631	628	82.9	9.76	LC FU	72	589	586	89.8	10.6
HC FU	72	630	628	83.4	9.83	HC FU	72	592	585	93.2	11.0
Spectralis TCT OD Vertical Paired Samples t-Test						Pentacam TCT OD Vertical Paired Samples t-Test					
BL	70	614	607	88.0	10.50	BL	71	586	572	97.9	11.6
LC FU	70	629	619	93.7	11.20	LC FU	71	594	578	101.2	12.0
BL	71	614	608	87.2	10.30	BL	71	586	572	97.9	11.6
HC FU	71	634	635	96.1	11.40	HC FU	71	597	586	105.7	12.5
LC FU	69	627	616	93.3	11.20	LC FU	71	594	578	101.2	12.0
HC FU	69	633	633	97.2	11.70	HC FU	71	597	586	105.7	12.5
Spectralis TCT OS Vertical Paired Samples t-Test						Pentacam TCT OS Vertical Paired Samples t-Test					
BL	72	627	627	89.9	10.60	BL	71	593	593	94.4	11.2
LC FU	72	637	629	94.0	11.10	LC FU	71	602	600	98.1	11.6
BL	72	627	627	89.9	10.60	BL	72	596	594	96.8	11.4
HC FU	72	641	636	100.8	11.90	HC FU	72	608	608	102.5	12.1
LC FU	72	637	629	94.0	11.10	LC FU	71	602	600	98.1	11.6
HC FU	72	641	636	100.8	11.90	HC FU	71	606	606	100.3	11.9
Spectralis TCT OD Inferior Temporal Paired Samples t-Test						Pentacam TCT OD Inferior Temporal Paired Samples t-Test					
BL	69	605	600	78.0	9.39	BL	72	576	569	93.1	11.0
LC FU	69	621	613	81.7	9.83	LC FU	72	584	577	97.0	11.4
BL	71	610	603	81.2	9.64	BL	72	576	569	93.1	11.0
HC FU	71	629	623	88.7	10.53	HC FU	72	586	581	97.3	11.5
LC FU	69	621	613	81.7	9.83	LC FU	72	584	577	97.0	11.4
HC FU	69	623	621	83.6	10.07	HC FU	72	586	581	97.3	11.5
Spectralis TCT OS Inferior Temporal Paired Samples t-Test						Pentacam TCT OS Inferior Temporal Paired Samples t-Test					
BL	67	615	610	87.3	10.70	BL	72	584	585	92.1	10.9
LC FU	67	628	625	88.1	10.80	LC FU	72	592	594	94.2	11.1
BL	66	615	609	87.9	10.80	BL	72	584	585	92.1	10.9
HC FU	66	629	623	98.0	12.10	HC FU	72	594	592	98.5	11.6
LC FU	65	624	617	88.6	11.00	LC FU	72	592	594	94.2	11.1
HC FU	65	626	618	97.4	12.10	HC FU	72	594	592	98.5	11.6
Spectralis TCT OD Inferior Nasal Paired Samples t-Test						Pentacam TCT OD Inferior Nasal Paired Samples t-Test					
BL	70	613	616	77.5	9.27	BL	72	577	575	91.8	10.8
LC FU	70	626	623	83.3	9.96	LC FU	72	586	579	96.9	11.4
BL	62	624	620	69.4	8.82	BL	72	577	575	91.8	10.8
HC FU	62	640	636	77.7	9.87	HC FU	72	587	582	99.1	11.7
LC FU	62	638	635	73.8	9.38	LC FU	72	586	579	96.9	11.4
HC FU	62	640	636	77.7	9.87	HC FU	72	587	582	99.1	11.7
Spectralis TCT OS Inferior Nasal Paired Samples t-Test						Pentacam TCT OS Inferior Nasal Paired Samples t-Test					
BL	71	626	628	84.3	10.00	BL	72	589	587	91.6	10.8
LC FU	71	636	632	91.1	10.80	LC FU	72	598	597	94.3	11.1
BL	71	627	628	85.4	10.10	BL	72	589	587	91.6	10.8
HC FU	71	643	632	97.3	11.60	HC FU	72	603	599	97.7	11.5
LC FU	70	635	631	91.6	11.00	LC FU	72	598	597	94.3	11.1
HC FU	70	641	632	95.8	11.40	HC FU	72	603	599	97.7	11.5

5.3.2 Corneal Epithelial Thickness: Non-Parametric RMANOVAs and Paired Samples Wilcoxon Testing

Friedman RMANOVAs in jamovi 1.8.1. were carried out on epithelial thickness by comparing all baseline measurements to all low and high clearance follow-up measurements.^{274,275,280} Data were not separated by location due to the nature of this rank-based analysis. See Table 5-7 below for analysis. One instance of statistical significance was noted, for the OD inferior nasal meridian measurements.

Table 5-7: Friedman RMANOVA for corneal epithelial thickness measured by the Spectralis®.

Eye	Direction	χ^2	df	p
OD	H	1.730	2	0.422
OS	H	0.478	2	0.788
OD	V	5.980	2	0.050
OS	V	0.064	2	0.969
OD	IT	4.830	2	0.089
OS	IT	2.840	2	0.241
OD	IN	7.020	2	*0.030
OS	IN	5.350	2	0.069

As with total corneal thickness measurements, to investigate statistically significant differences between conditions, it was determined that selective paired t-testing with Holm-Bonferroni correction would be carried out. After Shapiro-Wilk testing for normality, cases where data were not normally distributed were identified, and Wilcoxon signed rank t-testing was carried out in these cases. Results of paired t-testing for corneal epithelial thickness measurements are displayed below in Table 5-8, and thickness values used for statistical analysis are shown in Table 5-9. In all but two instances, changes across conditions were not statistically significant, shown in Table 5-8. Exceptions occurred in the OS inferior nasal meridian, specifically from the low to high clearance follow-up and from baseline to low clearance follow-up. In the latter case, a statistically significant decrease in average epithelial thickness was noted, indicating corneal epithelial thinning, as shown in Table 5-9.

Table 5-8: Results of specific paired t-tests for corneal epithelial thickness measurements comparing all locations between each combination of condition comparisons. Statistical significance is indicated as in Table 5-2 after Holm-Bonferroni correction.

Conditions Compared		Test Type	Statistic	df	p	Corrected α	Significance
Spectralis ECT OD Horizontal Paired Samples t-Test							
Baseline	LC Follow-Up	Wilcoxon rank	953	71	0.180	-	NS
Baseline	HC Follow-Up	Wilcoxon rank	1039	70	0.315	-	NS
LC Follow-Up	HC Follow-Up	Wilcoxon rank	904	70	0.889	-	NS
Spectralis ECT OS Horizontal Paired Samples t-Test							
Baseline	HC Follow-Up	Wilcoxon rank	1357	71	0.373	-	NS
LC Follow-Up	HC Follow-Up	Wilcoxon rank	976	71	0.495	-	NS
Baseline	LC Follow-Up	Wilcoxon rank	1288	71	0.632	-	NS
Spectralis ECT OD Vertical Paired Samples t-Test							
Baseline	HC Follow-Up	Wilcoxon rank	815	70	0.029	0.017	NS
Baseline	LC Follow-Up	Wilcoxon rank	929	70	0.067	-	NS
LC Follow-Up	HC Follow-Up	Wilcoxon rank	894	69	0.880	-	NS
Spectralis ECT OS Vertical Paired Samples t-Test							
Baseline	HC Follow-Up	Wilcoxon rank	1082	71	0.349	-	NS
LC Follow-Up	HC Follow-Up	Wilcoxon rank	1167	71	0.811	-	NS
Baseline	LC Follow-Up	Wilcoxon rank	1290	71	0.947	-	NS
Spectralis ECT OD Inferior Temporal Paired Samples t-Test							
Baseline	LC Follow-Up	Wilcoxon rank	868	70	0.063	-	NS
LC Follow-Up	HC Follow-Up	Wilcoxon rank	1276	70	0.186	-	NS
Baseline	HC Follow-Up	Wilcoxon rank	1197	71	0.886	-	NS
Spectralis ECT OS Inferior Temporal Paired Samples t-Test							
LC Follow-Up	HC Follow-Up	Wilcoxon rank	1142	71	0.160	-	NS
Baseline	HC Follow-Up	Wilcoxon rank	1518	71	0.170	-	NS
Baseline	LC Follow-Up	Wilcoxon rank	1157	71	0.765	-	NS
Spectralis ECT OD Inferior Nasal Paired Samples t-Test							
Baseline	HC Follow-Up	Wilcoxon rank	682	62	0.059	-	NS
LC Follow-Up	HC Follow-Up	Wilcoxon rank	580	62	0.232	-	NS
Baseline	LC Follow-Up	Wilcoxon rank	1371	71	0.454	-	NS
Spectralis ECT OS Inferior Nasal Paired Samples t-Test							
LC Follow-Up	HC Follow-Up	Wilcoxon rank	615	71	0.007	0.017	*
Baseline	LC Follow-Up	Wilcoxon rank	1531	71	0.014	0.025	*
Baseline	HC Follow-Up	Wilcoxon rank	1014	71	0.561	-	NS

Table 5-9: Descriptive values used for statistical analysis for corneal epithelial thickness, as displayed in Table 5-8. Values used for each paired t-test are listed.

Condition	N	Mean	Median	SD	SE	Condition	N	Mean	Median	SD	SE
Spectralis ECT OD Horizontal Paired Samples t-Test						Spectralis ECT OS Horizontal Paired Samples t-Test					
BL	72	64.2	63.9	8.97	1.06	BL	72	64.1	65.4	10.60	1.25
LC FU	72	65.3	65.8	11.61	1.37	LC FU	72	63.8	64.6	11.50	1.35
BL	71	64.2	63.9	9.03	1.07	BL	72	64.1	65.4	10.60	1.25
HC FU	71	65.2	64.8	10.16	1.21	HC FU	72	62.7	64.1	12.40	1.46
LC FU	71	65.0	65.7	11.46	1.36	LC FU	72	63.8	64.6	11.50	1.35
HC FU	71	65.2	64.8	10.16	1.21	HC FU	72	62.7	64.1	12.40	1.46
Spectralis ECT OD Vertical Paired Samples t-Test						Spectralis ECT OS Vertical Paired Samples t-Test					
BL	71	62.7	63.1	8.50	1.01	BL	72	63.7	63.7	8.73	1.03
LC FU	71	64.5	63.7	10.47	1.24	LC FU	72	63.7	64.3	10.23	1.21
BL	71	62.6	63.1	8.54	1.01	BL	72	63.7	63.7	8.73	1.03
HC FU	71	64.9	64.1	10.82	1.28	HC FU	72	64.2	65.4	11.34	1.34
LC FU	70	64.7	63.8	10.49	1.25	LC FU	72	63.7	64.3	10.23	1.21
HC FU	70	65.0	64.3	10.84	1.30	HC FU	72	64.2	65.4	11.34	1.34
Spectralis ECT OD Inferior Temporal Paired Samples t-Test						Spectralis ECT OS Inferior Temporal Paired Samples t-Test					
BL	71	62.9	63.4	12.20	1.45	BL	72	63.0	62.8	9.89	1.17
LC FU	71	65.4	66.4	11.30	1.34	LC FU	72	63.5	64.0	11.40	1.34
BL	72	62.8	63.2	12.20	1.43	BL	72	63.0	62.8	9.89	1.17
HC FU	72	63.8	64.3	12.60	1.48	HC FU	72	61.4	62.9	12.43	1.46
LC FU	71	65.4	66.4	11.30	1.34	LC FU	72	63.5	64.0	11.40	1.34
HC FU	71	63.8	64.2	12.60	1.50	HC FU	72	61.4	62.9	12.43	1.46
Spectralis ECT OD Inferior Nasal Paired Samples t-Test						Spectralis ECT OS Inferior Nasal Paired Samples t-Test					
BL	72	64.4	64.0	9.15	1.08	BL	72	65.6	65.7	10.30	1.22
LC FU	72	63.8	64.4	12.18	1.44	LC FU	72	62.9	64.2	11.40	1.34
BL	63	64.5	64.2	8.27	1.04	BL	72	65.6	65.7	10.30	1.22
HC FU	63	66.1	64.8	9.52	1.20	HC FU	72	66.6	65.8	12.10	1.43
LC FU	63	65.1	64.4	10.89	1.37	LC FU	72	62.9	64.2	11.40	1.34
HC FU	63	66.1	64.8	9.52	1.20	HC FU	72	66.6	65.8	12.10	1.43

5.4 Illustration of Regional Changes in Corneal Thickness

Following a more generalized statistical approach to the data previously described in 5.3, location-specific changes were explored. Further, these changes were examined on both an overall group basis (5.4.1, 5.4.2), as well as with a descriptive individual method (5.4.3). Both approaches are described and illustrated below.

5.4.1 Group Analysis: Estimated Marginal Means of Pentacam® Corneal Thickness

From RMANOVA testing in jamovi 1.8.1²⁸¹ described in 5.3.1 performed on all participants' data, estimated marginal means plots were generated for the group. These graphs illustrate the estimated marginal mean total corneal thickness measured at each corneal location under each condition, that is, at the averaged baseline (BL) and at both follow-up visits (LC and HC). Location parameters on the x-axis marked with an M (e.g., M4) refer to negative location values, and values without this letter are positive location values, according to the convention described in Chapter 4, section 4.4, shown in Table 4-3. These plots are shown for the group means of total corneal thickness measured by the Pentacam® HR for each eye and each meridian below in Figure 5-10 – Figure 5-17. It can be noted from these plots that there is a greater separation between baseline (blue line) and both follow-ups (grey and gold lines) at the conventionally negative corneal locations. That is, with scleral lens wear in general, there was a qualitatively greater increase in corneal thickness measured by the Pentacam® regionally in the temporal, inferior, inferior temporal, and superior temporal locations.

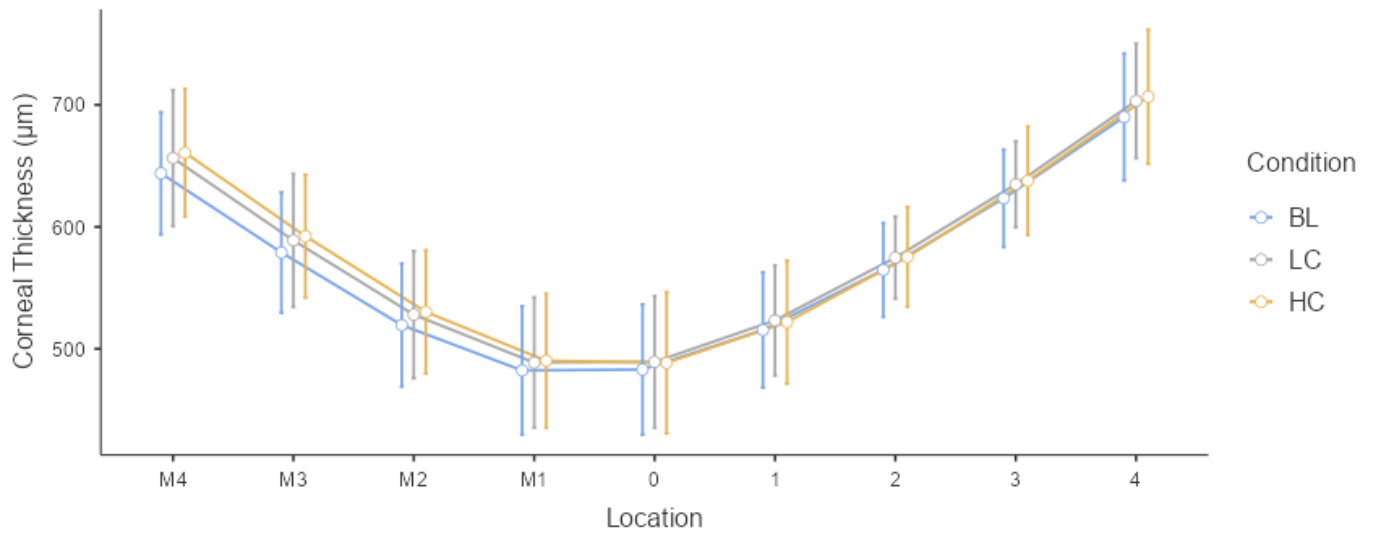


Figure 5-10: Estimated Marginal Means - Pentacam® OD Horizontal (T-N) Meridian. For Figure 5-10 – Figure 5-17, locations on the x-axis marked with “M” indicate negative location values previously described, and condition is colour-coded above by baseline average (BL), low clearance follow-up (LC) and high clearance follow-up (HC) visit measurements.

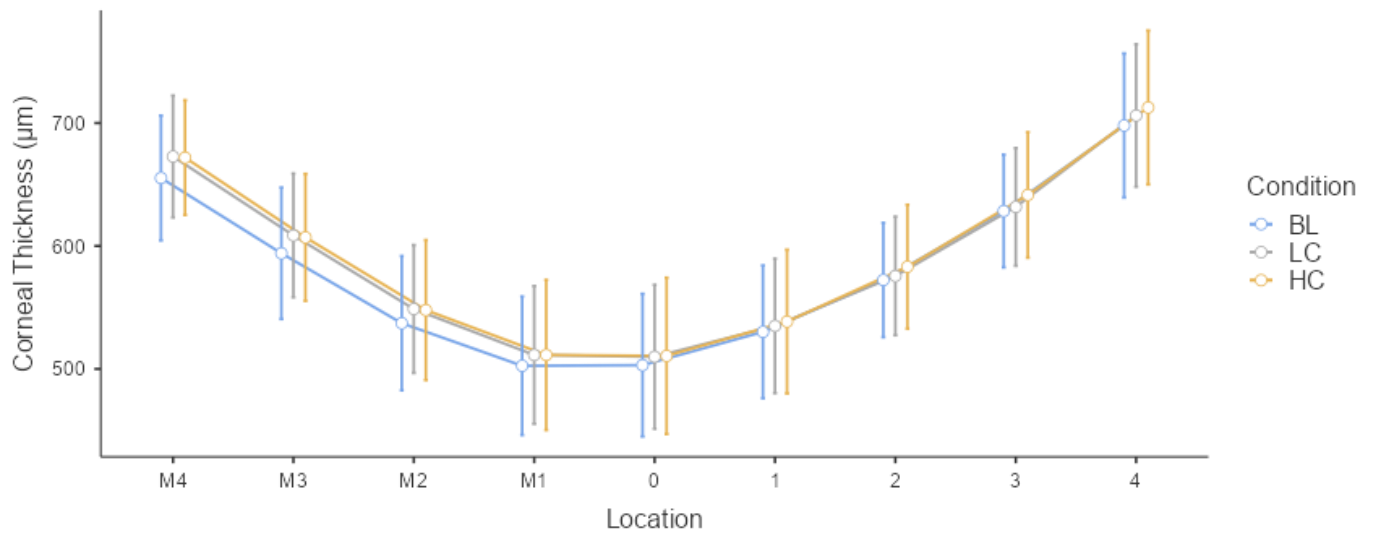


Figure 5-11: Estimated Marginal Means - Pentacam® OS Horizontal (T-N) Meridian

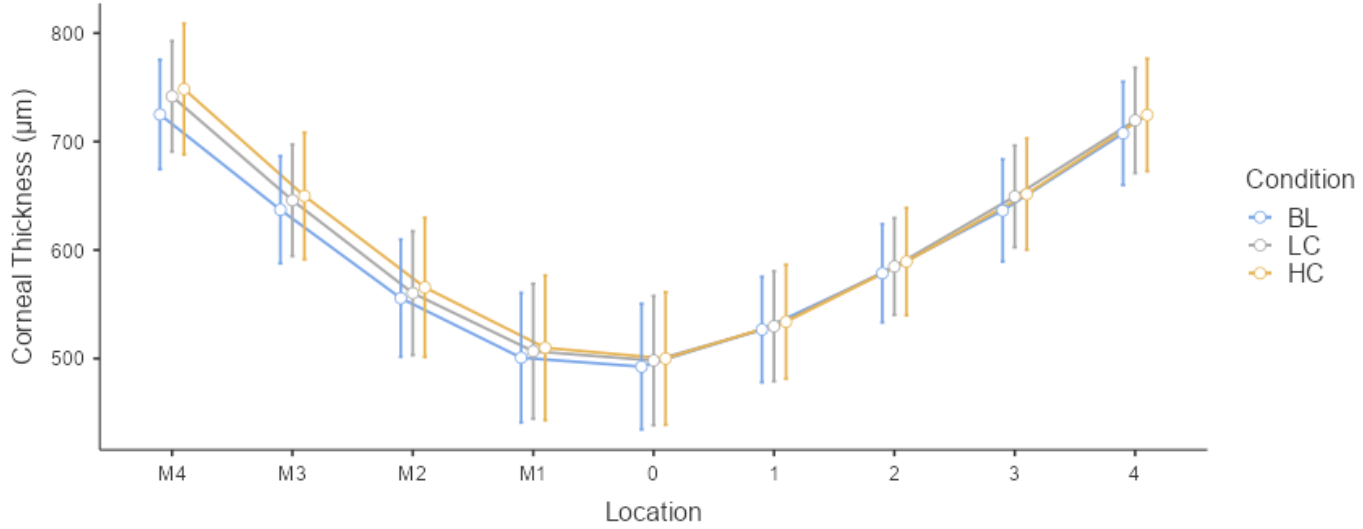


Figure 5-12: Estimated Marginal Means - Pentacam® OD Vertical (I-S) Meridian

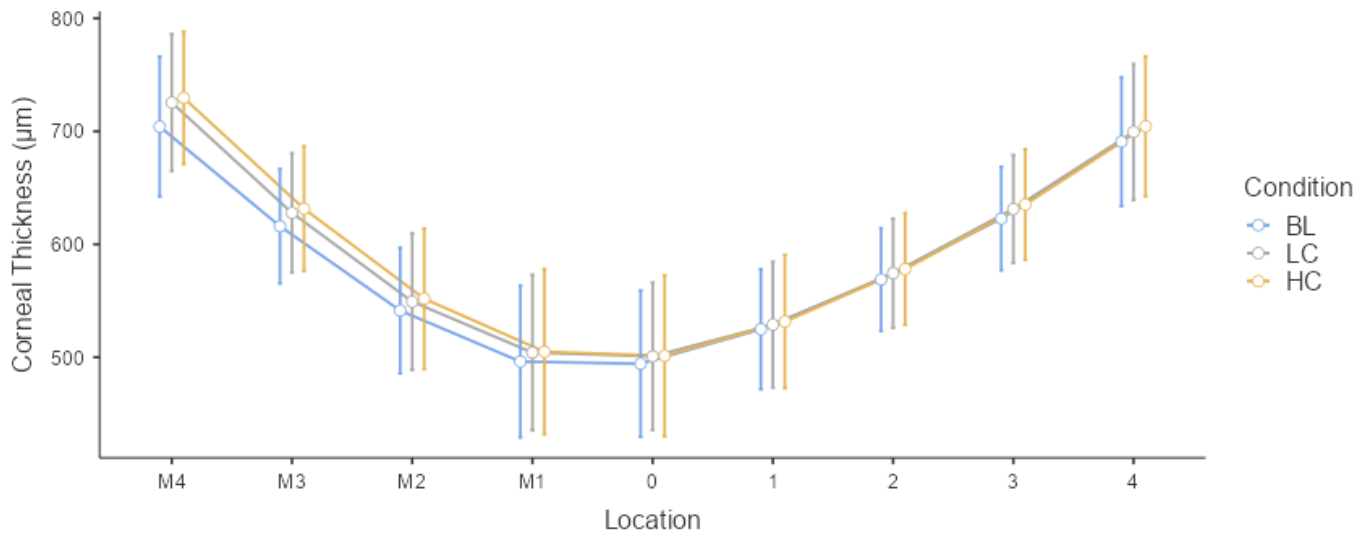


Figure 5-13: Estimated Marginal Means - Pentacam® OS Vertical (I-S) Meridian

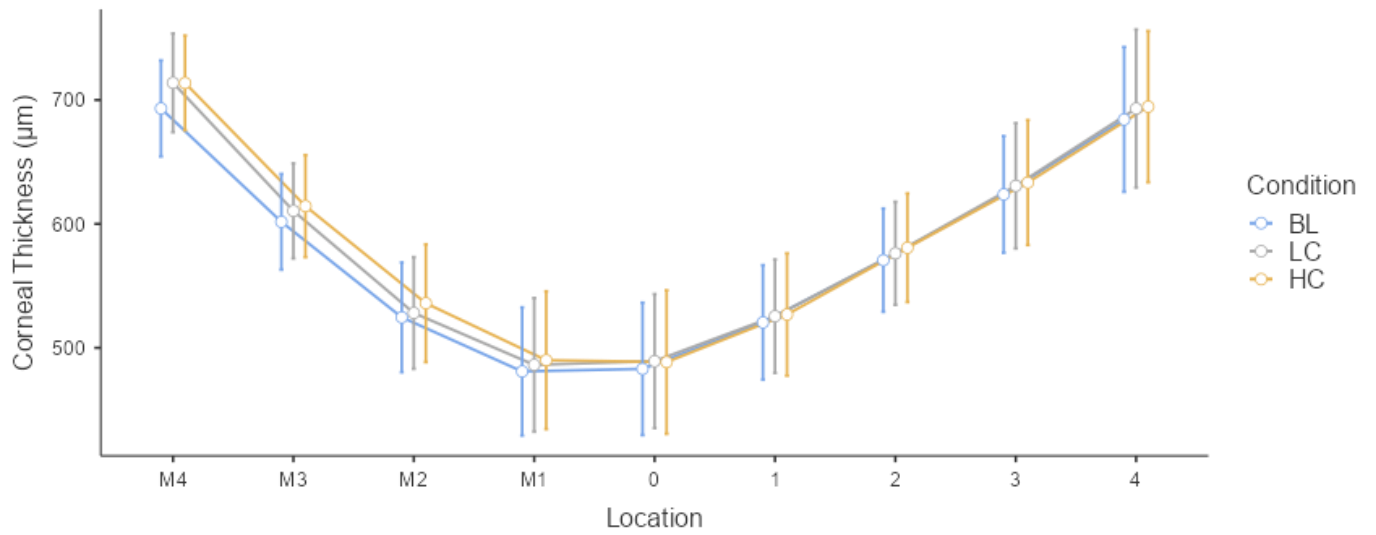


Figure 5-14: Estimated Marginal Means - Pentacam® OD Oblique (IT-SN) Meridian

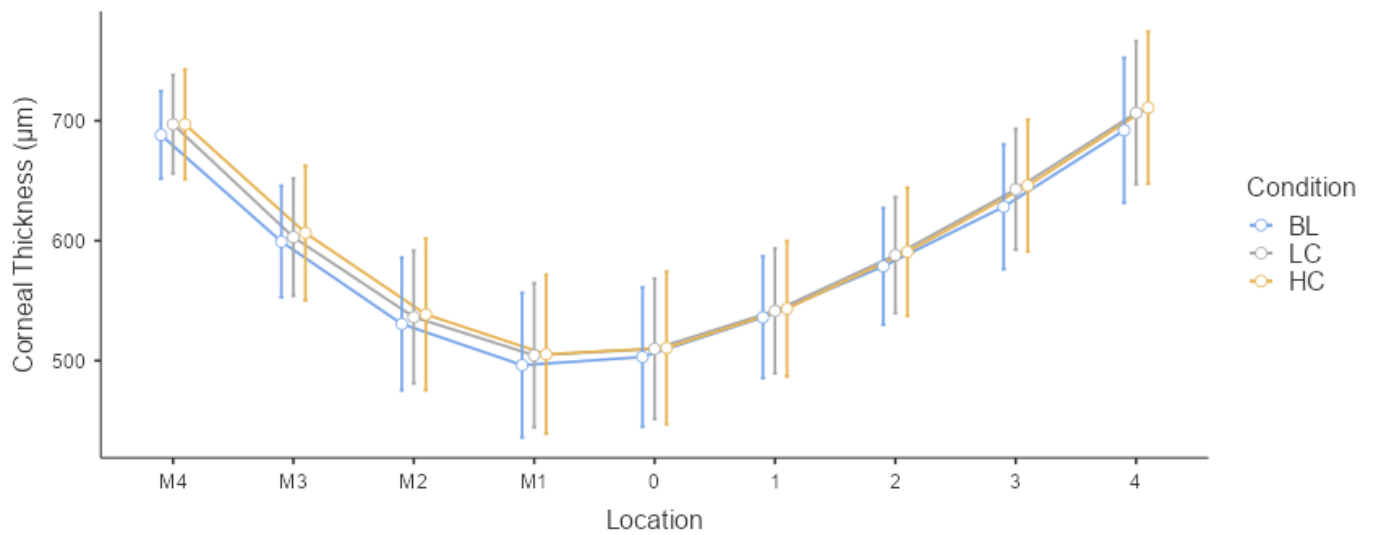


Figure 5-15: Estimated Marginal Means - Pentacam® OS Oblique (IT-SN) Meridian

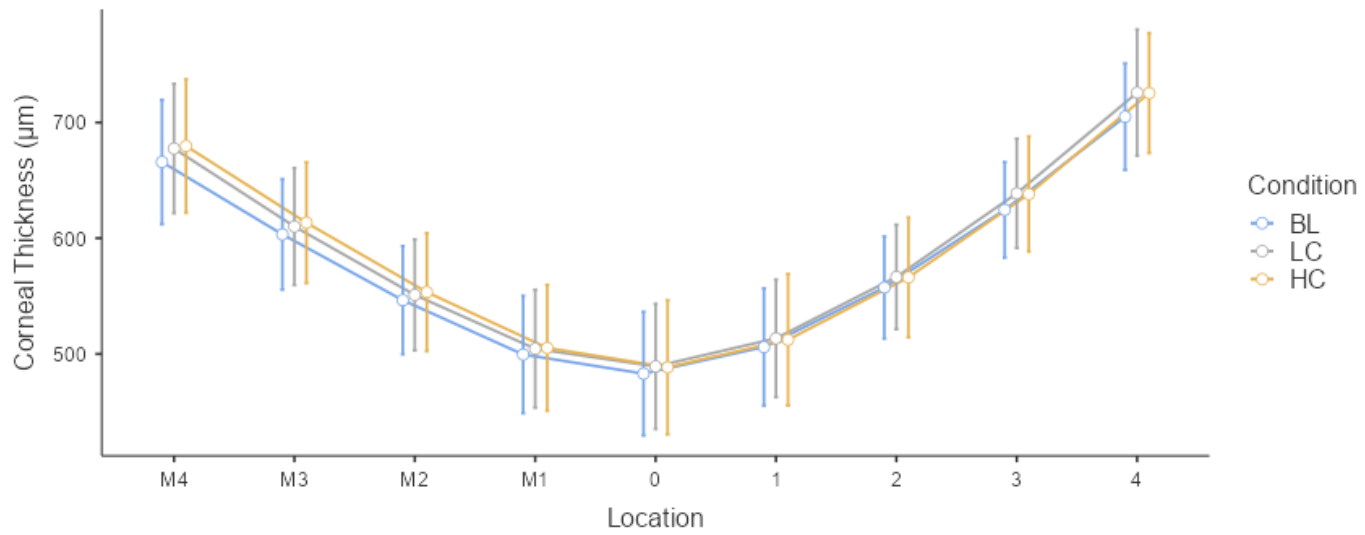


Figure 5-16: Estimated Marginal Means - Pentacam® OD Oblique (ST-IN)

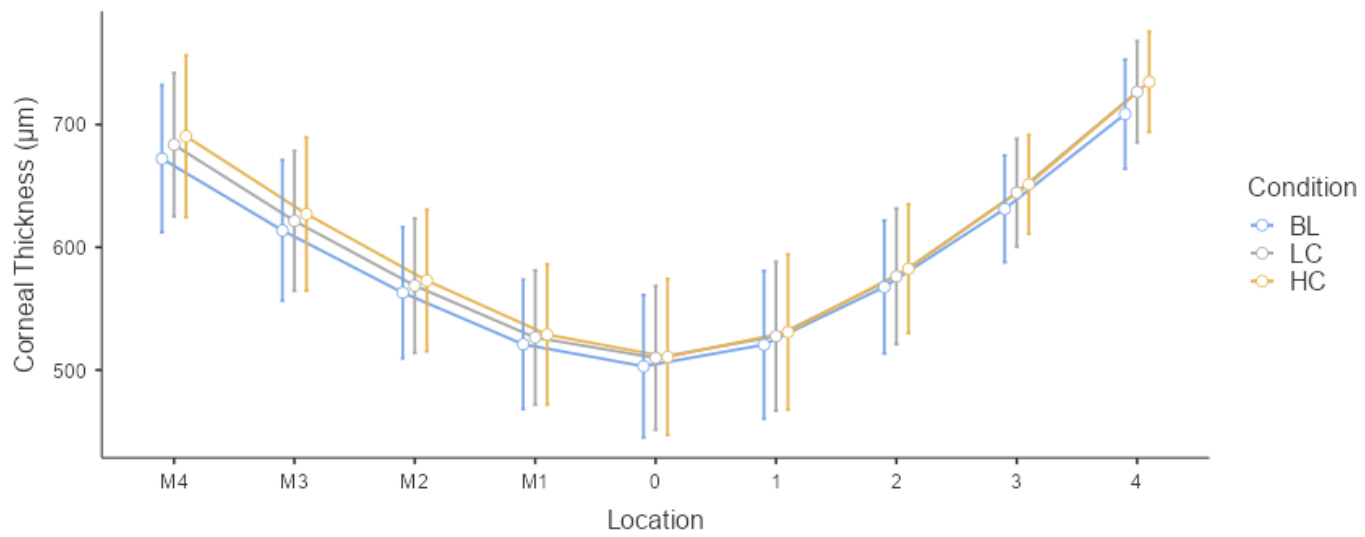


Figure 5-17: Estimated Marginal Means - Pentacam® OS Oblique (ST-IN)

5.4.2 Group Analysis: Descriptive Percent Changes in Corneal Thickness

Percent change in corneal thickness at each location was calculated for each eye and scan orientation from the average of the two baselines. The calculation was made as follows:

$$\% \text{change} = \frac{\text{follow up}_{\text{LC/HC}} - \text{baseline}_{\text{avg}}}{|\text{baseline}_{\text{avg}}|} \times 100\%$$

Since in most cases, there was not a significant difference in corneal epithelial thickness across visits (determined in 5.3.2, results displayed in Table 5-8), percent change was calculated only for total corneal thickness from baseline to low (Table 5-10) and high clearance (Table 5-11) follow-up visits, measured by the Spectralis® and Pentacam® HR.

Table 5-10: Percent change in total corneal thickness from baseline to low clearance

Eye	Instrument	Direction	Baseline to Low Clearance Follow-Up								
			-4	-3	-2	-1	0	1	2	3	4
OD	Spectralis	H	-0.65	1.53	-0.08	1.15	2.16	3.15	2.94	2.17	3.10
OS	Spectralis	H	1.55	0.66	0.53	0.30	1.79	2.32	3.37	3.34	3.99
OD	Spectralis	V	3.68	2.51	2.68	2.69	1.55	1.95	1.70	1.67	3.52
OS	Spectralis	V	1.12	0.63	2.31	1.92	0.95	1.52	1.20	1.35	2.55
OD	Spectralis	IT	4.53	1.86	1.60	2.11	2.60	2.30	2.24	3.25	2.68
OS	Spectralis	IT	-0.06	1.39	1.21	1.14	2.53	2.30	2.87	3.35	3.61
OD	Spectralis	IN	2.17	2.71	1.27	1.74	1.51	2.25	1.26	3.30	2.48
OS	Spectralis	IN	2.50	1.49	1.38	1.37	0.64	1.39	1.25	0.93	1.98
OD	Pentacam	H	1.88	1.65	1.64	1.34	1.30	1.59	1.88	1.93	2.00
OS	Pentacam	H	2.72	2.56	2.27	1.81	1.38	0.93	0.56	0.50	1.19
OD	Pentacam	V	2.33	0.48	0.06	0.85	1.30	0.88	1.37	2.41	2.45
OS	Pentacam	V	3.11	1.96	1.34	1.51	1.38	0.76	0.89	1.37	1.23
OD	Pentacam	IT	3.01	1.49	0.66	1.05	1.30	0.99	0.97	1.07	1.21
OS	Pentacam	IT	1.28	0.61	1.13	1.73	1.38	0.98	1.64	2.37	2.14
OD	Pentacam	IN	1.76	1.11	0.82	1.00	1.30	1.52	1.65	2.24	2.90
OS	Pentacam	IN	1.73	1.30	1.02	1.04	1.38	1.36	1.52	2.12	2.63

Table 5-11: Percent change in total corneal thickness from baseline to high clearance

Eye	Instrument	Direction	Baseline to High Clearance Follow-Up								
			-4	-3	-2	-1	0	1	2	3	4
OD	Spectralis	H	2.27	0.18	1.32	1.98	2.44	2.66	3.92	2.95	4.23
OS	Spectralis	H	1.96	0.97	1.09	1.13	2.94	1.72	1.62	1.80	3.10
OD	Spectralis	V	4.27	3.47	3.09	2.73	3.11	3.32	3.02	2.50	3.70
OS	Spectralis	V	4.39	2.25	3.32	2.66	-0.34	1.84	0.95	1.26	2.89
OD	Spectralis	IT	3.20	4.15	2.73	4.21	3.16	1.53	2.18	3.82	3.46
OS	Spectralis	IT	0.58	2.06	0.87	0.48	2.15	2.94	2.46	3.43	4.19
OD	Spectralis	IN	0.89	0.31	1.18	1.25	2.38	3.97	5.01	5.00	2.98
OS	Spectralis	IN	2.12	2.85	3.39	2.42	1.25	0.94	2.12	2.92	3.24
OD	Pentacam	H	2.63	2.34	2.15	1.65	1.05	1.22	1.87	2.28	2.42
OS	Pentacam	H	2.62	2.24	1.97	1.65	1.36	1.50	1.85	2.03	2.06
OD	Pentacam	V	3.17	1.67	1.36	1.28	1.05	1.13	1.81	2.21	2.21
OS	Pentacam	V	3.78	2.41	2.03	1.81	1.36	1.27	1.67	1.82	1.89
OD	Pentacam	IT	3.00	2.10	2.14	1.83	1.05	1.18	1.74	1.50	1.48
OS	Pentacam	IT	1.22	1.08	1.36	1.69	1.36	1.23	2.03	2.79	2.73
OD	Pentacam	IN	2.05	1.63	1.21	1.08	1.05	1.14	1.48	2.10	2.86
OS	Pentacam	IN	2.64	2.11	1.69	1.44	1.36	1.96	2.71	3.25	3.78

5.4.3 Individual and Subcategory Analysis: Corneal Thickness Difference Mapping

Due to the limitation of generalizing findings based on group analysis from a statistical perspective due to sample size, examination of data on an individual level, along with disease severity and surgical history subcategories, were explored. To visualize changes in total corneal and corneal epithelial thickness as measured, thickness values were entered into RStudio (version 1.4.1106),²⁸² where a custom code in R (Darwin Kernel Version 20.5.0)²⁸³ was written to generate maps displaying regional differences in thickness. Additional software packages referenced here were also used to generate these maps.^{284–287} Maps were produced via the subtraction of baseline from follow-up values at each location, displaying the amount and direction of change with an appropriate saturation and hue of colour, respectively. Cone apex locations were indicated with a small dot. As it was established in 5.2 that both baselines may be used, each baseline was used for their respective follow-up visit. Maps are displayed in a confrontation manner, that is, where the changes would be located as if one were looking directly at the participant. These maps for each participant are displayed in figures below for total corneal thickness (Spectralis®: Figure 5-18-Figure 5-25; Pentacam® Figure 5-26-Figure 5-33), followed by difference maps for corneal epithelial thickness measured by the Spectralis® in Figure 5-34-Figure 5-41.

SPECTRALIS: 02-KC Total Thickness Difference Follow-Up - Baseline

Classification	Status
Absolute Disease Stage	Early (Stage 2)
Relative Disease Stage (between eyes)	More Severe
100um thickness change	18.3%

Classification	Status
Absolute Disease Stage	Early (Stage 2)
Relative Disease Stage (between eyes)	Less Severe
100um thickness change	17.6%

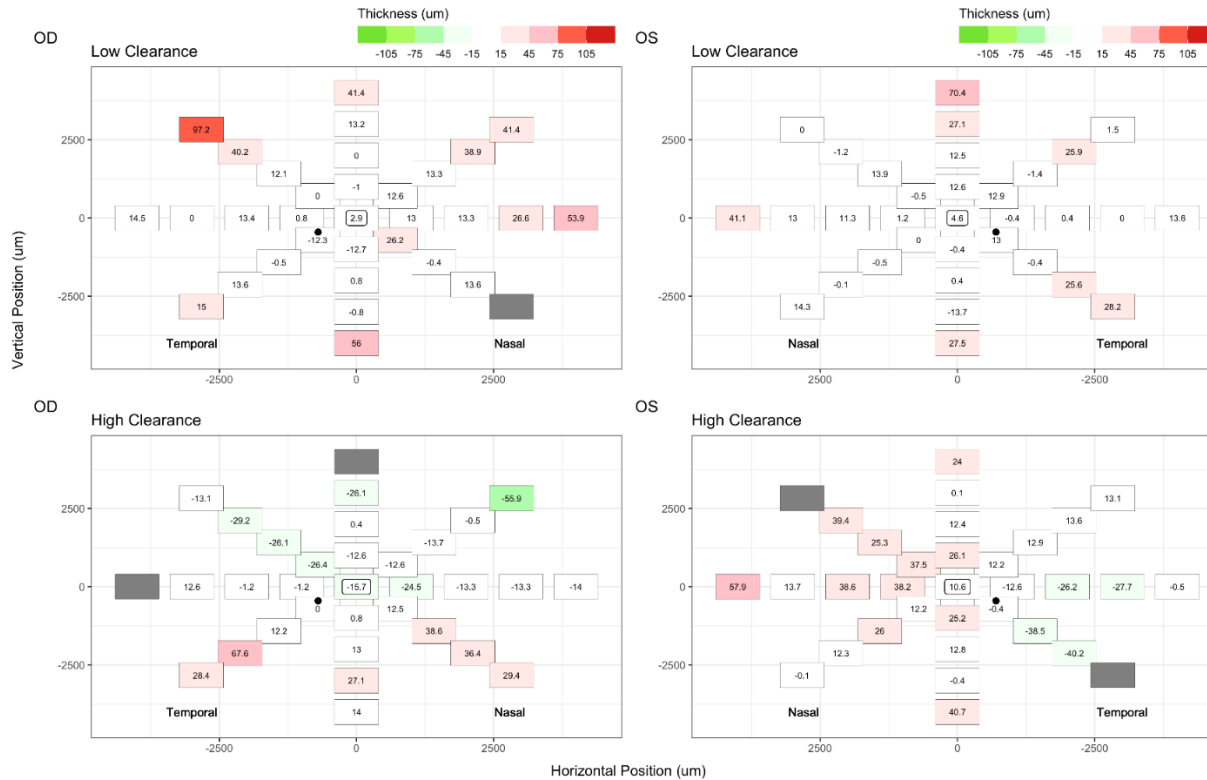


Figure 5-18: Difference maps of total corneal thickness subtracting baseline from follow-up values for Participant 02-KC, as measured by the Spectralis®. This individual has Stage 2 keratoconus OU. Maps are presented in confrontation view, with LC as the top two plots and HC as the bottom two, and cone apex location is indicated by a dot in each map. This is consistent for Figure 5-18-Figure 5-41. For Figure 5-18-Figure 5-33, red shades represent an increase in thickness, where green shades represent a decrease in thickness. Grey shades indicate missing data for Figure 5-18-Figure 5-41.

SPECTRALIS: 04-KC Total Thickness Difference Follow-Up - Baseline

Classification	Status
Absolute Disease Stage	Early (Stage 1)
Relative Disease Stage (between eyes)	Less Severe
100um thickness change	17.8%

Classification	Status
Absolute Disease Stage	Early (Stage 2)
Relative Disease Stage (between eyes)	More Severe
100um thickness change	18.3%

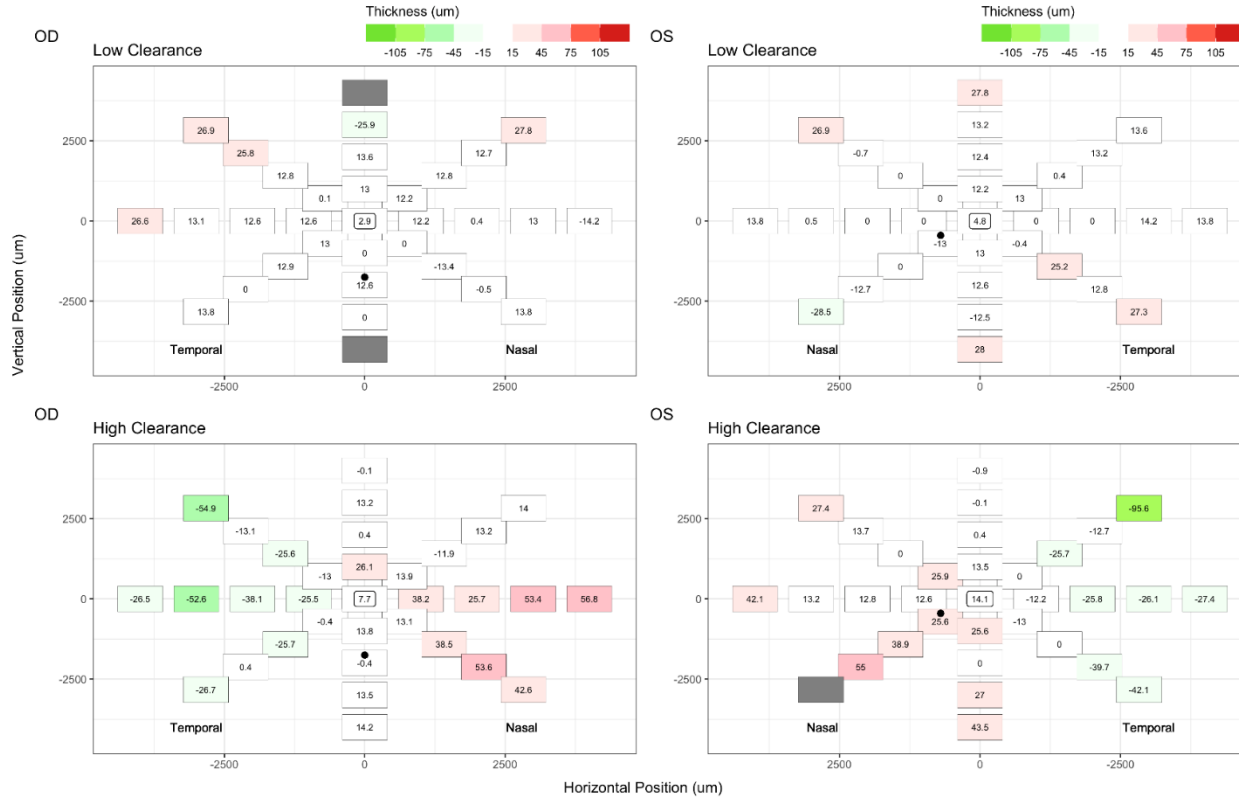


Figure 5-19: Difference maps of total corneal thickness subtracting baseline from follow-up values for Participant 04-KC, as measured by the Spectralis®. This individual has Stage 1 keratoconus OD, and Stage 2 OS.

SPECTRALIS: 07-KC Total Thickness Difference Follow-Up - Baseline

Classification	Status
Absolute Disease Stage	Severe (Stage 4)
Relative Disease Stage (between eyes)	Less Severe
100um thickness change	24.7%

Classification	Status
Absolute Disease Stage	Severe (Stage 4)
Relative Disease Stage (between eyes)	More Severe
100um thickness change	23.9%

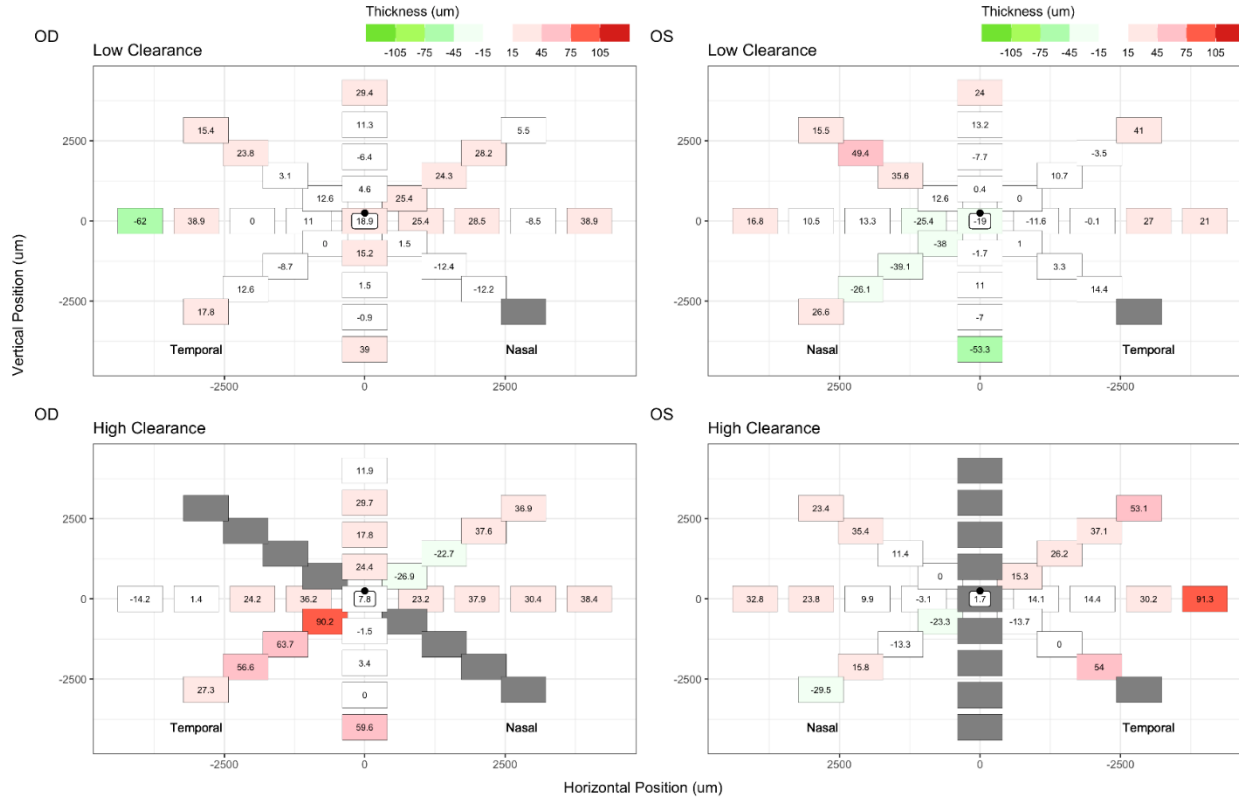


Figure 5-20: Difference maps of total corneal thickness subtracting baseline from follow-up values for Participant 07-KC, as measured by the Spectralis®. This individual has Stage 4 keratoconus OU.

SPECTRALIS: 09-KC Total Thickness Difference Follow-Up - Baseline

Classification	Status
Absolute Disease Stage	Severe (Stage 3)
Relative Disease Stage (between eyes)	More Severe
100um thickness change	17%

Classification	Status
Absolute Disease Stage	Early (Stage 1)
Relative Disease Stage (between eyes)	Less Severe
100um thickness change	14.8%

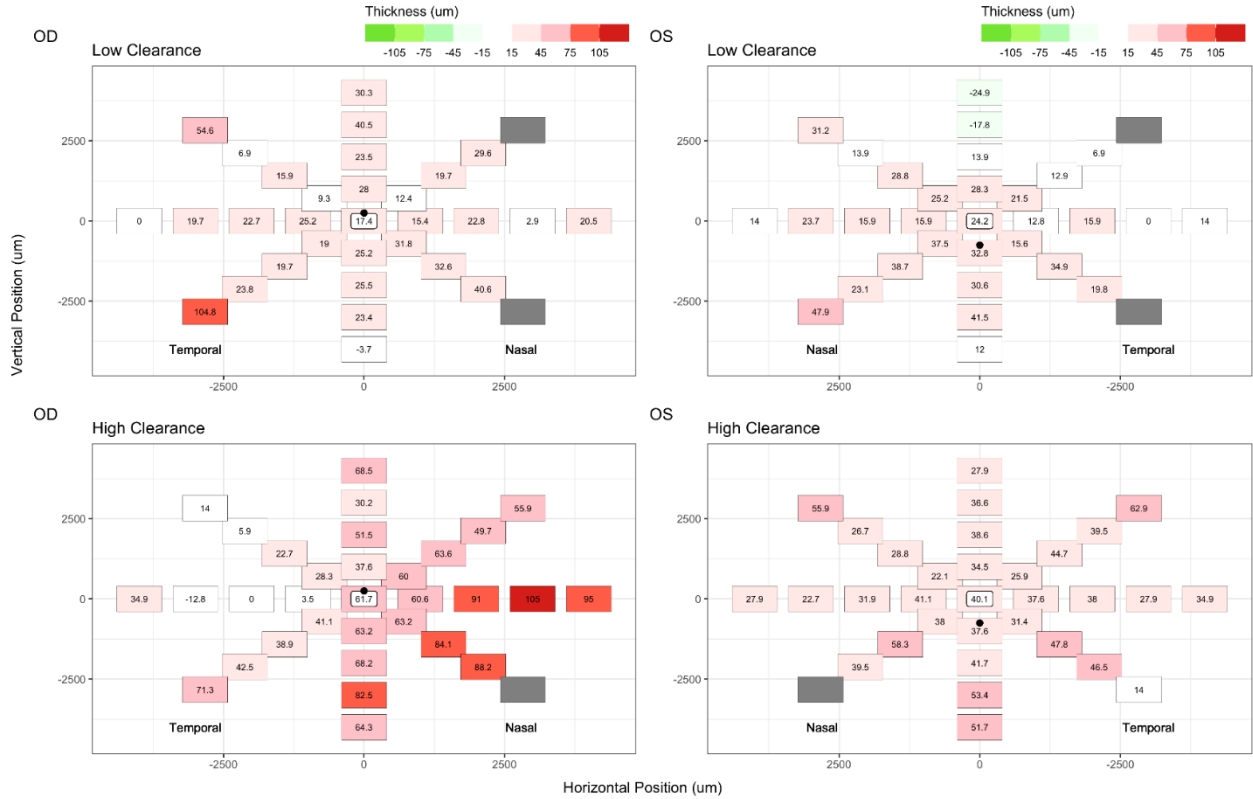


Figure 5-21: Difference maps of total corneal thickness subtracting baseline from follow-up values for Participant 09-KC, as measured by the Spectralis®. This individual has Stage 3 keratoconus OD, and Stage 1 OS.

SPECTRALIS: 11-KC Total Thickness Difference Follow-Up - Baseline

Classification	Status
Absolute Disease Stage	Early (Stage 1)
Relative Disease Stage (between eyes)	Less Severe
100um thickness change	18.3%

Classification	Status
Absolute Disease Stage	Early (Stage 2)
Relative Disease Stage (between eyes)	More Severe
100um thickness change	20.4%

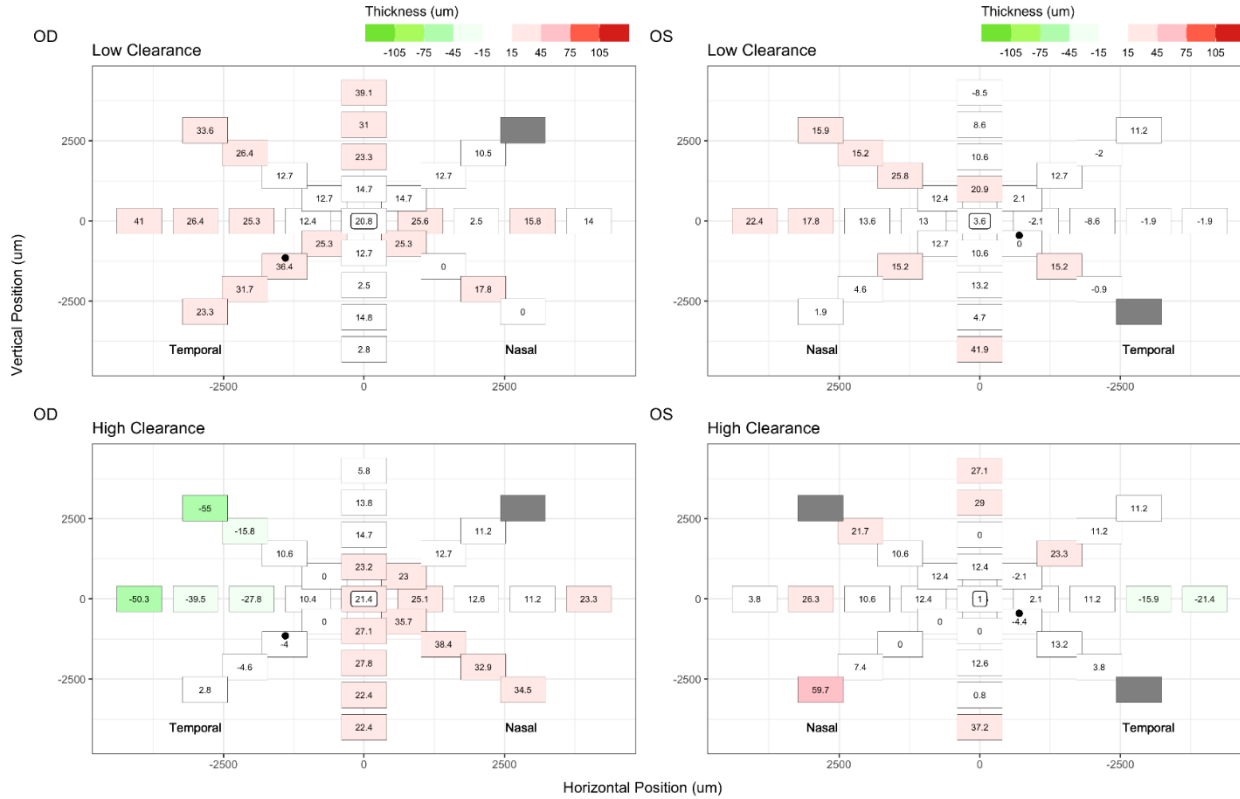


Figure 5-22: Difference maps of total corneal thickness subtracting baseline from follow-up values for Participant 11-KC, as measured by the Spectralis®. This individual has Stage 1 keratoconus OD, and Stage 2 OS.

SPECTRALIS: 13-KC Total Thickness Difference Follow-Up - Baseline

Classification	Status
Absolute Disease Stage	Early (Stage 1)
Relative Disease Stage (between eyes)	More Severe
100um thickness change	16.7%

Classification	Status
Absolute Disease Stage	Early (Stage 1)
Relative Disease Stage (between eyes)	Less Severe
100um thickness change	16.6%



Figure 5-23: Difference maps of total corneal thickness subtracting baseline from follow-up values for Participant 13-KC, as measured by the Spectralis®. This individual has Stage 1 keratoconus OU.

SPECTRALIS: 14-KC Total Thickness Difference Follow-Up - Baseline

Classification	Status
Absolute Disease Stage	Severe (Stage 4)
Relative Disease Stage (between eyes)	More Severe
100um thickness change	22.6%

Classification	Status
Absolute Disease Stage	Early (Stage 1)
Relative Disease Stage (between eyes)	Less Severe
100um thickness change	17.9%

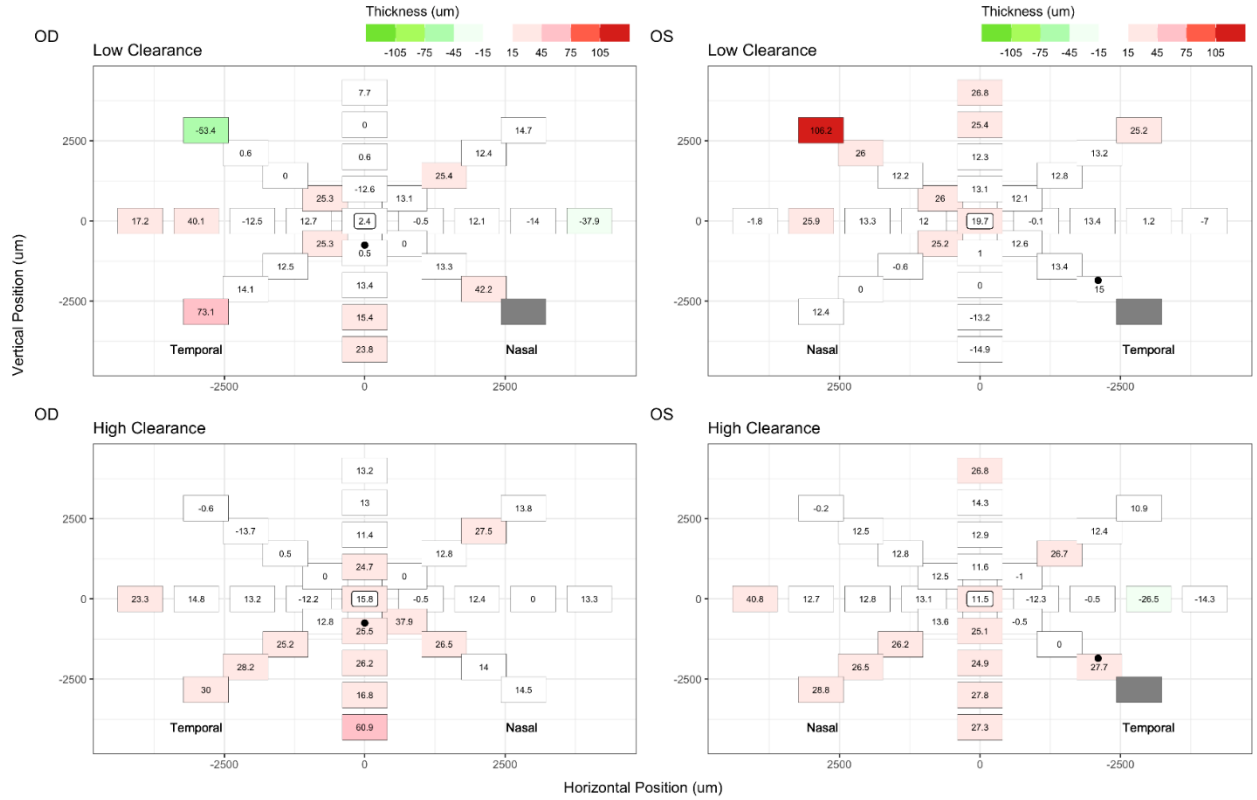


Figure 5-24: Difference maps of total corneal thickness subtracting baseline from follow-up values for Participant 14-KC, as measured by the Spectralis®. This individual has Stage 4 keratoconus OD, and Stage 1 OS.

SPECTRALIS: 15-KC Total Thickness Difference Follow-Up - Baseline

Classification	Status
Absolute Disease Stage	Early (Stage 1)
Relative Disease Stage (between eyes)	Less Severe
100um thickness change	15.6%

Classification	Status
Absolute Disease Stage	Severe (Stage 4)
Relative Disease Stage (between eyes)	More Severe
100um thickness change	16.2%

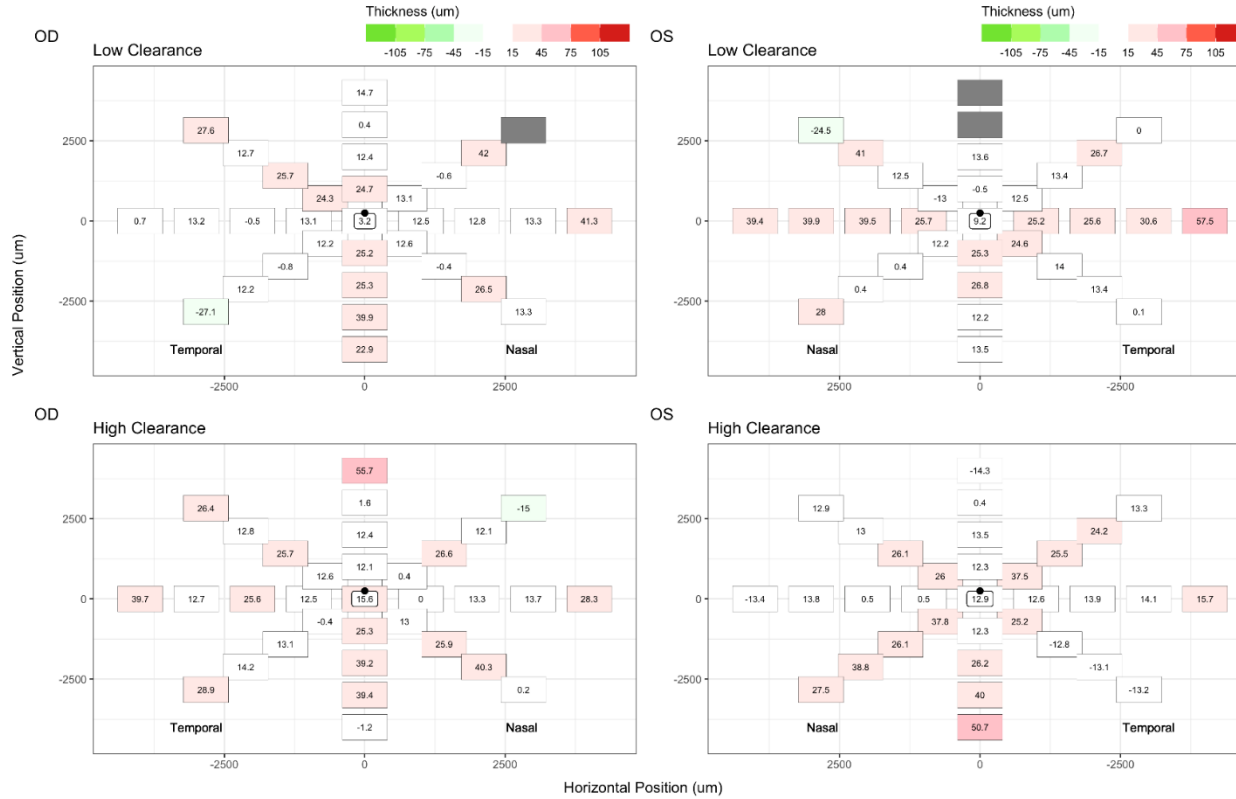


Figure 5-25: Difference maps of total corneal thickness subtracting baseline from follow-up values for Participant 15-KC, as measured by the Spectralis®. This individual has Stage 1 keratoconus OD, and Stage 4 OS.

PENTACAM: 02-KC Total Thickness Difference Follow-Up - Baseline

Classification	Status
Absolute Disease Stage	Early (Stage 2)
Relative Disease Stage (between eyes)	More Severe
100um thickness change	21.2%

Classification	Status
Absolute Disease Stage	Early (Stage 2)
Relative Disease Stage (between eyes)	Less Severe
100um thickness change	19.5%

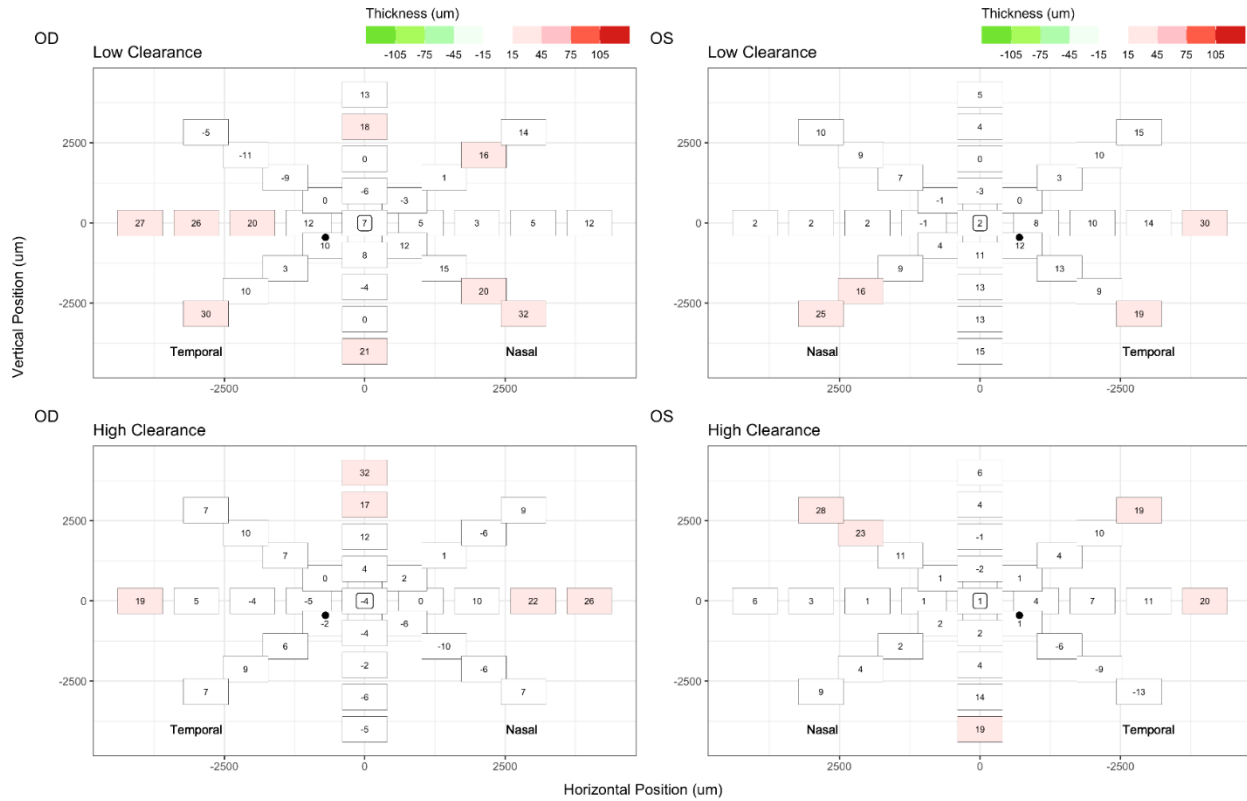


Figure 5-26: Difference maps of total corneal thickness subtracting baseline from follow-up values for Participant 02-KC, as measured by the Pentacam® HR. This individual has Stage 2 keratoconus OU.

PENTACAM: 04-KC Total Thickness Difference Follow-Up - Baseline

Classification	Status
Absolute Disease Stage	Early (Stage 1)
Relative Disease Stage (between eyes)	Less Severe
100um thickness change	20%

Classification	Status
Absolute Disease Stage	Early (Stage 2)
Relative Disease Stage (between eyes)	More Severe
100um thickness change	20.2%

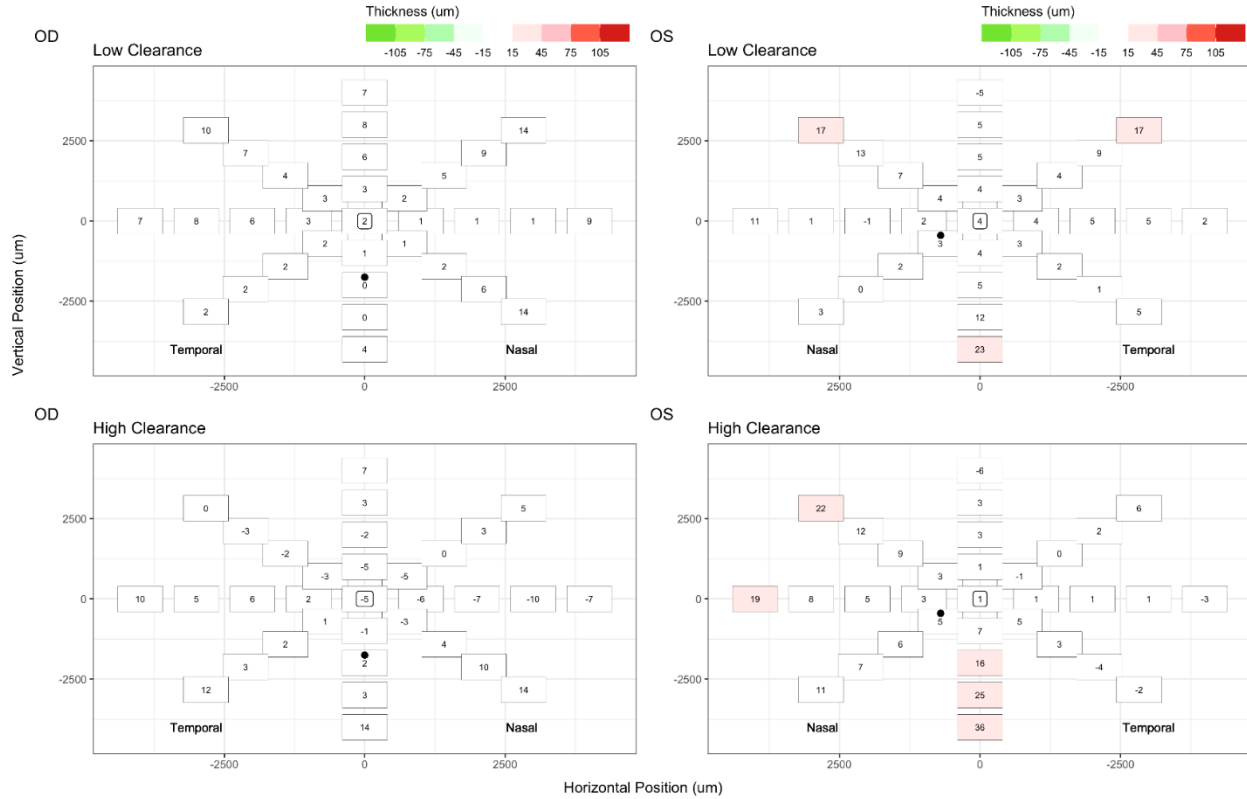


Figure 5-27: Difference maps of total corneal thickness subtracting baseline from follow-up values for Participant 04-KC, as measured by the Pentacam® HR. This individual has Stage 1 keratoconus OD, and Stage 2 OS.

PENTACAM: 07-KC Total Thickness Difference Follow-Up - Baseline

Classification	Status
Absolute Disease Stage	Severe (Stage 4)
Relative Disease Stage (between eyes)	Less Severe
100um thickness change	27%

Classification	Status
Absolute Disease Stage	Severe (Stage 4)
Relative Disease Stage (between eyes)	More Severe
100um thickness change	26.5%

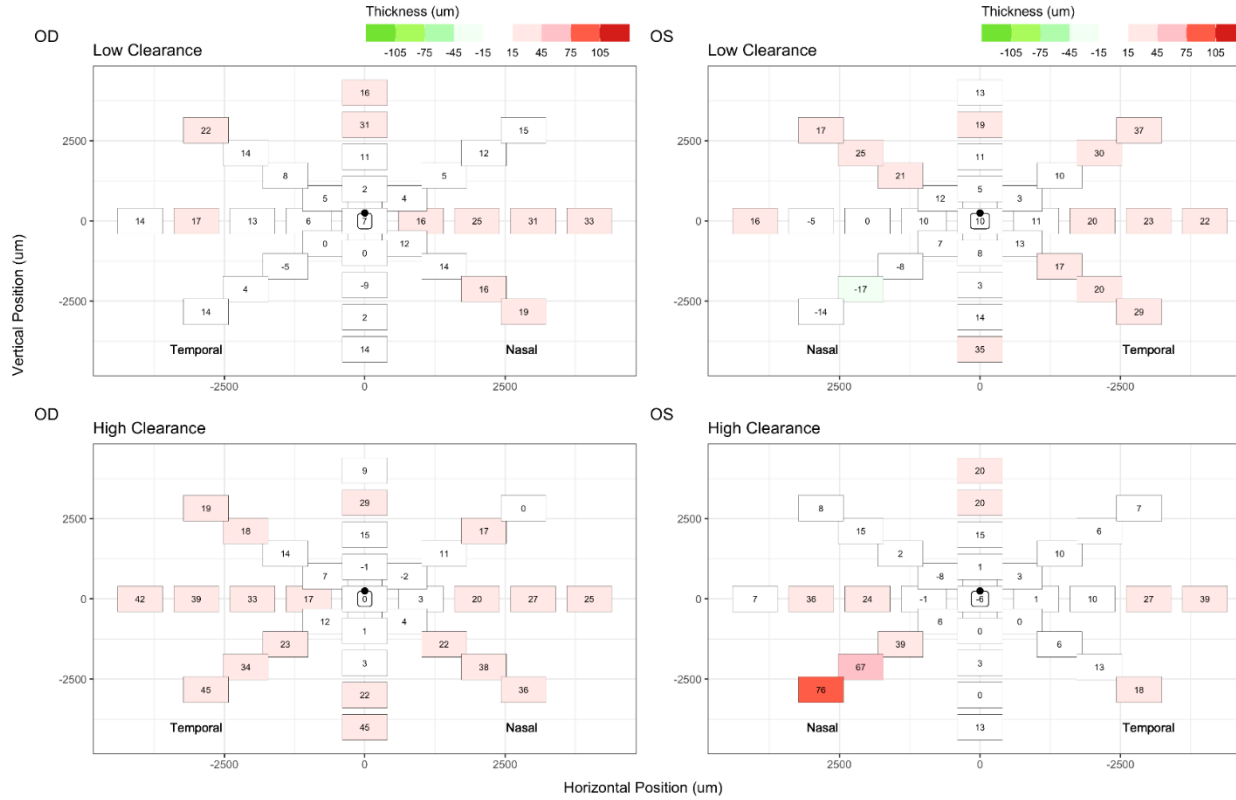


Figure 5-28: Difference maps of total corneal thickness subtracting baseline from follow-up values for Participant 07-KC, as measured by the Pentacam® HR. This individual has Stage 4 keratoconus OU.

PENTACAM: 09-KC Total Thickness Difference Follow-Up - Baseline

Classification	Status
Absolute Disease Stage	Severe (Stage 3)
Relative Disease Stage (between eyes)	More Severe
100um thickness change	19.6%

Classification	Status
Absolute Disease Stage	Early (Stage 1)
Relative Disease Stage (between eyes)	Less Severe
100um thickness change	16.8%

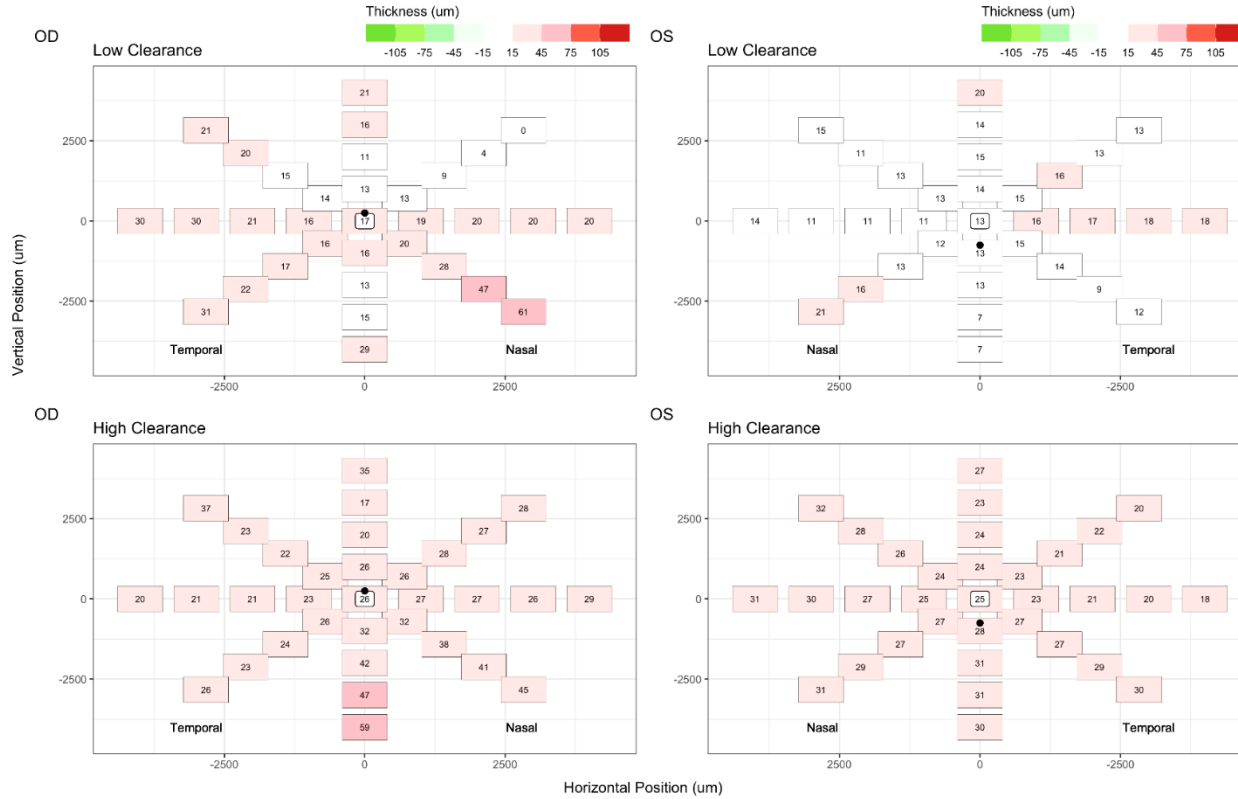


Figure 5-29: Difference maps of total corneal thickness subtracting baseline from follow-up values for Participant 09-KC, as measured by the Pentacam® HR. This individual has Stage 3 keratoconus OD, and Stage 1 OS.

PENTACAM: 11-KC Total Thickness Difference Follow-Up - Baseline

Classification	Status
Absolute Disease Stage	Early (Stage 1)
Relative Disease Stage (between eyes)	Less Severe
100um thickness change	20.3%

Classification	Status
Absolute Disease Stage	Early (Stage 2)
Relative Disease Stage (between eyes)	More Severe
100um thickness change	22.9%

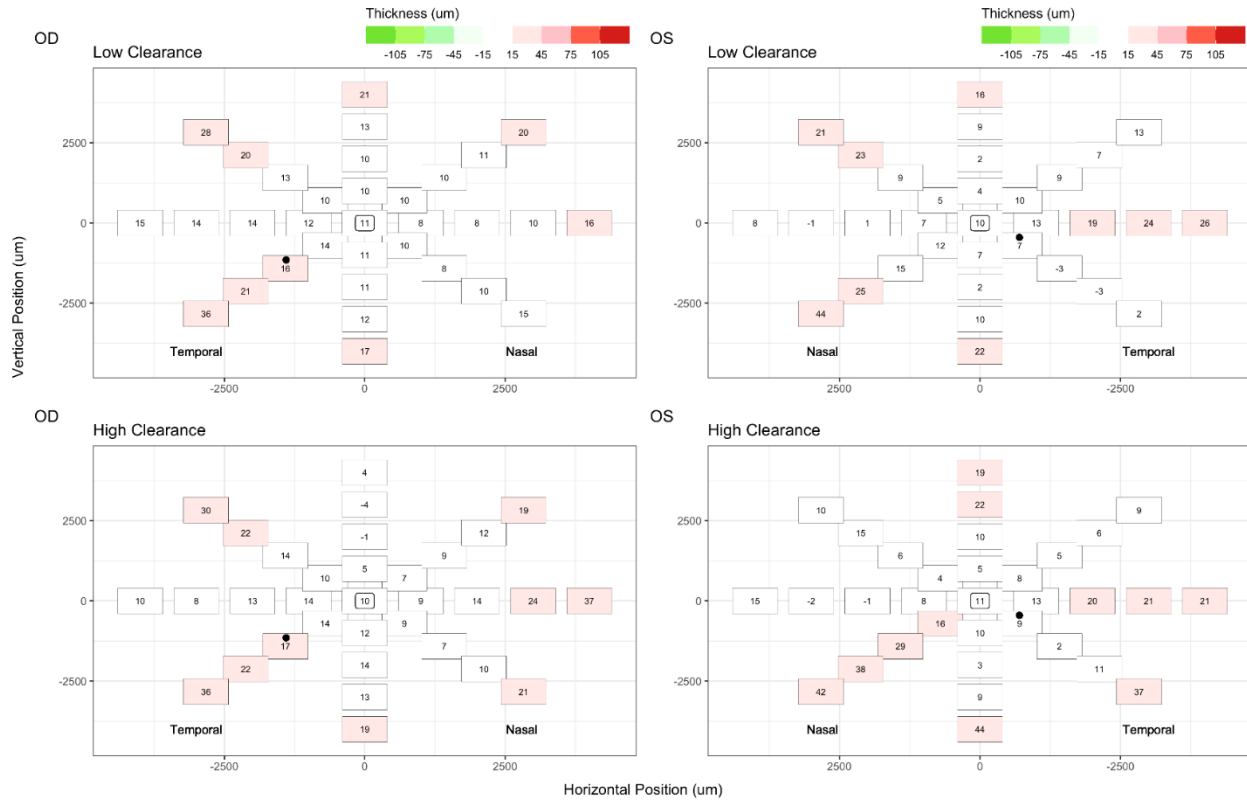


Figure 5-30: Difference maps of total corneal thickness subtracting baseline from follow-up values for Participant 11-KC, as measured by the Pentacam® HR. This individual has Stage 1 keratoconus OD, and Stage 2 OS.

PENTACAM: 13-KC Total Thickness Difference Follow-Up - Baseline

Classification	Status
Absolute Disease Stage	Early (Stage 1)
Relative Disease Stage (between eyes)	More Severe
100um thickness change	18.8%

Classification	Status
Absolute Disease Stage	Early (Stage 1)
Relative Disease Stage (between eyes)	Less Severe
100um thickness change	18.5%

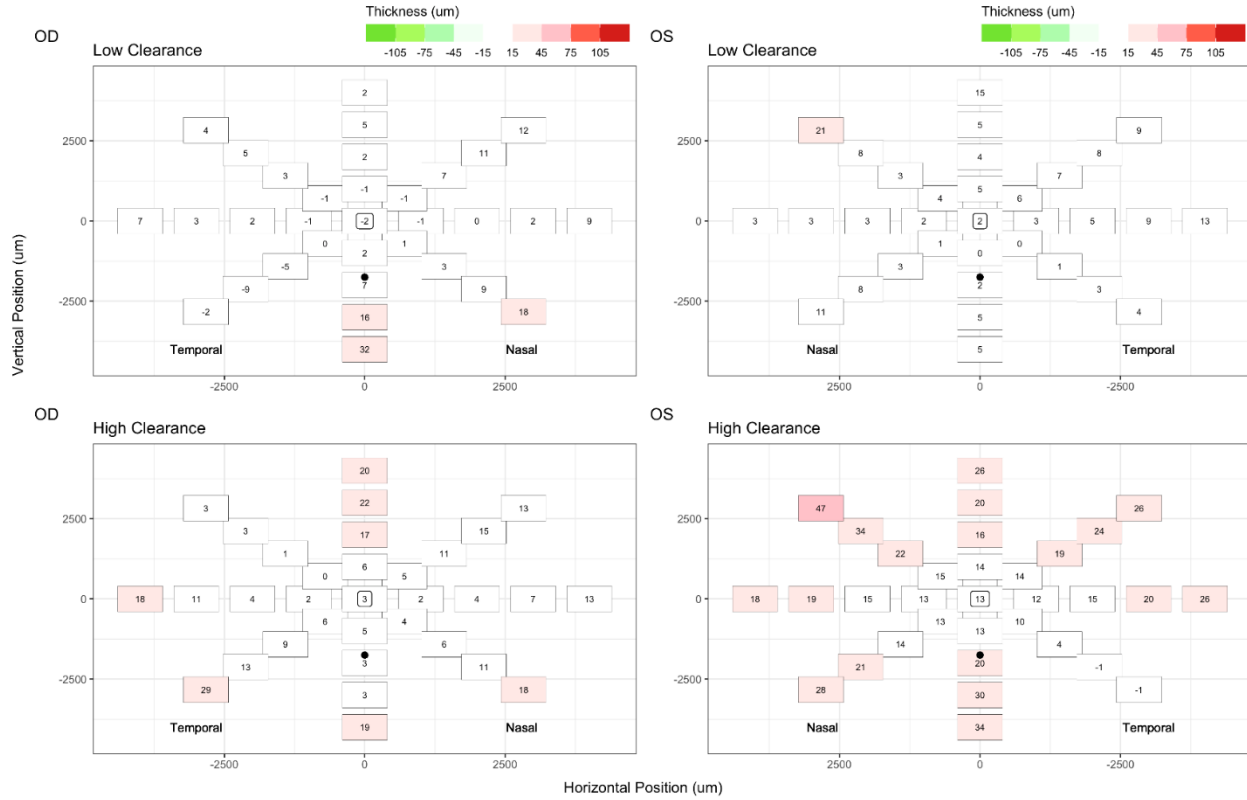


Figure 5-31: Difference maps of total corneal thickness subtracting baseline from follow-up values for Participant 13-KC, as measured by the Pentacam® HR. This individual has Stage 1 keratoconus OU.

PENTACAM: 14-KC Total Thickness Difference Follow-Up - Baseline

Classification	Status
Absolute Disease Stage	Severe (Stage 4)
Relative Disease Stage (between eyes)	More Severe
100um thickness change	24%

Classification	Status
Absolute Disease Stage	Early (Stage 1)
Relative Disease Stage (between eyes)	Less Severe
100um thickness change	20%

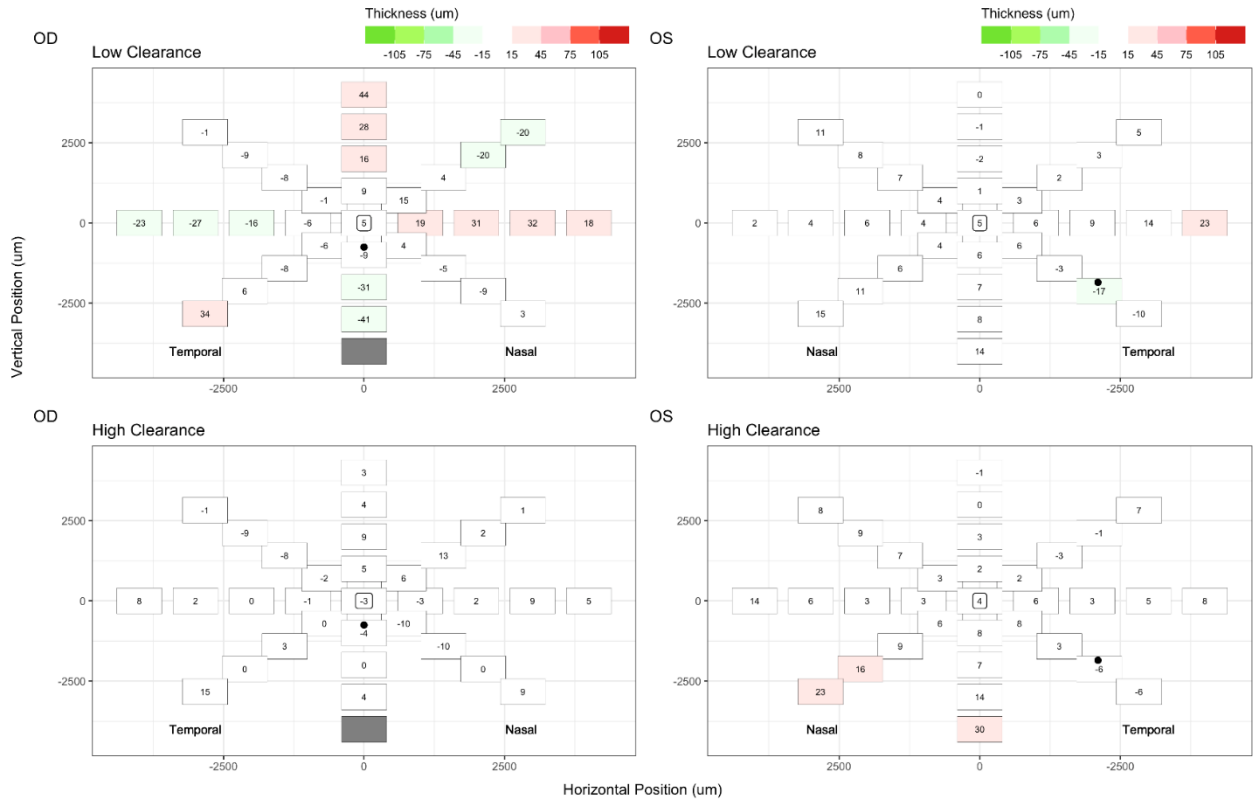


Figure 5-32: Difference maps of total corneal thickness subtracting baseline from follow-up values for Participant 14-KC, as measured by the Pentacam® HR. This individual has Stage 4 keratoconus OD, and Stage 1 OS.

PENTACAM: 15-KC Total Thickness Difference Follow-Up - Baseline

Classification	Status
Absolute Disease Stage	Early (Stage 1)
Relative Disease Stage (between eyes)	Less Severe
100um thickness change	17.5%

Classification	Status
Absolute Disease Stage	Severe (Stage 4)
Relative Disease Stage (between eyes)	More Severe
100um thickness change	17.7%

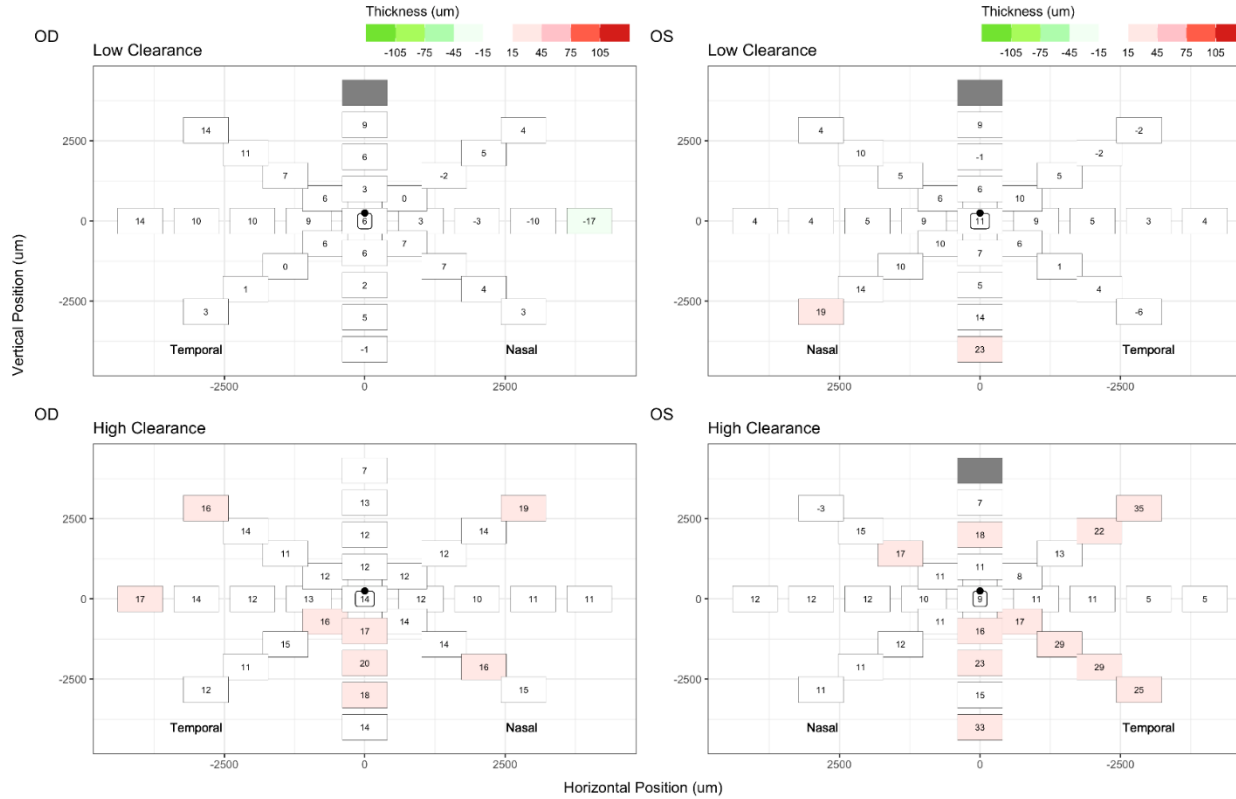


Figure 5-33: Difference maps of total corneal thickness subtracting baseline from follow-up values for Participant 15-KC, as measured by the Pentacam® HR. This individual has Stage 1 keratoconus OD, and Stage 4 OS.

SPECTRALIS: 02-KC Epithelial Thickness Difference Follow-Up - Baseline

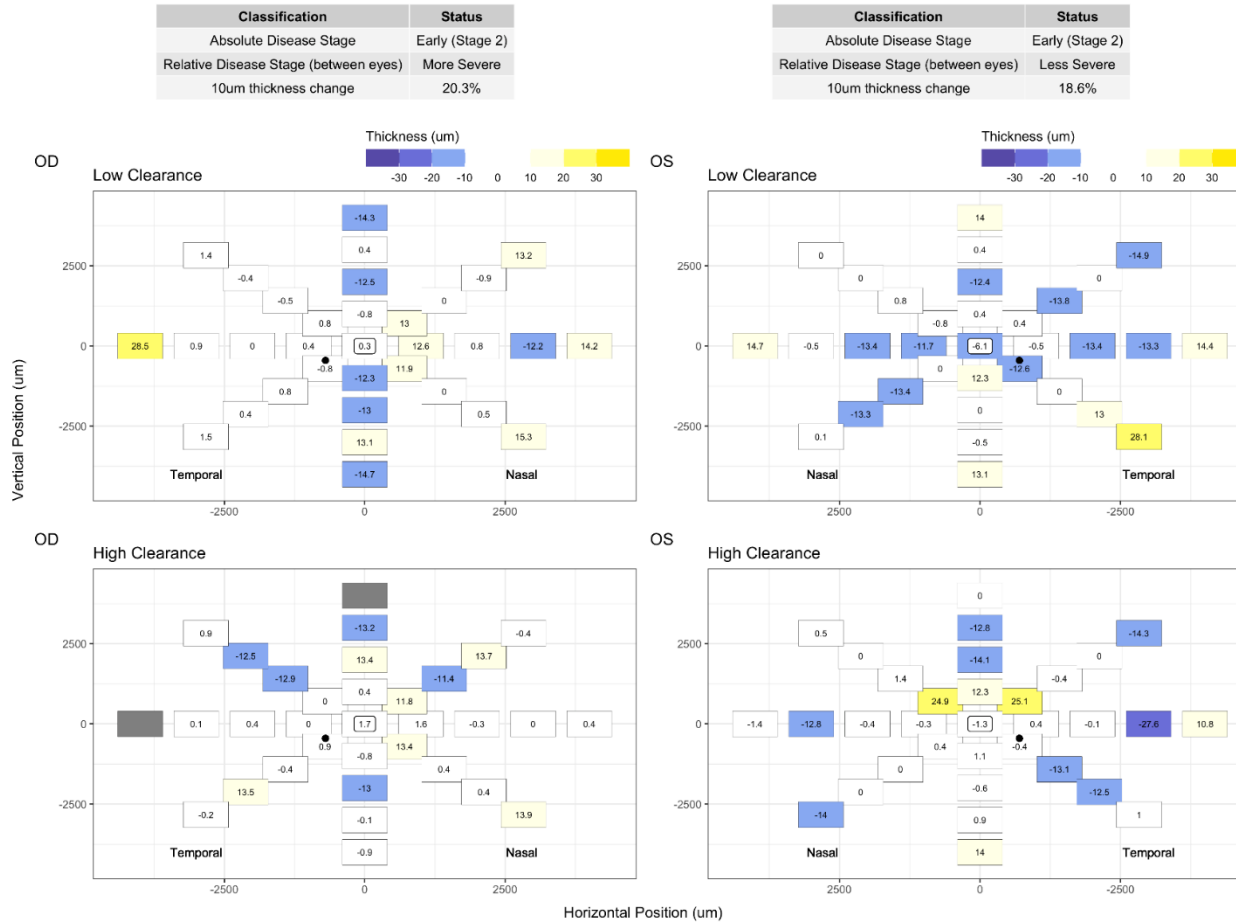


Figure 5-34: Difference maps of corneal epithelial thickness subtracting baseline from follow-up values for Participant 02-KC, as measured by the Spectralis®. This individual has Stage 2 keratoconus OU. For Figure 5-34-Figure 5-41, yellow shades represent an increase in thickness, where blue shades represent a decrease in thickness.

SPECTRALIS: 04-KC Epithelial Thickness Difference Follow-Up - Baseline

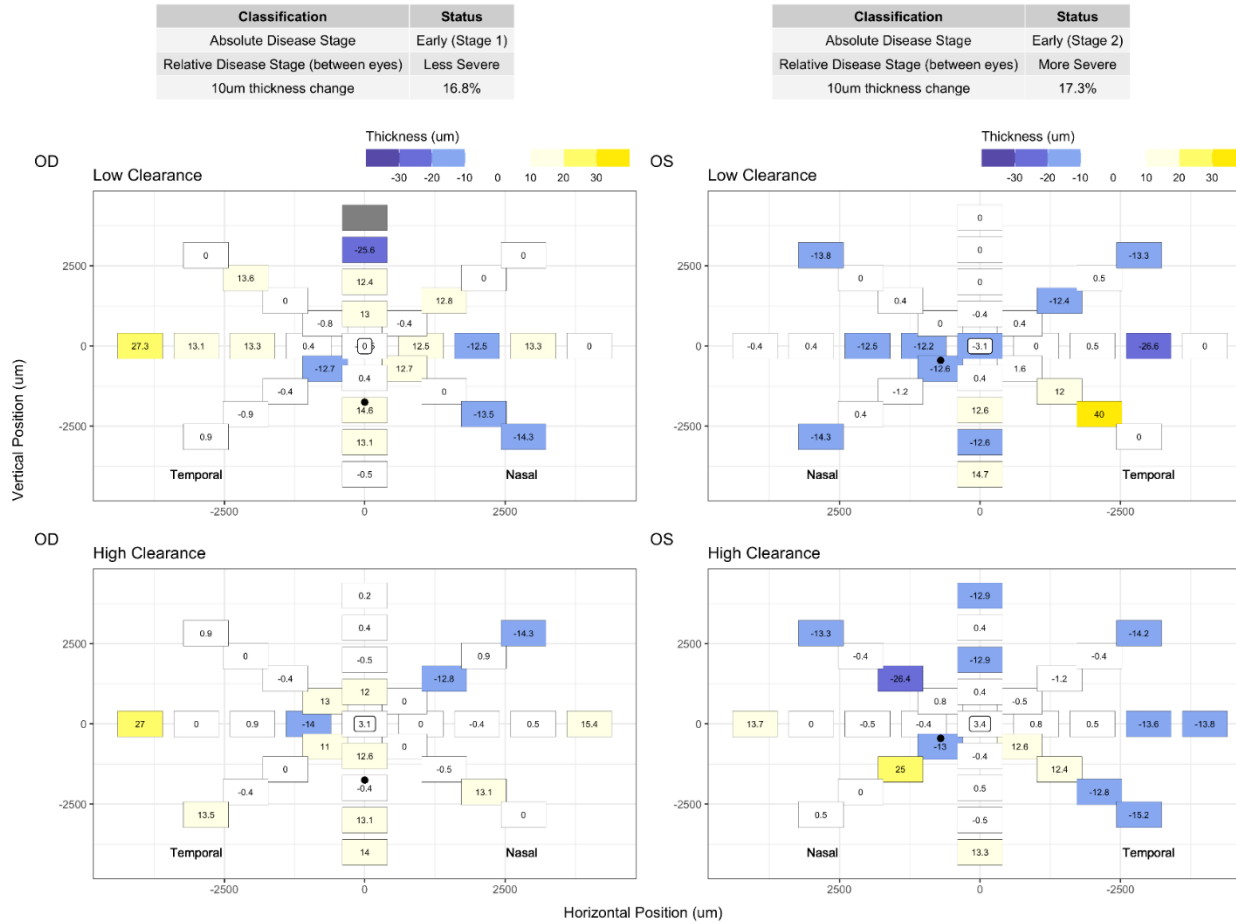


Figure 5-35: Difference maps of corneal epithelial thickness subtracting baseline from follow-up values for Participant 04-KC, as measured by the Spectralis®. This individual has Stage 1 keratoconus OD, and Stage 2 OS.

SPECTRALIS: 07-KC Epithelial Thickness Difference Follow-Up - Baseline

Classification	Status
Absolute Disease Stage	Severe (Stage 4)
Relative Disease Stage (between eyes)	Less Severe
10um thickness change	19.5%

Classification	Status
Absolute Disease Stage	Severe (Stage 4)
Relative Disease Stage (between eyes)	More Severe
10um thickness change	20%

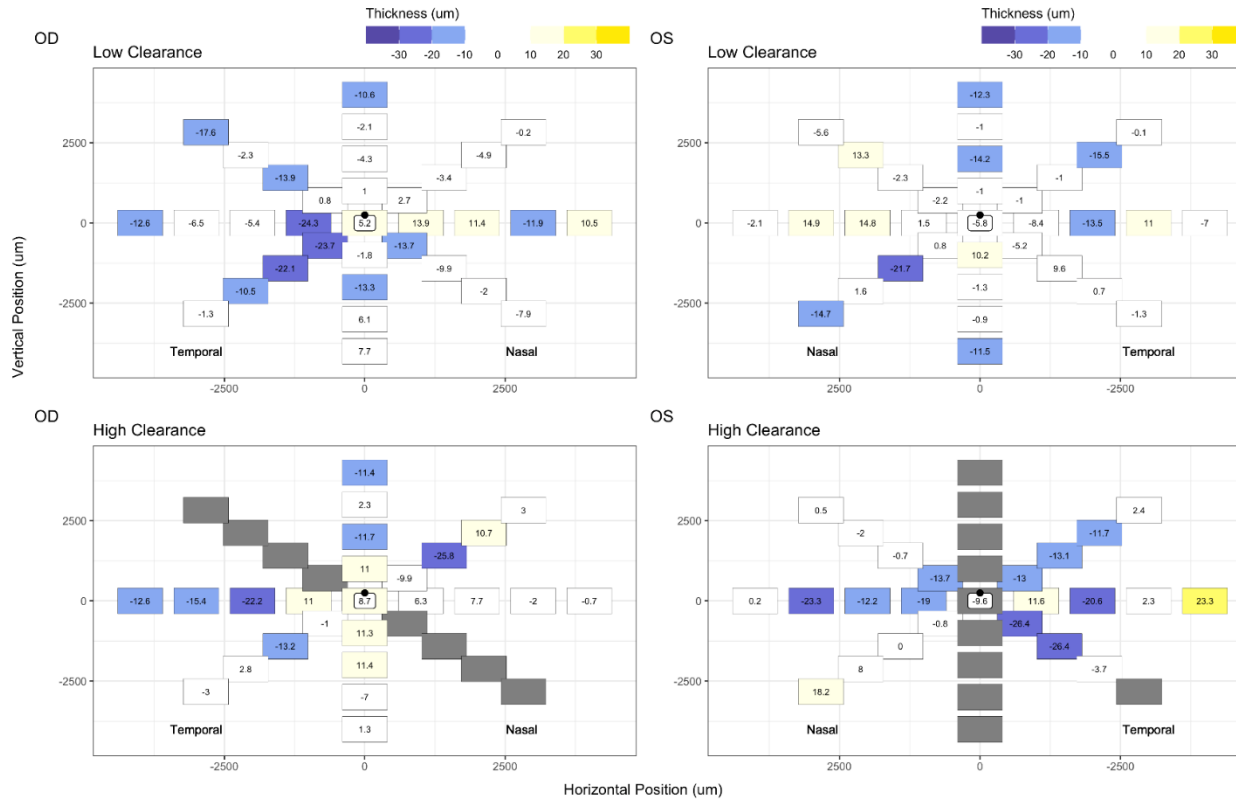


Figure 5-36: Difference maps of corneal epithelial thickness subtracting baseline from follow-up values for Participant 07-KC, as measured by the Spectralis®. This individual has Stage 4 keratoconus OU.

SPECTRALIS: 09-KC Epithelial Thickness Difference Follow-Up - Baseline

Classification	Status
Absolute Disease Stage	Severe (Stage 3)
Relative Disease Stage (between eyes)	More Severe
10um thickness change	15.6%

Classification	Status
Absolute Disease Stage	Early (Stage 1)
Relative Disease Stage (between eyes)	Less Severe
10um thickness change	13.4%

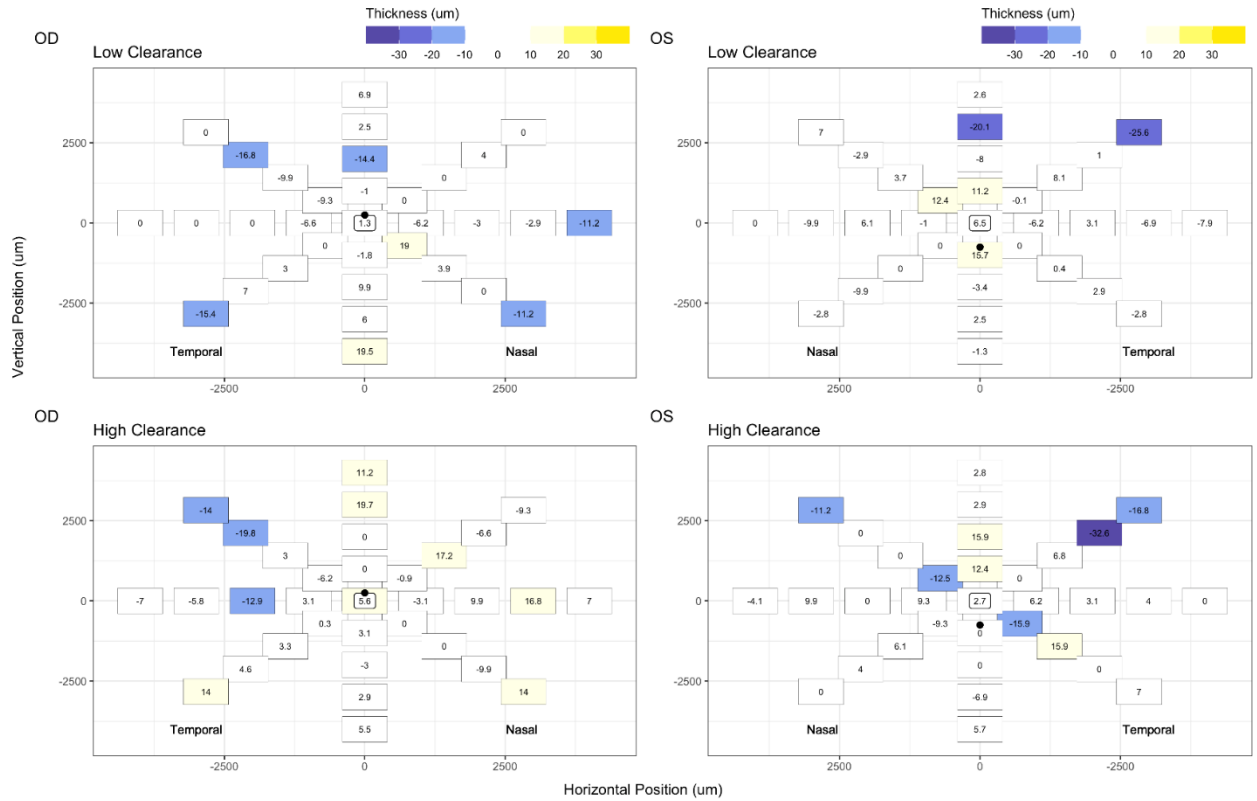


Figure 5-37: Difference maps of corneal epithelial thickness subtracting baseline from follow-up values for Participant 09-KC, as measured by the Spectralis®. This individual has Stage 3 keratoconus OD, and Stage 1 OS.

SPECTRALIS: 11-KC Epithelial Thickness Difference Follow-Up - Baseline

Classification	Status
Absolute Disease Stage	Early (Stage 1)
Relative Disease Stage (between eyes)	Less Severe
10um thickness change	16.5%

Classification	Status
Absolute Disease Stage	Early (Stage 2)
Relative Disease Stage (between eyes)	More Severe
10um thickness change	17.1%

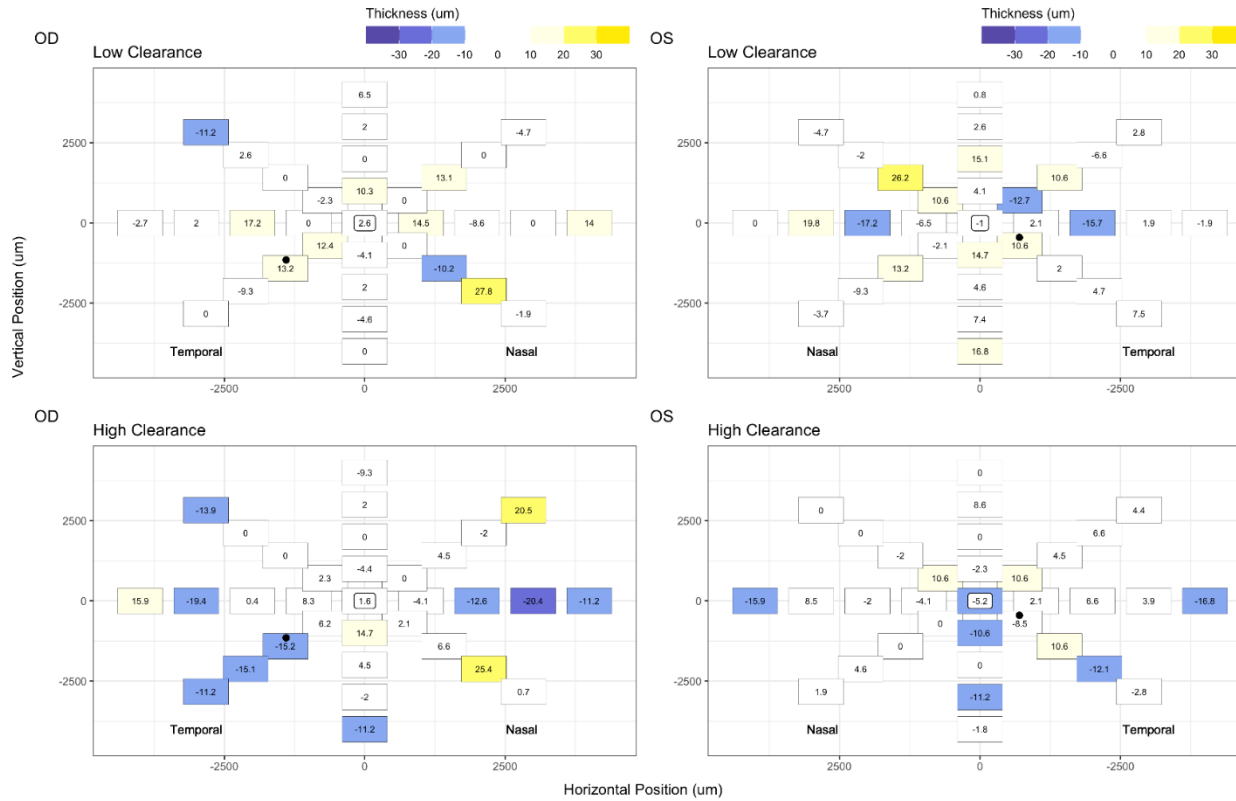


Figure 5-38: Difference maps of corneal epithelial thickness subtracting baseline from follow-up values for Participant 11-KC, as measured by the Spectralis®. This individual has Stage 1 keratoconus OD, and Stage 2 OS.

SPECTRALIS: 13-KC Epithelial Thickness Difference Follow-Up - Baseline

Classification	Status
Absolute Disease Stage	Early (Stage 1)
Relative Disease Stage (between eyes)	More Severe
10um thickness change	16.9%

Classification	Status
Absolute Disease Stage	Early (Stage 1)
Relative Disease Stage (between eyes)	Less Severe
10um thickness change	19.5%

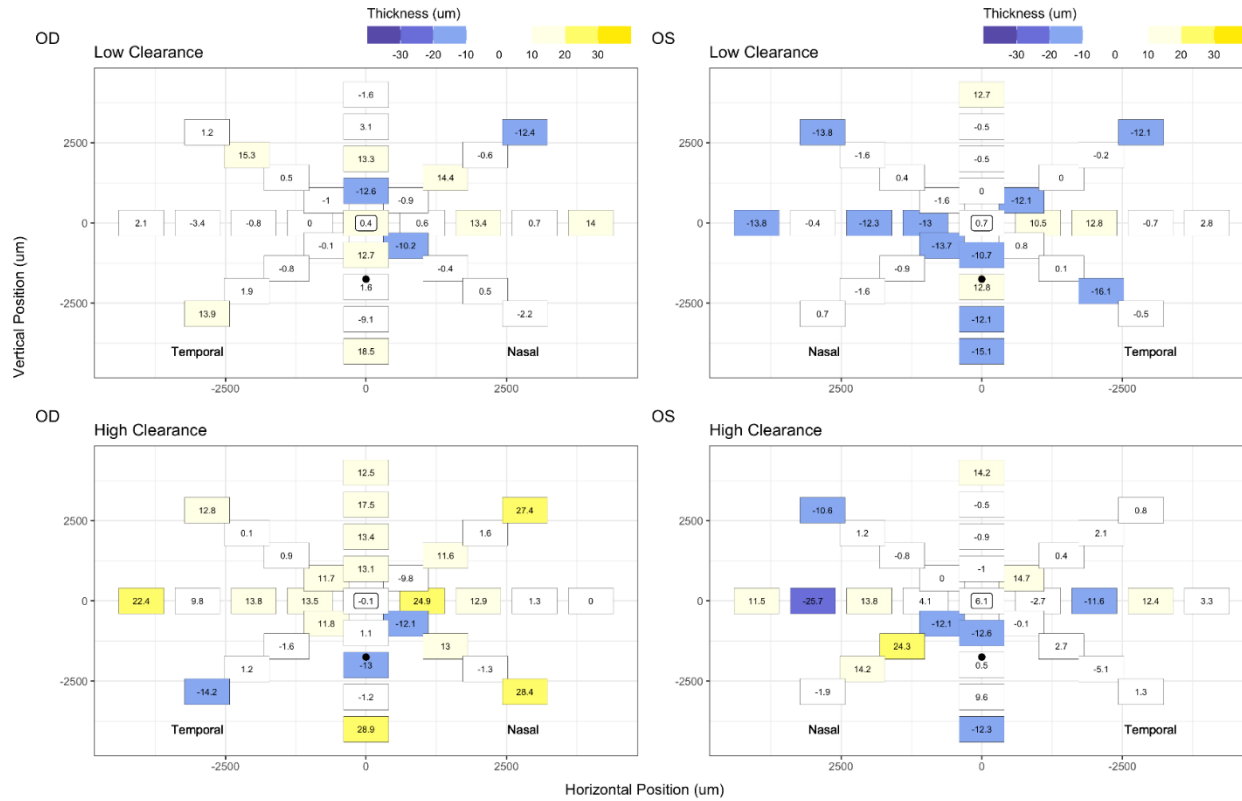


Figure 5-39: Difference maps of corneal epithelial thickness subtracting baseline from follow-up values for Participant 13-KC, as measured by the Spectralis®. This individual has Stage 1 keratoconus OU.

SPECTRALIS: 14-KC Epithelial Thickness Difference Follow-Up - Baseline

Classification	Status
Absolute Disease Stage	Severe (Stage 4)
Relative Disease Stage (between eyes)	More Severe
10um thickness change	15.8%

Classification	Status
Absolute Disease Stage	Early (Stage 1)
Relative Disease Stage (between eyes)	Less Severe
10um thickness change	14.1%

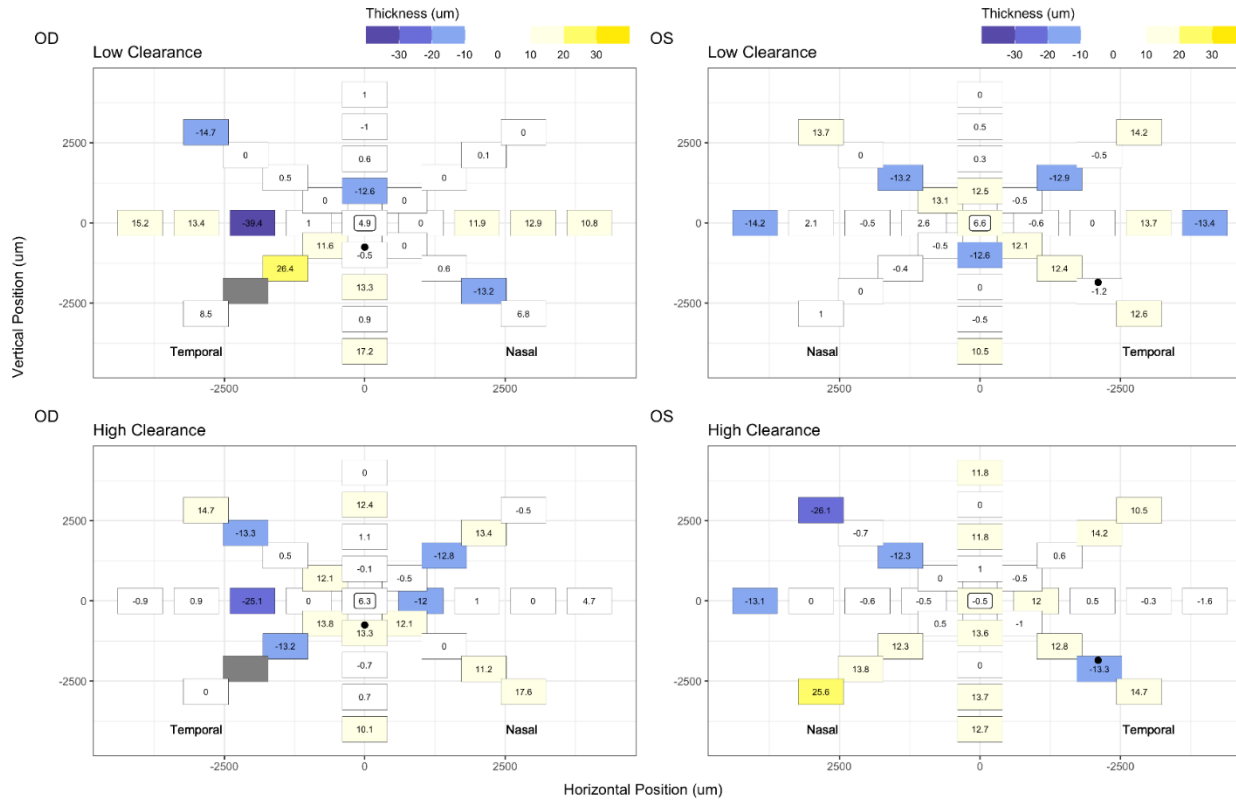


Figure 5-40: Difference maps of corneal epithelial thickness subtracting baseline from follow-up values for Participant 14-KC, as measured by the Spectralis®. This individual has Stage 4 keratoconus OD, and Stage 1 OS.

SPECTRALIS: 15-KC Epithelial Thickness Difference Follow-Up - Baseline

Classification	Status
Absolute Disease Stage	Early (Stage 1)
Relative Disease Stage (between eyes)	Less Severe
10um thickness change	18.2%

Classification	Status
Absolute Disease Stage	Severe (Stage 4)
Relative Disease Stage (between eyes)	More Severe
10um thickness change	20%

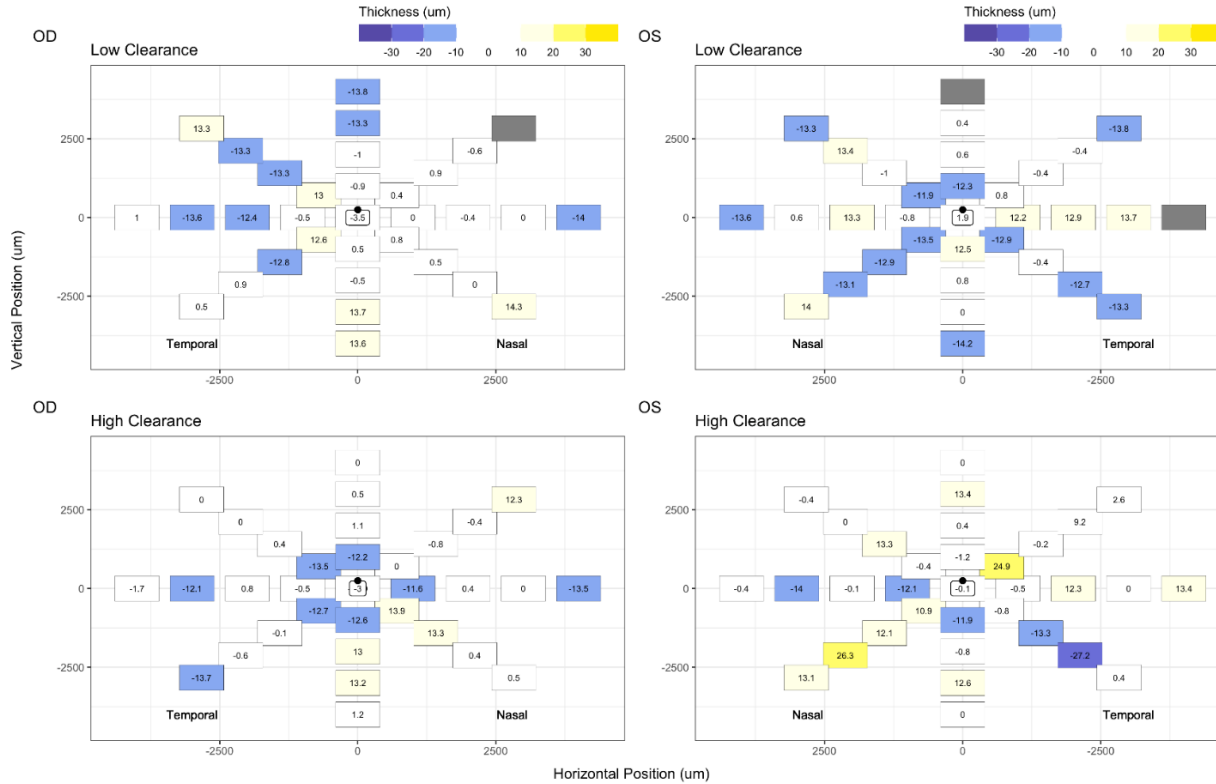


Figure 5-41: Difference maps of corneal epithelial thickness subtracting baseline from follow-up values for Participant 15-KC, as measured by the Spectralis®. This individual has Stage 1 keratoconus OD, and Stage 4 OS.

5.5 Additional Parameters Relating to Lens Fit and Ocular Health

5.5.1 Central Corneal Clearance

As previously discussed, central corneal clearance was measured in Fiji on images taken with Spectralis® OCT and subsequently corrected for magnification effects. Individual measured and magnification corrected central clearances are tabulated below in Table 5-12, and a group summary is presented in Table 5-13.

Table 5-12: Summary table of individual clearances measured for all participants for each lens. For each eye, Amsler-Krumeich disease stage¹⁷¹ is indicated. From left to right on this table, clearances are summarized as low clearance (LC) baseline (BL) and follow-up (FU), and then BL and FU for the high clearance (HC) lens.

Participant	A-K	Eye	Lens	Visit	CCC (μm)		Lens	Visit	CCC (μm)		Visit	CCC (μm)
	Disease Stage				Visit	CCC (μm)			Visit	CCC (μm)		
02-KC	2	OD	LC	BL	234	FU	179	HC	BL	337	FU	282
02-KC	2	OS	LC	BL	245	FU	245	HC	BL	376	FU	354
04-KC	1	OD	LC	BL	152	FU	101	HC	BL	238	FU	242
04-KC	2	OS	LC	BL	207	FU	135	HC	BL	272	FU	324
07-KC	4	OD	LC	BL	260	FU	145	HC	BL	383	FU	288
07-KC	4	OS	LC	BL	262	FU	209	HC	BL	386	FU	381
09-KC	3	OD	LC	BL	314	FU	300	HC	BL	529	FU	347
09-KC	1	OS	LC	BL	387	FU	245	HC	BL	489	FU	306
11-KC	1	OD	LC	BL	237	FU	201	HC	BL	309	FU	301
11-KC	2	OS	LC	BL	151	FU	103	HC	BL	259	FU	212
13-KC	1	OD	LC	BL	138	FU	146	HC	BL	312	FU	245
13-KC	1	OS	LC	BL	162	FU	154	HC	BL	339	FU	237
14-KC	4	OD	LC	BL	239	FU	250	HC	BL	436	FU	300
14-KC	1	OS	LC	BL	413	FU	378	HC	BL	523	FU	324
15-KC	1	OD	LC	BL	272	FU	203	HC	BL	477	FU	276
15-KC	4	OS	LC	BL	315	FU	219	HC	BL	477	FU	296

Table 5-13: Group summary and descriptive statistics for central corneal clearances. These values are shown for baseline (BL) and follow-up (FU) for each of the low clearance (LC) and high clearance (HC) lenses.

	LC		HC	
	BL	FU	BL	FU
Average CCC (µm)	249	201	384	295
SD	78	71	92	44
Range (µm)	138-413	101-378	238-529	212-381

5.5.2 High and Low Contrast Visual Acuity

For this study, high and low contrast visual acuity was measured with study lenses before and after best-spherical over refraction. As these measurements were recorded using Snellen notation, values were converted to logMAR using a validated method in Excel.²⁸⁸ Results of best-corrected high and low contrast visual acuity for each participant are displayed in Appendix G. These data are summarized below in Table 5-14 for high contrast visual acuity, and Table 5-15 for low contrast visual acuity.

Table 5-14: Summary of changes in high contrast visual acuity between baseline and follow-up for the low (left) and high clearance lens (right). Counts and averages of both decreases (colour coded in red) and increases (colour coded in green) in visual acuity are summarized at the bottom of the table.

Participant	High Contrast Acuity - Low Clearance Lens				High Contrast Acuity - High Clearance Lens			
	OD BCVA Change	OS BCVA Change	OS BCVA Change	OS BCVA Change	OD BCVA Change	OS BCVA Change	OS BCVA Change	OS BCVA Change
02KC	0.00	0	-0.04	-2	-0.02	-1	0.02	1
04KC	0.00	0	0.12	6	0.04	2	-0.02	-1
07KC	0.10	5	-0.06	-3	0.00	0	0.00	0
09KC	-0.02	-1	-0.04	-2	-0.18	-9	-0.06	-3
11KC	0.00	0	0.04	2	0.04	2	0.18	9
13KC	-0.06	-3	0.08	4	0.08	4	0.14	7
14KC	0.06	3	0.02	1	-0.08	-4	0.04	2
15KC	-0.06	-3	-0.04	-2	0.00	0	0.08	4
	Count Worse	3	Count Worse	4	Count Worse	3	Count Worse	2
	Count Better	2	Count Better	4	Count Better	3	Count Better	5
	Avg Worse	-2	Avg Worse	-2	Avg Worse	-5	Avg Worse	-2
	Avg Better	4	Avg Better	3	Avg Better	3	Avg Better	5

For the measurement of high contrast visual acuity summarized previously in Table 5-14, there was an overall roughly even division between case counts of improvement and worsening of VA with lens wear. The highest average of letters lost from baseline to follow-up was with the right eye, high clearance lens (five letters), however the same magnitude of letters gained was noted on average for the left eye with the same lens. Averages were otherwise similar.

Table 5-15: Summary of changes in low contrast visual acuity between baseline and follow-up for the low (left) and high clearance lens (right). Counts and averages are indicated as in Table 5-14.

Participant	Low Contrast Acuity - Low Clearance Lens				Low Contrast Acuity - High Clearance Lens			
	OD	OS	OD	OS	OD	OS	OD	OS
	BCVA Change	# Letters	BCVA Change	# Letters	BCVA Change	# Letters	BCVA Change	# Letters
02KC	-0.16	-8	-0.14	-7	0.00	0	0.16	8
04KC	0.24	12	0.60	30	-0.10	-5	-0.04	-2
07KC	-0.22	-11	-0.16	-8	-0.18	-9	-0.06	-3
09KC	0.30	15	-0.12	-6	0.00	0	-0.06	-3
11KC	-0.12	-6	0.14	7	-0.20	-10	-0.04	-2
13KC	0.06	3	0.32	16	0.08	4	-0.14	-7
14KC	-0.18	-9	0.12	6	0.00	0	0.04	2
15KC	-0.34	-17	-0.14	-7	0.06	3	0.02	1
	<i>Count Worse</i>	5	<i>Count Worse</i>	4	<i>Count Worse</i>	3	<i>Count Worse</i>	5
	<i>Count Better</i>	3	<i>Count Better</i>	4	<i>Count Better</i>	2	<i>Count Better</i>	3
	<i>Avg Worse</i>	-10	<i>Avg Worse</i>	-7	<i>Avg Worse</i>	-8	<i>Avg Worse</i>	-3
	<i>Avg Better</i>	10	<i>Avg Better</i>	15	<i>Avg Better</i>	4	<i>Avg Better</i>	4

For low contrast visual acuity shown above in Table 5-15, in all but one situation (low clearance, left eye), there were more cases of decreased visual acuity when comparing baseline to follow-up, compared to cases of improvement. However, this was generally only by 1-2 cases. When comparing averages of how many letters were lost or gained, in the low contrast acuity measurement for the high clearance lens for the right eye, the average number of letters lost was twice that of letters gained. On the other hand, the average number of letters gained was twice that of letters lost for the low contrast acuity measurement for the low clearance lens on the left eye. Otherwise, averages were similar.

5.5.3 Subjective Comfort

At each study visit, subjective comfort was assessed via written questionnaire, which is shown in Appendix A. Relevant answers to questions for scleral lens wear for each individual participant at all visits are tabulated in Appendix H. These questions refer to comfort and clarity ratings from 0 to 100, with 0 being poor and 100 being excellent, in addition to a determination of lens preference, if any. These values, in addition to the differences between clarity and comfort from baseline to follow-up for each lens are tabulated in Table 5-16 (low clearance lens) and Table 5-17 (high clearance lens).

Table 5-16: Summary of clarity and comfort values and change from baseline to follow-up for the low clearance lens. Improvements are indicated in green, and worsening of scores are in red.

Low Clearance										
Participant	Visit Type	Eye	Comfort	Clarity	Visit Type	Eye	Comfort	Clarity	FU - BL Comfort	FU - BL Clarity
02-KC	BL	OD	90	100	FU	OD	90	95	0	-5
02-KC	BL	OS	95	100	FU	OS	90	95	-5	-5
04-KC	BL	OD	65	95	FU	OD	75	85	10	-10
04-KC	BL	OS	65	95	FU	OS	65	85	0	-10
07-KC	BL	OD	95	100	FU	OD	100	100	5	0
07-KC	BL	OS	95	100	FU	OS	100	100	5	0
09-KC	BL	OD	95	90	FU	OD	90	90	-5	0
09-KC	BL	OS	90	85	FU	OS	90	85	0	0
11-KC	BL	OD	100	90	FU	OD	95	95	-5	5
11-KC	BL	OS	100	90	FU	OS	95	95	-5	5
13-KC	BL	OD	90	100	FU	OD	30	90	-60	-10
13-KC	BL	OS	75	100	FU	OS	30	90	-45	-10
14-KC	BL	OD	65	100	FU	OD	95	80	30	-20
14-KC	BL	OS	75	100	FU	OS	95	95	20	-5
15-KC	BL	OD	90	80	FU	OD	85	80	-5	0
15-KC	BL	OS	90	80	FU	OS	85	80	-5	0

In most cases, for the low clearance lens, clarity either decreased or remained the same from baseline to follow-up. Where decreases were noted, the magnitudes of these changes from baseline were significantly smaller than those noted with the high clearance lens (see Table 5-17 below). For 11-KC, there was a small improvement in clarity with the low clearance lens. In terms of comfort,

participants 04-KC, 07-KC and 14-KC all felt this parameter to improve from baseline to follow-up in at least one eye, where 13-KC noted a significant decrease in comfort in both eyes. Participants 02-KC, 09-KC, 11-KC, and 15-KC all reported less or equal comfort at follow-up compared to baseline. Changes in clarity and comfort from baseline to follow-up were more varied with the low clearance lens (Table 5-16), compared to the high clearance lens, shown in Table 5-17 below.

Table 5-17: Summary of clarity and comfort values and change from baseline to follow-up for the high clearance lens. Improvements are indicated in green, and worsening of scores are in red.

High Clearance										
Participant	Visit Type	Eye	Comfort	Clarity	Visit Type	Eye	Comfort	Clarity	FU - BL Comfort	FU - BL Clarity
02-KC	BL	OD	95	80	FU	OD	95	100	0	20
02-KC	BL	OS	95	80	FU	OS	95	100	0	20
04-KC	BL	OD	65	65	FU	OD	30	20	-35	-45
04-KC	BL	OS	50	55	FU	OS	20	10	-30	-45
07-KC	BL	OD	70	100	FU	OD	90	70	20	-30
07-KC	BL	OS	90	100	FU	OS	95	70	5	-30
09-KC	BL	OD	90	85	FU	OD	90	90	0	5
09-KC	BL	OS	85	90	FU	OS	90	85	5	-5
11-KC	BL	OD	95	90	FU	OD	85	85	-10	-5
11-KC	BL	OS	95	90	FU	OS	85	85	-10	-5
13-KC	BL	OD	90	100	FU	OD	90	100	0	0
13-KC	BL	OS	100	100	FU	OS	80	60	-20	-40
14-KC	BL	OD	100	100	FU	OD	85	80	-15	-20
14-KC	BL	OS	100	100	FU	OS	85	80	-15	-20
15-KC	BL	OD	100	80	FU	OD	90	75	-10	-5
15-KC	BL	OS	100	80	FU	OS	90	75	-10	-5

In general, from baseline to follow-up for the high clearance lens, both the clarity and the comfort of the lenses decreased, based on subjective scores given. Exceptions to this are participant 02-KC (OU), participant 09-KC (OD) and participant 13-KC (OD) where an improvement or stable score was noted. For comfort only, improvements in scores were noted for participant 07-KC in both eyes, and the left eye of 09-KC.

Lens preferences, both in terms of clearance and chronological order, for each participant are additionally summarized below in Table 5-18.

Table 5-18: Lens preference both by chronological order (first lens: navy blue, second lens: light blue), and by clearance (low clearance: grey, high clearance: beige).

Participant	Visit Type	Eye	Preferred Lens:	Preferred Lens:	Visit Type	Eye	Preferred Lens:	Preferred Lens:
			Order Worn	Type of Clearance			Order Worn	Type of Clearance
02-KC	BL	OD	L1	HC	FU	OD	L1	HC
02-KC	BL	OS	L1	HC	FU	OS	L1	HC
04-KC	BL	OD	L2	LC	FU	OD	L2	LC
04-KC	BL	OS	L2	LC	FU	OS	L2	LC
07-KC	BL	OD	L2	LC	FU	OD	L2	LC
07-KC	BL	OS	L2	LC	FU	OS	L2	LC
09-KC	BL	OD	L2	LC	FU	OD	L1=L2	LC=HC
09-KC	BL	OS	L1=L2	LC=HC	FU	OS	L1=L2	LC=HC
11-KC	BL	OD	L2	LC	FU	OD	L2	LC
11-KC	BL	OS	L2	LC	FU	OS	L2	LC
13-KC	BL	OD	L2	LC	FU	OD	L1	HC
13-KC	BL	OS	L1=L2	LC=HC	FU	OS	L1	HC
14-KC	BL	OD	L1=L2	LC=HC	FU	OD	L2	LC
14-KC	BL	OS	L1=L2	LC=HC	FU	OS	L2	LC
15-KC	BL	OD	L2	HC	FU	OD	L1=L2	LC=HC
15-KC	BL	OS	L2	HC	FU	OS	L1=L2	LC=HC

The majority of individuals preferred the low clearance lens at baseline and follow-up, which was the second lens worn in all but one case (15-KC). In approximately half of all cases, preference was the same from baseline to follow-up. Exceptions to this were participants 09-KC OD, 13-KC, 14-KC, and 15-KC (all OU), where the nature of changes in preferences varied among participants from baseline to follow-up.

5.5.4 Lens Centration

At each visit, any decentration of the scleral lens on-eye was recorded during slit-lamp biomicroscopy when lens fit was assessed. These results are detailed in Appendix I for each participant, and case counts for each direction of decentration are summarized below in Table 5-19 for all visits, and then at follow-up only.

Table 5-19: Summary of directions of decentration for all participants. All visits include baseline and follow-up, and follow-up only (centration after lens settling) is also detailed.

Direction of Decentration	All Visits	Follow-Up Only
Inferior temporal	30	17
Inferior	18	5
Centred	9	6
Superior	2	2
Temporal	2	0
Inferior nasal	2	1
Superior temporal	1	1
Nasal	0	0
Superior nasal	0	0

Most lenses showed a decentration towards the inferior temporal direction, when considering both baseline and follow-up visits (“all visits” column in Table 5-19). The second most common observation was inferior decentration with lateral centration, followed by the lens being centred both laterally and vertically. At follow-up only, inferior temporal decentration was still the most frequent, with a centred fit, followed by an inferiorly decentred fit, being the next most common.

5.5.5 Ocular Health Parameters

Ocular health parameters such as bulbar conjunctival and limbal hyperemia, and fluorescein staining were measured and documented at each study visit.

5.5.5.1 Bulbar and Limbal Hyperemia

Hyperemia was automatically graded with the K5® R-Scan for both the bulbar conjunctiva and the limbus, in the nasal and temporal regions. Results of individual measurements are displayed in Appendix J, and a summary of mean hyperemia and standard deviations of measurements at each location for each visit is tabulated below in Table 5-20.

Table 5-20: Mean and standard deviation of bulbar and limbal hyperemia both nasally and temporally at each visit for all participants.

Condition	Statistic	Bulbar Hyperemia		Limbal Hyperemia	
		T	N	T	N
LC BL	Mean	0.9	1.0	0.5	0.6
	SD	0.2	0.4	0.2	0.2
LC FU	Mean	1.2	1.2	0.6	0.6
	SD	0.3	0.4	0.2	0.3
HC BL	Mean	0.8	1.0	0.5	0.6
	SD	0.2	0.3	0.2	0.2
HC FU	Mean	1.1	1.1	0.6	0.5
	SD	0.3	0.4	0.2	0.2

Mean bulbar hyperemia increased qualitatively with scleral lens wear (i.e., from baseline to follow-up), by similar amounts for the low and high clearance lens. Nasal and temporal scores were similar. Limbal hyperemia average scores were similar at baseline and follow-up, and nasal and temporal measures were also similar.

Participants with decreases in both clarity and comfort, which occurred more with the high clearance lens (shown in Table 5-17) in comparison to the low clearance lens (Table 5-16), would often have an above average hyperemia grading (individual results shown in Appendix J). These individuals included, for high clearance, 04-KC OU, 11-KC OU, 13-KC OS, 14-KC OU, and 15-KC OU. For low clearance, these individuals were 02-KC OS and 13-KC OU. There was more often than not an increase in bulbar hyperemia in these cases from baseline to follow-up. However, decreases in these scores from baseline to follow-up were also at times noted for these individuals, and above average scores were also noted in individuals who did not have decreased clarity and comfort.

5.5.5.2 Corneal Fluorescein Staining

Corneal fluorescein staining was assessed at each visit with slit-lamp biomicroscopy. Grading was carried out by location (central, superior, inferior, nasal, temporal) and type on an integer scale of 1-4, representing micro-, macropunctate, coalescent, and patch staining, per the Brien Holden Vision

Institute (BHVI) grading system.²⁸⁹ If no staining was present, a grade of “0” was given. The presence and location of negative staining was also noted. Individual results are shown in Appendix K. Mean positive staining scores and their standard deviations at each location, along with presence or absence of negative staining are displayed below in Table 5-21 for each visit.

Table 5-21: Summary of corneal fluorescein staining using the BHVI scale.²⁸⁹ Mean and standard deviation are displayed at each corneal location for each visit for positive staining. Counts of the presence and absence of negative staining are detailed for each visit.

Condition	Statistic	Positive Staining					Negative Staining	
		Central	Superior	Inferior	Temporal	Nasal	Presence	Absence
LC BL	Mean	1	1	1	1	1	7	9
	SD	1	1	1	1	1		
HC BL	Mean	0	1	1	0	1	2	14
	SD	0	1	1	0	1		
LC FU	Mean	1	1	1	1	1	5	11
	SD	0	1	1	1	1		
HC FU	Mean	1	1	1	1	1	4	11
	SD	1	1	1	1	1		

Average positive staining with lens wear was very similar from baseline to follow-up, as well as between the low and high clearance lens follow-ups. The presence of negative staining was less often noted at baseline for the high clearance lens, which was the first baseline in all but one case.

However, the number of cases with and without negative staining were very similar between both lens follow-ups. In the same participants who reported decreases in both clarity and comfort from baseline to follow-up (referenced in 5.5.5.1), corneal fluorescein staining (results displayed in Appendix K) was not consistently above the average score. Similar to hyperemia scores, decreases in staining scores were also noted for these individuals, and above average staining scores were observed in individuals who did not report both decreases in clarity and comfort.

In general, group averages for ocular health parameters were stable throughout the study and were similar between the low and high clearance lenses.

Chapter 6

Discussion

6.1 Group Analysis Interpretation

This section will detail group analyses discussed in Chapter 5, performed on total (5.3.1, 5.4.1, 5.4.2) and corneal epithelial thickness measurements (5.3.2) collected at each visit. Firstly, total thickness group analysis will be discussed, followed by corneal epithelial thickness group analysis.

6.1.1 Total Corneal Thickness

Total corneal thickness measurements taken with both the Spectralis® and Pentacam® HR were initially analyzed via repeated-measures ANOVA (Chapter 5, section 5.3.1). The goal of this analysis was to determine if there was a statistically significant difference in corneal thickness measurements overall across the three conditions of averaged baseline, low clearance follow-up and high clearance follow-up visits, at each location. Separate analyses were performed for each instrument, eye, and meridian. Results of this analysis are shown in Table 5-4. With both Spectralis® and Pentacam® HR measurements, differences in total corneal thickness measurements across conditions were statistically significantly different in all but one case. The only instance where this was not noted was for the left eye, inferior temporal-superior nasal meridian analysis, measured with the Spectralis®.

Due to the spherical nature of the data, a repeated-measures method to determine specific differences between conditions would have been of limited value. In lieu of post-hoc testing, selective paired t-testing with Holm-Bonferroni correction applied was carried out on each of the three possible combinations of conditions to determine where statistically significant differences in corneal thickness occurred. Comparisons were made between the averaged baseline and low clearance follow-up measurements; averaged baseline and high clearance follow-up; and the low clearance and high clearance follow-up visits. Results of paired t-testing are shown in Chapter 5, Table 5-5, and

descriptive values used for each test are shown in Table 5-6. In this case, measurements were not tabulated separately by location, and all measurements taken at each visit type (e.g., baseline average) for all participants within the same eye, meridian, and instrument were matched with those corresponding measurements from the visit type they were being compared to (e.g., low clearance follow-up). For the Spectralis®, in five out of the eight analyses, there was a statistically significant increase in corneal thickness with scleral lens wear in general, that is, between baseline and both follow-up visits, however there was not a significant difference between low and high clearance follow-up measurements. One of these analyses was for the Spectralis® measurements for the left eye, inferior temporal-superior nasal meridian, where RMANOVA within-subject effects testing did not yield a significant difference. For the remaining three analyses, statistically significant differences were noted with both scleral lens wear in general, and between low and high clearance follow-ups. These three analyses were for the right and left eye in the vertical meridian, and the left eye superior temporal-inferior nasal meridian. For the Pentacam® HR measurements, the same two combinations of statistical significance were observed. However, in more of these analyses (five out of eight), significant differences were observed for scleral lens wear (between baseline and each follow-up), and between low and high clearance follow-up visits. For the right eye horizontal meridian, left eye inferior temporal-superior nasal meridian, and right eye superior temporal-inferior nasal meridian, there was a significant difference in measurements with scleral lens wear, but the difference between low and high clearance follow-ups was not significant. Of note, these three groupings where the change from the low to high clearance lens follow-ups measured with the Pentacam® were not significantly different paralleled statistical significance findings with the Spectralis® measurements. Whether statistically significant or not, all but one comparison yielded an increase in the mean total corneal thickness from baseline to follow-up, and from the low to high clearance follow-up. The exception to this is the analysis of the left eye measured with the Spectralis® in the horizontal

meridian, where mean thickness decreased very minimally (1 μm) from the low to high clearance lens. Mean total corneal thickness measurements referenced here are shown in Table 5-6.

To summarize the results of the group statistical analysis, when comparing follow-up to baseline total corneal thickness measurements, total corneal thickness measurements at follow-up were always statistically significantly greater than baseline measurements, whether the low or high clearance lens was worn. In other words, scleral lens wear always resulted in a statistically significant increase in total corneal thickness, compared to baseline. In some cases, this increase in corneal thickness was statistically significant with increased central clearance (i.e., when comparing the low to the high clearance follow-up corneal thickness measurements). Even if the amount of change was not statistically significant, either scleral lens wear, or increased central clearance in all but one case resulted in an increase in the mean corneal thickness, when analyzing all measurements of each meridian as above. An increase in corneal thickness as a result of conventional scleral lens wear, hypothesized to be due to a relative hypoxic state, is consistent with what has been reported in the literature for eyes with keratoconus,^{243,244,246} and eyes without⁷⁸⁻⁸⁵ measured with both OCT and Pentacam® for both populations. Central, as well as midperipheral increases in thickness has been noted with scleral lens wear in healthy eyes, where a largely symmetrical and uniform response has been suggested, but with a suggestion of a greater amount of swelling inferiorly.^{78,85} However, it should be noted that studies done on eyes without pathology far outnumber those carried out in individuals with keratoconus, and comparisons with all studies should be done with caution, due to pathological and biomechanical differences between these two groups.²⁴⁵

As mentioned, the other important question investigated in this study was whether varying central corneal clearance in scleral lens wear influenced the degree of induction of corneal edema secondary to subclinical hypoxia.

Results of this group statistical analysis suggests that there may be an effect of increased clearance, that is location dependent. Uniformly and with both instruments, corneal thickness along the vertical meridian increased significantly with wear of scleral lenses with an increased corneal clearance, meaning from the low to high clearance follow-up measurements. In most, but not all comparisons, the horizontal and the inferior temporal-superior nasal oblique meridians were not measured to be significantly different across varying clearances, and for the other oblique meridian (superior temporal-inferior nasal), there appeared to be an even division for significance across instruments where the right eye was unaffected by clearance for both, and the left eye was affected. To the best of current knowledge, of the few studies published on scleral lens wear in keratoconus, none have varied central clearance and simultaneously investigated midperipheral changes across various meridians in total corneal thickness. One study where limbal clearance was varied did note corneal swelling to be particularly greater in the inferior and temporal regions.²⁴⁶ In contrast to this cited study and the current study, another group reported inferior total corneal thinning with scleral lens wear alone compared to baseline measurements, which will be discussed further in a later section.²⁴⁵ It is challenging to compare our study results to the results of both of these studies, as analyses were performed by meridian in the current study, rather than quadrant. Also, central corneal clearance was not varied in the cited investigations. When potential edematous effects of lenses of different central corneal clearances have been retrospectively investigated in the healthy population, measurements averaged over the central 4mm of the cornea were reported to increase with increased central clearance, but not by a statistically significant amount, and a preference for location was not mentioned.⁸³ As previously stated, a greater amount of swelling due to scleral lens wear in the inferior meridian has been reported in healthy eyes, and so this finding may be one shared by eyes with and without keratoconus.^{78,290} We carried out a pilot study of similar design to the current study on a small sample size of healthy individuals for a two week period in order to obtain the parameters of a healthy

corneal response to scleral lens wear.²⁹⁰ This pilot study yielded significant total corneal thickness increases across all compared conditions in the vertical meridian, similar to the current study, but in the horizontal meridian, a non-significant increase in thickness with low clearance scleral lens wear was observed, alongside statistically significant increases in corneal thickness from baseline to high clearance follow-up measurements, and between both follow-ups.²⁹⁰ These measurements were taken from images taken with the Pentacam® HR, analyzed along the horizontal and vertical meridians only. In contrast, Pentacam® HR measurements from the current study yielded significant increases in these meridians for all combinations of conditions except for the low versus high clearance follow-up visit in the horizontal meridian. Further work is needed to ascertain this, but it is possible that the keratoconic cornea is more influenced by scleral lens wear in general in the horizontal meridian, in comparison to the non-keratoconic cornea. This observation could potentially be related to the fact that the horizontal meridian, irregularly protruding in keratoconic eyes, is subjected to different influences than the vertical meridian in terms of pressure changes and mechanical rubbing since it follows and falls on the closure line of the eyelids.

A proposed reason for the consistently affected vertical meridian in the case of increased central corneal clearance in this study would be that the cone apex (indicated by a dot in thickness maps, Figure 5-18-Figure 5-41) is quite often located on (31% of cases) or adjacent to this meridian (69% - however, these apices are equidistant to the horizontal meridian). The cone area in its entirety, would lie along or very close to this meridian. In keratoconus, it is known that corneal biomechanical strength is compromised^{215,216,218} due to the pathological process, which would theoretically make this region more vulnerable to edematous changes.^{219,291} However, with 31% of cone apices being located exactly along the inferior temporal-superior nasal meridian, one would expect this uniform effect of significant swelling with increased clearance for this meridian as well, however this was only noted for the right eye, Pentacam® measurements. Similarly, lens decentration coincided with the inferior

temporal meridian in approximately half of follow-up visits, and along the vertical meridian about 20% of the time which would again partially but not fully explain the consistently affected vertical, but not inferior temporal oblique meridian. The interplay between these two factors, as well as probable individual differences are possibly responsible for there not being a consistently affected region across these meridians.

Much of the literature reports on changes in central corneal thickness when central clearance has been varied in scleral lens wear in the healthy population. An association between increased initial clearance and the increase in central corneal thickness both has⁸⁴ and has not⁸¹ been postulated, and significant differences have been noted especially where clearance was intentionally varied and controlled,⁷⁷ while it has otherwise been suggested this not to be the case.^{79,240} Further, a greater influence of clearance on oxygen transmissibility has been suggested where the lens material has a Dk of greater than 100.⁸⁴ In this study, percent changes from baseline to follow-up in the centre were approximately 1-2% for the low clearance lens (Table 5-10), and 1-3% for the high clearance lens (Table 5-11). Scleral lens wear in both cases resulted in an increase in central corneal thickness, and a descriptively greater increase at this location with the high clearance lens.

Estimated marginal mean plots were generated following RMANOVA testing. These results from analysis of data taken with the Pentacam® HR are displayed in Chapter 5, section 5.4.1. Mean total corneal thickness values at each location are graphed, and individual graphs separated by instrument, eye, and meridian are shown. It can be noted that there appears to be a greater separation between the baseline and two follow-up means at the negatively assigned locations, denoted with an “M” on the x axes. For horizontal meridians, this refers to the temporal region, for vertical this is inferior, for the oblique inferior temporal-superior nasal meridian this is the inferior temporal hemi-meridian, and for the superior temporal-inferior nasal meridian, this is the superior temporal meridian. Descriptively, it appears that there are greater increases in thickness between baseline and follow-up measurements

regionally in the temporal, inferior, inferior-temporal, and superior-temporal hemi-meridians compared to their counterparts, in general. Estimated marginal means plots generated from analysis of Spectralis® data did not reveal any clear or consistent regional trends. This general trend in keratoconic eyes was also noted by Yeung et al, where more significant increases in thickness were noted in the inferior and temporal quadrants,²⁴⁶ and in the inferior region, when investigated in healthy eyes,⁷⁸ both measured with the Pentacam®. This observation of descriptively greater edema in these regions would be feasibly explained by both frequent inferior temporal lens decentration, as well as the position of the mechanically weaker cone apex located along the inferior temporal meridian. These observations represent corneal behaviour minutes after lens removal, that is, as it is recovering from scleral lens wear, since this is when Pentacam® measurements were taken. This will be further discussed in later sections.

As mentioned, further descriptive analysis was carried out in the calculation of percent changes from baseline to low clearance (Table 5-10) and baseline to high clearance (Table 5-11), described in 5.4.2. Again, analyses were done separately per instrument, eye, and meridian. Percent changes were reported at each location. Regional descriptive trends discussed previously for Pentacam® HR data were reflected in these tables, that is, descriptively, greater percent changes from baseline were observed in the conventionally assigned negative location values, compared to the positive. Again, Spectralis® data did not exhibit a clear preference for location in this analysis. For both instruments, in many cases, greater percent changes were noted in the more peripheral locations (3 and 4mm from the centre) when comparing baseline to low clearance (Table 5-10). High percent changes were observed closer to the centre (i.e., 1 and 2mm from the centre) in many cases of comparing baseline to high clearance (Table 5-11), in addition to the periphery specifically with Spectralis® measurements. As Spectralis® measurements were taken prior to the Pentacam® HR, it is possible that by the time Pentacam® imaging was done, edema closer to the centre present initially after lens

removal had dissipated. From these results, it can be suggested that as the level of central clearance increases, corneal edema may begin in the periphery and then occupy the central cornea as the degree of hypoxia increases. In the literature, values of corneal edema have reported to range from 0.38-5.44%^{77,78,240,243,244,246,79-85,232} In this study, the range of -0.65-5.01% corneal edema, with an average of $1.96 \pm 0.96\%$ are aligned with what has been described by others.

Descriptively, when examining ocular health parameters overall, there was a greater amount of bulbar hyperemia at both lens follow-ups compared to baseline. However, a descriptive difference between these values at follow-up visits after lens wear of varying clearance was not obvious. Limbal hyperemia appeared to remain consistent at all visits. This may suggest that bulbar hyperemia may be associated with subclinical hypoxia induced by scleral lens wear, in theory due to vascular autoregulation,⁴⁹ but varying levels of clearance used for this study does not appear to substantially affect the overall average amount of hyperemia, from a purely descriptive perspective. This contrasts the more well-established link in the literature between limbal hyperemia and hypoxia in comparison to bulbar hyperemia.^{45,47,48} Bulbar and limbal hyperemia group results are summarized in Table 5-20.

It was descriptively noted that positive corneal fluorescein staining did not change substantially from baseline to follow-up (i.e., with scleral lens wear alone). Negative staining may occur more frequently as scleral lenses are worn, as this was more often noted at the second baseline visit, however there was not a great difference in its occurrence between follow-up visits after lens wear of varying clearances. These results contrast the theoretical prediction that scleral lens-induced hypoxia may be associated with increased positive corneal fluorescein staining.^{43,44} A group summary of corneal fluorescein staining results is displayed in Table 5-21. Further work in a larger sample size of individuals is required to contribute to the investigation of ocular hyperemia and corneal fluorescein staining and its possible relationship with scleral lens-induced hypoxia.

6.1.2 Corneal Epithelial Thickness

Initially, RMANOVAs were also carried out for corneal epithelial thickness data to compare between baseline and both follow-up visits. Results of non-parametric Friedman RMANOVA were in most cases not statistically significant, apart from analysis of the right eye, superior temporal-inferior nasal meridian, where a significance difference was noted. Specific analyses to test for differences between combinations of conditions mentioned in 6.1.1 were similarly carried out with selective paired t-testing, rather than pairwise Durbin-Conover comparisons in the repeated-measures analysis. In general, there was not a statistically significant change in epithelial thickness across any of the three comparisons. That is, scleral lens wear in general did not yield a significant increase in epithelial thickness, and there was not a significant difference between wear of the low and higher clearance lens. Results of paired t-testing with Holm-Bonferroni correction applied (see Table 5-8) revealed only two instances of statistically significant change, those being for the left eye superior temporal-inferior nasal meridian from both the low to high clearance follow-up, and from the baseline to low clearance follow-up. When comparing low to high clearance there was a statistically significant increase in epithelial thickness, however, the change from baseline to low clearance follow-up revealed a significant decrease in epithelial thickness. Descriptive values of epithelial thickness used for these comparisons are shown in Table 5-9. All other pairs of conditions were not significantly different from one another. For epithelial thickness, there was not a consistent trend for a descriptive increase in mean corneal epithelial thickness from baseline to either follow-up visit, or from the low to high clearance follow-up visit, as there was for mean total corneal thickness. These results of largely non-significant and inconsistent changes in epithelial thickness with scleral lens wear are similar to that in the literature, as studies thus far have suggested that total corneal edema secondary to scleral lens wear primarily occurs in the stroma.^{83,84} However, with resolution limitations with current imaging technology, changes in epithelial thickness are presumably more difficult to detect in

comparison to changes in total corneal thickness. It would be worth continuing to investigate this parameter with scleral lens wear, especially with improvements in imaging technology and resolution, in this disease population. In particular, the response to scleral lens wear in locations where the epithelium is pathologically affected would be of clinical interest. However, local variations in epithelial thickness due to pathology alone present practical difficulties in measuring this parameter and may result in a range of responses to scleral lens wear which may not be feasibly generalized.

6.2 Subcategory and Individual Exploratory Analysis Interpretation

With this study being of limited sample size and statistical power, it was determined that it would be of value to describe individual changes and explore patterns across participants with common characteristics in a qualitative manner. Visual depiction of changes in total corneal and corneal epithelial thickness was presented in Chapter 5 in the form of corneal thickness difference mapping. These maps are shown in Figure 5-18-Figure 5-33 (total corneal thickness) and in Figure 5-34-Figure 5-41 (corneal epithelial thickness). When all maps were examined, swelling was defined by a positive difference from baseline to follow-up that was detected by the warmer colour scale of the maps (red for total corneal thickness, yellow for corneal epithelial thickness). Thinning conversely was defined by a negative difference from baseline to follow-up detected by the cooler colour scale of the maps (green for total corneal thickness, blue for corneal epithelial thickness). For both directions of change, the magnitudes necessary to yield a visible colour on the maps were 10 μ m for corneal epithelial thickness maps, and 15 μ m for total corneal thickness maps. Initially, all maps were surveyed in a broad manner. Following this, individual cases grouped by swelling patterns were analyzed. Finally, eyes were sorted firstly by instrument type and disease stage and then, instrument type and positive or negative history of CXL to elucidate patterns. In accordance with the labelling of the difference maps, Stages 1 and 2 will be referred to as “early” keratoconus and Stages 3 and 4 as “severe” keratoconus.

6.2.1 Total Corneal Thickness Analysis

It was generally noted that apparent corneal swelling was much more frequently detected by the Spectralis®, in comparison to the Pentacam® HR. Visually, this meant that Spectralis® maps appeared much redder, indicating swelling, compared to the Pentacam® maps, which conversely appeared much whiter, suggesting minimal change in corneal thickness. As mentioned, Spectralis® measurements were taken immediately after scleral lens removal. The reversal of corneal swelling with scleral lens wear has been reported to occur immediately after removal of a scleral lens,⁶⁸ which would provide a reasonable explanation for greater changes in corneal thickness noted by the Spectralis®, compared to the Pentacam®. However, because the Spectralis® measurements were always taken immediately after scleral lens removal, and Pentacam® measurements were taken minutes later, it cannot be assertively stated that these differences in observations were not also due to instrument variation. To confirm this, randomization of the order of imaging instruments used following lens removal could have been employed. Measurement procedures could have also been repeated, where the other instrument not used after the first measurement session would then be used immediately after lens removal for the repeated session. The latter option would also assist in ruling out the possibility of individual differences. If in both cases with both instruments, measurements were found to be similar immediately following lens removal and during recovery regardless of the instrument used, the change in corneal swelling between those two time points could be fully attributed to the passage of time alone as the cornea recovers from scleral lens wear. Additionally, in most cases, maps showing high clearance lens data appeared “redder” indicating more regions of swelling, compared to the low clearance lens for both instruments. This further supports a link between increased corneal clearance and increased corneal edema secondary to hypoxia.

6.2.1.1 Patterns in Changes in Total Corneal Thickness: Individual Observations

6.2.1.1.1 Diffuse Total Corneal Swelling

With the Spectralis®, some individuals tended to exhibit a more diffuse effect of swelling in terms of location, and swell more, quantitatively, manifesting as a deeper saturation of red, indicating a greater increase in corneal thickness. The three individuals who were most noteworthy for diffuse swelling were 09-KC, 13-KC, and 07-KC.

Participant 09-KC had asymmetrical disease severity between eyes. Specifically, their right eye was graded a Stage 3, or severe stage and their left eye Stage 1, or early stage. In nearly all cases of scleral lens wear for 09-KC, almost the entire total corneal area appeared to swell. High amounts of swelling were noted (in the range of 45-105 μm), which were among the highest amounts of corneal thickness increase observed in this study. This was noted particularly for the right eye high clearance map in the vertical meridian and superior nasal, nasal, and inferior nasal hemimeridians, and to a lesser degree (in the approximate 15-60 μm range) for the left eye high clearance map affecting inferior hemimeridians slightly more than superior regions. In all situations, the cone was affected by total corneal swelling, but it was most intensely affected in terms of swelling amount in the case of the right eye, high clearance lens. The corneal epithelium did not appear to exhibit great amounts of changes in thickness, and exhibited both areas of swelling and thinning, which were sparsely distributed across the cornea. For this participant, the general diffuse nature of swelling was detected by the Pentacam® and can be noted from the thickness maps, but the same degree of swelling as with the Spectralis® was not observed. Instead, difference values tended to range from approximately 15-60 μm , generally falling in the 20-40 μm range for the right eye and stay within the range of 18-31 μm for the left eye. For the Pentacam®, cone apices appeared to be similarly affected for right and left eyes in the cases of low and high clearance lenses, unlike the asymmetric (OD>OS) swelling at the cone noted with the Spectralis®. In the right eye, the substantially increased inferior nasal sectoral

swelling did not correlate exactly with the inferior temporal noted lens decentration, however there was an association between higher values of swelling inferiorly in the left eye and the inferior decentration of this lens.

The above noted nasal swelling in both oblique hemimeridians was paralleled in participant 13-KC with the Spectralis®, who also exhibited a diffuse pattern of swelling but on essentially half of the cornea on the more superior nasal side, where the superior temporal to inferior nasal meridian divides the cornea in two, in addition to swelling along this meridian. Greater total corneal swelling was noted in this region compared to the more inferior temporal section, with the cornea divided as such. This was noted in both eyes, for the higher clearance lens. Specifically, the superior temporal-inferior nasal oblique meridian was affected, as well as the superior, superior nasal, nasal, and inferior nasal hemimeridians. Epithelial swelling appeared to parallel these locations of total corneal swelling for the right eye much more so than for the left for the high clearance lens. Of note, participant 13-KC has Stage 1 (early) keratoconus in both eyes. In all cases, located inferiorly in both eyes, the cone apex was not affected by swelling. Both high clearance lenses were reported to be centred at follow-up, which would not correspond to this sectoral preference for swelling. The Pentacam® did detect greater swelling comparatively with the high, compared to the low clearance lens, but the location of swelling was more diffuse in nature, in contrast to Spectralis® mapping. This may reflect a dissipation of corneal swelling as it recovers from scleral lens wear. With the Pentacam® measurements, it appeared that the cone was affected by swelling only in the case of the left eye, high clearance lens.

For participant 07-KC, diffuse swelling was also noted, similarly to 09-KC, but due to missing data with the Spectralis®, this was difficult to ascertain with these maps alone. From what was available to analyze, the region where the greatest amount of swelling (i.e., where difference maps were most saturated with colour) was noted was for the right eye, high clearance, inferior temporal

hemimeridian. Swelling across entire meridians but of lesser amounts include the nasal region for the right eye, high clearance lens, and for the left eye in this scenario, in the superior temporal region. For the Pentacam®, the same regions of the right eye were affected, as well as more swelling inferior nasal for the left. For the Pentacam®, the centre and adjacent areas 1mm from the centre were largely unaffected by swelling, that is, the swelling appeared to be more paracentrally located compared to Spectralis® measurements. This may loosely parallel the general findings of the Pentacam® detecting less of an increase in the adjacent paracentral regions, compared to more midperipheral paracentral regions, potentially due to the dissipation of corneal swelling at those locations at the time of Pentacam® imaging, minutes after lens removal. The cone apex, located in the centre, appeared to be generally unaffected by swelling for both the Pentacam® and Spectralis®, except for the right eye, low clearance lens. The centrally located cone apices were coincident with the lens being perfectly centred in all situations, meaning that for this individual, scleral lens centration did not overlap well with the strict individual central area of swelling. However, neighbouring locations 1mm from the centre were noted to swell with the Spectralis®, particularly for the right eye. Locations of epithelial swelling were at times coincident with locations of total corneal swelling, both measured by the Spectralis®, most notably for the right eye, low clearance lens. The single location of high corneal epithelial swelling (4mm temporal to centre, left eye, high clearance lens) did overlap with a great amount of total corneal swelling at this location, measured at the same time by the Spectralis®.

When examining individually measured central corneal clearances for these participants, it was noted that for both 07- and 09-KC, one eye exceeded the target range for the low and high clearance lenses. This was the left eye for 07-KC and the right for 09-KC. However, only the left eye of 07-KC was at the extreme of the measured range for the high clearance lens. These observations correlated with descriptive swelling interpretations more so for 09-KC, however a difference between eyes for 07-KC was more difficult to establish due to missing data. Measurements for 13-KC fell within and

not towards the higher extremes of both targeted and measured ranges for both lenses. However, for this participant, stable endothelial guttata throughout study visits were noted, which may explain a slightly greater vulnerability to swelling in this participant. Diffuse corneal swelling occurred in individuals with ranging disease stages. Therefore, this may be a property of the individual's corneal biomechanics. These individuals may have a more even distribution of corneal strength, resulting in a symmetrical pattern of swelling across the cornea.

6.2.1.1.2 Sectoral Total Corneal Swelling

In the majority of cases, distinct corneal swelling was noted in certain hemimeridians. To begin, swelling in the inferior meridian was noted in participants 11-KC, 14-KC, and 15-KC. These participants all had asymmetric disease staging, specifically for 11-KC, their right eye was graded as Stage 1, and left Stage 2, and to a greater degree of asymmetry, early and severe stages in each eye for participants 14-KC (right eye Stage 4, left eye Stage 1) and 15-KC (right eye Stage 1, left eye Stage 4). For participant 11-KC, greater swelling inferiorly was noted for the right eye, high clearance lens only. For 14-KC and 15-KC, inferior swelling was most consistently noted in both eyes for the high clearance lens, but was also observed for the right eye, low clearance lens in 15-KC. The cone apex was affected by swelling in the case of the high clearance lens except for in 11-KC, and in 15-KC left eye, where regions neighboring the cone were affected. Otherwise, corneal swelling at the cone apex was noted for the low clearance lens for 11-KC, where the entire inferior temporal hemimeridian was also affected. This meridian was also affected in 14-KC (right eye, high clearance lens). For both 14-KC and 15-KC, the inferior nasal hemimeridian exhibited some swelling for both high clearance lenses. Other participants also exhibited swelling in the oblique hemimeridians, which will be later detailed. For participants 11-, 14- and 15-KC, lens centration and regions of swelling were well-correlated, particularly for 11-KC and for the right eye, high clearance lens for 14-KC. For all other instances for 14- and 15-KC, both lens centration and corneal swelling were located

inferiorly, but not technically in the same hemimeridians. Some overlap between total corneal and corneal epithelial swelling as measured with the Spectralis® was noted, cases where this was quite apparent were 11-KC in both eyes, low clearance lens, and for both 14- and 15-KC, the left eye, high clearance lens. Pentacam® images most often showed similar regions of swelling and usually swelling to a lesser degree in comparison to the Spectralis®. The exceptions to this would be with 11-KC left eye, high clearance lens where more inferior swelling was noted with the Pentacam®, and for 14-KC, right eye, low clearance lens, where more swelling was noted in the superior and nasal hemimeridians.

Other hemimeridians notably affected by swelling were on the nasal side. Participant 11-KC was previously discussed in detail, as with the high clearance lens, diffuse swelling was noted in the right eye's inferior nasal hemimeridian. This meridian was consistently affected in participant 02-KC and 04-KC with the same lens (high clearance) and eye (right eye), along with the left eye, high clearance lens for 04-KC. Additionally, diffuse swelling in the superior nasal meridian was noted for participant 02-KC for the left eye, high clearance lens. For 04-KC, diffuse and in a few areas, substantial swelling was noted in the nasal hemimeridian for the right eye, and inferiorly in the left eye, both with the high clearance lens. Participants 02- and 04-KC are like one another in terms of disease stage, as well as to participant 11-KC, as all eyes have early keratoconus (Stages 1 and 2). Specifically, participant 02-KC has Stage 2 keratoconus bilaterally, and both participants 04- and 11-KC have Stage 1 in the right, and Stage 2 in the left eye. In all but one case for 02- and 04-KC, the cone apex was unaffected by swelling. The exception to this was 04-KC, left eye, high clearance lens. Lens centration did not perfectly correlate with meridians where greater swelling was noted, however, in all cases except one (02-KC left eye, high clearance lens), both lens centration and swelling were inferiorly noted. In terms of regional parallels to epithelial swelling, this was noted for both 02- and 11-KC with the left eye, low clearance lens, and sparsely noted for the left eye, high clearance lens

for 02-KC. Comparing Pentacam® to Spectralis® mapping revealed in general less total corneal swelling as measured with the Pentacam®, except for a few diffuse areas of swelling noted with Pentacam® and not the Spectralis® for all four maps for participant 02-KC. As stated, Spectralis® measurements were taken prior to those of them Pentacam® after lens removal. The change in pattern of swelling may indicate the dissipation of corneal swelling from a more sectoral to diffuse pattern in the minutes of recovery following lens removal, however, differences in instrumentation may also be responsible. Sectoral corneal swelling patterns appeared to be independent of disease stage, and weakly associated with the location of lens decentration. Thus, these patterns are more likely to be related to individual biomechanics.

6.2.1.1.3 Sectoral Corneal Thinning

In a few isolated cases, total corneal thinning relative to baseline was noted. This was observed in the following participants: 02-KC, 04-KC, 07-KC, 11-KC. All individuals except 07-KC had early keratoconus, who had severe keratoconus bilaterally. Also, thinning was noted more so on the temporal side for early cases, whereas thinning noted for 07-KC was predominantly observed on the nasal side. In all early cases, this occurred with the high clearance lens, but with 07-KC who had severe keratoconus, thinning was noted for the low clearance lens as well. For this group, in all but one case, thinning occurred near the cone but not at the exact conical apex. The exception to this was 07-KC (left eye, low clearance lens), where thinning occurred at the conical apex. In some, but not all cases, these regions overlapped with relative epithelial thinning.

A previous study has reported a noted “rebound” corneal thinning, or deswelling following scleral lens removal, which this very well may be.⁷⁸ In healthy eyes, a regional significance for this phenomenon was not reported.⁷⁸ In contrast, one study carried out in individuals with keratoconus did note significant thinning inferiorly.²⁴⁵ Despite this thinning effect being noted in the extreme groups of disease staging, its nature may vary across these groups. Specifically, since it tended to occur more

nasally in severe cases as opposed to temporally in early, one may expect the location of thinning to change with disease severity. If this thinning is related to the hypoxic effect of scleral lens wear, more severely diseased corneas may also have a lower clearance (and therefore hypoxia) threshold for this effect to occur, as thinning was noted for both the low and high clearance lens for 07-KC, whereas it was only noted in the high clearance lenses for other participants. In particular, the left eye of 07-KC where thinning was noted for the low clearance lens, was the intrasubject “more severe” eye, in terms of possessing more advanced disease characteristics of Stage 4 keratoconus. This thinning effect, if related to corneal edema, may be occurring because of the uneven distribution of mechanical strength across the keratoconic cornea. In particular, it may be a consequence of other, weaker areas (such as the diseased area)^{219,291} of the cornea swelling prior to lens removal if this occurs, placing greater tension and strain on other these regions, resulting in thinning.²⁴⁵ As mentioned, corneal thinning in eyes with keratoconus after scleral lens wear has been reported to be significant inferiorly, in addition to superior corneal thinning in individuals who had both keratoconus and intrastromal corneal ring segments.²⁴⁵ Differences in locations of thinning depending on a history of surgery which has altered the shape, and by consequence, biomechanics of the cornea, provides further support for the possibility of this phenomenon being related to this trait. In the present study, thinning appeared to occur approximately equally in the inferior, superior, and nasal regions. Further, the most dominant effect of scleral lens wear on this group of participants was corneal edema, rather than corneal thinning, as was the case with the group analysis for the study discussed. Since for the current study, this phenomenon was not noted in all participants, it may be more related to individual biomechanical traits. Another possible reason why it was not uniformly noted in all participants was slightly varied timing of image acquisition following scleral lens removal across participants, despite maximal efforts to acquire an image instantly following lens removal. Further, some participants may “de-swell” at a faster rate than others. Additionally, since this was noted in both early and severe stages, it

may not be related to disease stage in terms of its likelihood but may present itself differently in varying disease severity as suggested. Further investigation in a greater number of individuals with a range of disease severity is needed to fully establish this.

6.2.1.2 Subcategory Analysis

6.2.1.2.1 By Disease Severity

For disease stage, three groups were formed according to previously mentioned Amsler-Krumeich staging for keratoconus (see Table 1-1). Eight eyes belonged to the Stage 1 disease group, four to the Stage 2 group, and five had a disease stage of either 3 or 4. Stages 3 and 4 were grouped together, as only one eye in the study had a Stage 3 severity of keratoconus.

When examining thickness maps generated for total corneal thickness measured by both the Spectralis® and the Pentacam® HR, it can be noted that quite often, the measured area closest to the cone apex (labelled with a dot on all thickness maps) is spared from swelling. It was very rare for there to be corneal swelling coinciding with the cone area for the Pentacam®, and this occurrence was more frequent for the Spectralis® maps, which as mentioned exhibited more instances of swelling in general. When maps of the above-mentioned disease severity groupings were analyzed for the Spectralis®, it appeared that the cone apex area was affected by swelling in 35-40% of cases for both Stage 1 and in the severe grouping (Stages 3 and 4), and only approximately in 13% of cases for participants with Stage 2 keratoconus. These comparisons are limited in that they are purely descriptive; however, it may provide insight into a unique resilience at the cone apex of individuals with Stage 2 disease, perhaps due to the specific characteristics and morphological changes occurring during tissue remodeling at this disease stage.

Potential regional patterns in swelling for each instrument were noted. Specifically, when measured with the Spectralis®, swelling more frequently occurred nasally in terms of location, particularly for

individuals with early keratoconus. Conversely, when measured with the Pentacam®, slightly more swelling was noted temporally in general. This finding is consistent with group measurements for the Pentacam® previously mentioned, particularly the estimated marginal means plots as well as percent changes on the conventionally “negative” locations, which includes areas temporal to the centre. When visually inspecting the difference maps, there was not however a particular preference for inferior swelling. The shift in nasal to temporal corneal swelling from the Spectralis® to Pentacam® measurements may indicate how regional corneal swelling changes in the minutes following lens removal, barring differences between instrumentation. This is further discussed in section 6.2.1.3.

6.2.1.2.1.1 Lens Decentration

For each case, lens fit as measured at follow-up visits were noted, and the area on the map corresponding to the lens decentration was examined. This was carried out on groups sorted by instrument, and then examined by disease severity and lens clearance. Lens decentration at follow-up visits were tabulated alongside whether there was substantial regional overlap with the corneal swelling on thickness maps. Substantial regional swelling was determined to be two or more boxes on thickness maps in each area. These results are tabulated by disease severity in Table 6-1 and by lens clearance in Table 6-2.

Table 6-1: Direction of decentration for each eye, sorted by Amsler-Krumeich disease stage.¹⁷¹ Presence (Y) or absence of regional overlap (N) with corneal swelling on thickness maps as measured by each instrument is indicated and totalled for each disease stage.

Participant	Lens	A-K Disease Stage	Eye	Lens Fit		Decentration	Overlap with Spectralis Swelling	Overlap with Pentacam Swelling
				Lateral (x)	Vertical (y)			
04-KC	LC	1	OD	-0.5	-1	IT	N	N
09-KC	LC	1	OS	0	-1	I	Y	N
11-KC	LC	1	OD	-0.5	-1	IT	Y	Y
13-KC	LC	1	OD	0	0.5	S	Y	N
13-KC	LC	1	OS	-1	0.5	ST	N	N
14-KC	LC	1	OS	-1	-1.5	IT	N	N
15-KC	LC	1	OD	-1	-1.5	IT	N	N
04-KC	HC	1	OD	-1	-2	IT	N	N
09-KC	HC	1	OS	0	-1	I	Y	Y
11-KC	HC	1	OD	0	0	C	Y	N
13-KC	HC	1	OD	0	0.5	S	Y	Y
13-KC	HC	1	OS	0	0	C	Y	N
14-KC	HC	1	OS	-1	-1	IT	N	N
15-KC	HC	1	OD	-1	-1	IT	N	N
Counts of presence (Y) and absence of overlap (N)						Stage 1, Y	7	3
						Stage 1, N	7	11
02-KC	LC	2	OD	-1	-1	IT	N	N
02-KC	LC	2	OS	-1	-1	IT	Y	N
04-KC	LC	2	OS	1	-1	IN	N	N
11-KC	LC	2	OS	-1	-1	IT	N	N
02-KC	HC	2	OD	-1	-1	IT	Y	N
02-KC	HC	2	OS	-1	-1.5	IT	N	N
04-KC	HC	2	OS	-1	-2	IT	N	N
11-KC	HC	2	OS	0	-1	I	N	N
Counts of presence (Y) and absence of overlap (N)						Stage 2, Y	2	0
						Stage 2, N	6	8
09-KC	LC	3	OD	0	-1	I	Y	Y
09-KC	HC	3	OD	-1	-1	IT	Y	Y
07-KC	LC	4	OD	0	0	C	Y	N
07-KC	LC	4	OS	0	0	C	N	N
14-KC	LC	4	OD	-0.5	-1.5	IT	Y	N
15-KC	LC	4	OS	-1	-1.5	IT	N	N
07-KC	HC	4	OD	0	0	C	Y	N
07-KC	HC	4	OS	0	0	C	N	N
14-KC	HC	4	OD	0	-1.5	I	Y	N
15-KC	HC	4	OS	-1	-1	IT	N	Y
Counts of presence (Y) and absence of overlap (N)						Stage 3/4, Y	6	3
						Stage 3/4, N	4	7

From these results, taken from individual analyses, overlap between corneal swelling and the direction of decentration was more often noted with the Spectralis® than the Pentacam®. This may be due to the recovery of corneal swelling in general following lens removal. Regional overlap and the lack thereof appeared to equally occur in both early (Stage 1) and late disease stages (Stages 3 and 4). In individuals with Stage 2 disease, there tended to be less regional overlap with lens decentration and swelling. This may indicate that regional swelling due to lens decentration when individually examined is independent of disease stage, or that individuals with Stage 2 disease may be less vulnerable to swelling due to morphology at this disease stage, as previously referenced.

These results were also explored in terms of lens clearance, see below in Table 6-2. As shown, and consistent with results displayed in Table 6-1, there tended to be fewer instances of regional overlap with the Pentacam® compared to the Spectralis®. Instances of regional overlap between corneal swelling and lens decentration were very similar in amount across varying lens clearances, and there was an almost equal occurrence of overlap and lack thereof for both the high and low clearance lens. From this method of analysis, it may be suggested that varying lens central clearance may not have a great effect on regional swelling due to lens decentration.

Table 6-2: Settled direction of decentration for each eye, sorted by lens clearance. Presence (Y) or absence of regional overlap (N) with corneal swelling on thickness maps as measured by each instrument is indicated and totalled for both the low and high clearance lens groups.

Participant	Lens	A-K Disease Stage	Eye	Lens Fit		Decentration	Overlap with Spectralis Swelling	Overlap with Pentacam Swelling
				Lateral (x)	Vertical (y)			
02-KC	LC	2	OD	-1	-1	IT	N	N
02-KC	LC	2	OS	-1	-1	IT	Y	N
04-KC	LC	1	OD	-0.5	-1	IT	N	N
04-KC	LC	2	OS	1	-1	IN	N	N
07-KC	LC	4	OD	0	0	C	Y	N
07-KC	LC	4	OS	0	0	C	N	N
09-KC	LC	3	OD	0	-1	I	Y	Y
09-KC	LC	1	OS	0	-1	I	Y	N
11-KC	LC	1	OD	-0.5	-1	IT	Y	Y
11-KC	LC	2	OS	-1	-1	IT	N	N
13-KC	LC	1	OD	0	0.5	S	Y	N
13-KC	LC	1	OS	-1	0.5	ST	N	N
14-KC	LC	4	OD	-0.5	-1.5	IT	Y	N
14-KC	LC	1	OS	-1	-1.5	IT	N	N
15-KC	LC	1	OD	-1	-1.5	IT	N	N
15-KC	LC	4	OS	-1	-1.5	IT	N	N
Counts of presence (Y) and absence of overlap (N)						LC, Y	7	2
						LC, N	9	14
02-KC	HC	2	OD	-1	-1	IT	Y	N
02-KC	HC	2	OS	-1	-1.5	IT	N	N
04-KC	HC	1	OD	-1	-2	IT	N	N
04-KC	HC	2	OS	-1	-2	IT	N	N
07-KC	HC	4	OD	0	0	C	Y	N
07-KC	HC	4	OS	0	0	C	N	N
09-KC	HC	3	OD	-1	-1	IT	Y	Y
09-KC	HC	1	OS	0	-1	I	Y	Y
11-KC	HC	1	OD	0	0	C	Y	N
11-KC	HC	2	OS	0	-1	I	N	N
13-KC	HC	1	OD	0	0.5	S	Y	Y
13-KC	HC	1	OS	0	0	C	Y	N
14-KC	HC	4	OD	0	-1.5	I	Y	N
14-KC	HC	1	OS	-1	-1	IT	N	N
15-KC	HC	1	OD	-1	-1	IT	N	N
15-KC	HC	4	OS	-1	-1	IT	N	Y
Counts of presence (Y) and absence of overlap (N)						HC, Y	8	4
						HC, N	8	12

When examined in this manner, results are contrary to what was previously discussed for that of the Pentacam®, where a qualitatively greater swelling was suspected in the general region of lens centration (displayed in estimated marginal means plots, see Figure 5 11-Figure 5 18). However, it should be noted that the analysis discussed in this section refers to the presence or absence of a certain magnitude of swelling in a particular region as shown by the thickness maps, and prior analysis in the estimated marginal means plots displayed descriptive differences in amounts of swelling in certain regions compared to other regions. That is, the area of lens decentration (typically inferior temporal) does likely exhibit a greater amount of corneal swelling than its superior nasal counterpart when measured with the Pentacam®, however this magnitude was not deemed to be substantial in the context of this section’s analysis. Further work is needed to explore this phenomenon.

6.2.1.2.1.2 Central Total Corneal Swelling and Changes in Visual Acuity

Where central swelling was noted, the change in both high and low contrast visual acuity from baseline to follow-up was examined for that lens and eye. A change of one line (0.1 logMAR units) or greater was considered a substantial change, as this would be clinically significant. Again, difference maps were sorted by instrument and disease severity. A substantially decreased visual acuity was not consistently observed in cases of centrally located swelling. However, the instance where decreased visual acuity was most frequently observed with central corneal swelling was in individuals with Stage 1 and Stage 4 keratoconus, with corneal thickness measured by the Spectralis®. In both disease categories, 50% of cases of central swelling were associated with a decrease in low contrast visual acuity from baseline to follow-up. In severe keratoconus, there was one case (17%) of a decrease in high contrast visual acuity from baseline to follow-up, and in Stage 1, there was one case of an improvement in high contrast visual acuity (10%). There may be an association between increased total corneal thickness centrally and decreased low contrast visual acuity, but this finding was not

consistently observed. With the Pentacam®, central swelling was much less frequently observed, specifically, it was only noted in participants 09-KC and 15-KC. These individuals both exhibited extreme asymmetrical disease staging between eyes, paralleling the range of disease stages where central swelling was noted with the Spectralis®. Where central swelling was noted for these participants, a clinically significant decrease in visual acuity was only noted for 09-KC OD with the high clearance lens and measured with high contrast visual acuity, and low contrast visual acuity remained stable, in contrast with individuals with central swelling noted with the Spectralis®. Due to the more frequent occurrence of central swelling immediately after lens removal (Spectralis®) compared to minutes later (Pentacam®), along with differences in the nature of the change in visual acuity between individuals exhibiting central swelling with each instrument, visual acuity may also return to baseline as the cornea recovers from swelling, aside from possible differences between instruments. This would be better asserted by measuring visual acuity as the cornea recovers. This however may be practically difficult in severely diseased eyes with irregular astigmatism without a scleral lens to adequately correct one's vision.

6.2.1.2.2 By Surgical History

Comparisons were also made between individuals with and without a history of CXL surgery. Individuals with a history of CXL included participants 02-KC OU, 04-KC OU, 09-KC OD, and 15-KC OU, as shown in Table 5-1. Swelling at the cone area previously detailed appeared to be similar for those with and without a history of CXL when examining Spectralis® maps, which was just under one third of cases for both groups of participants. However, for the Pentacam® maps, there was less corneal swelling measured at the cone apex in those with a history of CXL (7%), compared to those without (22%). This may indicate a unique resiliency at the cone region in its recovery from edema in eyes with prior CXL, unless instrumentation differences are responsible. Regionally, both eyes that had undergone and had not undergone CXL, when imaged with the Spectralis® exhibited a nasal

location preference for swelling, as was noted in general. With the Pentacam®, there did not appear to be a preference for a particular region of swelling. Plausibly, cross-linking surgery may provide greater resistance to corneal swelling secondary to hypoxia with scleral lens wear, although further investigation is needed to determine this. Otherwise, patterns of corneal swelling secondary to scleral lens wear did not appear to differ greatly across these two groups. Our findings, if confirmed with a larger study, would suggest that patients who had undergone CXL would potentially recover more rapidly at the cone region from hypoxia-induced corneal swelling, if subsequent scleral lens wear is necessary. Theoretically, these eyes would be less susceptible to hypoxia-induced corneal swelling, however, this must also be confirmed in larger study. This could represent an additional possible benefit of CXL together with the expected therapeutic and preventive benefits of this treatment.

6.2.1.3 Interpretation of Common Locations of Swelling

Quite often, in Spectralis® mapping, representing differences in corneal thickness immediately after scleral lens removal, both entire meridians inferiorly and inferior nasally exhibited a diffuse pattern of swelling. Additionally, the region closest to the cone apex was often spared but swelling in neighbouring regions was noted. Regions on the nasal side tended to swell by a substantial amount in individuals who exhibited a more diffuse pattern of swelling (09-KC, 13-KC). Most of these instances were noted in situations where the individual had worn the higher clearance lens in this study. In addition, Pentacam® mapping, representing corneal thickness minutes after lens removal, displayed a general location preference for swelling on the temporal side. These patterns provide insight into the location of greatest swelling in scleral lens wear in individuals with keratoconus, and how this swelling may recover in the time after lens removal. In most cases, both the cone apex and lens centration are located inferior temporally. Presumably, where the lens apex centres on the eye is the location of maximum negative fluid pressure, placing this region under comparatively greatest strain. If these locations are coincident, the cone apex region, already vulnerable due to pathology, is being

placed under great mechanical strain. Perhaps, neighbouring regions to the cone apex, as well as nasal regions exhibit a sympathetic adaptive response in swelling by a greater amount, which varies by the individual. It is also possible that instantaneously with lens removal and relief of this pressure, greater swelling at the vulnerable inferior temporal and cone regions rapidly migrates to this nasal region. Then, a few minutes after removal, residual swelling is more apparent in the originally vulnerable temporal area as the cornea recovers. On the contrary, it is also possible that neighbouring regions are swelling comparatively more due to the cone area being of more compact architecture.¹²⁴ This would be fully asserted with lens-on imaging, followed by imaging immediately after (as was done in this study), and then imaging at set time increments following lens removal with the same instrument. To the best of current knowledge, this has not been reported on in keratoconus. In healthy eyes, initial corneal swelling following scleral lens removal after a short period of wear appeared to be greatest inferiorly, and in that study, it was suspected that the superior region would be more compromised in terms of oxygen delivery due to the upper lid presence.⁷⁸ This would imply a similar hypothesis as proposed here, that perhaps neighbouring regions to those most affected may swell more immediately after lens removal.

6.2.2 Corneal Epithelial Thickness Analysis

Unlike changes in total corneal thickness, there was not a uniform effect of an increase in epithelial thickness. Rather, there appeared to be a roughly even distribution of epithelial swelling and thinning, excepting participants with early (Stage 1) keratoconus, where there were more occurrences of swelling than thinning when considering individual cases. This was especially noted for 04-KC OD, 13-KC OU, and 14-KC OS. The cone apex was again largely unaffected, but when affected, there were more cases of epithelial swelling at the cone apex in severe cases, and more cases of epithelial thinning at the cone apex in Stage 2 keratoconus. For individuals with Stage 1 keratoconus, there was a similar amount of thinning and thickening of the corneal epithelium at the cone apex. The

epithelium may be more vulnerable to swelling as keratoconus advances, as early as Stage 2. There was a slight preference for epithelial swelling at locations of lens centration for individuals with Stages 1 and 2 keratoconus, however thinning and thickening at this location was equally likely for severe cases. Further regional trends, and differences between the low and high clearance lenses could not be assertively elucidated for the group.

Literature on epithelial behaviour in scleral lens wear is limited in healthy eyes, and to the best of current knowledge, not yet reported in eyes with keratoconus. In studies carried out, an initial epithelial swelling, followed by thinning during an 8-hour period of wear has been suggested.⁸³ Additionally, a non-significant increase of the epithelium has been noted.⁸⁴ Our study's largely non-significant results in both individual and group analysis parallels these mixed, yet limited results reported.

6.3 Lens Fit and Ocular Health

6.3.1 Central Corneal Clearance

On average, measurements of follow-up central corneal clearance fell exactly within targeted ranges for both the low and high clearance lenses, as shown in Table 5-13. There was one isolated occurrence where the settled clearance for the high clearance lens was lower than that of the low clearance lens settled clearance, by 54 μm (participant 14-KC OS, see Table 5-12). It is not likely that lenses were reversed in error, as the lens of the other eye settled accordingly, but it is possible that the force used by the participant was greater, or the amount of fluid in the lens bowl was slightly less than what was used for insertion that day, compared to at the delivery appointment to assess the lens clearance. Settling was 48 μm on average for the low clearance lens, and 89 μm for the high clearance lens. This observation is consistent with previous reports that lenses of higher initial clearance settle more than those of lower initial clearance.²⁹²

6.3.2 High and Low Contrast Visual Acuity

Clinically significant decreases in BCVA from baseline to follow-up rarely occurred in the case of high contrast visual acuity, where this was only noted for participant 09-KC OS, high clearance lens. This individual exhibited diffuse swelling of considerable magnitude all cases of lens wear, but especially in this case, as shown in Figure 5-21. In many other circumstances, there was a clinically significant improvement in high contrast visual acuity. Low contrast visual acuity was much more frequently decreased by a clinically significant amount when comparing baseline to follow-up, and on average, there were more letters lost compared to when measured with high contrast visual acuity. For low contrast visual acuity alone, average amounts of letters lost were similar and technically more substantial for the low clearance lens follow-up compared to the high clearance lens follow-up. However, average amounts of improvement were often similar to amounts of decreased acuity, except for the right eye, high clearance lens where on average more letters were lost, and for the left eye, low clearance lens where on average more letters were gained. These results suggest that low contrast visual acuity may slightly decrease with scleral lens wear, however since improvements in this parameter were similarly noted, this cannot be assertively stated. As corneal edema increases in magnitude, it may induce clinically significant decreases in high contrast visual acuity, as shown for participant 09-KC.

Visual acuity findings were also discussed previously in section 6.2.1.2.1.2 and investigated for possible correlation to central corneal edema.

6.3.3 Subjective Comfort Results

Most participants preferred the lower clearance lens between the two. Also, from baseline to follow-up, there were more cases of decreased clarity and comfort and a greater magnitude in the decrease of these scores for the high clearance compared to the low clearance lens. For all but one participant, this was the second lens worn. The participant for whom the low clearance was worn first, the preferred

lens was the high clearance initially, and equal at follow-up. Because order did not stay randomized as planned, it cannot be definitively stated that the low clearance was exclusively preferred due to fitting characteristics, as adaptation to scleral lens wear was also a factor. The preference for the lower clearance lens with a scleral lens system of an overall lower Dk is indirectly in alignment with reports of a preferred higher Dk lens,⁸⁴ and in contrast to another study, reporting a lens of higher limbal clearance being preferred.²⁴⁶ However, central clearance in both studies were not altered, and so these two studies could not be compared with certainty.

6.3.4 Lens Centration

As is typical with scleral lens wear, many of the study lens fits, despite optimal prediction of alignment with scleral toricity per the CSP, were slightly decentred inferiorly and temporally.⁵¹ Additionally, lenses were often inferiorly decentred and centred laterally. Specific groupings of these cases were detailed as they potentially related to changes corneal thickness in 6.1.1 and additionally in 6.2.1.2.1.1.

6.3.5 Ocular Health Parameters

Ocular health parameters, including hyperemia and corneal fluorescein staining are detailed individually in Appendix J and Appendix K, respectively, and summarized for the group in Table 5-20. These parameters as they relate to scleral lens wear were previously discussed in section 6.1.1. These results indicate that scleral lens wear was well-tolerated in all participants. Hyperemia rarely exceeded a grade of 2.0 on the 0.0-4.0 JENVIS scale²⁵⁷ at follow-up visits, apart from two cases of bulbar hyperemia for participant 07-KC, nasally in the left eye both times (2.5 at low clearance follow-up, 2.1 at high). This was due to mild blanching which was deemed acceptable for this study time frame. However, these results should be interpreted with caution, since this method has been shown to underestimate ocular redness compared to subjective methods.^{293,294}

Corneal fluorescein staining, an indicator of both the ocular response to scleral lens wear and nonspecific ocular surface insult rarely exceeded a grade 1, or micropunctate type per the BHVI grading scale.²⁸⁹ Of note, for participant 15-KC's right eye at the high clearance lens follow up visit, grade 3 coalescent staining was noted centrally, superiorly and inferiorly. This was determined to be secondary to desiccation from a noted bubble in the post-lens fluid reservoir, coincident with these regions. This finding resolved at the subsequent visit. Across participants, there was not any significant impairment of ocular health parameters noted, due to scleral lens wear.

6.4 Comparison to Findings of Michaud et al.

As detailed in 2.1, theoretical calculations made by Michaud et al. advise that practitioners use scleral lenses of the highest Dk possible, greater than 150, with a centre thickness not exceeding 250 μm , and a central corneal clearance no greater than 200 μm to prevent corneal edema secondary to hypoxia.⁶¹ In this study, two of these criteria could not be met due to lens specifications available for the study. Specifically, the scleral lenses used (Zenlens™) were composed of Boston XO® (Dk=100), with a standard centre thickness of 350 μm .²⁵² As discussed in section 4.6, a negative flex control factor was considered for lenses whose centre thicknesses exceeded this standard value due to the lens power, however this was not employed since it would alter the lens thickness profile. The central corneal clearance recommendation of 200 μm is highly congruent with the average settled clearance for the low clearance lens used in this study, as shown in Table 5-13, which is also in the centre of the targeted low clearance range. It would be expected that corneal edema would be induced in all cases of scleral lens wear in this study, whether the low or high clearance lens was worn, predicted by Michaud's calculations. A statistically significant amount of edema was indeed observed in this study with the wear of both lenses, but these levels were largely within the physiological range, as noted in other clinical studies.^{77,78,240,243,244,246,79–85,232} It should be noted that the goal of Michaud et al. was to determine levels to completely prevent any corneal edema from occurring, regardless of whether this

was within the physiological range. The Dk/t predicted by this paper, when using average settled clearance values, would range from 13.8-16.7 Dk/t units for the high and low clearance lens, respectively. From predictions by Morgan et al.,²² both Dk/t values would result in a less than 1% increase in corneal thickness (see Figure 4-9). In this study, percentage total corneal swelling more commonly did exceed 1%, likely because initial levels of clearance exceeded these values prior to settling, inducing greater corneal edema. Therefore, the results of this study did follow what was predicted by this theoretical study in that edema was induced, however, the wear of both lenses appeared to be clinically safe due to its low level.

When considering cases where the clearance did exceed 200 μm (i.e., after wear of the high clearance lens for all participants), there was descriptively less comfort and clarity, and the lower clearance lens was often preferred. Scleral lens wear alone did result in decreased visual acuity, more frequently low contrast, however there was not a consistent effect of lens clearance noted, and improvements in this parameter were similarly noted. Likewise, bulbar redness was increased with scleral lens wear, but not particularly more so with the higher clearance lens. Positive corneal fluorescein staining remained stable throughout the study.

In individuals whose settled clearances greatly exceeded 200 μm in the low clearance lens group (i.e., 250 μm or greater), perceptual and ocular health parameters were examined. Specifically, this was for participant 09-KC OD, and 14-KC OU. Visual acuity shown in Table 5-14 remained stable from baseline to follow-up for 09-KC OD, where a clinically significant decrease in low contrast VA was noted in the right eye of 14-KC, and a clinically significant increase was noted in the left eye. Subjective changes in clarity and comfort from baseline to follow-up were stable for 09-KC OD, where for 14-KC there was an increase in comfort but a decrease in clarity for both eyes (see Table 5-16). As shown in Appendix J, hyperemia remained stable from baseline to follow-up for 09-KC OD, where there was an increase in limbal hyperemia nasally and temporally for 14-KC OD, and in

temporal bulbar hyperemia OS. Corneal fluorescein staining slightly increased inferiorly and temporally for 09-KC, and for 14-KC there was a slight increase centrally and nasally (OD) and superior and temporally (OS), as shown in Appendix K.

Overall, changes in these parameters were noted with lens wear, however they were not consistently observed for these participants, nor was there a trend in location of ocular health parameter changes. Subjective scores most consistently indicate that there may be subclinical differences between the low and high clearance lens due to hypoxia, which may result in decreased lens comfort.

6.5 Study Limitations

This study was primarily limited due to its sample size. As mentioned, the COVID-19 pandemic, an external factor, was the reason for the unforeseen changes to the study, which necessitated protocol adjustments and a smaller sample size than originally intended. However, study results still have provided excellent insight into scleral lens wear in individuals with keratoconus and have generated multiple hypotheses on corneal swelling secondary to hypoxia with this lens modality. A healthy control group studied under identical conditions would have assisted in the assertion that regional changes observed were related to the pathological process of keratoconus.

As mentioned, corneal imaging was carried out immediately following scleral lens removal. This was done as quickly as possible, however could not be guaranteed to be immediately following this for all images. This was due to each volume scan taking a small amount of time, exacerbated by participant movement, which could vary by individual and across study visits within each individual case. Measurements with the Spectralis® were always carried out before those taken with the Pentacam®, resulting in higher thickness measurements being recorded with the Spectralis®. It is unclear whether this finding was solely due to this order of measurement or if it must be attributed to

the instruments as well – future studies comparing these multiple devices should include device-order randomization. The image processing method used to generate corneal thickness measurements from Spectralis® images was largely manual, with automatic aspects. The development of this process was incredibly valuable from an image processing learning perspective. However, its manual nature gave way to potential human error, despite the process being highly systematic, and maximal efforts by the investigator to remain unbiased.

Lastly, in this study, a difference of 100µm of initial targeted clearance between lenses was used, which may have not been sufficiently different, due to settling differences, to confirm if varying clearance truly influenced corneal physiology. Perhaps if a greater difference between lenses was targeted, a more consistent effect of varying clearance would have been observed. However, the fact that there were significant changes noted at times with this chosen target difference does provide unique insight into location-specific changes in corneal thickness in response to scleral lens wear. Additionally, it has made a valuable contribution to answering the clinical question of how subtle changes in clearance influence corneal physiology in the keratoconic population, for whom scleral lenses are primarily indicated.

Chapter 7

Conclusions and Future Work

7.1 Conclusions

7.1.1 Corneal Thickness Changes

Analyzing corneal thickness data with scleral lens wear both as a group, and with individual mapping has provided further insight into the nature of corneal swelling with scleral lens wear in this at-risk population.

Without question, scleral lens wear is associated with increased corneal thickness secondary to hypoxia, with both the lens and fluid reservoir as barriers to oxygen delivery. With the amount of clearance varied, a statistically significant difference in the group analysis was not always noted between corneal thickness measurements at follow-up. However, greater consistency of descriptive swelling patterns from difference maps noted at the high clearance follow-up visit compared to the low clearance follow-up suggests that corneal swelling with scleral lens wear does depend on the amount of scleral lens clearance. As depicted in difference mapping, this swelling is quite likely location-specific in individuals with keratoconus.

The changing of location preference of corneal swelling when comparing Spectralis® to Pentacam® maps, taken minutes apart after lens removal suggests that during recovery, the location of this swelling shifts, assuming instrumentation was consistent. A complex interaction between the nature of recovery, unique corneal biomechanics, and relief of lens pressure may very well be responsible for the change in the location of corneal swelling.

7.1.2 Individual Differences

An important finding from this work is that there are individual differences in patterns of swelling in this disease population, that is not always related to disease severity. This is significant, as many

individuals with keratoconus have asymmetric disease stages between eyes. Therefore, individuals may possess characteristics of swelling that are both unique to them, as well as their disease stage.

In some individuals, corneal thinning immediately following lens removal was observed. This phenomenon is likely related to corneal biomechanics in keratoconus, as well as how the individual's cornea responds to the relief of fluid pressure and reversal of hypoxia.

7.1.3 Association of Total Corneal Thickness Changes and Varying Lens Clearance with Other Factors

Associations between total corneal and epithelial swelling were sometimes, but not consistently noted. Additionally, cases of increased central corneal swelling did at times correspond with a decrease in low contrast visual acuity, but this was again not a uniform finding. Lens centration location was not consistently perfectly coincident with areas of noted swelling. The nature of corneal swelling secondary to scleral lens wear in eyes with and without clinical history of CXL may vary between these groups qualitatively in terms of swelling at the cone apex, but this was only noted with Pentacam® measurements. Otherwise, these two parties did not drastically differ from one another in their patterns of swelling, despite the intended increase in biomechanical strength of the cornea with this treatment. Decreases in subjective clarity and comfort were descriptively noted more often and of greater magnitude for the high clearance, compared to the low clearance lens, which was more often preferred. A descriptive increase in bulbar hyperemia with scleral lens wear from baseline was noted for both lenses but similar between lenses. Corneal staining remained stable on average throughout the study. Decreased low contrast visual acuity was at times observed with scleral lens wear, with inconsistent differences between lens clearances.

7.2 Future Work

To gain more insight into the pan-corneal effects of hypoxia secondary to scleral lens wear in individuals with keratoconus, further work is needed. Firstly, a greater number of individuals should be studied to fully establish the effects of increased central corneal clearance with scleral lens wear. Secondly, greater representation of individuals with more advanced stages of keratoconus would be valuable, particularly including more patients with severe keratoconus, as these individuals tend to more often require and benefit from optical correction through scleral lenses. Individuals with asymmetrical disease staging between eyes represent a large percentage of this disease population, and thus should continue to be studied. Additionally, a direct comparison with individuals without ocular pathology would also be of value, to confirm whether regional trends in corneal swelling are truly unique to this disease process, and resultant biomechanical properties of the cornea.

Further work on image processing, where corneal measurements could be taken with lenses on would also be feasible and would provide important insight into corneal behaviour immediately before and after scleral lens removal. An automatic method of image processing would be of value in the reduction of human error and increasing efficiency in the collection of corneal thickness measurements. Corneal thickness difference mapping beyond the four principal meridians would also be useful, to gain a greater understanding of how corneal thickness behaves beyond these regions, and the cone region in its entirety. This would likely be achieved most effectively by using automatic image processing algorithms which commercially available instruments may be equipped with.

The relationship between total corneal swelling with epithelial changes in thickness, low contrast visual acuity decrease, and scleral lens decentration could not be definitively established. However, association between these factors were at times noted. Subjective comfort and bulbar hyperemia may provide greater insight into the effects of scleral lens-induced edema. Further exploration of the

interaction between these elements, in addition to a history of CXL, in a larger group of individuals with keratoconus would be of interest to be evaluated in further studies, some of which are ongoing.

It was valuable to note that a difference of 100 μ m between targeted clearances may affect corneal physiology. This difference, in conjunction with a third lens of a greater targeted clearance from the low clearance lens would provide insight into the influence of both subtle, as well as changes of a greater magnitude in scleral lens central clearance, on the corneal physiology in those with keratoconus.

Letters of Copyright Permission

Figure 1-2

ELSEVIER LICENSE
TERMS AND CONDITIONS

Jun 19, 2021

This Agreement between Dr. Kirsten Carter ("You") and Elsevier ("Elsevier") consists of your license details and the terms and conditions provided by Elsevier and Copyright Clearance Center.

License Number	5092810293859
License date	Jun 19, 2021
Licensed Content Publisher	Elsevier
Licensed Content Publication	Elsevier Books
Licensed Content Title	Contact Lens Complications
Licensed Content Author	Nathan Efron
Licensed Content Date	Jan 1, 2012
Licensed Content Pages	13
Start Page	185
End Page	197
Type of Use	reuse in a thesis/dissertation
Portion	figures/tables/illustrations

Number of figures/tables/illustrations	1
Format	both print and electronic
Are you the author of this Elsevier chapter?	No
Will you be translating?	No
Title	Changes in corneal thickness in keratoconic eyes with variation in scleral contact lens central clearance
Institution name	University of Waterloo
Expected presentation date	Aug 2021
Portions	Figure 20.9
Requestor Location	Dr. Kirsten Carter 78A Mill Street East P.O Box 152 Milverton, ON N0K 1M0 Canada Attn: Kirsten Carter
Publisher Tax ID	GB 494 6272 12
Total	0.00 CAD
Terms and Conditions	

INTRODUCTION

1. The publisher for this copyrighted material is Elsevier. By clicking "accept" in connection with completing this licensing transaction, you agree that the following terms and conditions apply to this transaction (along with the Billing and Payment terms and conditions established by Copyright Clearance Center, Inc. ("CCC"), at the time that you opened your Rightslink account and that are available at any time at <http://myaccount.copyright.com>).

GENERAL TERMS

2. Elsevier hereby grants you permission to reproduce the aforementioned material subject to the terms and conditions indicated.

3. Acknowledgement: If any part of the material to be used (for example, figures) has appeared in our publication with credit or acknowledgement to another source, permission must also be sought from that source. If such permission is not obtained then that material may not be included in your publication/copies. Suitable acknowledgement to the source must be made, either as a footnote or in a reference list at the end of your publication, as follows:

"Reprinted from Publication title, Vol /edition number, Author(s), Title of article / title of chapter, Pages No., Copyright (Year), with permission from Elsevier [OR APPLICABLE SOCIETY COPYRIGHT OWNER]." Also Lancet special credit - "Reprinted from The Lancet, Vol. number, Author(s), Title of article, Pages No., Copyright (Year), with permission from Elsevier."

4. Reproduction of this material is confined to the purpose and/or media for which permission is hereby given.

5. Altering/Modifying Material: Not Permitted. However figures and illustrations may be altered/adapted minimally to serve your work. Any other abbreviations, additions, deletions and/or any other alterations shall be made only with prior written authorization of Elsevier Ltd. (Please contact Elsevier's permissions helpdesk [here](#)). No modifications can be made to any Lancet figures/tables and they must be reproduced in full.

6. If the permission fee for the requested use of our material is waived in this instance, please be advised that your future requests for Elsevier materials may attract a fee.

7. Reservation of Rights: Publisher reserves all rights not specifically granted in the combination of (i) the license details provided by you and accepted in the course of this licensing transaction, (ii) these terms and conditions and (iii) CCC's Billing and Payment terms and conditions.

8. License Contingent Upon Payment: While you may exercise the rights licensed immediately upon issuance of the license at the end of the licensing process for the transaction, provided that you have disclosed complete and accurate details of your proposed use, no license is finally effective unless and until full payment is received from you (either by publisher or by CCC) as provided in CCC's Billing and Payment terms and conditions. If full payment is not received on a timely basis, then any license preliminarily granted shall be deemed automatically revoked and shall be void as if never granted. Further, in the event that you breach any of these terms and conditions or any of CCC's Billing and Payment terms and conditions, the license is automatically revoked and shall be void as if never granted. Use of materials as described in a revoked license, as well as any use of the materials beyond the scope of an unrevoked license, may constitute copyright infringement and publisher reserves the right to take any and all action to protect its copyright in the materials.

9. Warranties: Publisher makes no representations or warranties with respect to the licensed material.

10. Indemnity: You hereby indemnify and agree to hold harmless publisher and CCC, and their respective officers, directors, employees and agents, from and against any and all claims arising out of your use of the licensed material other than as specifically authorized pursuant to this license.

11. **No Transfer of License:** This license is personal to you and may not be sublicensed, assigned, or transferred by you to any other person without publisher's written permission.

12. **No Amendment Except in Writing:** This license may not be amended except in a writing signed by both parties (or, in the case of publisher, by CCC on publisher's behalf).

13. **Objection to Contrary Terms:** Publisher hereby objects to any terms contained in any purchase order, acknowledgment, check endorsement or other writing prepared by you, which terms are inconsistent with these terms and conditions or CCC's Billing and Payment terms and conditions. These terms and conditions, together with CCC's Billing and Payment terms and conditions (which are incorporated herein), comprise the entire agreement between you and publisher (and CCC) concerning this licensing transaction. In the event of any conflict between your obligations established by these terms and conditions and those established by CCC's Billing and Payment terms and conditions, these terms and conditions shall control.

14. **Revocation:** Elsevier or Copyright Clearance Center may deny the permissions described in this License at their sole discretion, for any reason or no reason, with a full refund payable to you. Notice of such denial will be made using the contact information provided by you. Failure to receive such notice will not alter or invalidate the denial. In no event will Elsevier or Copyright Clearance Center be responsible or liable for any costs, expenses or damage incurred by you as a result of a denial of your permission request, other than a refund of the amount(s) paid by you to Elsevier and/or Copyright Clearance Center for denied permissions.

LIMITED LICENSE

The following terms and conditions apply only to specific license types:

15. **Translation:** This permission is granted for non-exclusive world **English** rights only unless your license was granted for translation rights. If you licensed translation rights you may only translate this content into the languages you requested. A professional translator must perform all translations and reproduce the content word for word preserving the integrity of the article.

16. **Posting licensed content on any Website:** The following terms and conditions apply as follows: Licensing material from an Elsevier journal: All content posted to the web site must maintain the copyright information line on the bottom of each image; A hyper-text must be included to the Homepage of the journal from which you are licensing at <http://www.sciencedirect.com/science/journal/xxxxx> or the Elsevier homepage for books at <http://www.elsevier.com>; Central Storage: This license does not include permission for a scanned version of the material to be stored in a central repository such as that provided by Heron/XanEdu.

Licensing material from an Elsevier book: A hyper-text link must be included to the Elsevier homepage at <http://www.elsevier.com>. All content posted to the web site must maintain the copyright information line on the bottom of each image.

Posting licensed content on Electronic reserve: In addition to the above the following clauses are applicable: The web site must be password-protected and made available only to bona fide students registered on a relevant course. This permission is granted for 1 year only. You may obtain a new license for future website posting.

17. **For journal authors:** the following clauses are applicable in addition to the above:

Preprints:

A preprint is an author's own write-up of research results and analysis, it has not been peer-reviewed, nor has it had any other value added to it by a publisher (such as formatting, copyright, technical enhancement etc.).

Authors can share their preprints anywhere at any time. Preprints should not be added to or enhanced in any way in order to appear more like, or to substitute for, the final versions of articles however authors can update their preprints on arXiv or RePEc with their Accepted Author Manuscript (see below).

If accepted for publication, we encourage authors to link from the preprint to their formal publication via its DOI. Millions of researchers have access to the formal publications on ScienceDirect, and so links will help users to find, access, cite and use the best available version. Please note that Cell Press, The Lancet and some society-owned have different preprint policies. Information on these policies is available on the journal homepage.

Accepted Author Manuscripts: An accepted author manuscript is the manuscript of an article that has been accepted for publication and which typically includes author-incorporated changes suggested during submission, peer review and editor-author communications.

Authors can share their accepted author manuscript:

- immediately
 - via their non-commercial person homepage or blog
 - by updating a preprint in arXiv or RePEc with the accepted manuscript
 - via their research institute or institutional repository for internal institutional uses or as part of an invitation-only research collaboration work-group
 - directly by providing copies to their students or to research collaborators for their personal use
 - for private scholarly sharing as part of an invitation-only work group on commercial sites with which Elsevier has an agreement
- After the embargo period
 - via non-commercial hosting platforms such as their institutional repository
 - via commercial sites with which Elsevier has an agreement

In all cases accepted manuscripts should:

- link to the formal publication via its DOI
- bear a CC-BY-NC-ND license - this is easy to do
- if aggregated with other manuscripts, for example in a repository or other site, be shared in alignment with our hosting policy not be added to or enhanced in any way to appear more like, or to substitute for, the published journal article.

Published journal article (JPA): A published journal article (PJA) is the definitive final record of published research that appears or will appear in the journal and embodies all value-adding publishing activities including peer review co-ordination, copy-editing, formatting, (if relevant) pagination and online enrichment.

Policies for sharing publishing journal articles differ for subscription and gold open access articles:

Subscription Articles: If you are an author, please share a link to your article rather than the full-text. Millions of researchers have access to the formal publications on ScienceDirect,

and so links will help your users to find, access, cite, and use the best available version.

Theses and dissertations which contain embedded PJAs as part of the formal submission can be posted publicly by the awarding institution with DOI links back to the formal publications on ScienceDirect.

If you are affiliated with a library that subscribes to ScienceDirect you have additional private sharing rights for others' research accessed under that agreement. This includes use for classroom teaching and internal training at the institution (including use in course packs and courseware programs), and inclusion of the article for grant funding purposes.

Gold Open Access Articles: May be shared according to the author-selected end-user license and should contain a [CrossMark logo](#), the end user license, and a DOI link to the formal publication on ScienceDirect.

Please refer to Elsevier's [posting policy](#) for further information.

18. **For book authors** the following clauses are applicable in addition to the above: Authors are permitted to place a brief summary of their work online only. You are not allowed to download and post the published electronic version of your chapter, nor may you scan the printed edition to create an electronic version. **Posting to a repository:** Authors are permitted to post a summary of their chapter only in their institution's repository.

19. **Thesis/Dissertation:** If your license is for use in a thesis/dissertation your thesis may be submitted to your institution in either print or electronic form. Should your thesis be published commercially, please reapply for permission. These requirements include permission for the Library and Archives of Canada to supply single copies, on demand, of the complete thesis and include permission for Proquest/UMI to supply single copies, on demand, of the complete thesis. Should your thesis be published commercially, please reapply for permission. Theses and dissertations which contain embedded PJAs as part of the formal submission can be posted publicly by the awarding institution with DOI links back to the formal publications on ScienceDirect.

Elsevier Open Access Terms and Conditions

You can publish open access with Elsevier in hundreds of open access journals or in nearly 2000 established subscription journals that support open access publishing. Permitted third party re-use of these open access articles is defined by the author's choice of Creative Commons user license. See our [open access license policy](#) for more information.

Terms & Conditions applicable to all Open Access articles published with Elsevier:

Any reuse of the article must not represent the author as endorsing the adaptation of the article nor should the article be modified in such a way as to damage the author's honour or reputation. If any changes have been made, such changes must be clearly indicated.

The author(s) must be appropriately credited and we ask that you include the end user license and a DOI link to the formal publication on ScienceDirect.

If any part of the material to be used (for example, figures) has appeared in our publication with credit or acknowledgement to another source it is the responsibility of the user to ensure their reuse complies with the terms and conditions determined by the rights holder.

Additional Terms & Conditions applicable to each Creative Commons user license:

CC BY: The CC-BY license allows users to copy, to create extracts, abstracts and new works from the Article, to alter and revise the Article and to make commercial use of the Article (including reuse and/or resale of the Article by commercial entities), provided the user gives appropriate credit (with a link to the formal publication through the relevant DOI), provides a link to the license, indicates if changes were made and the licensor is not represented as endorsing the use made of the work. The full details of the license are available at <http://creativecommons.org/licenses/by/4.0>.

CC BY NC SA: The CC BY-NC-SA license allows users to copy, to create extracts, abstracts and new works from the Article, to alter and revise the Article, provided this is not done for commercial purposes, and that the user gives appropriate credit (with a link to the formal publication through the relevant DOI), provides a link to the license, indicates if changes were made and the licensor is not represented as endorsing the use made of the work. Further, any new works must be made available on the same conditions. The full details of the license are available at <http://creativecommons.org/licenses/by-nc-sa/4.0>.

CC BY NC ND: The CC BY-NC-ND license allows users to copy and distribute the Article, provided this is not done for commercial purposes and further does not permit distribution of the Article if it is changed or edited in any way, and provided the user gives appropriate credit (with a link to the formal publication through the relevant DOI), provides a link to the license, and that the licensor is not represented as endorsing the use made of the work. The full details of the license are available at <http://creativecommons.org/licenses/by-nc-nd/4.0>. Any commercial reuse of Open Access articles published with a CC BY NC SA or CC BY NC ND license requires permission from Elsevier and will be subject to a fee.

Commercial reuse includes:

- Associating advertising with the full text of the Article
- Charging fees for document delivery or access
- Article aggregation
- Systematic distribution via e-mail lists or share buttons

Posting or linking by commercial companies for use by customers of those companies.

20. Other Conditions:

v1.10

Questions? customercare@copyright.com or +1-855-239-3415 (toll free in the US) or +1-978-646-2777.

Figure 1-3

ELSEVIER LICENSE TERMS AND CONDITIONS

Jun 21, 2021

This Agreement between Dr. Kirsten Carter ("You") and Elsevier ("Elsevier") consists of your license details and the terms and conditions provided by Elsevier and Copyright Clearance Center.

License Number	5093781121595
License date	Jun 21, 2021
Licensed Content Publisher	Elsevier
Licensed Content Publication	Contact Lens and Anterior Eye
Licensed Content Title	The official guide to scleral lens terminology
Licensed Content Author	Langis Michaud,Michael Lipson,Elise Kramer,Maria Walker
Licensed Content Date	Dec 1, 2020
Licensed Content Volume	43
Licensed Content Issue	6
Licensed Content Pages	6
Start Page	529
End Page	534

Type of Use	reuse in a thesis/dissertation
Portion	figures/tables/illustrations
Number of figures/tables/illustrations	1
Format	both print and electronic
Are you the author of this Elsevier article?	No
Will you be translating?	No
Title	Changes in corneal thickness in keratoconic eyes with variation in scleral contact lens central clearance
Institution name	University of Waterloo
Expected presentation date	Aug 2021
Portions	Figure 2
Requestor Location	Dr. Kirsten Carter 78A Mill Street East P.O. Box 152 Milverton, ON N0K 1M0 Canada Attn: Kirsten Carter
Publisher Tax ID	GB 494 6272 12
Total	0.00 CAD
Terms and Conditions	

INTRODUCTION

1. The publisher for this copyrighted material is Elsevier. By clicking "accept" in connection with completing this licensing transaction, you agree that the following terms and conditions apply to this transaction (along with the Billing and Payment terms and conditions established by Copyright Clearance Center, Inc. ("CCC"), at the time that you opened your Rightslink account and that are available at any time at <http://myaccount.copyright.com>).

GENERAL TERMS

2. Elsevier hereby grants you permission to reproduce the aforementioned material subject to the terms and conditions indicated.

3. Acknowledgement: If any part of the material to be used (for example, figures) has appeared in our publication with credit or acknowledgement to another source, permission must also be sought from that source. If such permission is not obtained then that material may not be included in your publication/copies. Suitable acknowledgement to the source must be made, either as a footnote or in a reference list at the end of your publication, as follows:

"Reprinted from Publication title, Vol /edition number, Author(s), Title of article / title of chapter, Pages No., Copyright (Year), with permission from Elsevier [OR APPLICABLE SOCIETY COPYRIGHT OWNER]." Also Lancet special credit - "Reprinted from The Lancet, Vol. number, Author(s), Title of article, Pages No., Copyright (Year), with permission from Elsevier."

4. Reproduction of this material is confined to the purpose and/or media for which permission is hereby given.

5. Altering/Modifying Material: Not Permitted. However figures and illustrations may be altered/adapted minimally to serve your work. Any other abbreviations, additions, deletions and/or any other alterations shall be made only with prior written authorization of Elsevier Ltd. (Please contact Elsevier's permissions helpdesk [here](#)). No modifications can be made to any Lancet figures/tables and they must be reproduced in full.

6. If the permission fee for the requested use of our material is waived in this instance, please be advised that your future requests for Elsevier materials may attract a fee.

7. Reservation of Rights: Publisher reserves all rights not specifically granted in the combination of (i) the license details provided by you and accepted in the course of this licensing transaction, (ii) these terms and conditions and (iii) CCC's Billing and Payment terms and conditions.

8. License Contingent Upon Payment: While you may exercise the rights licensed immediately upon issuance of the license at the end of the licensing process for the transaction, provided that you have disclosed complete and accurate details of your proposed use, no license is finally effective unless and until full payment is received from you (either by publisher or by CCC) as provided in CCC's Billing and Payment terms and conditions. If full payment is not received on a timely basis, then any license preliminarily granted shall be deemed automatically revoked and shall be void as if never granted. Further, in the event that you breach any of these terms and conditions or any of CCC's Billing and Payment terms and conditions, the license is automatically revoked and shall be void as if never granted. Use of materials as described in a revoked license, as well as any use of the materials beyond the scope of an unrevoked license, may constitute copyright infringement and publisher reserves the right to take any and all action to protect its copyright in the materials.

9. **Warranties:** Publisher makes no representations or warranties with respect to the licensed material.

10. **Indemnity:** You hereby indemnify and agree to hold harmless publisher and CCC, and their respective officers, directors, employees and agents, from and against any and all claims arising out of your use of the licensed material other than as specifically authorized pursuant to this license.

11. **No Transfer of License:** This license is personal to you and may not be sublicensed, assigned, or transferred by you to any other person without publisher's written permission.

12. **No Amendment Except in Writing:** This license may not be amended except in a writing signed by both parties (or, in the case of publisher, by CCC on publisher's behalf).

13. **Objection to Contrary Terms:** Publisher hereby objects to any terms contained in any purchase order, acknowledgment, check endorsement or other writing prepared by you, which terms are inconsistent with these terms and conditions or CCC's Billing and Payment terms and conditions. These terms and conditions, together with CCC's Billing and Payment terms and conditions (which are incorporated herein), comprise the entire agreement between you and publisher (and CCC) concerning this licensing transaction. In the event of any conflict between your obligations established by these terms and conditions and those established by CCC's Billing and Payment terms and conditions, these terms and conditions shall control.

14. **Revocation:** Elsevier or Copyright Clearance Center may deny the permissions described in this License at their sole discretion, for any reason or no reason, with a full refund payable to you. Notice of such denial will be made using the contact information provided by you. Failure to receive such notice will not alter or invalidate the denial. In no event will Elsevier or Copyright Clearance Center be responsible or liable for any costs, expenses or damage incurred by you as a result of a denial of your permission request, other than a refund of the amount(s) paid by you to Elsevier and/or Copyright Clearance Center for denied permissions.

LIMITED LICENSE

The following terms and conditions apply only to specific license types:

15. **Translation:** This permission is granted for non-exclusive world **English** rights only unless your license was granted for translation rights. If you licensed translation rights you may only translate this content into the languages you requested. A professional translator must perform all translations and reproduce the content word for word preserving the integrity of the article.

16. **Posting licensed content on any Website:** The following terms and conditions apply as follows: Licensing material from an Elsevier journal: All content posted to the web site must maintain the copyright information line on the bottom of each image; A hyper-text must be included to the Homepage of the journal from which you are licensing at <http://www.sciencedirect.com/science/journal/xxxxx> or the Elsevier homepage for books at <http://www.elsevier.com>; Central Storage: This license does not include permission for a scanned version of the material to be stored in a central repository such as that provided by Heron/XanEdu.

Licensing material from an Elsevier book: A hyper-text link must be included to the Elsevier homepage at <http://www.elsevier.com>. All content posted to the web site must maintain the copyright information line on the bottom of each image.

Posting licensed content on Electronic reserve: In addition to the above the following clauses are applicable: The web site must be password-protected and made available only to bona fide students registered on a relevant course. This permission is granted for 1 year only. You may obtain a new license for future website posting.

17. For journal authors: the following clauses are applicable in addition to the above:

Preprints:

A preprint is an author's own write-up of research results and analysis, it has not been peer-reviewed, nor has it had any other value added to it by a publisher (such as formatting, copyright, technical enhancement etc.).

Authors can share their preprints anywhere at any time. Preprints should not be added to or enhanced in any way in order to appear more like, or to substitute for, the final versions of articles however authors can update their preprints on arXiv or RePEc with their Accepted Author Manuscript (see below).

If accepted for publication, we encourage authors to link from the preprint to their formal publication via its DOI. Millions of researchers have access to the formal publications on ScienceDirect, and so links will help users to find, access, cite and use the best available version. Please note that Cell Press, The Lancet and some society-owned have different preprint policies. Information on these policies is available on the journal homepage.

Accepted Author Manuscripts: An accepted author manuscript is the manuscript of an article that has been accepted for publication and which typically includes author-incorporated changes suggested during submission, peer review and editor-author communications.

Authors can share their accepted author manuscript:

- immediately
 - via their non-commercial person homepage or blog
 - by updating a preprint in arXiv or RePEc with the accepted manuscript
 - via their research institute or institutional repository for internal institutional uses or as part of an invitation-only research collaboration work-group
 - directly by providing copies to their students or to research collaborators for their personal use
 - for private scholarly sharing as part of an invitation-only work group on commercial sites with which Elsevier has an agreement
- After the embargo period
 - via non-commercial hosting platforms such as their institutional repository
 - via commercial sites with which Elsevier has an agreement

In all cases accepted manuscripts should:

- link to the formal publication via its DOI
- bear a CC-BY-NC-ND license - this is easy to do
- if aggregated with other manuscripts, for example in a repository or other site, be shared in alignment with our hosting policy not be added to or enhanced in any way to appear more like, or to substitute for, the published journal article.

Published journal article (JPA): A published journal article (PJA) is the definitive final record of published research that appears or will appear in the journal and embodies all

value-adding publishing activities including peer review co-ordination, copy-editing, formatting, (if relevant) pagination and online enrichment.

Policies for sharing publishing journal articles differ for subscription and gold open access articles:

Subscription Articles: If you are an author, please share a link to your article rather than the full-text. Millions of researchers have access to the formal publications on ScienceDirect, and so links will help your users to find, access, cite, and use the best available version.

Theses and dissertations which contain embedded PJAs as part of the formal submission can be posted publicly by the awarding institution with DOI links back to the formal publications on ScienceDirect.

If you are affiliated with a library that subscribes to ScienceDirect you have additional private sharing rights for others' research accessed under that agreement. This includes use for classroom teaching and internal training at the institution (including use in course packs and courseware programs), and inclusion of the article for grant funding purposes.

Gold Open Access Articles: May be shared according to the author-selected end-user license and should contain a [CrossMark logo](#), the end user license, and a DOI link to the formal publication on ScienceDirect.

Please refer to Elsevier's [posting policy](#) for further information.

18. **For book authors** the following clauses are applicable in addition to the above: Authors are permitted to place a brief summary of their work online only. You are not allowed to download and post the published electronic version of your chapter, nor may you scan the printed edition to create an electronic version. **Posting to a repository:** Authors are permitted to post a summary of their chapter only in their institution's repository.

19. **Thesis/Dissertation:** If your license is for use in a thesis/dissertation your thesis may be submitted to your institution in either print or electronic form. Should your thesis be published commercially, please reapply for permission. These requirements include permission for the Library and Archives of Canada to supply single copies, on demand, of the complete thesis and include permission for Proquest/UMI to supply single copies, on demand, of the complete thesis. Should your thesis be published commercially, please reapply for permission. Theses and dissertations which contain embedded PJAs as part of the formal submission can be posted publicly by the awarding institution with DOI links back to the formal publications on ScienceDirect.

Elsevier Open Access Terms and Conditions

You can publish open access with Elsevier in hundreds of open access journals or in nearly 2000 established subscription journals that support open access publishing. Permitted third party re-use of these open access articles is defined by the author's choice of Creative Commons user license. See our [open access license policy](#) for more information.

Terms & Conditions applicable to all Open Access articles published with Elsevier:

Any reuse of the article must not represent the author as endorsing the adaptation of the article nor should the article be modified in such a way as to damage the author's honour or reputation. If any changes have been made, such changes must be clearly indicated.

The author(s) must be appropriately credited and we ask that you include the end user license and a DOI link to the formal publication on ScienceDirect.

If any part of the material to be used (for example, figures) has appeared in our publication with credit or acknowledgement to another source it is the responsibility of the user to ensure their reuse complies with the terms and conditions determined by the rights holder.

Additional Terms & Conditions applicable to each Creative Commons user license:

CC BY: The CC-BY license allows users to copy, to create extracts, abstracts and new works from the Article, to alter and revise the Article and to make commercial use of the Article (including reuse and/or resale of the Article by commercial entities), provided the user gives appropriate credit (with a link to the formal publication through the relevant DOI), provides a link to the license, indicates if changes were made and the licensor is not represented as endorsing the use made of the work. The full details of the license are available at <http://creativecommons.org/licenses/by/4.0>.

CC BY NC SA: The CC BY-NC-SA license allows users to copy, to create extracts, abstracts and new works from the Article, to alter and revise the Article, provided this is not done for commercial purposes, and that the user gives appropriate credit (with a link to the formal publication through the relevant DOI), provides a link to the license, indicates if changes were made and the licensor is not represented as endorsing the use made of the work. Further, any new works must be made available on the same conditions. The full details of the license are available at <http://creativecommons.org/licenses/by-nc-sa/4.0>.

CC BY NC ND: The CC BY-NC-ND license allows users to copy and distribute the Article, provided this is not done for commercial purposes and further does not permit distribution of the Article if it is changed or edited in any way, and provided the user gives appropriate credit (with a link to the formal publication through the relevant DOI), provides a link to the license, and that the licensor is not represented as endorsing the use made of the work. The full details of the license are available at <http://creativecommons.org/licenses/by-nc-nd/4.0>. Any commercial reuse of Open Access articles published with a CC BY NC SA or CC BY NC ND license requires permission from Elsevier and will be subject to a fee.

Commercial reuse includes:

- Associating advertising with the full text of the Article
- Charging fees for document delivery or access
- Article aggregation
- Systematic distribution via e-mail lists or share buttons

Posting or linking by commercial companies for use by customers of those companies.

20. Other Conditions:

v1.10

Questions? customercare@copyright.com or +1-855-239-3415 (toll free in the US) or +1-978-646-2777.

Figure 1-4

ELSEVIER LICENSE TERMS AND CONDITIONS

Jun 22, 2021

This Agreement between Dr. Kirsten Carter ("You") and Elsevier ("Elsevier") consists of your license details and the terms and conditions provided by Elsevier and Copyright Clearance Center.

The publisher has provided special terms related to this request that can be found at the end of the Publisher's Terms and Conditions.

License Number	5094310002309
License date	Jun 22, 2021
Licensed Content Publisher	Elsevier
Licensed Content Publication	Ophthalmology: Journal of the American Academy of Ophthalmology
Licensed Content Title	Round and Oval Cones in Keratoconus
Licensed Content Author	Henry D. Perry, Jorge N. Buxton, Ben S. Fine
Licensed Content Date	Sep 1, 1980
Licensed Content Volume	87
Licensed Content Issue	9
Licensed Content Pages	5
Start Page	905

End Page	909
Type of Use	reuse in a thesis/dissertation
Portion	figures/tables/illustrations
Number of figures/tables/illustrations	1
Format	both print and electronic
Are you the author of this Elsevier article?	No
Will you be translating?	No
Title	Changes in corneal thickness in keratoconic eyes with variation in scleral contact lens central clearance
Institution name	University of Waterloo
Expected presentation date	Aug 2021
Portions	Figure 1
Attachment	Perry_Fig1.png
Requestor Location	Dr. Kirsten Carter 78A Mill Street East P.O. Box 152 Milverton, ON N0K 1M0 Canada Attn: Kirsten Carter
Publisher Tax ID	GB 494 6272 12
Billing Type	Invoice

Billing Address Kirsten Carter
78A Mill Street East P.O Box 152

Milverton, ON N0K 1M0
Canada
Attn: Kirsten Carter

Total 0.00 CAD

Terms and Conditions

INTRODUCTION

1. The publisher for this copyrighted material is Elsevier. By clicking "accept" in connection with completing this licensing transaction, you agree that the following terms and conditions apply to this transaction (along with the Billing and Payment terms and conditions established by Copyright Clearance Center, Inc. ("CCC"), at the time that you opened your Rightslink account and that are available at any time at <http://myaccount.copyright.com>).

GENERAL TERMS

2. Elsevier hereby grants you permission to reproduce the aforementioned material subject to the terms and conditions indicated.

3. Acknowledgement: If any part of the material to be used (for example, figures) has appeared in our publication with credit or acknowledgement to another source, permission must also be sought from that source. If such permission is not obtained then that material may not be included in your publication/copies. Suitable acknowledgement to the source must be made, either as a footnote or in a reference list at the end of your publication, as follows:

"Reprinted from Publication title, Vol /edition number, Author(s), Title of article / title of chapter, Pages No., Copyright (Year), with permission from Elsevier [OR APPLICABLE SOCIETY COPYRIGHT OWNER]." Also Lancet special credit - "Reprinted from The Lancet, Vol. number, Author(s), Title of article, Pages No., Copyright (Year), with permission from Elsevier."

4. Reproduction of this material is confined to the purpose and/or media for which permission is hereby given.

5. Altering/Modifying Material: Not Permitted. However figures and illustrations may be altered/adapted minimally to serve your work. Any other abbreviations, additions, deletions and/or any other alterations shall be made only with prior written authorization of Elsevier Ltd. (Please contact Elsevier's permissions helpdesk [here](#)). No modifications can be made to any Lancet figures/tables and they must be reproduced in full.

6. If the permission fee for the requested use of our material is waived in this instance, please be advised that your future requests for Elsevier materials may attract a fee.

7. Reservation of Rights: Publisher reserves all rights not specifically granted in the combination of (i) the license details provided by you and accepted in the course of this

licensing transaction, (ii) these terms and conditions and (iii) CCC's Billing and Payment terms and conditions.

8. License Contingent Upon Payment: While you may exercise the rights licensed immediately upon issuance of the license at the end of the licensing process for the transaction, provided that you have disclosed complete and accurate details of your proposed use, no license is finally effective unless and until full payment is received from you (either by publisher or by CCC) as provided in CCC's Billing and Payment terms and conditions. If full payment is not received on a timely basis, then any license preliminarily granted shall be deemed automatically revoked and shall be void as if never granted. Further, in the event that you breach any of these terms and conditions or any of CCC's Billing and Payment terms and conditions, the license is automatically revoked and shall be void as if never granted. Use of materials as described in a revoked license, as well as any use of the materials beyond the scope of an unrevoked license, may constitute copyright infringement and publisher reserves the right to take any and all action to protect its copyright in the materials.

9. Warranties: Publisher makes no representations or warranties with respect to the licensed material.

10. Indemnity: You hereby indemnify and agree to hold harmless publisher and CCC, and their respective officers, directors, employees and agents, from and against any and all claims arising out of your use of the licensed material other than as specifically authorized pursuant to this license.

11. No Transfer of License: This license is personal to you and may not be sublicensed, assigned, or transferred by you to any other person without publisher's written permission.

12. No Amendment Except in Writing: This license may not be amended except in a writing signed by both parties (or, in the case of publisher, by CCC on publisher's behalf).

13. Objection to Contrary Terms: Publisher hereby objects to any terms contained in any purchase order, acknowledgment, check endorsement or other writing prepared by you, which terms are inconsistent with these terms and conditions or CCC's Billing and Payment terms and conditions. These terms and conditions, together with CCC's Billing and Payment terms and conditions (which are incorporated herein), comprise the entire agreement between you and publisher (and CCC) concerning this licensing transaction. In the event of any conflict between your obligations established by these terms and conditions and those established by CCC's Billing and Payment terms and conditions, these terms and conditions shall control.

14. Revocation: Elsevier or Copyright Clearance Center may deny the permissions described in this License at their sole discretion, for any reason or no reason, with a full refund payable to you. Notice of such denial will be made using the contact information provided by you. Failure to receive such notice will not alter or invalidate the denial. In no event will Elsevier or Copyright Clearance Center be responsible or liable for any costs, expenses or damage incurred by you as a result of a denial of your permission request, other than a refund of the amount(s) paid by you to Elsevier and/or Copyright Clearance Center for denied permissions.

LIMITED LICENSE

The following terms and conditions apply only to specific license types:

15. **Translation:** This permission is granted for non-exclusive world **English** rights only unless your license was granted for translation rights. If you licensed translation rights you may only translate this content into the languages you requested. A professional translator must perform all translations and reproduce the content word for word preserving the integrity of the article.

16. **Posting licensed content on any Website:** The following terms and conditions apply as follows: Licensing material from an Elsevier journal: All content posted to the web site must maintain the copyright information line on the bottom of each image; A hyper-text must be included to the Homepage of the journal from which you are licensing at <http://www.sciencedirect.com/science/journal/xxxxx> or the Elsevier homepage for books at <http://www.elsevier.com>; Central Storage: This license does not include permission for a scanned version of the material to be stored in a central repository such as that provided by Heron/XanEdu.

Licensing material from an Elsevier book: A hyper-text link must be included to the Elsevier homepage at <http://www.elsevier.com>. All content posted to the web site must maintain the copyright information line on the bottom of each image.

Posting licensed content on Electronic reserve: In addition to the above the following clauses are applicable: The web site must be password-protected and made available only to bona fide students registered on a relevant course. This permission is granted for 1 year only. You may obtain a new license for future website posting.

17. **For journal authors:** the following clauses are applicable in addition to the above:

Preprints:

A preprint is an author's own write-up of research results and analysis, it has not been peer-reviewed, nor has it had any other value added to it by a publisher (such as formatting, copyright, technical enhancement etc.).

Authors can share their preprints anywhere at any time. Preprints should not be added to or enhanced in any way in order to appear more like, or to substitute for, the final versions of articles however authors can update their preprints on arXiv or RePEc with their Accepted Author Manuscript (see below).

If accepted for publication, we encourage authors to link from the preprint to their formal publication via its DOI. Millions of researchers have access to the formal publications on ScienceDirect, and so links will help users to find, access, cite and use the best available version. Please note that Cell Press, The Lancet and some society-owned have different preprint policies. Information on these policies is available on the journal homepage.

Accepted Author Manuscripts: An accepted author manuscript is the manuscript of an article that has been accepted for publication and which typically includes author-incorporated changes suggested during submission, peer review and editor-author communications.

Authors can share their accepted author manuscript:

- immediately
 - via their non-commercial person homepage or blog
 - by updating a preprint in arXiv or RePEc with the accepted manuscript

- via their research institute or institutional repository for internal institutional uses or as part of an invitation-only research collaboration work-group
- directly by providing copies to their students or to research collaborators for their personal use
- for private scholarly sharing as part of an invitation-only work group on commercial sites with which Elsevier has an agreement
- After the embargo period
 - via non-commercial hosting platforms such as their institutional repository
 - via commercial sites with which Elsevier has an agreement

In all cases accepted manuscripts should:

- link to the formal publication via its DOI
- bear a CC-BY-NC-ND license - this is easy to do
- if aggregated with other manuscripts, for example in a repository or other site, be shared in alignment with our hosting policy not be added to or enhanced in any way to appear more like, or to substitute for, the published journal article.

Published journal article (JPA): A published journal article (PJA) is the definitive final record of published research that appears or will appear in the journal and embodies all value-adding publishing activities including peer review co-ordination, copy-editing, formatting, (if relevant) pagination and online enrichment.

Policies for sharing publishing journal articles differ for subscription and gold open access articles:

Subscription Articles: If you are an author, please share a link to your article rather than the full-text. Millions of researchers have access to the formal publications on ScienceDirect, and so links will help your users to find, access, cite, and use the best available version.

Theses and dissertations which contain embedded PJAs as part of the formal submission can be posted publicly by the awarding institution with DOI links back to the formal publications on ScienceDirect.

If you are affiliated with a library that subscribes to ScienceDirect you have additional private sharing rights for others' research accessed under that agreement. This includes use for classroom teaching and internal training at the institution (including use in course packs and courseware programs), and inclusion of the article for grant funding purposes.

Gold Open Access Articles: May be shared according to the author-selected end-user license and should contain a [CrossMark logo](#), the end user license, and a DOI link to the formal publication on ScienceDirect.

Please refer to Elsevier's [posting policy](#) for further information.

18. For book authors the following clauses are applicable in addition to the above: Authors are permitted to place a brief summary of their work online only. You are not allowed to download and post the published electronic version of your chapter, nor may you scan the printed edition to create an electronic version. **Posting to a repository:** Authors are permitted to post a summary of their chapter only in their institution's repository.

19. Thesis/Dissertation: If your license is for use in a thesis/dissertation your thesis may be submitted to your institution in either print or electronic form. Should your thesis be published commercially, please reapply for permission. These requirements include permission for the Library and Archives of Canada to supply single copies, on demand, of

the complete thesis and include permission for Proquest/UMI to supply single copies, on demand, of the complete thesis. Should your thesis be published commercially, please reapply for permission. Theses and dissertations which contain embedded PJAs as part of the formal submission can be posted publicly by the awarding institution with DOI links back to the formal publications on ScienceDirect.

Elsevier Open Access Terms and Conditions

You can publish open access with Elsevier in hundreds of open access journals or in nearly 2000 established subscription journals that support open access publishing. Permitted third party re-use of these open access articles is defined by the author's choice of Creative Commons user license. See our [open access license policy](#) for more information.

Terms & Conditions applicable to all Open Access articles published with Elsevier:

Any reuse of the article must not represent the author as endorsing the adaptation of the article nor should the article be modified in such a way as to damage the author's honour or reputation. If any changes have been made, such changes must be clearly indicated.

The author(s) must be appropriately credited and we ask that you include the end user license and a DOI link to the formal publication on ScienceDirect.

If any part of the material to be used (for example, figures) has appeared in our publication with credit or acknowledgement to another source it is the responsibility of the user to ensure their reuse complies with the terms and conditions determined by the rights holder.

Additional Terms & Conditions applicable to each Creative Commons user license:

CC BY: The CC-BY license allows users to copy, to create extracts, abstracts and new works from the Article, to alter and revise the Article and to make commercial use of the Article (including reuse and/or resale of the Article by commercial entities), provided the user gives appropriate credit (with a link to the formal publication through the relevant DOI), provides a link to the license, indicates if changes were made and the licensor is not represented as endorsing the use made of the work. The full details of the license are available at <http://creativecommons.org/licenses/by/4.0>.

CC BY NC SA: The CC BY-NC-SA license allows users to copy, to create extracts, abstracts and new works from the Article, to alter and revise the Article, provided this is not done for commercial purposes, and that the user gives appropriate credit (with a link to the formal publication through the relevant DOI), provides a link to the license, indicates if changes were made and the licensor is not represented as endorsing the use made of the work. Further, any new works must be made available on the same conditions. The full details of the license are available at <http://creativecommons.org/licenses/by-nc-sa/4.0>.

CC BY NC ND: The CC BY-NC-ND license allows users to copy and distribute the Article, provided this is not done for commercial purposes and further does not permit distribution of the Article if it is changed or edited in any way, and provided the user gives appropriate credit (with a link to the formal publication through the relevant DOI), provides a link to the license, and that the licensor is not represented as endorsing the use made of the work. The full details of the license are available at <http://creativecommons.org/licenses/by-nc-nd/4.0>. Any commercial reuse of Open Access articles published with a CC BY NC SA or CC BY NC ND license requires permission from Elsevier and will be subject to a fee.

Commercial reuse includes:

- Associating advertising with the full text of the Article
- Charging fees for document delivery or access
- Article aggregation
- Systematic distribution via e-mail lists or share buttons

Posting or linking by commercial companies for use by customers of those companies.

20. **Other Conditions:** null

v1.10

Questions? customercare@copyright.com or +1-855-239-3415 (toll free in the US) or +1-978-646-2777.



Figure 1-5A-B

Kirsten Carter

From: kirstiescarter@gmail.com
Sent: June 28, 2021 12:54 PM
To: Kirsten Carter
Subject: Bennett, Edward S. and Henry, Vinita Allee Permissions Book Request [ref:_00Dd0dixc._5003w1TQ9km:ref]
Attachments: WK-Terms-and-Conditions-03-2019.pdf

From: "["RIP - Book Permissions"](#) <permissions@lww.com>
Sent: June 23, 2021 2:24 PM
To: kirstiescarter@gmail.com
Subject: RE: Bennett, Edward S. and Henry, Vinita Allee Permissions Book Request [ref:_00Dd0dixc._5003w1TQ9km:ref]

Hello Kirsten.

Thank you for contacting us. Your request to use Figures 19.3 and 19.4 from Bennett: Clinical Manual of Contact Lenses 4e in your thesis "Changes in corneal thickness in keratoconic eyes with variation in scleral contact lens central clearance" at University of Waterloo is granted for print and e-formats.

I've attached a copy of our Terms and Conditions. Please consider those, and this email your grant of permission.

Thank you.

Caren Erlichman

Â

[Caren Erlichman](#)

Wolters Kluwer Permissions

Â

Wolters Kluwer

Two Commerce Square

2001 Market Street

Philadelphia, PA 19103

www.wolterskluwerhealth.com

www.lww.com

Confidentiality Notice: This email and its attachments (if any) contain confidential information of the sender. The information is intended only for the use by the direct addresses of the original sender of this email. If you are not an intended recipient of the original sender (or responsible for delivering the message to such person), you are hereby notified that any review, disclosure, copying, distribution or the taking of any action in reliance of the

contents of and attachments to this email is strictly prohibited. If you have received this email in error, please immediately notify the sender at the address show herein and permanently delete any copies of this email (digital or paper) in your possession.

Â

----- Original Message -----

From: Kirsten Carter [kirstiescarter@gmail.com]

Sent: 6/23/2021 1:02 PM

To: permissions@lww.com

Subject: Bennett, Edward S. and Henry, Vinita Allee Permissions Book Request

Â

Â

Â	[Inline image URL : https://cdn.jotfor.ms/assets/img/builder/email_logo_small.png]	Book Permissions Request Form
Name	Kirsten Carter	
Company/Organization	University of Waterloo School of Optometry and Vision Science	
Street Address	78A Mill Street East P.O Box 152	
City	Milverton	
State or Province	ON	
Postal Code	N0K 1M0	
Country	Canada	
E-mail	kirstiescarter@gmail.com	
Phone Number	5193018487	
Requestor Type:	University/College	
Are you requesting permission from a book or an ACC Chart?	Book	
Author	Bennett, Edward S. and Henry, Vinita Allee	
Title	Clinical Manual of Contact Lenses	
Â	Edition	4
ISBN (without dashes)	9781451175325	
I would like to use:	Figure/Table/Illustration	
Content Requested [List the specific figures, tables, or text for permission]	Figures 19.3 (Vogt's striae) and 19.4 (Fleischer's ring)	
Are you the author of this Wolters Kluwer content?	No	
How Will Our Content Be Used?	Thesis/Dissertation	
Please Provide:	Title of Thesis: Changes in corneal thickness in keratoconic eyes with variation in scleral contact lens central clearance; Quantity of Copies Needed: 4 (for self and supervisor/committee); Website Thesis Will Be Posted: https://uwspace.uwaterloo.ca/handle/10012/6	

2

Where do you attend university?	University of Waterloo
Will this be posted to your university website?	Yes
Is the website password protected?	No
Additional languages (other than English)	No
Format	Print and Electronic
Notes/Comments	Specifically, I would like to slightly modify both figures (19.3, 19.4) for the purpose of formatting. I would like to crop both figures, and place a letter (A, and B, respectively) in the bottom left corner with a text box to label parts of these figures. A third image of apical scarring from another source will be placed alongside these two figures. Thank you in advance for reviewing my request.

Ã

Ã

Ã



ref:_00Dd0dixc._5003w1TQ9km:ref

Wolters Kluwer Terms and Conditions

1. **Duration of License:** Permission is granted for a one time use only. Rights herein do not apply to future reproductions, editions, revisions, or other derivative works. This permission shall be effective as of the date of execution by the parties for the maximum period of 12 months and should be renewed after the term expires.
 - i. When content is to be republished in a book or journal the validity of this agreement should be the life of the book edition or journal issue.
 - ii. When content is licensed for use on a website, internet, intranet, or any publicly accessible site (not including a journal or book), you agree to remove the material from such site after 12 months, or request to renew your permission license.
2. **Credit Line:** A credit line must be prominently placed and include: For book content: the author(s), title of book, edition, copyright holder, year of publication; For journal content: the author(s), titles of article, title of journal, volume number, issue number, inclusive pages and website URL to the journal page; If a journal is published by a learned society the credit line must include the details of that society.
3. **Warranties:** The requestor warrants that the material shall not be used in any manner which may be considered derogatory to the title, content, authors of the material, or to Wolters Kluwer Health, Inc.
4. **Indemnity:** You hereby indemnify and hold harmless Wolters Kluwer Health, Inc. and its respective officers, directors, employees and agents, from and against any and all claims, costs, proceeding or demands arising out of your unauthorized use of the Licensed Material
5. **Geographical Scope:** Permission granted is non-exclusive and is valid throughout the world in the English language and the languages specified in the license.
6. **Copy of Content:** Wolters Kluwer Health, Inc. cannot supply the requestor with the original artwork, high-resolution images, electronic files or a clean copy of content.
7. **Validity:** Permission is valid if the borrowed material is original to a Wolters Kluwer Health, Inc. imprint (J.B Lippincott, Lippincott-Raven Publishers, Williams & Wilkins, Lea & Febiger, Harwal, Rapid Science, Little Brown & Company, Harper & Row Medical, American Journal of Nursing Co, and Urban & Schwarzenberg - English Language, Raven Press, Paul Hoeber, Springhouse, Ovid), and the Anatomical Chart Company
8. **Third Party Material:** This permission does not apply to content that is credited to publications other than Wolters Kluwer Health, Inc. or its Societies. For images credited to non-Wolters Kluwer Health, Inc. books or journals, you must obtain permission from the source referenced in the figure or table legend or credit line before making any use of the image(s), table(s) or other content.
9. **Adaptations:** Adaptations are protected by copyright. For images that have been adapted, permission must be sought from the rightsholder of the original material and the rightsholder of the adapted material.
10. **Modifications:** Wolters Kluwer Health, Inc. material is not permitted to be modified or adapted without written approval from Wolters Kluwer Health, Inc. with the exception of text size or color. The adaptation should be credited as follows: Adapted with permission from Wolters Kluwer Health, Inc.: [the author(s), title of book, edition, copyright holder, year of publication] or [the author(s), titles of article, title of journal, volume number, issue number, inclusive pages and website URL to the journal page].
11. **Full Text Articles:** Republication of full articles in English is prohibited.
12. **Branding and Marketing:** No drug name, trade name, drug logo, or trade logo can be included on the same page as material borrowed from *Diseases of the Colon & Rectum, Plastic Reconstructive Surgery, Obstetrics & Gynecology (The Green Journal), Critical Care Medicine, Pediatric Critical Care Medicine, the American Heart Association publications and the American Academy of Neurology publications.*
13. **Open Access:** Unless you are publishing content under the same Creative Commons license, the following statement must be added when reprinting material in Open Access journals: "The Creative Commons license does not apply to this content. Use of the material in any format is prohibited without written permission from the publisher, Wolters Kluwer Health, Inc. Please contact permissions@jhw.com for further information."
14. **Translations:** The following disclaimer must appear on all translated copies: Wolters Kluwer Health, Inc. and its Societies take no responsibility for the accuracy of the translation from the published English original and are not liable for any errors which may occur.
15. **Published Ahead of Print (PAP):** Articles in the PAP stage of publication can be cited using the online publication date and the unique DOI number.
 - i. Disclaimer: Articles appearing in the PAP section have been peer-reviewed and accepted for publication in the relevant journal and posted online before print publication. Articles appearing as PAP may contain statements, opinions, and information that have errors in facts, figures, or interpretation. Any final changes in manuscripts will be made at the time of print publication and will be reflected in the final electronic version of the issue. Accordingly, Wolters Kluwer Health, Inc., the editors, authors and their respective employees are not responsible or liable for the use of any such inaccurate or misleading data, opinion or information contained in the articles in this section.
16. **Termination of Contract:** Wolters Kluwer Health, Inc. must be notified within 90 days of the original license date if you opt not to use the requested material.
17. **Waived Permission Fee:** Permission fees that have been waived are not subject to future waivers, including similar requests or renewing a license.
18. **Contingent on Payment:** You may exercise these rights licensed immediately upon issuance of the license, however until full payment is received either by the publisher or our authorized vendor, this license is not valid. If full payment is not received on a timely basis, then any license preliminarily granted shall be deemed automatically revoked and shall be void as if never granted. Further, in the event that you breach any of these terms and conditions or any of Wolters Kluwer Health, Inc.'s other billing and payment terms and conditions, the license is automatically revoked and shall be void as if never granted. Use of materials as described in a revoked license, as well as any use of the materials beyond the scope of an unrevoked license, may constitute copyright infringement and publisher reserves the right to take any and all action to protect its copyright in the materials.
19. **STM Signatories Only:** Any permission granted for a particular edition will apply to subsequent editions and for editions in other languages, provided such editions are for the work as a whole in situ and do not involve the separate exploitation of the permitted illustrations or excerpts. Please view: [STM Permissions Guidelines](#)
20. **Warranties and Obligations:** LICENSOR further represents and warrants that, to the best of its knowledge and belief, LICENSEE's contemplated use of the Content as represented to LICENSOR does not infringe any valid rights to any third party.
21. **Breach:** If LICENSEE fails to comply with any provisions of this agreement, LICENSOR may serve written notice of breach of LICENSEE and, unless such breach is fully cured within fifteen (15) days from the receipt of notice by LICENSEE, LICENSOR may thereupon, at its option, serve notice of cancellation on LICENSEE, whereupon this Agreement shall immediately terminate.
22. **Assignment:** License conveyed hereunder by the LICENSOR shall not be assigned or granted in any manner conveyed to any third party by the LICENSEE without the consent in writing to the LICENSOR.
23. **Governing Law:** The laws of The State of New York shall govern interpretation of this Agreement and all rights and liabilities arising hereunder.
24. **Unlawful:** If any provision of this Agreement shall be found unlawful or otherwise legally unenforceable, all other conditions and provisions of this Agreement shall remain in full force and effect.

For Copyright Clearance Center Only (CCC)/RightsLink Only:

1. **Service Description for Content Services:** Subject to these terms of use, any terms set forth on the particular order, and payment of the applicable fee, you may make the following uses of the ordered materials:
 - i. **Content Rental:** You may access and view a single electronic copy of the materials ordered for the time period designated at the time the order is placed. Access to the materials will be provided through a dedicated content viewer or other portal, and access will be discontinued upon expiration of the designated time period. An order for Content Rental does not include any rights to print, download, save, create additional copies, to distribute or to reuse in any way the full text or parts of the materials.
 - ii. **Content Purchase:** You may access and download a single electronic copy of the materials ordered. Copies will be provided by email or by such other means as publisher may make available from time to time. An order for Content Purchase does not include any rights to create additional copies or to distribute copies of the materials.

Figure 1-5C

ELSEVIER LICENSE TERMS AND CONDITIONS

Jun 19, 2021

This Agreement between Dr. Kirsten Carter ("You") and Elsevier ("Elsevier") consists of your license details and the terms and conditions provided by Elsevier and Copyright Clearance Center.

License Number	5092820551280
License date	Jun 19, 2021
Licensed Content Publisher	Elsevier
Licensed Content Publication	Contact Lens and Anterior Eye
Licensed Content Title	Collaborative Longitudinal Evaluation of Keratoconus (CLEK) Study: Methods and findings to date
Licensed Content Author	H. Wagner, J.T. Barr, K. Zadnik
Licensed Content Date	Sep 1, 2007
Licensed Content Volume	30
Licensed Content Issue	4
Licensed Content Pages	10
Start Page	223
End Page	232

Type of Use	reuse in a thesis/dissertation
Portion	figures/tables/illustrations
Number of figures/tables/illustrations	1
Format	both print and electronic
Are you the author of this Elsevier article?	No
Will you be translating?	No
Title	Changes in corneal thickness in keratoconic eyes with variation in scleral contact lens central clearance
Institution name	University of Waterloo
Expected presentation date	Aug 2021
Portions	Figure 2
Requestor Location	Dr. Kirsten Carter 78A Mill Street East P.O. Box 152 Milverton, ON N0K 1M0 Canada Attn: Kirsten Carter
Publisher Tax ID	GB 494 6272 12
Total	0.00 USD
Terms and Conditions	

INTRODUCTION

1. The publisher for this copyrighted material is Elsevier. By clicking "accept" in connection with completing this licensing transaction, you agree that the following terms and conditions apply to this transaction (along with the Billing and Payment terms and conditions established by Copyright Clearance Center, Inc. ("CCC"), at the time that you opened your Rightslink account and that are available at any time at <http://myaccount.copyright.com>).

GENERAL TERMS

2. Elsevier hereby grants you permission to reproduce the aforementioned material subject to the terms and conditions indicated.

3. Acknowledgement: If any part of the material to be used (for example, figures) has appeared in our publication with credit or acknowledgement to another source, permission must also be sought from that source. If such permission is not obtained then that material may not be included in your publication/copies. Suitable acknowledgement to the source must be made, either as a footnote or in a reference list at the end of your publication, as follows:

"Reprinted from Publication title, Vol /edition number, Author(s), Title of article / title of chapter, Pages No., Copyright (Year), with permission from Elsevier [OR APPLICABLE SOCIETY COPYRIGHT OWNER]." Also Lancet special credit - "Reprinted from The Lancet, Vol. number, Author(s), Title of article, Pages No., Copyright (Year), with permission from Elsevier."

4. Reproduction of this material is confined to the purpose and/or media for which permission is hereby given.

5. Altering/Modifying Material: Not Permitted. However figures and illustrations may be altered/adapted minimally to serve your work. Any other abbreviations, additions, deletions and/or any other alterations shall be made only with prior written authorization of Elsevier Ltd. (Please contact Elsevier's permissions helpdesk [here](#)). No modifications can be made to any Lancet figures/tables and they must be reproduced in full.

6. If the permission fee for the requested use of our material is waived in this instance, please be advised that your future requests for Elsevier materials may attract a fee.

7. Reservation of Rights: Publisher reserves all rights not specifically granted in the combination of (i) the license details provided by you and accepted in the course of this licensing transaction, (ii) these terms and conditions and (iii) CCC's Billing and Payment terms and conditions.

8. License Contingent Upon Payment: While you may exercise the rights licensed immediately upon issuance of the license at the end of the licensing process for the transaction, provided that you have disclosed complete and accurate details of your proposed use, no license is finally effective unless and until full payment is received from you (either by publisher or by CCC) as provided in CCC's Billing and Payment terms and conditions. If full payment is not received on a timely basis, then any license preliminarily granted shall be deemed automatically revoked and shall be void as if never granted. Further, in the event that you breach any of these terms and conditions or any of CCC's Billing and Payment terms and conditions, the license is automatically revoked and shall be void as if never granted. Use of materials as described in a revoked license, as well as any use of the materials beyond the scope of an unrevoked license, may constitute copyright infringement and publisher reserves the right to take any and all action to protect its copyright in the materials.

9. **Warranties:** Publisher makes no representations or warranties with respect to the licensed material.

10. **Indemnity:** You hereby indemnify and agree to hold harmless publisher and CCC, and their respective officers, directors, employees and agents, from and against any and all claims arising out of your use of the licensed material other than as specifically authorized pursuant to this license.

11. **No Transfer of License:** This license is personal to you and may not be sublicensed, assigned, or transferred by you to any other person without publisher's written permission.

12. **No Amendment Except in Writing:** This license may not be amended except in a writing signed by both parties (or, in the case of publisher, by CCC on publisher's behalf).

13. **Objection to Contrary Terms:** Publisher hereby objects to any terms contained in any purchase order, acknowledgment, check endorsement or other writing prepared by you, which terms are inconsistent with these terms and conditions or CCC's Billing and Payment terms and conditions. These terms and conditions, together with CCC's Billing and Payment terms and conditions (which are incorporated herein), comprise the entire agreement between you and publisher (and CCC) concerning this licensing transaction. In the event of any conflict between your obligations established by these terms and conditions and those established by CCC's Billing and Payment terms and conditions, these terms and conditions shall control.

14. **Revocation:** Elsevier or Copyright Clearance Center may deny the permissions described in this License at their sole discretion, for any reason or no reason, with a full refund payable to you. Notice of such denial will be made using the contact information provided by you. Failure to receive such notice will not alter or invalidate the denial. In no event will Elsevier or Copyright Clearance Center be responsible or liable for any costs, expenses or damage incurred by you as a result of a denial of your permission request, other than a refund of the amount(s) paid by you to Elsevier and/or Copyright Clearance Center for denied permissions.

LIMITED LICENSE

The following terms and conditions apply only to specific license types:

15. **Translation:** This permission is granted for non-exclusive world **English** rights only unless your license was granted for translation rights. If you licensed translation rights you may only translate this content into the languages you requested. A professional translator must perform all translations and reproduce the content word for word preserving the integrity of the article.

16. **Posting licensed content on any Website:** The following terms and conditions apply as follows: Licensing material from an Elsevier journal: All content posted to the web site must maintain the copyright information line on the bottom of each image; A hyper-text must be included to the Homepage of the journal from which you are licensing at <http://www.sciencedirect.com/science/journal/xxxxx> or the Elsevier homepage for books at <http://www.elsevier.com>; Central Storage: This license does not include permission for a scanned version of the material to be stored in a central repository such as that provided by Heron/XanEdu.

Licensing material from an Elsevier book: A hyper-text link must be included to the Elsevier homepage at <http://www.elsevier.com>. All content posted to the web site must maintain the copyright information line on the bottom of each image.

Posting licensed content on Electronic reserve: In addition to the above the following clauses are applicable: The web site must be password-protected and made available only to bona fide students registered on a relevant course. This permission is granted for 1 year only. You may obtain a new license for future website posting.

17. For journal authors: the following clauses are applicable in addition to the above:

Preprints:

A preprint is an author's own write-up of research results and analysis, it has not been peer-reviewed, nor has it had any other value added to it by a publisher (such as formatting, copyright, technical enhancement etc.).

Authors can share their preprints anywhere at any time. Preprints should not be added to or enhanced in any way in order to appear more like, or to substitute for, the final versions of articles however authors can update their preprints on arXiv or RePEc with their Accepted Author Manuscript (see below).

If accepted for publication, we encourage authors to link from the preprint to their formal publication via its DOI. Millions of researchers have access to the formal publications on ScienceDirect, and so links will help users to find, access, cite and use the best available version. Please note that Cell Press, The Lancet and some society-owned have different preprint policies. Information on these policies is available on the journal homepage.

Accepted Author Manuscripts: An accepted author manuscript is the manuscript of an article that has been accepted for publication and which typically includes author-incorporated changes suggested during submission, peer review and editor-author communications.

Authors can share their accepted author manuscript:

- immediately
 - via their non-commercial person homepage or blog
 - by updating a preprint in arXiv or RePEc with the accepted manuscript
 - via their research institute or institutional repository for internal institutional uses or as part of an invitation-only research collaboration work-group
 - directly by providing copies to their students or to research collaborators for their personal use
 - for private scholarly sharing as part of an invitation-only work group on commercial sites with which Elsevier has an agreement
- After the embargo period
 - via non-commercial hosting platforms such as their institutional repository
 - via commercial sites with which Elsevier has an agreement

In all cases accepted manuscripts should:

- link to the formal publication via its DOI
- bear a CC-BY-NC-ND license - this is easy to do
- if aggregated with other manuscripts, for example in a repository or other site, be shared in alignment with our hosting policy not be added to or enhanced in any way to appear more like, or to substitute for, the published journal article.

Published journal article (JPA): A published journal article (PJA) is the definitive final record of published research that appears or will appear in the journal and embodies all

value-adding publishing activities including peer review co-ordination, copy-editing, formatting, (if relevant) pagination and online enrichment.

Policies for sharing publishing journal articles differ for subscription and gold open access articles:

Subscription Articles: If you are an author, please share a link to your article rather than the full-text. Millions of researchers have access to the formal publications on ScienceDirect, and so links will help your users to find, access, cite, and use the best available version.

Theses and dissertations which contain embedded PJAs as part of the formal submission can be posted publicly by the awarding institution with DOI links back to the formal publications on ScienceDirect.

If you are affiliated with a library that subscribes to ScienceDirect you have additional private sharing rights for others' research accessed under that agreement. This includes use for classroom teaching and internal training at the institution (including use in course packs and courseware programs), and inclusion of the article for grant funding purposes.

Gold Open Access Articles: May be shared according to the author-selected end-user license and should contain a [CrossMark logo](#), the end user license, and a DOI link to the formal publication on ScienceDirect.

Please refer to Elsevier's [posting policy](#) for further information.

18. **For book authors** the following clauses are applicable in addition to the above: Authors are permitted to place a brief summary of their work online only. You are not allowed to download and post the published electronic version of your chapter, nor may you scan the printed edition to create an electronic version. **Posting to a repository:** Authors are permitted to post a summary of their chapter only in their institution's repository.

19. **Thesis/Dissertation:** If your license is for use in a thesis/dissertation your thesis may be submitted to your institution in either print or electronic form. Should your thesis be published commercially, please reapply for permission. These requirements include permission for the Library and Archives of Canada to supply single copies, on demand, of the complete thesis and include permission for Proquest/UMI to supply single copies, on demand, of the complete thesis. Should your thesis be published commercially, please reapply for permission. Theses and dissertations which contain embedded PJAs as part of the formal submission can be posted publicly by the awarding institution with DOI links back to the formal publications on ScienceDirect.

Elsevier Open Access Terms and Conditions

You can publish open access with Elsevier in hundreds of open access journals or in nearly 2000 established subscription journals that support open access publishing. Permitted third party re-use of these open access articles is defined by the author's choice of Creative Commons user license. See our [open access license policy](#) for more information.

Terms & Conditions applicable to all Open Access articles published with Elsevier:

Any reuse of the article must not represent the author as endorsing the adaptation of the article nor should the article be modified in such a way as to damage the author's honour or reputation. If any changes have been made, such changes must be clearly indicated.

The author(s) must be appropriately credited and we ask that you include the end user license and a DOI link to the formal publication on ScienceDirect.

If any part of the material to be used (for example, figures) has appeared in our publication with credit or acknowledgement to another source it is the responsibility of the user to ensure their reuse complies with the terms and conditions determined by the rights holder.

Additional Terms & Conditions applicable to each Creative Commons user license:

CC BY: The CC-BY license allows users to copy, to create extracts, abstracts and new works from the Article, to alter and revise the Article and to make commercial use of the Article (including reuse and/or resale of the Article by commercial entities), provided the user gives appropriate credit (with a link to the formal publication through the relevant DOI), provides a link to the license, indicates if changes were made and the licensor is not represented as endorsing the use made of the work. The full details of the license are available at <http://creativecommons.org/licenses/by/4.0>.

CC BY NC SA: The CC BY-NC-SA license allows users to copy, to create extracts, abstracts and new works from the Article, to alter and revise the Article, provided this is not done for commercial purposes, and that the user gives appropriate credit (with a link to the formal publication through the relevant DOI), provides a link to the license, indicates if changes were made and the licensor is not represented as endorsing the use made of the work. Further, any new works must be made available on the same conditions. The full details of the license are available at <http://creativecommons.org/licenses/by-nc-sa/4.0>.

CC BY NC ND: The CC BY-NC-ND license allows users to copy and distribute the Article, provided this is not done for commercial purposes and further does not permit distribution of the Article if it is changed or edited in any way, and provided the user gives appropriate credit (with a link to the formal publication through the relevant DOI), provides a link to the license, and that the licensor is not represented as endorsing the use made of the work. The full details of the license are available at <http://creativecommons.org/licenses/by-nc-nd/4.0>. Any commercial reuse of Open Access articles published with a CC BY NC SA or CC BY NC ND license requires permission from Elsevier and will be subject to a fee.

Commercial reuse includes:

- Associating advertising with the full text of the Article
- Charging fees for document delivery or access
- Article aggregation
- Systematic distribution via e-mail lists or share buttons

Posting or linking by commercial companies for use by customers of those companies.

20. Other Conditions:

v1.10

Questions? customercare@copyright.com or +1-855-239-3415 (toll free in the US) or +1-978-646-2777.

Figure 1-7



This is a License Agreement between Dr. Kirsten Carter ("User") and Copyright Clearance Center, Inc. ("CCC") on behalf of the Rightsholder identified in the order details below. The license consists of the order details, the CCC Terms and Conditions below, and any Rightsholder Terms and Conditions which are included below.
 All payments must be made in full to CCC in accordance with the CCC Terms and Conditions below.

Order Date	12-Jul-2021	Type of Use	Republish in a thesis/dissertation
Order License ID	1132552-1	Publisher	LIPPINCOTT WILLIAMS & WILKINS
ISSN	1040-5488	Portion	Image/photo/illustration

LICENSED CONTENT

Publication Title	Optometry and vision science : official publication of the American Academy of Optometry	Rightsholder	Wolters Kluwer Health, Inc.
Article Title	Clinical Manual of Contact Lenses, 4th ed., Edward Bennett and Vinita Henry	Publication Type	Journal
Author/Editor	AMERICAN ACADEMY OF OPTOMETRY.	Start Page	e95
Date	01/01/1989	Issue	4
Language	English	Volume	91
Country	United States of America	URL	http://journals.lww.com/optvissci/pages/default.aspx

REQUEST DETAILS

Portion Type	Image/photo/illustration	Distribution	Worldwide
Number of images / photos / illustrations	1	Translation	Original language of publication
Format (select all that apply)	Print, Electronic	Copies for the disabled?	No
Who will republish the content?	Publisher, not-for-profit	Minor editing privileges?	No
Duration of Use	Current edition and up to 15 years	Incidental promotional use?	No
Lifetime Unit Quantity	Up to 499	Currency	CAD
Rights Requested	Main product		

NEW WORK DETAILS

Title	Changes in corneal thickness in keratoconic eyes with variation in scleral contact lens central clearance	Institution name	University of Waterloo
		Expected presentation date	2021-08-06

Instructor name Denise Hileeto

ADDITIONAL DETAILS

Order reference number	N/A	The requesting person / organization to appear on the license	Dr. Kirsten Carter
------------------------	-----	---	--------------------

REUSE CONTENT DETAILS

Title, description or numeric reference of the portion(s)	Figure 19.9	Title of the article/chapter the portion is from	Clinical Manual of Contact Lenses, 4th ed., Edward Bennett and Vinita Henry
Editor of portion(s)	N/A	Author of portion(s)	Edward S. Bennett, Joseph T. Barr, and Loretta Szczotka-Flynn
Volume of serial or monograph	4th Edition	Issue, if republishing an article from a serial	N/A
Page or page range of portion	534	Publication date of portion	2014-04-01

RIGHTSHOLDER TERMS AND CONDITIONS

If you are placing a request on behalf of/for a corporate organisation, please use [RightsLink](#). For more information, visit [LWW Journals Permissions](#).

It is Wolters Kluwer Lippincott Williams and Wilkins' policy not to allow modifications of text in the image/figure, only colour and size can be altered.

CCC Terms and Conditions

1. Description of Service; Defined Terms. This Republication License enables the User to obtain licenses for republication of one or more copyrighted works as described in detail on the relevant Order Confirmation (the "Work(s)"). Copyright Clearance Center, Inc. ("CCC") grants licenses through the Service on behalf of the rightsholder identified on the Order Confirmation (the "Rightsholder"). "Republication", as used herein, generally means the inclusion of a Work, in whole or in part, in a new work or works, also as described on the Order Confirmation. "User", as used herein, means the person or entity making such republication.
2. The terms set forth in the relevant Order Confirmation, and any terms set by the Rightsholder with respect to a particular Work, govern the terms of use of Works in connection with the Service. By using the Service, the person transacting for a republication license on behalf of the User represents and warrants that he/she/it (a) has been duly authorized by the User to accept, and hereby does accept, all such terms and conditions on behalf of User, and (b) shall inform User of all such terms and conditions. In the event such person is a "freelancer" or other third party independent of User and CCC, such party shall be deemed jointly a "User" for purposes of these terms and conditions. In any event, User shall be deemed to have accepted and agreed to all such terms and conditions if User republishes the Work in any fashion.
3. Scope of License; Limitations and Obligations.
 - 3.1. All Works and all rights therein, including copyright rights, remain the sole and exclusive property of the Rightsholder. The license created by the exchange of an Order Confirmation (and/or any invoice) and payment by User of the full amount set forth on that document includes only those rights expressly set forth in the Order Confirmation and in these terms and conditions, and conveys no other rights in the Work(s) to User. All rights not expressly granted are hereby reserved.
 - 3.2.

General Payment Terms: You may pay by credit card or through an account with us payable at the end of the month. If you and we agree that you may establish a standing account with CCC, then the following terms apply: Remit Payment to: Copyright Clearance Center, 29118 Network Place, Chicago, IL 60673-1291. Payments Due: Invoices are payable upon their delivery to you (or upon our notice to you that they are available to you for downloading). After 30 days, outstanding amounts will be subject to a service charge of 1-1/2% per month or, if less, the maximum rate allowed by applicable law. Unless otherwise specifically set forth in the Order Confirmation or in a separate written agreement signed by CCC, invoices are due and payable on "net 30" terms. While User may exercise the rights licensed immediately upon issuance of the Order Confirmation, the license is automatically revoked and is null and void, as if it had never been issued, if complete payment for the license is not received on a timely basis either from User directly or through a payment agent, such as a credit card company.

- 3.3. Unless otherwise provided in the Order Confirmation, any grant of rights to User (i) is "one-time" (including the editions and product family specified in the license), (ii) is non-exclusive and non-transferable and (iii) is subject to any and all limitations and restrictions (such as, but not limited to, limitations on duration of use or circulation) included in the Order Confirmation or invoice and/or in these terms and conditions. Upon completion of the licensed use, User shall either secure a new permission for further use of the Work(s) or immediately cease any new use of the Work(s) and shall render inaccessible (such as by deleting or by removing or severing links or other locators) any further copies of the Work (except for copies printed on paper in accordance with this license and still in User's stock at the end of such period).
 - 3.4. In the event that the material for which a republication license is sought includes third party materials (such as photographs, illustrations, graphs, inserts and similar materials) which are identified in such material as having been used by permission, User is responsible for identifying, and seeking separate licenses (under this Service or otherwise) for, any of such third party materials; without a separate license, such third party materials may not be used.
 - 3.5. Use of proper copyright notice for a Work is required as a condition of any license granted under the Service. Unless otherwise provided in the Order Confirmation, a proper copyright notice will read substantially as follows: "Republished with permission of [Rightsholder's name], from [Work's title, author, volume, edition number and year of copyright]; permission conveyed through Copyright Clearance Center, Inc. " Such notice must be provided in a reasonably legible font size and must be placed either immediately adjacent to the Work as used (for example, as part of a by-line or footnote but not as a separate electronic link) or in the place where substantially all other credits or notices for the new work containing the republished Work are located. Failure to include the required notice results in loss to the Rightsholder and CCC, and the User shall be liable to pay liquidated damages for each such failure equal to twice the use fee specified in the Order Confirmation, in addition to the use fee itself and any other fees and charges specified.
 - 3.6. User may only make alterations to the Work if and as expressly set forth in the Order Confirmation. No Work may be used in any way that is defamatory, violates the rights of third parties (including such third parties' rights of copyright, privacy, publicity, or other tangible or intangible property), or is otherwise illegal, sexually explicit or obscene. In addition, User may not conjoin a Work with any other material that may result in damage to the reputation of the Rightsholder. User agrees to inform CCC if it becomes aware of any infringement of any rights in a Work and to cooperate with any reasonable request of CCC or the Rightsholder in connection therewith.
4. Indemnity. User hereby indemnifies and agrees to defend the Rightsholder and CCC, and their respective employees and directors, against all claims, liability, damages, costs and expenses, including legal fees and expenses, arising out of any use of a Work beyond the scope of the rights granted herein, or any use of a Work which has been altered in any unauthorized way by User, including claims of defamation or infringement of rights of copyright, publicity, privacy or other tangible or intangible property.
 5. Limitation of Liability. UNDER NO CIRCUMSTANCES WILL CCC OR THE RIGHTSHOLDER BE LIABLE FOR ANY DIRECT, INDIRECT, CONSEQUENTIAL OR INCIDENTAL DAMAGES (INCLUDING WITHOUT LIMITATION DAMAGES FOR LOSS OF BUSINESS PROFITS OR INFORMATION, OR FOR BUSINESS INTERRUPTION) ARISING OUT OF THE USE OR INABILITY

TO USE A WORK, EVEN IF ONE OF THEM HAS BEEN ADVISED OF THE POSSIBILITY OF SUCH DAMAGES. In any event, the total liability of the Rightsholder and CCC (including their respective employees and directors) shall not exceed the total amount actually paid by User for this license. User assumes full liability for the actions and omissions of its principals, employees, agents, affiliates, successors and assigns.

6. Limited Warranties. THE WORK(S) AND RIGHT(S) ARE PROVIDED "AS IS". CCC HAS THE RIGHT TO GRANT TO USER THE RIGHTS GRANTED IN THE ORDER CONFIRMATION DOCUMENT. CCC AND THE RIGHTSHOLDER DISCLAIM ALL OTHER WARRANTIES RELATING TO THE WORK(S) AND RIGHT(S), EITHER EXPRESS OR IMPLIED, INCLUDING WITHOUT LIMITATION IMPLIED WARRANTIES OF MERCHANTABILITY OR FITNESS FOR A PARTICULAR PURPOSE. ADDITIONAL RIGHTS MAY BE REQUIRED TO USE ILLUSTRATIONS, GRAPHS, PHOTOGRAPHS, ABSTRACTS, INSERTS OR OTHER PORTIONS OF THE WORK (AS OPPOSED TO THE ENTIRE WORK) IN A MANNER CONTEMPLATED BY USER; USER UNDERSTANDS AND AGREES THAT NEITHER CCC NOR THE RIGHTSHOLDER MAY HAVE SUCH ADDITIONAL RIGHTS TO GRANT.
7. Effect of Breach. Any failure by User to pay any amount when due, or any use by User of a Work beyond the scope of the license set forth in the Order Confirmation and/or these terms and conditions, shall be a material breach of the license created by the Order Confirmation and these terms and conditions. Any breach not cured within 30 days of written notice thereof shall result in immediate termination of such license without further notice. Any unauthorized (but licensable) use of a Work that is terminated immediately upon notice thereof may be liquidated by payment of the Rightsholder's ordinary license price therefor; any unauthorized (and unlicensable) use that is not terminated immediately for any reason (including, for example, because materials containing the Work cannot reasonably be recalled) will be subject to all remedies available at law or in equity, but in no event to a payment of less than three times the Rightsholder's ordinary license price for the most closely analogous licensable use plus Rightsholder's and/or CCC's costs and expenses incurred in collecting such payment.
8. Miscellaneous.
 - 8.1. User acknowledges that CCC may, from time to time, make changes or additions to the Service or to these terms and conditions, and CCC reserves the right to send notice to the User by electronic mail or otherwise for the purposes of notifying User of such changes or additions; provided that any such changes or additions shall not apply to permissions already secured and paid for.
 - 8.2. Use of User-related information collected through the Service is governed by CCC's privacy policy, available online here:<https://marketplace.copyright.com/rs-ui-web/mp/privacy-policy>
 - 8.3. The licensing transaction described in the Order Confirmation is personal to User. Therefore, User may not assign or transfer to any other person (whether a natural person or an organization of any kind) the license created by the Order Confirmation and these terms and conditions or any rights granted hereunder; provided, however, that User may assign such license in its entirety on written notice to CCC in the event of a transfer of all or substantially all of User's rights in the new material which includes the Work(s) licensed under this Service.
 - 8.4. No amendment or waiver of any terms is binding unless set forth in writing and signed by the parties. The Rightsholder and CCC hereby object to any terms contained in any writing prepared by the User or its principals, employees, agents or affiliates and purporting to govern or otherwise relate to the licensing transaction described in the Order Confirmation, which terms are in any way inconsistent with any terms set forth in the Order Confirmation and/or in these terms and conditions or CCC's standard operating procedures, whether such writing is prepared prior to, simultaneously with or subsequent to the Order Confirmation, and whether such writing appears on a copy of the Order Confirmation or in a separate instrument.
 - 8.5. The licensing transaction described in the Order Confirmation document shall be governed by and construed under the law of the State of New York, USA, without regard to the principles thereof of conflicts of law. Any case, controversy, suit, action, or proceeding arising out of, in connection with, or related to such licensing transaction shall be brought, at CCC's sole discretion, in any federal or state court located in the County of New York, State of New York, USA, or in any federal or state court whose geographical

jurisdiction covers the location of the Rightsholder set forth in the Order Confirmation. The parties expressly submit to the personal jurisdiction and venue of each such federal or state court. If you have any comments or questions about the Service or Copyright Clearance Center, please contact us at 978-750-8400 or send an e-mail to support@copyright.com.

v 1.1

Figure 3-1

Kirsten Carter

From: Lee Hall <leehall980@hotmail.com>
Sent: June 22, 2021 12:11 PM
To: Kirsten Carter
Cc: Lisa Starcher
Subject: Ocular Sagittal Height Figures

Hello Kirsten,

I received a request from Lisa Starcher this morning saying that you'd requested publishing permission for some figures I'd produced a few years back. The answer is yes and I've let Lisa know! :)

I'd be very interested to hear more about your work and please let me know if I can be of assistance in any other way.

Good luck with your MSc.

Kind Regards,
Dr Lee Hall

Sent from my iPhone

Kirsten Carter

From: Lisa Starcher <Lisa.Starcher@pentavisionmedia.com>
Sent: June 22, 2021 12:41 PM
To: Kirsten Carter
Subject: Re: Request for permission to reproduce figure from PentaVision + Contact Lens Spectrum article

Hi Dr. Carter. Dr. Hall copied me on his email to you, so I see that he gave you permission. You can simply credit Dr. Hall for the image, no need to mention Contact Lens Spectrum.

Good luck on your thesis!
Lisa

From: Roger Zimmer <roger.zimmer@pentavisionmedia.com>
Date: Tuesday, June 22, 2021 at 7:54 AM
To: Kirsten Carter <kirsten.carter@uwaterloo.ca>
Cc: Lisa Starcher <Lisa.Starcher@pentavisionmedia.com>
Subject: Re: Request for permission to reproduce figure from PentaVision + Contact Lens Spectrum article

Hi Dr. Carter,

Thank you for your message, and for inquiring about the use of the attached illustration.

I have copied *Contact Lens Spectrum* managing editor Lisa Starcher, who will respond to your request.

Best of luck with your master's thesis.

Regards,
Roger

Roger Zimmer
Executive Vice President and Publisher
Contact Lens Spectrum
Global Specialty Lens Symposium
Global Myopia Symposium

PentaVision LLC
2003 South Easton Road, Suite 203
Doylestown, PA 18901
(203) 856-9660 tel

From: Kirsten Carter <kirsten.carter@uwaterloo.ca>
Date: Monday, June 21, 2021 at 10:21 AM
To: Roger Zimmer <roger.zimmer@pentavisionmedia.com>
Subject: Request for permission to reproduce figure from PentaVision + Contact Lens Spectrum article

Dear Mr. Zimmer,

My name is Kirsten Carter and I am an MSc candidate at The University of Waterloo School of Optometry and Vision Science. I write to you requesting permission to reproduce an illustration published by PentaVision + Contact Lens Spectrum in my Master's thesis. Here is the reference to the article:

Hall L. What you need to know about sagittal height and scleral lenses. Contact Lens Spectrum. <https://www.clspectrum.com/issues/2015/may-2015/what-you-need-to-know-about-sagittal-height-and-sc>. Published 2015.

Specifically, I wish to reproduce Figure 1, and provide additional annotation to the illustration indicating ocular sagittal height. This involves adding two arrows, one dotted line, and a text box to label this parameter. I have attached to this email screenshots of both the original image used in the article, and my proposed modified image for ease of access and personal use at this time only. Please let me know if permission may be granted, and if there would be a charge for my request. Thank you in advance for your time.

All the best,
Kirsten

Dr. Kirsten Carter, BSc, OD
MSc Candidate – Vision Science
School of Optometry and Vision Science
University of Waterloo
200 University Avenue West, Waterloo, ON, N2L 3G1



Figure 3-8

BAUSCH + LOMB

Karen J. Tyler
Senior Legal Administrator
1400 N. Goodman Street, Area 62
Rochester, NY 14609
T 585 338 5556
F 585 338 8706
E karen.tyler@bausch.com

July 6, 2021

Attn: Dr. Kirsten Carter
School of Optometry and Vision Science
University of Waterloo
200 University Avenue West, Waterloo, ON, N2L 3G1

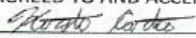
Re: Master's thesis (the "Publication")

Bausch & Lomb Incorporated or its affiliates (collectively "Bausch + Lomb") provides consent to Dr. Kirsten Carter, School of Optometry and Vision Science, University of Waterloo, 200 University Avenue West, Waterloo, ON, N2L 3G1, (hereinafter "Publisher") to use the Diagnostic Set Configuration (hereinafter the "Images"), attached as Exhibit A, for use in the Publication in Master's thesis, subject to the following terms and conditions:

1. Publisher acknowledges Bausch + Lomb's right, title and interest in and to the Images;
2. That Bausch + Lomb is given appropriate trademark and copyright attribution as the owner in all Use of the Images in the Chapter, i.e., © Images provided courtesy of Bausch + Lomb.
3. That the Images will be used only in a manner consistent with the educational aim of the Use of the Images;
4. Publisher acknowledges Bausch + Lomb does not make any representations or warranties of the Images and further acknowledges Bausch + Lomb will not indemnify Publisher or its affiliates for any causes of action, claims or losses arising out of the Use of the Images that does not comply with the Use in the Publication or any other use of the Images;
5. That Publisher shall indemnify and hold harmless Bausch + Lomb against any and all causes of action, claims or losses which arise from any aspect of the Use of the Images in the Publication or any other use of the Images by the Publisher;
6. That the Images will be included in the Publisher's archive for internal storage and viewing purposes only and will not be re-used in any other publication or media without written permission;
7. The rights granted hereunder will in no way restrict republication of the Images in any form or manner by Bausch + Lomb or others licensed, permitted or otherwise authorized by Bausch + Lomb; and
8. The Images will be used in a manner so as not to denigrate, damage or harm Bausch + Lomb or Bausch + Lomb's goodwill.

Please sign and date where indicated below to accept and agree to the aforementioned terms.

AGREED TO AND ACCEPTED BY:


Authorized Officer / Title

Dated: 7 July 2021 By:

EXHIBIT A

DIAGNOSTIC SET CONFIGURATION

		QUARK						TORIC PC _s
PROLATE	16MM	Z-1 4200 SAG 8.20 BC	Z-2 4500 SAG 7.60 BC	Z-3 4800 SAG 7.00 BC	Z-4 5100 SAG 6.70 BC	Z-5 5400 SAG 6.40 BC	Z-6 5700 SAG 6.30 BC	ZT-5 5400 SAG 6.40 BC
	17MM	Z-7 4300 SAG 9.20 BC	Z-8 4600 SAG 8.40 BC	Z-9 4900 SAG 7.80 BC	Z-10 5200 SAG 7.30 BC	Z-11 5500 SAG 6.90 BC	Z-12 5800 SAG 6.60 BC	ZT-11 5500 SAG 6.90 BC
OBLATE	16MM	Z-13 4100 SAG 10.00 BC	Z-14 4400 SAG 9.50 BC	Z-15 4700 SAG 9.00 BC	Z-16 5000 SAG 8.50 BC	Z-17 5300 SAG 8.00 BC	Z-18 5600 SAG 7.50 BC	ZT-17 5300 SAG 8.00 BC
	17MM	Z-19 4200 SAG 10.90 BC	Z-20 4500 SAG 10.30 BC	Z-21 4800 SAG 9.70 BC	Z-22 5100 SAG 9.10 BC	Z-23 5400 SAG 8.50 BC	Z-24 5700 SAG 7.90 BC	ZT-23 5400 SAG 8.50 BC

Appendix B

Kirsten Carter

From: Ledermann, Nadine <n.ledermann@oculus.de>
Sent: June 22, 2021 5:20 AM
To: Kirsten Carter
Cc: TJ Flynn
Subject: AW: Request for permission to reproduce illustration from OCULUS Pentacam® CSP Report Fitting Guide in Master's thesis

Dear Kirsten,

thank you for asking, we appreciate it!

We grant our permission to use parts of our Pentacam® CSP Report Scleral Lens Fitting Guide in your master's thesis with referring to it.

Please do not hesitate to contact us in case of any further questions!

Best regards,

Nadine Ledermann
International Sales



OCULUS Optikgeräte GmbH
Münchholzhäuser Straße 29 | 35582 Wetzlar | GERMANY

Tel. +49 641 2005-236 | Fax +49 641 2005-295

n.ledermann@oculus.de | www.oculus.de



Von: Kirsten Carter <kirsten.carter@uwaterloo.ca>

Gesendet: Montag, 21. Juni 2021 16:49

An: export <export@oculus.de>

Betreff: Request for permission to reproduce illustration from OCULUS Pentacam® CSP Report Fitting Guide in Master's thesis

To Whom It May Concern,

My name is Kirsten Carter and I am an MSc candidate at The University of Waterloo School of Optometry and Vision Science. I write to you requesting permission to reproduce an illustration published by OCULUS in my Master's thesis.

Specifically, I wish to reproduce the first page of the "Pentacam® CSP Report: Scleral Lens Fitting Guide for Zenlens or Zen RC" as an appendix. Here is the reference to the fitting guide:

OCULUS, Alden Optical. Pentacam® CSP Report Scleral Lens Fitting Guide for Zenlens or Zen RC. 2019.

I have also attached here the .pdf copy of the fitting guide for ease of access and personal use only at this time. Please let me know if permission may be granted, and if there would be a charge for my request. Thank you in advance for your time.

All the best,
Kirsten

Dr. Kirsten Carter, BSc, OD
MSc Candidate – Vision Science
School of Optometry and Vision Science
University of Waterloo
200 University Avenue West, Waterloo, ON, N2L 3G1



Figure 4-7



This is a License Agreement between Kirsten Carter ("User") and Copyright Clearance Center, Inc. ("CCC") on behalf of the Rightsholder identified in the order details below. The license consists of the order details, the CCC Terms and Conditions below, and any Rightsholder Terms and Conditions which are included below.

All payments must be made in full to CCC in accordance with the CCC Terms and Conditions below.

Order Date	20-Jun-2021	Type of Use	Republish in a thesis/dissertation
Order License ID	1127247-1	Publisher	JOHN WILEY & SONS
ISSN	1552-4973	Portion	Chart/graph/table/figure

LICENSED CONTENT

Publication Title	Journal of biomedical materials research. Part B, Applied biomaterials	Rightsholder	John Wiley & Sons - Books
Article Title	Central and peripheral oxygen transmissibility thresholds to avoid corneal swelling during open eye soft contact lens wear.	Publication Type	Journal
Author/Editor	Society for Biomaterials., Nihon Baiomateriaru Gakkai., Australian Society for Biomaterials., Korean Society for Biomaterials.	Start Page	NA
Date	01/01/2004	End Page	NA
Language	English	Issue	2
Country	United States of America	Volume	92

REQUEST DETAILS

Portion Type	Chart/graph/table/figure	Distribution	Worldwide
Number of charts / graphs / tables / figures requested	1	Translation	Original language of publication
Format (select all that apply)	Print, Electronic	Copies for the disabled?	No
Who will republish the content?	Academic institution	Minor editing privileges?	Yes
Duration of Use	Life of current and all future editions	Incidental promotional use?	No
Lifetime Unit Quantity	Up to 499	Currency	CAD
Rights Requested	Main product		

NEW WORK DETAILS

Title	Changes in corneal thickness in keratoconic eyes with variation in scleral contact lens central clearance	Institution name	University of Waterloo
		Expected presentation date	2021-08-12
Instructor name	Kirsten Carter		

ADDITIONAL DETAILS

The requesting person / organization to appear on the license	Kirsten Carter
--	----------------

REUSE CONTENT DETAILS

Title, description or numeric reference of the portion(s)	Figure 1	Title of the article/chapter the portion is from	Central and peripheral oxygen transmissibility thresholds to avoid corneal swelling during open eye soft contact lens wear.
Editor of portion(s)	Morgan, Philip B.; Brennan, Noel A.; Maldonado-Codina, Carole; Quhill, Walead; Rashid, Khaled; Efron, Nathan	Author of portion(s)	Morgan, Philip B.; Brennan, Noel A.; Maldonado-Codina, Carole; Quhill, Walead; Rashid, Khaled; Efron, Nathan
Volume of serial or monograph	92		
Page or page range of portion	NA-NA	Publication date of portion	2010-02-01

RIGHTSHOLDER TERMS AND CONDITIONS

No right, license or interest to any trademark, trade name, service mark or other branding ("Marks") of WILEY or its licensors is granted hereunder, and you agree that you shall not assert any such right, license or interest with respect thereto. You may not alter, remove or suppress in any manner any copyright, trademark or other notices displayed by the Wiley material. This Agreement will be void if the Type of Use, Format, Circulation, or Requestor Type was misrepresented during the licensing process. In no instance may the total amount of Wiley Materials used in any Main Product, Compilation or Collective work comprise more than 5% (if figures/tables) or 15% (if full articles/chapters) of the (entirety of the) Main Product, Compilation or Collective Work. Some titles may be available under an Open Access license. It is the Licensors' responsibility to identify the type of Open Access license on which the requested material was published, and comply fully with the terms of that license for the type of use specified. Further details can be found on Wiley Online Library <http://olabout.wiley.com/WileyCDA/Section/id-410895.html>.

CCC Terms and Conditions

1. Description of Service; Defined Terms. This Republication License enables the User to obtain licenses for republication of one or more copyrighted works as described in detail on the relevant Order Confirmation (the "Work(s)"). Copyright Clearance Center, Inc. ("CCC") grants licenses through the Service on behalf of the rightsholder identified on the Order Confirmation (the "Rightsholder"). "Republication", as used herein, generally means the inclusion of a Work, in whole or in part, in a new work or works, also as described on the Order Confirmation. "User", as used herein, means the person or entity making such republication.
2. The terms set forth in the relevant Order Confirmation, and any terms set by the Rightsholder with respect to a particular Work, govern the terms of use of Works in connection with the Service. By using the Service, the person transacting for a republication license on behalf of the User represents and warrants that he/she/it (a) has been

duly authorized by the User to accept, and hereby does accept, all such terms and conditions on behalf of User, and (b) shall inform User of all such terms and conditions. In the event such person is a "freelancer" or other third party independent of User and CCC, such party shall be deemed jointly a "User" for purposes of these terms and conditions. In any event, User shall be deemed to have accepted and agreed to all such terms and conditions if User republishes the Work in any fashion.

3. Scope of License; Limitations and Obligations.

- 3.1. All Works and all rights therein, including copyright rights, remain the sole and exclusive property of the Rightsholder. The license created by the exchange of an Order Confirmation (and/or any invoice) and payment by User of the full amount set forth on that document includes only those rights expressly set forth in the Order Confirmation and in these terms and conditions, and conveys no other rights in the Work(s) to User. All rights not expressly granted are hereby reserved.
- 3.2. General Payment Terms: You may pay by credit card or through an account with us payable at the end of the month. If you and we agree that you may establish a standing account with CCC, then the following terms apply: Remit Payment to: Copyright Clearance Center, 29118 Network Place, Chicago, IL 60673-1291. Payments Due: Invoices are payable upon their delivery to you (or upon our notice to you that they are available to you for downloading). After 30 days, outstanding amounts will be subject to a service charge of 1-1/2% per month or, if less, the maximum rate allowed by applicable law. Unless otherwise specifically set forth in the Order Confirmation or in a separate written agreement signed by CCC, invoices are due and payable on "net 30" terms. While User may exercise the rights licensed immediately upon issuance of the Order Confirmation, the license is automatically revoked and is null and void, as if it had never been issued, if complete payment for the license is not received on a timely basis either from User directly or through a payment agent, such as a credit card company.
- 3.3. Unless otherwise provided in the Order Confirmation, any grant of rights to User (i) is "one-time" (including the editions and product family specified in the license), (ii) is non-exclusive and non-transferable and (iii) is subject to any and all limitations and restrictions (such as, but not limited to, limitations on duration of use or circulation) included in the Order Confirmation or invoice and/or in these terms and conditions. Upon completion of the licensed use, User shall either secure a new permission for further use of the Work(s) or immediately cease any new use of the Work(s) and shall render inaccessible (such as by deleting or by removing or severing links or other locators) any further copies of the Work (except for copies printed on paper in accordance with this license and still in User's stock at the end of such period).
- 3.4. In the event that the material for which a republication license is sought includes third party materials (such as photographs, illustrations, graphs, inserts and similar materials) which are identified in such material as having been used by permission, User is responsible for identifying, and seeking separate licenses (under this Service or otherwise) for, any of such third party materials; without a separate license, such third party materials may not be used.
- 3.5. Use of proper copyright notice for a Work is required as a condition of any license granted under the Service. Unless otherwise provided in the Order Confirmation, a proper copyright notice will read substantially as follows: "Republished with permission of [Rightsholder's name], from [Work's title, author, volume, edition number and year of copyright]; permission conveyed through Copyright Clearance Center, Inc. " Such notice must be provided in a reasonably legible font size and must be placed either immediately adjacent to the Work as used (for example, as part of a by-line or footnote but not as a separate electronic link) or in the place where substantially all other credits or notices for the new work containing the republished Work are located. Failure to include the required notice results in loss to the Rightsholder and CCC, and the User shall be liable to pay liquidated damages for each such failure equal to twice the use fee specified in the Order Confirmation, in addition to the use fee itself and any other fees and charges specified.
- 3.6. User may only make alterations to the Work if and as expressly set forth in the Order Confirmation. No Work may be used in any way that is defamatory, violates the rights of third parties (including such third parties' rights of copyright, privacy, publicity, or other tangible or intangible property), or is otherwise illegal, sexually explicit or obscene. In addition, User may not conjoin a Work with any other material that

may result in damage to the reputation of the Rightsholder. User agrees to inform CCC if it becomes aware of any infringement of any rights in a Work and to cooperate with any reasonable request of CCC or the Rightsholder in connection therewith.

4. Indemnity. User hereby indemnifies and agrees to defend the Rightsholder and CCC, and their respective employees and directors, against all claims, liability, damages, costs and expenses, including legal fees and expenses, arising out of any use of a Work beyond the scope of the rights granted herein, or any use of a Work which has been altered in any unauthorized way by User, including claims of defamation or infringement of rights of copyright, publicity, privacy or other tangible or intangible property.
5. Limitation of Liability. UNDER NO CIRCUMSTANCES WILL CCC OR THE RIGHTSHOLDER BE LIABLE FOR ANY DIRECT, INDIRECT, CONSEQUENTIAL OR INCIDENTAL DAMAGES (INCLUDING WITHOUT LIMITATION DAMAGES FOR LOSS OF BUSINESS PROFITS OR INFORMATION, OR FOR BUSINESS INTERRUPTION) ARISING OUT OF THE USE OR INABILITY TO USE A WORK, EVEN IF ONE OF THEM HAS BEEN ADVISED OF THE POSSIBILITY OF SUCH DAMAGES. In any event, the total liability of the Rightsholder and CCC (including their respective employees and directors) shall not exceed the total amount actually paid by User for this license. User assumes full liability for the actions and omissions of its principals, employees, agents, affiliates, successors and assigns.
6. Limited Warranties. THE WORK(S) AND RIGHT(S) ARE PROVIDED "AS IS". CCC HAS THE RIGHT TO GRANT TO USER THE RIGHTS GRANTED IN THE ORDER CONFIRMATION DOCUMENT. CCC AND THE RIGHTSHOLDER DISCLAIM ALL OTHER WARRANTIES RELATING TO THE WORK(S) AND RIGHT(S), EITHER EXPRESS OR IMPLIED, INCLUDING WITHOUT LIMITATION IMPLIED WARRANTIES OF MERCHANTABILITY OR FITNESS FOR A PARTICULAR PURPOSE. ADDITIONAL RIGHTS MAY BE REQUIRED TO USE ILLUSTRATIONS, GRAPHS, PHOTOGRAPHS, ABSTRACTS, INSERTS OR OTHER PORTIONS OF THE WORK (AS OPPOSED TO THE ENTIRE WORK) IN A MANNER CONTEMPLATED BY USER; USER UNDERSTANDS AND AGREES THAT NEITHER CCC NOR THE RIGHTSHOLDER MAY HAVE SUCH ADDITIONAL RIGHTS TO GRANT.
7. Effect of Breach. Any failure by User to pay any amount when due, or any use by User of a Work beyond the scope of the license set forth in the Order Confirmation and/or these terms and conditions, shall be a material breach of the license created by the Order Confirmation and these terms and conditions. Any breach not cured within 30 days of written notice thereof shall result in immediate termination of such license without further notice. Any unauthorized (but licensable) use of a Work that is terminated immediately upon notice thereof may be liquidated by payment of the Rightsholder's ordinary license price therefor; any unauthorized (and unlicensable) use that is not terminated immediately for any reason (including, for example, because materials containing the Work cannot reasonably be recalled) will be subject to all remedies available at law or in equity, but in no event to a payment of less than three times the Rightsholder's ordinary license price for the most closely analogous licensable use plus Rightsholder's and/or CCC's costs and expenses incurred in collecting such payment.
8. Miscellaneous.
 - 8.1. User acknowledges that CCC may, from time to time, make changes or additions to the Service or to these terms and conditions, and CCC reserves the right to send notice to the User by electronic mail or otherwise for the purposes of notifying User of such changes or additions; provided that any such changes or additions shall not apply to permissions already secured and paid for.
 - 8.2. Use of User-related information collected through the Service is governed by CCC's privacy policy, available online here:<https://marketplace.copyright.com/rs-ui-web/mp/privacy-policy>
 - 8.3. The licensing transaction described in the Order Confirmation is personal to User. Therefore, User may not assign or transfer to any other person (whether a natural person or an organization of any kind) the license created by the Order Confirmation and these terms and conditions or any rights granted hereunder; provided, however, that User may assign such license in its entirety on written notice to CCC in the event of a transfer of all or substantially all of User's rights in the new material which includes the Work(s) licensed under this Service.
 - 8.4.

No amendment or waiver of any terms is binding unless set forth in writing and signed by the parties. The Rightsholder and CCC hereby object to any terms contained in any writing prepared by the User or its principals, employees, agents or affiliates and purporting to govern or otherwise relate to the licensing transaction described in the Order Confirmation, which terms are in any way inconsistent with any terms set forth in the Order Confirmation and/or in these terms and conditions or CCC's standard operating procedures, whether such writing is prepared prior to, simultaneously with or subsequent to the Order Confirmation, and whether such writing appears on a copy of the Order Confirmation or in a separate instrument.

- 8.5. The licensing transaction described in the Order Confirmation document shall be governed by and construed under the law of the State of New York, USA, without regard to the principles thereof of conflicts of law. Any case, controversy, suit, action, or proceeding arising out of, in connection with, or related to such licensing transaction shall be brought, at CCC's sole discretion, in any federal or state court located in the County of New York, State of New York, USA, or in any federal or state court whose geographical jurisdiction covers the location of the Rightsholder set forth in the Order Confirmation. The parties expressly submit to the personal jurisdiction and venue of each such federal or state court. If you have any comments or questions about the Service or Copyright Clearance Center, please contact us at 978-750-8400 or send an e-mail to support@copyright.com.

v 1.1

Appendix A

Ocular Symptom Questionnaire

Subjective Ratings of Ocular Symptoms

Date _____ CCT Scleral Study _____ Investigator _____ ID _____ Lens <u>1 and 2</u>
--

The following questions relate to a number of symptoms which you may or may not be experiencing with the contact lenses you are wearing in the study. Please select a value between 0 and 100 which most adequately describes how you feel about your study lenses and enter this in the box next to each question's scale. R=right eye; L=left eye

Baseline

<p>1. How would you rate your <u>comfort</u> with your own lenses?</p> <div style="text-align: center;"> <p>0 100</p> <p>_____</p> <p>Very poor comfort excellent comfort</p> </div>	<p>R <input style="width: 50px; height: 20px;" type="text"/></p> <p>L <input style="width: 50px; height: 20px;" type="text"/></p>
<p>2. How would you rate your <u>dryness</u> with your own lenses?</p> <div style="text-align: center;"> <p>0 100</p> <p>_____</p> <p>Very dry not dry at <u>all</u></p> </div>	<p>R <input style="width: 50px; height: 20px;" type="text"/></p> <p>L <input style="width: 50px; height: 20px;" type="text"/></p>
<p>3. How would you rate <u>burning</u> with your own lenses?</p> <div style="text-align: center;"> <p>0 100</p> <p>_____</p> <p>Severe burning no burning</p> </div>	<p>R <input style="width: 50px; height: 20px;" type="text"/></p> <p>L <input style="width: 50px; height: 20px;" type="text"/></p>
<p>4. How would you rate your <u>clarity of vision</u> with respect to cloudy/filminess (blinking to clear) with your own lenses?</p> <div style="text-align: center;"> <p>0 100</p> <p>_____</p> <p>Very poor excellent (constantly having to blink to clear) (never having to blink to clear)</p> </div>	<p>R <input style="width: 50px; height: 20px;" type="text"/></p> <p>L <input style="width: 50px; height: 20px;" type="text"/></p>
<p>Comments:</p>	
Signed _____	Date _____

Delivery Visit Insertion Lens 1 or 2 please circle

<p>1. How would you rate your <u>comfort</u> with your study lenses?</p> <p style="text-align: center;">0 100</p> <p>Very poor comfort excellent comfort</p>	R	<input style="width: 60px; height: 20px;" type="text"/>
	L	<input style="width: 60px; height: 20px;" type="text"/>
<p>2. How would you rate your <u>dryness</u> with your study lenses?</p> <p style="text-align: center;">0 100</p> <p>Very dry not dry at all</p>	R	<input style="width: 60px; height: 20px;" type="text"/>
	L	<input style="width: 60px; height: 20px;" type="text"/>
<p>3. How would you rate <u>burning</u> with your study lenses?</p> <p style="text-align: center;">0 100</p> <p>Severe burning no burning</p>	R	<input style="width: 60px; height: 20px;" type="text"/>
	L	<input style="width: 60px; height: 20px;" type="text"/>
<p>4. How would you rate your <u>clarity of vision</u> with respect to cloudy/filminess (blinking to clear) with your study lenses?</p> <p style="text-align: center;">0 100</p> <p>Very poor excellent (constantly having to blink to clear) (never having to blink to clear)</p>	R	<input style="width: 60px; height: 20px;" type="text"/>
	L	<input style="width: 60px; height: 20px;" type="text"/>
<p>5. How would you rate your <u>overall preference</u> with your study lenses?</p> <p style="text-align: center;">100 0 100</p> <p>Strongly prefer L1 No Difference strongly prefer L2</p>	R	<input style="width: 60px; height: 20px;" type="text"/>
		OR
	L	<input style="width: 60px; height: 20px;" type="text"/>
<p>Comments:</p>		
Signed	Date	

Follow up Visit Lens 1 or 2 please circle

<p>1. How would you rate your <u>comfort</u> with your study lenses?</p> <p style="text-align: center;">0 100</p> <p style="text-align: center;">Very poor comfort excellent comfort</p>	R	<input style="width: 50px; height: 20px;" type="text"/>
	L	<input style="width: 50px; height: 20px;" type="text"/>
<p>2. How would you rate your <u>dryness</u> with your study lenses?</p> <p style="text-align: center;">0 100</p> <p style="text-align: center;">Very dry not dry at all</p>	R	<input style="width: 50px; height: 20px;" type="text"/>
	L	<input style="width: 50px; height: 20px;" type="text"/>
<p>3. How would you rate <u>burning</u> with your study lenses?</p> <p style="text-align: center;">0 100</p> <p style="text-align: center;">Severe burning no burning</p>	R	<input style="width: 50px; height: 20px;" type="text"/>
	L	<input style="width: 50px; height: 20px;" type="text"/>
<p>4. How would you rate your <u>clarity of vision</u> with respect to cloudy/filminess (blinking to clear) with your study lenses?</p> <p style="text-align: center;">0 100</p> <p style="text-align: center;">Very poor excellent (constantly having to blink to clear) (never having to blink to clear)</p>	R	<input style="width: 50px; height: 20px;" type="text"/>
	L	<input style="width: 50px; height: 20px;" type="text"/>
<p>5. How would you rate your <u>overall preference</u> with your study lenses?</p> <p style="text-align: center;">100 0 100</p> <p style="text-align: center;">Strongly prefer L1 No Difference strongly prefer <u>L2</u></p>	R	<input style="width: 50px; height: 20px;" type="text"/>
		OR
	L	<input style="width: 50px; height: 20px;" type="text"/>
<p>Comments:</p>		
<p>Signed Date</p>		

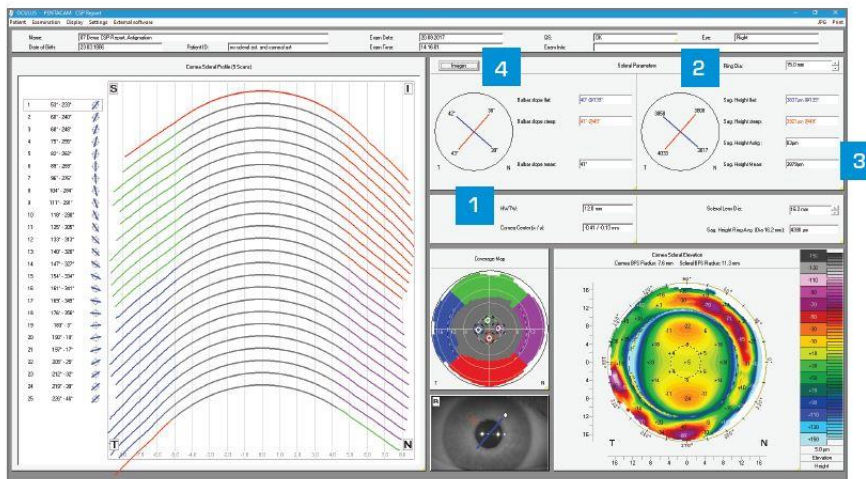
Appendix B

Oculus Pentacam® Cornea Sclera Profile Scleral Fitting Guide. ©

Image provided courtesy of Oculus.²⁶⁰

Pentacam® CSP Report

Scleral Lens Fitting Guide for Zenlens or Zen RC



1 Select Scleral Lens Diameter:

Choose scleral lens diameter based on HWTW value:

- 11.8 mm or greater -> choose Zenlens 17 mm or Zen RC 15.4 mm
- 11.7 mm or less -> choose Zenlens 16 mm or Zen RC 14.8 mm

2 Adapt Ring Diameter:

Set **Ring Dia** to lens diameter determined in step 1

3 Select Sagittal Height

Select **Sag. Height Mean** and add 300 microns for initial clearance

4 Select APS

Use bulbar slope values to select APS from the grid to the right:

-> e.g. when **Bulbar slope flat** = 38 and **Bulbar slope steep** = 42, select APS of standard and steep 4

When the steep and flat slopes are less than 3 degrees different, select a spherical APS using slope mean:

-> e.g. when slope flat = 37 and slope steep = 39, select APS of standard

Bulbar Slope [°]	APS
28	Flat 10
30	Flat 8
32	Flat 6
34	Flat 4
36	Flat 2
38	Standard
40	Steep 2
42	Steep 4
44	Steep 6
46	Steep 8
48	Steep 10



Appendix C

Personal Communication, Annie Kwan, Technical and Clinical Support Representative, Innova-Heidelberg Supplier, 23 February 2021

From: Annie Kwan <akwan@innovamed.com>
Sent: February 23, 2021 12:28 PM
To: Kirsten Carter <kirsten.carter@uwaterloo.ca>
Subject: RE: Questions Re Corneal Thickness Measurements with Spectralis Anterior Segment Imaging Module

Hello Kirsten,

Here is the response from the manufacturer:

No, no further correction is required for corneal thickness measurements. The images are refraction corrected so that the 200 μm scale applies to the area above the Anterior Cornea as well as to the cornea itself.

However, this is not the case for the anterior chamber itself, i.e. the area behind the posterior cornea, so the images are not suitable for measurements within the anterior chamber.

This is explained by the procedure used:

The Anterior Cornea is segmented, see red line in the appendix. Then the light rays incident vertically in parallel from the upper edge of the image are followed. When the light ray hits the anterior cornea, it is on the one hand refracted, i.e. deflected towards the center of the image, and on the other hand shortened from here according to the refractive index. For the cornea we assume a refractive index of 1.376. Thus the lower edge of the image is bent upwards in the center.

Actually, the light beam is then refracted again at the posterior cornea during the transition from the cornea to the anterior chamber. However, since we cannot reliably segment the posterior cornea, this refraction is not included in the refraction correction. Therefore, we represent the pixels in the anterior chamber as if they had the same refractive index as the cornea. However, this is irrelevant for thickness measurements of the cornea.

The refractive index 1.40 is only relevant for images in sclera mode. There, in fact, only all pixels are rescaled as if they were in a medium with refractive index 1.40, which we assume for the sclera.

I hope this helps.

Regards,

Annie Kwan

Technology Support Group, Ext. 8027



a. 136 Sparks Ave, Toronto ON M2H 2S4

t. 416 615 0185 | 800 461 1200

f. 416 631 8272 | 800 313 8696

Appendix D

Personal Communication, Annie Kwan, Technical and Clinical Support Representative, Innova-Heidelberg Supplier, 4 March 2021



Annie Kwan <akwan@innovamed.com>
To: Kirsten Carter

[↩ Reply](#) [↶ Reply All](#) [→ Forward](#) [⋮](#)

Thu 2021-03-04 11:04 AM

Follow up. Completed on May 5, 2021.

This message is part of a tracked conversation. [Click here to find all related messages or to open the original flagged message.](#)
[Click here to download pictures.](#) To help protect your privacy, Outlook prevented automatic download of some pictures in this message.

Hello Kirsten,

Here is the response from Heidelberg:

There are 3 different types of ASM images:

1. Cornea
2. Chamber Angle
3. Sclera

The following refers to Cornea images (below the segmentation line):

In Oct images every pixel has the same optical way length.

For the Spectralis this is roughly about 5.2 μm . This means:

1; A single raw pixel in air is about 5.2 μm long.

2; A single raw pixel in cornea is about 5.2/1.376 μm long.

In the preprocessing of the image (some sort of ray tracing) the different scaling of the pixels and the refraction on the surface of the cornea are done via software. Thus everything below the segmentation line has the scaling of the cornea.

To get the correct length for something other than cornea below the segmentation line, you have first to compute the optical path length of the structure. To do so you have to multiply its length by the refractive index of the cornea. After that you have to divide the optical path length by the refractive index of the structure. In case of tear film this would be:

$\text{CorrectedLength} = \text{Length} * n_{\text{Cornea}} / n_{\text{TearFilm}}$

This is also valid for the scleral lens. If you know the refractive index of the lens you can verify the formula above by replacing the refractive index of the tear film by the refractive index of the lens.

Please note:

1; To avoid errors due to different refraction indices of cornea and lens you should measure as close to the apex as possible.

2; The visibility of the apex is also important, because then you know that you measure perpendicular to the cornea. In this case the 2D refraction correction of the image is correct.

3; The formula above is only valid for vertical distances.

Regards,

Annie Kwan

Clinical and Technical Support

OFFICE 416.615.0185 ext 8027 | 800.461.1200

Appendix E

Descriptive Statistics: Total Corneal Thickness Measurements

Table E-1: Spectralis OD Horizontal (-Temporal to +Nasal). In all tables in this appendix, “M” refers to negative location values.

	Visit Type	Lens Only	M4	M3	M2	M1	0	1	2	3	4
N	BL	LC	8	8	8	8	8	8	8	8	8
		HC	8	8	8	8	8	8	8	8	8
	FU	LC	8	8	8	8	8	8	8	8	8
		HC	7	8	8	8	8	8	8	8	8
Missing	BL	LC	0	0	0	0	0	0	0	0	0
		HC	0	0	0	0	0	0	0	0	0
	FU	LC	0	0	0	0	0	0	0	0	0
		HC	1	0	0	0	0	0	0	0	0
Mean	BL	LC	656	609	574	553	541	582	619	665	695
		HC	676	630	593	566	543	573	610	651	680
	FU	LC	662	628	583	566	552	595	632	672	709
		HC	678	620	590	570	555	593	638	678	717
Median	BL	LC	653	620	574	548	551	580	618	659	686
		HC	686	653	613	574	563	586	611	652	679
	FU	LC	673	627	587	560	563	593	624	663	716
		HC	662	626	593	560	570	592	618	659	699
Standard deviation	BL	LC	57.9	58.8	59.6	58.7	81.8	66.5	55.6	49.5	53.8
		HC	36.5	61.1	60.6	63.9	88.0	69.1	55.5	53.2	54.1
	FU	LC	60.5	47.3	63.4	61.0	80.5	64.7	55.2	52.5	69.3
		HC	63.6	61.5	57.8	61.4	90.8	73.6	64.3	66.6	66.3
Minimum	BL	LC	574	524	487	469	402	468	522	594	616
		HC	626	534	487	456	384	445	511	587	605
	FU	LC	564	563	487	480	427	494	551	609	627
		HC	591	535	511	493	409	468	549	607	639
Maximum	BL	LC	723	675	664	642	644	666	691	740	794
		HC	730	696	665	654	651	666	691	722	752
	FU	LC	724	688	664	655	656	678	704	743	814
		HC	765	701	691	667	653	684	741	807	847

Table E-2: Spectralis OS Horizontal (-Temporal to +Nasal)

	Visit Type	Lens Only	M4	M3	M2	M1	0	1	2	3	4
N	BL	LC	8	8	8	8	8	8	8	8	8
		HC	8	8	8	8	8	8	8	8	8
	FU	LC	8	8	8	8	8	8	8	8	8
		HC	8	8	8	8	8	8	8	8	8
Missing	BL	LC	0	0	0	0	0	0	0	0	0
		HC	0	0	0	0	0	0	0	0	0
	FU	LC	0	0	0	0	0	0	0	0	0
		HC	0	0	0	0	0	0	0	0	0
Mean	BL	LC	657	621	589	567	565	595	624	662	700
		HC	667	636	599	570	556	578	607	648	681
	FU	LC	673	633	598	572	571	601	636	676	718
		HC	675	635	601	575	577	599	627	667	712
Median	BL	LC	653	617	587	567	569	599	632	659	712
		HC	673	637	613	573	562	574	605	637	660
	FU	LC	666	627	587	567	578	605	629	662	726
		HC	687	626	587	561	572	599	630	659	708
Standard deviation	BL	LC	51.0	64.1	66.6	71.7	82.5	66.4	65.7	55.0	54.3
		HC	52.9	57.1	66.5	64.6	80.3	81.7	77.2	64.1	65.6
	FU	LC	61.3	64.5	75.7	80.6	90.0	76.3	68.9	59.8	61.4
		HC	63.9	66.3	72.0	74.3	89.3	93.0	82.3	63.8	60.6
Minimum	BL	LC	608	530	494	467	425	494	527	593	629
		HC	603	554	507	481	413	432	474	556	607
	FU	LC	601	557	494	456	413	469	540	618	627
		HC	595	562	522	493	428	429	484	580	640
Maximum	BL	LC	755	728	705	692	688	692	715	750	776
		HC	741	716	692	680	672	692	709	744	779
	FU	LC	769	728	721	705	703	707	731	774	790
		HC	776	744	730	717	725	733	741	767	807

Table E-3: Spectralis OD Vertical (-Inferior to +Superior)

	Visit Type	Lens Only	M4	M3	M2	M1	0	1	2	3	4
N	BL	LC	8	8	8	8	8	8	8	8	8
		HC	8	8	8	8	8	8	8	8	8
	FU	LC	7	8	8	8	8	8	8	8	7
		HC	8	8	8	8	8	8	8	8	7
Missing	BL	LC	0	0	0	0	0	0	0	0	0
		HC	0	0	0	0	0	0	0	0	0
	FU	LC	1	0	0	0	0	0	0	0	1
		HC	0	0	0	0	0	0	0	0	1
Mean	BL	LC	690	635	584	545	543	577	620	667	696
		HC	681	628	574	535	541	575	621	668	697
	FU	LC	712	648	595	555	550	587	631	679	723
		HC	714	655	598	556	559	595	640	684	720
Median	BL	LC	675	616	576	550	557	586	629	665	694
		HC	676	615	566	536	560	592	635	661	708
	FU	LC	697	622	582	549	561	592	635	674	747
		HC	698	628	582	555	566	598	635	672	682
Standard deviation	BL	LC	79.0	70.4	74.6	78.3	81.0	63.7	61.5	59.3	66.2
		HC	77.0	61.7	69.2	81.0	82.4	75.4	66.4	64.3	61.7
	FU	LC	79.1	79.1	81.7	83.6	82.4	73.0	67.5	67.1	72.4
		HC	72.8	83.4	85.1	92.4	87.6	73.7	72.7	67.2	88.8
Minimum	BL	LC	579	541	494	404	396	471	541	594	600
		HC	572	554	494	394	400	456	530	584	595
	FU	LC	603	557	499	419	421	475	534	597	608
		HC	633	571	499	393	411	481	547	597	608
Maximum	BL	LC	839	737	709	656	638	656	710	749	787
		HC	789	719	696	655	637	668	722	762	767
	FU	LC	835	771	734	681	650	680	722	789	817
		HC	850	801	735	681	663	680	735	792	827

Table E-4: Spectralis OS Vertical (-Inferior to +Superior)

	Visit Type	Lens Only	M4	M3	M2	M1	0	1	2	3	4
N	BL	LC	8	8	8	8	8	8	8	7	7
		HC	7	7	7	7	7	7	7	7	7
	FU	LC	8	8	8	8	8	8	8	8	8
		HC	8	8	8	8	8	8	8	8	8
Missing	BL	LC	0	0	0	0	0	0	0	1	1
		HC	1	1	1	1	1	1	1	1	1
	FU	LC	0	0	0	0	0	0	0	0	0
		HC	0	0	0	0	0	0	0	0	0
Mean	BL	LC	691	651	596	551	565	595	632	651	684
		HC	694	656	613	577	580	610	644	676	707
	FU	LC	697	652	608	560	570	604	640	679	719
		HC	720	662	612	563	565	608	640	679	721
Median	BL	LC	678	645	593	567	563	586	616	638	663
		HC	688	669	597	552	569	604	643	679	701
	FU	LC	706	632	593	567	572	598	629	672	715
		HC	720	645	592	572	572	611	629	657	702
Standard deviation	BL	LC	56.2	72.4	91.0	109	77.5	68.2	67.6	55.9	62.4
		HC	63.4	68.6	70.4	69.9	59.8	54.9	61.3	78.3	76.9
	FU	LC	68.7	85.7	97.4	116	89.8	68.3	70.7	66.1	66.6
		HC	68.4	86.3	88.8	113	108	87.0	84.7	80.5	70.6
Minimum	BL	LC	631	546	442	330	425	491	551	593	627
		HC	604	576	545	481	502	541	577	591	625
	FU	LC	585	539	453	328	400	492	543	602	634
		HC	631	556	492	344	350	445	505	592	652
Maximum	BL	LC	763	754	723	673	669	676	728	742	805
		HC	780	742	711	680	684	692	741	803	828
	FU	LC	777	784	749	706	700	704	742	803	828
		HC	832	796	746	717	713	726	754	803	818

Table E-5: Spectralis OD Oblique (-Inferior Temporal to +Superior Nasal)

	Lens Only	Visit Type	M4	M3	M2	M1	0	1	2	3	4
N	LC	BL	8	8	8	8	8	8	8	8	8
		FU	8	8	8	8	8	8	8	8	5
	HC	BL	8	8	8	8	8	8	8	8	8
		FU	8	8	8	8	8	8	8	8	7
Missing	LC	BL	0	0	0	0	0	0	0	0	0
		FU	0	0	0	0	0	0	0	0	3
	HC	BL	0	0	0	0	0	0	0	0	0
		FU	0	0	0	0	0	0	0	0	1
Mean	LC	BL	664	612	566	536	544	589	622	658	678
		FU	697	626	575	546	557	602	637	681	692
	HC	BL	671	617	567	535	541	588	625	662	696
		FU	689	639	581	554	560	598	638	686	724
Median	LC	BL	651	603	557	536	558	593	623	656	686
		FU	699	610	569	554	581	605	636	684	694
	HC	BL	671	610	570	548	551	592	628	652	682
		FU	672	617	563	548	573	593	620	679	689
Standard deviation	LC	BL	55.5	59.1	68.0	76.8	80.0	64.4	58.8	45.9	57.2
		FU	62.8	59.8	68.9	79.5	83.1	59.6	53.1	54.4	51.5
	HC	BL	64.7	60.9	80.0	83.2	74.2	59.1	48.1	63.2	77.7
		FU	74.2	57.9	70.9	63.9	88.0	74.4	69.2	69.0	79.4
Minimum	LC	BL	593	535	465	393	406	482	531	595	596
		FU	611	547	457	393	413	508	555	607	611
	HC	BL	568	506	418	367	425	495	566	592	604
		FU	595	563	482	457	413	468	543	603	624
Maximum	LC	BL	762	713	692	655	650	667	707	728	760
		FU	818	725	692	667	650	681	706	757	744
	HC	BL	760	712	692	655	637	681	693	754	799
		FU	804	726	705	655	663	681	731	804	855

Table E-6: Spectralis OS Oblique (-Inferior Temporal to +Superior Nasal)

	Visit Type	Lens Only	M4	M3	M2	M1	0	1	2	3	4
N	BL	LC	5	8	8	8	8	8	8	8	8
		HC	4	8	8	8	8	8	8	8	7
	FU	LC	5	8	8	8	8	8	8	8	7
		HC	5	8	8	8	8	8	8	8	6
Missing	BL	LC	3	0	0	0	0	0	0	0	0
		HC	4	0	0	0	0	0	0	0	1
	FU	LC	3	0	0	0	0	0	0	0	1
		HC	3	0	0	0	0	0	0	0	2
Mean	BL	LC	630	609	573	552	558	597	628	662	698
		HC	723	625	585	556	556	589	625	658	710
	FU	LC	676	625	586	560	572	607	644	682	719
		HC	689	628	584	559	571	611	642	683	739
Median	BL	LC	641	597	561	549	560	598	618	656	705
		HC	725	643	587	555	563	579	616	643	701
	FU	LC	693	617	573	561	581	604	631	680	706
		HC	680	606	567	554	575	611	629	681	726
Standard deviation	BL	LC	90.5	79.5	82.2	82.3	78.1	67.1	65.7	59.8	74.4
		HC	57.4	92.8	88.7	87.3	77.5	66.2	64.7	68.0	71.3
	FU	LC	82.9	82.6	87.6	88.6	86.5	65.8	63.9	63.7	57.9
		HC	83.6	84.6	94.9	101	95.0	74.8	73.3	69.5	88.0
Minimum	BL	LC	494	490	446	419	419	493	544	590	599
		HC	666	473	446	406	418	493	543	590	631
	FU	LC	553	504	449	420	417	505	580	616	637
		HC	595	527	446	393	400	493	554	603	641
Maximum	BL	LC	742	724	690	680	672	680	722	744	822
		HC	777	751	703	683	675	695	719	773	811
	FU	LC	756	737	713	696	700	705	734	785	797
		HC	791	769	742	715	714	717	747	786	857

Table E-7: Spectralis OD Oblique (-Superior Temporal to +Inferior Nasal)

	Visit Type	Lens Only	M4	M3	M2	M1	0	1	2	3	4
N	BL	LC	8	8	8	8	8	8	8	8	4
		HC	8	8	8	8	8	8	8	8	7
	FU	LC	8	8	8	8	8	8	8	8	6
		HC	7	7	7	7	7	7	7	7	6
Missing	BL	LC	0	0	0	0	0	0	0	0	4
		HC	0	0	0	0	0	0	0	0	1
	FU	LC	0	0	0	0	0	0	0	0	2
		HC	1	1	1	1	1	1	1	1	2
Mean	BL	LC	674	643	599	565	541	557	609	655	687
		HC	697	651	605	571	541	554	600	650	691
	FU	LC	701	664	609	577	549	569	613	674	692
		HC	699	661	624	592	572	593	646	689	695
Median	BL	LC	666	640	604	580	554	562	609	647	685
		HC	705	659	635	593	556	550	579	653	698
	FU	LC	706	673	616	580	563	581	607	659	693
		HC	714	662	618	579	563	579	637	687	699
Standard deviation	BL	LC	52.6	58.1	60.8	66.4	83.6	75.9	60.0	55.1	60.2
		HC	66.1	69.3	69.2	70.0	72.3	68.2	55.2	55.9	75.8
	FU	LC	65.0	57.7	66.0	65.8	76.1	82.4	68.5	64.2	59.6
		HC	82.1	71.9	63.1	60.9	67.7	65.0	65.4	74.1	48.4
Minimum	BL	LC	601	578	513	458	400	430	511	592	622
		HC	599	555	490	446	430	456	551	576	603
	FU	LC	601	584	516	471	419	431	499	599	622
		HC	594	556	530	493	451	494	583	609	637
Maximum	BL	LC	746	724	682	643	650	656	696	735	757
		HC	790	743	695	669	638	656	696	728	818
	FU	LC	800	731	707	668	638	669	708	776	771
		HC	804	756	720	681	650	679	747	817	743

Table E-8: Spectralis OS Oblique (-Superior Temporal to +Inferior Nasal)

	Visit Type	Lens Only	M4	M3	M2	M1	0	1	2	3	4
N	BL	LC	7	8	8	8	8	8	8	8	8
		HC	8	8	8	8	8	8	8	8	7
	FU	LC	7	8	8	8	8	8	8	8	8
		HC	8	8	8	8	8	8	8	8	7
Missing	BL	LC	1	0	0	0	0	0	0	0	0
		HC	0	0	0	0	0	0	0	0	1
	FU	LC	1	0	0	0	0	0	0	0	0
		HC	0	0	0	0	0	0	0	0	1
Mean	BL	LC	684	656	616	581	566	575	619	670	706
		HC	694	657	618	582	556	563	602	651	688
	FU	LC	701	666	625	591	566	579	619	667	716
		HC	708	675	638	596	569	578	625	681	728
Median	BL	LC	673	640	615	579	566	581	615	660	713
		HC	712	659	628	585	563	575	605	649	668
	FU	LC	687	659	615	592	574	593	615	654	703
		HC	701	660	621	591	572	588	631	674	729
Standard deviation	BL	LC	81.1	67.2	72.2	72.6	80.3	90.2	71.5	62.5	51.3
		HC	75.7	73.9	70.8	69.2	81.1	96.0	76.0	72.4	48.9
	FU	LC	73.9	72.5	73.0	77.5	94.4	108	84.3	70.9	58.7
		HC	86.1	80.0	75.5	78.4	92.0	115	93.2	77.5	67.7
Minimum	BL	LC	604	580	510	457	424	406	525	593	623
		HC	603	567	522	468	405	379	486	569	628
	FU	LC	621	592	521	457	388	368	486	589	649
		HC	614	580	548	483	413	356	472	585	625
Maximum	BL	LC	838	760	707	682	678	680	709	757	766
		HC	812	776	713	692	675	692	700	754	759
	FU	LC	838	787	720	704	700	717	746	780	814
		HC	825	801	742	717	716	730	759	794	831

Table E-9: Pentacam OD Horizontal (-Temporal to +Nasal)

	Visit Type	Lens Only	M4	M3	M2	M1	0	1	2	3	4
N	BL	LC	8	8	8	8	8	8	8	8	8
		HC	8	8	8	8	8	8	8	8	8
	FU	LC	8	8	8	8	8	8	8	8	8
		HC	8	8	8	8	8	8	8	8	8
Missing	BL	LC	0	0	0	0	0	0	0	0	0
		HC	0	0	0	0	0	0	0	0	0
	FU	LC	0	0	0	0	0	0	0	0	0
		HC	0	0	0	0	0	0	0	0	0
Mean	BL	LC	645	579	519	482	483	515	564	624	691
		HC	643	579	520	482	483	516	565	623	689
	FU	LC	656	589	528	489	489	523	575	635	703
		HC	661	592	530	490	489	522	575	638	707
Median	BL	LC	646	589	532	487	495	517	563	612	683
		HC	640	588	537	490	496	517	560	612	682
	FU	LC	653	594	545	495	502	522	570	626	696
		HC	654	596	538	493	499	519	564	622	693
Standard deviation	BL	LC	57.0	56.4	57.7	61.5	64.8	58.2	46.5	46.5	61.3
		HC	63.4	62.2	63.2	64.4	63.2	55.0	46.0	49.9	63.8
	FU	LC	66.7	65.3	62.4	63.9	64.7	54.1	40.4	42.2	56.1
		HC	62.6	60.4	60.5	65.7	69.3	60.5	48.9	53.2	65.8
Minimum	BL	LC	569	495	425	376	364	405	491	577	623
		HC	558	486	419	377	377	420	496	562	606
	FU	LC	577	499	438	382	371	421	516	587	639
		HC	587	511	445	394	377	423	516	585	639
Maximum	BL	LC	709	648	596	568	571	593	630	691	787
		HC	719	650	602	573	572	593	627	711	804
	FU	LC	738	659	606	577	577	596	630	711	807
		HC	739	664	614	586	586	605	651	737	833

Table E-10: Pentacam OS Horizontal (-Temporal to +Nasal)

	Visit Type	Lens Only	M4	M3	M2	M1	0	1	2	3	4
N	BL	LC	8	8	8	8	8	8	8	8	8
		HC	8	8	8	8	8	8	8	8	8
	FU	LC	8	8	8	8	8	8	8	8	8
		HC	8	8	8	8	8	8	8	8	8
Missing	BL	LC	0	0	0	0	0	0	0	0	0
		HC	0	0	0	0	0	0	0	0	0
	FU	LC	0	0	0	0	0	0	0	0	0
		HC	0	0	0	0	0	0	0	0	0
Mean	BL	LC	656	595	538	503	503	530	572	629	699
		HC	655	593	537	503	503	531	572	628	697
	FU	LC	673	609	549	511	510	535	576	632	706
		HC	672	607	548	511	511	539	583	642	713
Median	BL	LC	645	591	529	499	506	533	569	620	698
		HC	647	591	535	502	508	535	567	614	692
	FU	LC	662	601	539	506	510	535	569	620	705
		HC	665	602	540	507	511	537	573	634	710
Standard deviation	BL	LC	61.8	63.9	64.9	66.8	69.9	65.5	54.9	54.0	68.9
		HC	60.4	64.4	65.9	67.9	69.0	63.9	56.5	56.2	71.7
	FU	LC	59.3	60.2	62.2	67.1	70.0	65.4	57.7	57.3	69.3
		HC	55.8	61.8	68.1	73.0	76.1	70.0	60.3	61.1	74.9
Minimum	BL	LC	569	498	433	388	378	420	508	565	602
		HC	549	482	425	382	378	423	498	572	601
	FU	LC	591	521	453	399	388	430	508	564	610
		HC	588	509	435	383	372	422	519	570	616
Maximum	BL	LC	749	684	623	595	596	614	649	715	808
		HC	732	675	622	594	592	608	651	709	802
	FU	LC	753	690	640	611	609	625	660	726	822
		HC	743	690	643	617	617	633	670	739	833

Table E-11: Pentacam OD Vertical (-Inferior to +Superior)

	Visit Type	Lens Only	M4	M3	M2	M1	0	1	2	3	4
N	BL	LC	7	8	8	8	8	8	8	8	7
		HC	7	8	8	8	8	8	8	8	8
	FU	LC	7	8	8	8	8	8	8	8	8
		HC	7	8	8	8	8	8	8	8	8
Missing	BL	LC	1	0	0	0	0	0	0	0	1
		HC	1	0	0	0	0	0	0	0	0
	FU	LC	1	0	0	0	0	0	0	0	0
		HC	1	0	0	0	0	0	0	0	0
Mean	BL	LC	725	640	556	495	483	517	569	622	673
		HC	725	636	552	495	483	516	569	625	687
	FU	LC	742	641	554	499	489	521	576	638	702
		HC	748	649	562	502	489	523	579	637	702
Median	BL	LC	720	631	546	495	495	518	568	622	693
		HC	735	637	545	492	496	516	563	620	698
	FU	LC	749	626	538	501	502	518	571	640	709
		HC	754	638	544	498	499	516	568	643	717
Standard deviation	BL	LC	53.7	50.1	53.9	61.9	64.8	57.2	53.6	61.2	76.2
		HC	57.0	49.7	55.0	62.6	63.2	56.9	52.9	59.9	75.3
	FU	LC	55.2	53.2	59.6	65.8	64.7	56.7	50.9	57.7	69.8
		HC	65.3	58.6	65.0	70.7	69.3	61.7	57.1	65.7	82.9
Minimum	BL	LC	625	564	485	381	364	429	500	527	534
		HC	613	557	477	383	377	438	500	532	539
	FU	LC	642	576	476	381	371	431	516	555	578
		HC	632	570	480	384	377	437	509	536	542
Maximum	BL	LC	798	719	651	594	571	601	650	698	766
		HC	790	703	651	597	572	600	652	709	773
	FU	LC	827	734	653	600	577	604	656	714	787
		HC	849	750	671	614	586	612	664	726	802

Table E-12: Pentacam OS Vertical (-Inferior to +Superior)

	Visit Type	Lens Only	M4	M3	M2	M1	0	1	2	3	4
N	BL	LC	8	8	8	8	8	8	8	8	8
		HC	8	8	8	8	8	8	8	8	7
	FU	LC	8	8	8	8	8	8	8	8	7
		HC	8	8	8	8	8	8	8	8	8
Missing	BL	LC	0	0	0	0	0	0	0	0	0
		HC	0	0	0	0	0	0	0	0	1
	FU	LC	0	0	0	0	0	0	0	0	1
		HC	0	0	0	0	0	0	0	0	0
Mean	BL	LC	710	628	557	508	503	535	586	641	704
		HC	703	624	554	507	503	536	584	640	691
	FU	LC	728	638	563	515	510	540	590	649	699
		HC	733	641	567	518	511	543	595	652	718
Median	BL	LC	723	628	553	507	506	533	574	624	706
		HC	719	616	545	509	508	534	574	627	701
	FU	LC	746	637	560	515	510	533	576	634	684
		HC	742	638	558	514	511	533	575	630	713
Standard deviation	BL	LC	63.3	60.3	69.6	75.3	69.9	61.6	65.1	68.1	68.9
		HC	61.6	55.5	66.8	74.3	69.0	60.6	63.3	67.2	62.1
	FU	LC	61.1	60.3	71.9	75.9	70.0	63.7	65.4	69.5	65.1
		HC	59.4	61.4	75.8	81.4	76.1	67.0	68.1	67.8	73.0
Minimum	BL	LC	609	548	458	373	378	446	521	573	614
		HC	599	544	458	372	378	443	518	563	610
	FU	LC	623	556	461	381	388	451	523	576	630
		HC	629	558	461	372	372	444	530	585	629
Maximum	BL	LC	808	721	654	608	596	611	700	765	800
		HC	795	708	651	602	592	610	693	761	791
	FU	LC	815	728	664	621	609	625	699	774	812
		HC	825	739	674	630	617	634	711	768	818

Table E-13: Pentacam OD Oblique (-Inferior Temporal to +Superior Nasal)

	Visit Type	Lens Only	M4	M3	M2	M1	0	1	2	3	4
N	BL	LC	8	8	8	8	8	8	8	8	8
		HC	8	8	8	8	8	8	8	8	8
	FU	LC	8	8	8	8	8	8	8	8	8
		HC	8	8	8	8	8	8	8	8	8
Missing	BL	LC	0	0	0	0	0	0	0	0	0
		HC	0	0	0	0	0	0	0	0	0
	FU	LC	0	0	0	0	0	0	0	0	0
		HC	0	0	0	0	0	0	0	0	0
Mean	BL	LC	695	603	526	481	483	521	571	625	686
		HC	691	600	524	481	483	521	570	623	683
	FU	LC	714	611	528	486	489	526	576	631	693
		HC	714	614	536	490	489	527	581	633	695
Median	BL	LC	698	596	520	483	495	522	567	616	688
		HC	685	587	514	482	496	520	567	618	686
	FU	LC	712	594	525	491	502	523	570	628	701
		HC	712	593	525	489	499	521	567	620	694
Standard deviation	BL	LC	42.7	43.3	50.5	61.1	64.8	56.8	50.9	57.8	74.4
		HC	50.5	49.4	55.5	62.7	63.2	53.9	49.0	55.3	65.9
	FU	LC	47.6	45.9	53.9	64.5	64.7	54.8	49.7	60.5	76.3
		HC	45.7	49.3	56.9	66.5	69.3	59.0	52.4	60.3	73.0
Minimum	BL	LC	626	555	452	371	364	423	504	566	585
		HC	619	548	438	370	377	437	511	555	577
	FU	LC	656	557	447	371	371	427	509	548	565
		HC	655	562	461	382	377	435	522	557	578
Maximum	BL	LC	758	663	615	577	571	601	648	718	805
		HC	772	670	619	580	572	598	644	698	771
	FU	LC	789	681	615	583	577	601	646	722	805
		HC	798	693	634	596	586	610	656	724	799

Table E-14: Pentacam OS Oblique (-Inferior Temporal to +Superior Nasal)

	Visit Type	Lens Only	M4	M3	M2	M1	0	1	2	3	4
N	BL	LC	8	8	8	8	8	8	8	8	8
		HC	8	8	8	8	8	8	8	8	8
	FU	LC	8	8	8	8	8	8	8	8	8
		HC	8	8	8	8	8	8	8	8	8
Missing	BL	LC	0	0	0	0	0	0	0	0	0
		HC	0	0	0	0	0	0	0	0	0
	FU	LC	0	0	0	0	0	0	0	0	0
		HC	0	0	0	0	0	0	0	0	0
Mean	BL	LC	690	600	531	497	503	536	579	630	692
		HC	686	599	530	496	503	537	578	627	692
	FU	LC	697	603	536	505	510	542	588	643	707
		HC	697	607	539	505	511	543	591	646	711
Median	BL	LC	695	594	519	493	506	537	574	625	699
		HC	675	587	522	497	508	537	571	618	690
	FU	LC	709	594	524	502	510	538	581	636	716
		HC	698	592	522	501	511	539	581	635	715
Standard deviation	BL	LC	43.3	55.1	66.3	72.3	69.9	62.4	59.8	63.5	74.0
		HC	45.8	56.6	66.4	72.0	69.0	59.2	56.7	61.0	71.1
	FU	LC	49.1	58.6	66.3	71.9	70.0	62.3	57.9	60.2	71.4
		HC	54.8	67.3	75.6	79.3	76.1	67.5	63.9	65.8	75.9
Minimum	BL	LC	627	541	426	365	378	438	513	556	591
		HC	624	535	420	362	378	444	519	564	605
	FU	LC	622	531	443	378	388	450	528	573	612
		HC	618	539	426	362	372	436	521	573	615
Maximum	BL	LC	747	681	622	595	596	613	667	722	794
		HC	746	685	619	592	592	609	666	725	796
	FU	LC	759	685	635	610	609	626	672	732	809
		HC	776	714	648	619	617	633	683	740	817

Table E-15: Pentacam OD Oblique (-Superior Temporal to +Inferior Nasal)

	Visit Type	Lens Only	M4	M3	M2	M1	0	1	2	3	4
N	BL	LC	8	8	8	8	8	8	8	8	8
		HC	8	8	8	8	8	8	8	8	8
	FU	LC	8	8	8	8	8	8	8	8	8
		HC	8	8	8	8	8	8	8	8	8
Missing	BL	LC	0	0	0	0	0	0	0	0	0
		HC	0	0	0	0	0	0	0	0	0
	FU	LC	0	0	0	0	0	0	0	0	0
		HC	0	0	0	0	0	0	0	0	0
Mean	BL	LC	666	603	547	500	483	505	558	626	705
		HC	666	604	546	499	483	507	557	623	705
	FU	LC	678	610	551	505	489	514	567	639	726
		HC	680	613	553	505	489	512	566	638	725
Median	BL	LC	671	602	551	504	495	508	555	622	705
		HC	664	597	546	504	496	508	557	623	708
	FU	LC	675	602	548	506	502	513	564	631	721
		HC	673	605	549	504	499	511	554	627	724
Standard deviation	BL	LC	65.4	57.1	55.0	59.8	64.8	60.8	49.9	45.5	52.9
		HC	63.6	57.5	57.0	61.6	63.2	60.4	55.6	53.6	57.8
	FU	LC	66.8	60.4	57.4	61.0	64.7	60.7	54.0	56.5	65.2
		HC	69.0	62.4	60.9	65.1	69.3	68.0	61.9	59.5	62.0
Minimum	BL	LC	577	534	480	406	364	390	484	561	606
		HC	582	534	473	412	377	397	470	561	608
	FU	LC	576	525	472	411	371	402	498	571	621
		HC	581	530	465	413	377	401	492	571	629
Maximum	BL	LC	767	681	629	585	571	593	632	695	784
		HC	754	683	632	587	572	597	639	701	789
	FU	LC	788	701	636	591	577	600	642	742	845
		HC	791	705	643	599	586	611	655	742	834

Table E-16: Pentacam OS Oblique (-Superior Temporal to +Inferior Nasal)

	Visit Type	Lens Only	M4	M3	M2	M1	0	1	2	3	4
N	BL	LC	8	8	8	8	8	8	8	8	8
		HC	8	8	8	8	8	8	8	8	8
	FU	LC	8	8	8	8	8	8	8	8	8
		HC	8	8	8	8	8	8	8	8	8
Missing	BL	LC	0	0	0	0	0	0	0	0	0
		HC	0	0	0	0	0	0	0	0	0
	FU	LC	0	0	0	0	0	0	0	0	0
		HC	0	0	0	0	0	0	0	0	0
Mean	BL	LC	670	612	562	520	503	521	570	635	711
		HC	674	616	564	522	503	520	565	627	706
	FU	LC	684	622	569	527	510	528	576	645	727
		HC	690	627	573	529	511	531	583	651	735
Median	BL	LC	662	596	550	515	506	524	566	632	718
		HC	664	600	554	518	508	526	568	629	720
	FU	LC	678	605	553	516	510	528	572	636	725
		HC	676	606	556	519	511	530	575	643	740
Standard deviation	BL	LC	74.2	71.0	64.5	62.8	69.9	72.1	62.2	48.4	49.9
		HC	69.7	66.5	63.6	63.4	69.0	72.1	67.7	56.6	57.8
	FU	LC	69.9	68.1	65.6	65.5	70.0	72.5	66.1	52.6	49.4
		HC	78.8	74.8	69.1	68.4	76.1	75.8	62.7	48.1	49.0
Minimum	BL	LC	570	532	489	426	378	394	483	574	632
		HC	585	547	482	419	378	393	464	556	624
	FU	LC	583	539	498	429	388	401	475	582	676
		HC	594	553	492	422	372	399	503	594	666
Maximum	BL	LC	790	737	662	604	596	614	654	715	799
		HC	788	736	664	603	592	607	655	707	794
	FU	LC	788	735	667	619	609	626	667	731	820
		HC	823	758	677	626	617	634	673	736	825

Appendix F

Descriptive Statistics: Corneal Epithelial Thickness Measurements

Table F-1: Spectralis OD Horizontal (-Temporal to +Nasal). In all tables in this appendix, “M” refers to negative location values.

	Visit Type	Lens Only	M4	M3	M2	M1	0	1	2	3	4
N	BL	LC	8	8	8	8	8	8	8	8	8
		HC	8	8	8	8	8	8	8	8	8
	FU	LC	8	8	8	8	8	8	8	8	8
		HC	7	8	8	8	8	8	8	8	8
Missing	BL	LC	0	0	0	0	0	0	0	0	0
		HC	0	0	0	0	0	0	0	0	0
	FU	LC	0	0	0	0	0	0	0	0	0
		HC	1	0	0	0	0	0	0	0	0
Mean	BL	LC	63.7	60.4	62.5	57.4	56.0	63.1	67.5	73.7	65.3
		HC	66.2	65.5	67.9	60.0	57.1	63.5	68.6	69.7	68.2
	FU	LC	71.1	61.2	59.0	53.7	60.6	69.1	69.1	73.7	70.1
		HC	71.6	60.3	62.4	62.7	58.4	63.8	71.0	69.2	68.4
Median	BL	LC	61.8	65.1	64.4	55.3	55.6	63.0	64.3	72.0	62.8
		HC	66.2	65.8	63.9	62.5	59.1	62.9	68.0	66.4	68.5
	FU	LC	71.1	66.6	64.2	51.0	62.7	68.4	64.7	76.7	69.1
		HC	70.7	56.5	64.7	62.6	60.0	63.3	70.7	67.0	70.7
Standard deviation	BL	LC	10.1	9.81	16.5	8.32	6.49	8.00	9.14	9.47	11.4
		HC	9.51	7.80	10.5	9.08	6.10	11.9	7.63	6.74	9.42
	FU	LC	9.38	15.6	14.5	9.79	7.33	6.39	6.75	7.03	10.9
		HC	9.82	12.7	13.4	7.04	7.91	9.18	8.05	7.33	9.27
Minimum	BL	LC	54.0	41.3	35.1	50.2	49.0	49.5	52.4	63.9	53.1
		HC	54.3	54.7	58.4	50.4	50.0	44.4	56.5	64.4	55.0
	FU	LC	55.1	34.7	29.6	35.8	50.0	62.3	63.6	63.9	53.9
		HC	54.6	41.3	40.0	50.5	50.0	50.6	62.2	59.3	54.4

Maximum	BL	LC	81.8	69.3	91.8	72.5	62.5	79.1	81.1	91.1	83.2
		HC	81.8	78.9	90.6	76.4	63.0	76.0	77.5	81.3	81.8
	FU	LC	84.7	79.3	77.4	65.9	71.9	76.4	78.1	80.1	93.6
		HC	82.5	78.9	77.4	75.7	71.9	74.5	81.1	81.3	81.1
Shapiro-Wilk W	BL	LC	0.892	0.845	0.896	0.828	0.751	0.812	0.929	0.874	0.894
		HC	0.936	0.958	0.752	0.854	0.784	0.884	0.919	0.689	0.923
	FU	LC	0.964	0.796	0.897	0.898	0.864	0.779	0.715	0.804	0.796
		HC	0.938	0.940	0.862	0.929	0.875	0.886	0.804	0.840	0.902
Shapiro-Wilk p	BL	LC	0.246	0.084	0.264	0.057	0.008	0.038	0.509	0.165	0.253
		HC	0.569	0.794	0.009	0.105	0.019	0.204	0.421	0.002	0.454
	FU	LC	0.849	0.026	0.274	0.275	0.133	0.017	0.003	0.032	0.026
		HC	0.623	0.610	0.124	0.509	0.167	0.214	0.031	0.076	0.303

Table F-2: Spectralis OS Horizontal (-Temporal to +Nasal)

	Visit Type	Lens Only	M4	M3	M2	M1	0	1	2	3	4
N	BL	LC	7	8	8	8	8	8	8	8	8
		HC	8	8	8	8	8	8	8	8	8
	FU	LC	8	8	8	8	8	8	8	8	8
		HC	8	8	8	8	8	8	8	8	8
Missing	BL	LC	1	0	0	0	0	0	0	0	0
		HC	0	0	0	0	0	0	0	0	0
	FU	LC	0	0	0	0	0	0	0	0	0
		HC	0	0	0	0	0	0	0	0	0
Mean	BL	LC	69.3	62.8	57.9	63.3	58.0	64.9	68.2	68.8	72.2
		HC	65.7	62.8	61.1	58.8	57.6	65.2	60.5	72.7	66.1
	FU	LC	66.0	61.9	56.2	64.5	59.7	59.8	65.5	72.2	68.5
		HC	68.0	60.4	59.9	62.6	60.7	62.3	60.2	65.6	65.0
Median	BL	LC	71.1	60.3	64.3	63.3	59.2	68.2	73.7	66.4	68.7
		HC	67.5	66.1	63.6	57.2	51.0	63.2	63.4	73.1	62.4
Median	FU	LC	68.8	66.3	57.7	63.2	60.4	57.0	64.6	66.6	68.6
		HC	67.8	60.5	64.6	57.4	55.6	63.1	64.2	66.2	67.4

Standard deviation	BL	LC	6.87	18.7	12.7	11.5	8.29	11.9	11.6	5.76	14.3
		HC	8.96	13.3	9.16	14.4	11.1	6.93	8.35	7.83	12.0
	FU	LC	5.82	7.28	14.8	11.9	10.9	11.6	8.23	11.5	14.5
		HC	15.3	12.4	10.7	15.4	14.1	14.2	10.3	11.7	10.1
Minimum	BL	LC	56.0	39.9	38.6	47.4	47.9	49.1	50.9	63.7	55.2
		HC	55.3	39.8	39.6	37.0	50.0	57.0	50.4	63.3	54.8
	FU	LC	55.7	52.1	27.7	39.0	47.9	48.3	51.3	64.8	53.9
		HC	53.1	39.8	41.2	48.6	49.2	38.0	39.5	52.2	54.4
Maximum	BL	LC	76.9	93.1	73.6	81.8	71.9	76.6	77.9	79.7	97.2
		HC	76.9	80.5	70.5	81.8	75.0	76.0	73.6	80.6	83.2
	FU	LC	70.4	69.3	76.6	75.6	81.3	76.0	76.6	94.6	95.0
		HC	99.7	80.1	73.6	88.0	87.5	84.9	73.6	88.3	83.4
Shapiro-Wilk W	BL	LC	0.908	0.951	0.862	0.927	0.922	0.834	0.789	0.765	0.926
		HC	0.870	0.957	0.713	0.958	0.698	0.818	0.875	0.763	0.836
	FU	LC	0.708	0.766	0.919	0.803	0.891	0.828	0.901	0.653	0.890
		HC	0.864	0.978	0.908	0.849	0.825	0.967	0.864	0.918	0.863
Shapiro-Wilk p	BL	LC	0.382	0.719	0.127	0.490	0.443	0.066	0.022	0.012	0.478
		HC	0.149	0.777	0.003	0.790	0.002	0.045	0.169	0.011	0.068
	FU	LC	0.003	0.012	0.426	0.031	0.240	0.057	0.295	< .001	0.234
		HC	0.131	0.955	0.342	0.094	0.053	0.870	0.133	0.416	0.129

Table F-3: Spectralis OD Vertical (-Inferior to +Superior)

	Visit Type	Lens Only	M4	M3	M2	M1	0	1	2	3	4
N	BL	LC	8	8	8	8	8	8	8	8	8
		HC	8	8	8	8	8	8	8	8	8
	FU	LC	8	8	8	8	8	8	8	8	7
		HC	8	8	8	8	8	8	8	8	7
Missing	BL	LC	0	0	0	0	0	0	0	0	0
		HC	0	0	0	0	0	0	0	0	0

	FU	LC	0	0	0	0	0	0	0	0	1
		HC	0	0	0	0	0	0	0	0	1
Mean	BL	LC	63.5	62.3	61.7	63.5	56.2	62.9	65.5	71.5	64.6
		HC	63.9	65.4	61.7	55.1	57.3	59.8	64.7	65.0	61.7
	FU	LC	71.1	67.2	63.5	62.6	59.6	62.4	64.8	67.2	62.1
		HC	70.0	67.8	61.5	60.5	61.2	62.3	66.8	70.2	63.1
Median	BL	LC	64.1	66.0	63.6	63.7	53.3	63.1	64.1	71.5	65.0
		HC	63.7	67.1	64.0	50.9	59.9	62.8	63.3	65.5	57.0
	FU	LC	69.6	66.8	64.9	62.8	62.2	62.4	63.8	66.0	66.5
		HC	70.9	67.0	64.7	63.1	62.5	62.8	69.4	67.7	65.6
Standard deviation	BL	LC	11.9	9.98	9.90	9.83	8.24	9.37	8.13	8.41	8.33
		HC	7.98	11.3	9.24	9.60	6.02	8.83	7.55	10.8	9.47
	FU	LC	9.55	13.5	15.2	8.78	5.50	9.22	8.95	10.6	10.6
		HC	8.54	12.5	13.2	9.76	7.38	9.93	12.5	13.7	6.82
Minimum	BL	LC	45.8	42.3	50.9	49.7	49.0	49.7	52.1	59.6	54.8
		HC	54.4	54.1	51.6	48.3	50.0	38.0	51.9	51.4	54.8
	FU	LC	56.6	43.2	37.6	50.9	50.5	49.9	47.8	53.5	41.0
		HC	55.5	53.0	38.6	50.5	50.4	49.1	40.2	53.0	54.8
Maximum	BL	LC	85.8	74.3	77.8	76.0	71.9	75.0	77.3	82.8	80.1
		HC	72.9	88.2	78.1	76.0	62.9	63.8	76.0	87.1	81.8
	FU	LC	83.9	81.6	80.6	74.2	64.6	75.8	76.9	80.7	71.3
		HC	84.1	91.1	76.9	79.1	71.9	75.8	77.1	89.4	70.4
Shapiro-Wilk W	BL	LC	0.961	0.900	0.889	0.878	0.861	0.868	0.868	0.926	0.935
		HC	0.856	0.841	0.872	0.708	0.765	0.467	0.891	0.856	0.777
	FU	LC	0.960	0.912	0.922	0.888	0.714	0.889	0.844	0.906	0.819
		HC	0.942	0.924	0.937	0.833	0.862	0.908	0.809	0.921	0.853
Shapiro-Wilk p	BL	LC	0.820	0.286	0.229	0.182	0.123	0.143	0.145	0.479	0.559
		HC	0.109	0.078	0.158	0.003	0.012	< .001	0.242	0.111	0.016
	FU	LC	0.806	0.370	0.447	0.222	0.003	0.228	0.082	0.328	0.062
		HC	0.629	0.461	0.578	0.064	0.127	0.337	0.036	0.440	0.130

Table F-4: Spectralis OS Vertical (-Inferior to +Superior)

	Visit Type	Lens Only	M4	M3	M2	M1	0	1	2	3	4
N	BL	LC	8	8	8	8	8	8	8	8	7
		HC	7	7	7	7	7	7	7	7	7
	FU	LC	8	8	8	8	8	8	8	8	8
		HC	8	8	8	8	8	8	8	8	8
Missing	BL	LC	0	0	0	0	0	0	0	0	1
		HC	1	1	1	1	1	1	1	1	1
	FU	LC	0	0	0	0	0	0	0	0	0
		HC	0	0	0	0	0	0	0	0	0
Mean	BL	LC	63.3	63.4	60.7	59.2	60.4	60.9	66.4	70.1	63.9
		HC	60.3	67.7	64.7	62.8	61.2	66.4	69.6	67.1	60.3
	FU	LC	64.9	61.3	64.0	64.5	59.2	62.7	64.1	67.9	64.9
		HC	63.2	67.2	61.3	61.7	60.6	65.3	65.7	68.2	64.1
Median	BL	LC	61.3	66.3	62.0	55.5	62.5	62.9	64.5	66.4	63.5
		HC	57.7	67.2	64.8	63.3	60.4	63.6	65.0	65.9	56.4
	FU	LC	66.3	60.6	64.7	63.1	53.6	63.0	64.2	66.0	68.1
		HC	62.7	67.5	65.1	57.9	57.2	68.8	64.7	66.7	66.6
Standard deviation	BL	LC	9.33	5.69	12.3	11.3	7.27	4.40	7.96	9.65	9.11
		HC	11.2	11.0	10.9	7.51	11.5	9.17	6.64	7.86	6.27
	FU	LC	11.7	8.16	13.0	11.8	11.2	9.26	11.2	10.8	6.30
		HC	10.1	10.0	13.9	12.1	13.4	16.8	12.7	4.50	7.24
Minimum	BL	LC	54.3	52.5	40.9	48.6	50.0	50.7	51.4	63.3	55.6
		HC	41.3	52.0	50.6	49.6	50.0	50.6	63.7	54.4	54.5
	FU	LC	44.2	52.0	39.5	50.8	50.0	49.7	50.5	53.0	54.7
		HC	52.0	45.7	37.6	49.4	47.9	35.8	38.7	64.3	55.6
Maximum	BL	LC	81.9	68.1	77.6	76.2	71.9	63.2	77.1	92.9	80.4
		HC	72.7	83.0	78.7	75.6	84.4	75.6	78.0	79.8	69.0
	FU	LC	83.0	75.5	78.4	86.4	76.6	75.5	87.5	91.9	70.1
		HC	78.4	79.8	77.9	75.9	84.4	88.0	79.7	76.1	75.0

Shapiro-Wilk W	BL	LC	0.864	0.808	0.970	0.822	0.860	0.599	0.903	0.647	0.879
		HC	0.915	0.945	0.893	0.828	0.849	0.868	0.767	0.914	0.813
	FU	LC	0.953	0.907	0.918	0.888	0.784	0.888	0.818	0.720	0.763
		HC	0.869	0.825	0.921	0.794	0.867	0.947	0.840	0.802	0.875
Shapiro-Wilk p	BL	LC	0.130	0.035	0.900	0.049	0.119	< .001	0.309	< .001	0.223
		HC	0.433	0.685	0.291	0.077	0.121	0.180	0.019	0.427	0.055
	FU	LC	0.746	0.330	0.413	0.226	0.019	0.225	0.045	0.004	0.011
		HC	0.148	0.053	0.435	0.025	0.140	0.682	0.075	0.030	0.170

Table F-5: Spectralis OD Oblique (-Inferior Temporal to +Superior Nasal)

	Visit Type	Lens Only	M4	M3	M2	M1	0	1	2	3	4
N	BL	LC	8	7	8	8	8	8	8	8	8
		HC	8	7	8	8	8	8	8	8	8
	FU	LC	8	8	8	8	8	8	8	8	7
		HC	8	8	8	8	8	8	8	8	8
Missing	BL	LC	0	1	0	0	0	0	0	0	0
		HC	0	1	0	0	0	0	0	0	0
	FU	LC	0	0	0	0	0	0	0	0	1
		HC	0	0	0	0	0	0	0	0	0
Mean	BL	LC	62.5	60.9	60.2	58.0	63.1	68.9	65.3	72.6	66.6
		HC	63.9	60.5	60.1	56.3	56.2	63.9	71.8	69.0	66.1
	FU	LC	63.6	60.8	61.1	57.9	64.7	70.7	70.0	72.2	67.8
		HC	62.1	64.2	55.0	60.1	58.6	62.7	68.0	73.0	70.9
Median	BL	LC	60.2	64.6	58.0	56.1	62.9	72.9	64.6	73.3	67.9
		HC	65.9	54.0	58.9	55.2	59.4	63.4	70.1	66.2	63.0
	FU	LC	66.2	60.9	63.3	56.6	63.0	73.8	73.8	73.8	67.7
		HC	63.9	61.0	51.3	62.4	58.9	63.4	66.5	71.4	69.4
Standard deviation	BL	LC	15.5	6.90	10.3	9.09	7.01	8.53	10.9	11.4	8.12
		HC	11.1	9.41	9.54	11.5	7.50	10.1	9.27	7.56	12.4
	FU	LC	10.8	10.1	12.4	13.1	7.86	7.54	15.1	10.9	7.11
		HC	15.2	12.8	14.3	9.17	8.49	10.7	15.5	9.69	9.07

Minimum	BL	LC	36.6	51.1	49.5	50.3	49.5	52.2	42.1	53.0	54.6
		HC	45.1	53.0	51.1	37.8	43.8	49.5	63.4	63.3	54.9
	FU	LC	45.1	46.2	41.2	37.9	50.0	54.8	38.7	52.4	55.5
		HC	41.2	51.5	37.9	49.6	50.0	39.6	37.6	61.3	54.5
Maximum	BL	LC	85.3	67.5	76.9	76.0	75.4	76.0	76.4	91.9	79.7
		HC	78.3	76.6	77.8	75.7	63.0	75.4	89.1	82.4	85.7
	FU	LC	78.3	74.3	79.1	76.0	75.0	76.0	89.5	87.0	79.7
		HC	88.1	83.9	81.1	76.0	75.0	74.9	92.5	90.4	83.4
Shapiro-Wilk W	BL	LC	0.963	0.850	0.882	0.821	0.833	0.819	0.826	0.975	0.913
		HC	0.963	0.799	0.841	0.966	0.845	0.891	0.843	0.726	0.827
	FU	LC	0.962	0.919	0.962	0.933	0.914	0.737	0.896	0.958	0.905
		HC	0.963	0.861	0.931	0.890	0.880	0.826	0.909	0.928	0.947
Shapiro-Wilk p	BL	LC	0.839	0.122	0.198	0.047	0.063	0.046	0.054	0.935	0.372
		HC	0.835	0.040	0.077	0.861	0.085	0.238	0.081	0.004	0.056
	FU	LC	0.832	0.419	0.832	0.548	0.386	0.006	0.268	0.792	0.364
		HC	0.837	0.123	0.529	0.232	0.189	0.054	0.348	0.501	0.680

Table F-6: Spectralis OS Oblique (-Inferior Temporal to +Superior Nasal)

	Visit Type	Lens Only	M4	M3	M2	M1	0	1	2	3	4
N	BL	LC	8	8	8	8	8	8	8	8	8
		HC	7	8	8	8	8	8	8	8	8
	FU	LC	8	8	8	8	8	8	8	8	8
		HC	8	8	8	8	8	8	8	8	8
Missing	BL	LC	0	0	0	0	0	0	0	0	0
		HC	1	0	0	0	0	0	0	0	0
	FU	LC	0	0	0	0	0	0	0	0	0
		HC	0	0	0	0	0	0	0	0	0
Mean	BL	LC	56.3	58.7	58.7	61.2	57.0	60.2	63.7	70.1	69.3
		HC	65.1	66.9	62.1	59.6	57.6	60.0	68.9	69.1	70.1
	FU	LC	60.1	62.6	63.2	60.5	59.0	62.7	65.6	72.7	65.5
		HC	64.4	56.0	62.3	54.6	57.4	61.2	65.4	68.9	62.5

Median	BL	LC	56.3	56.9	56.4	62.6	50.4	63.1	64.1	66.8	69.1
		HC	69.5	66.0	64.4	54.9	50.2	57.0	70.9	66.6	68.6
	FU	LC	56.3	65.3	63.9	62.2	53.3	62.4	64.4	66.7	67.5
		HC	66.0	53.0	63.3	50.4	56.4	62.9	64.3	66.5	58.8
Standard deviation	BL	LC	9.54	12.9	12.8	8.00	10.4	10.6	6.66	10.6	8.90
		HC	10.6	15.2	10.6	13.0	11.5	12.7	9.52	10.1	9.34
	FU	LC	6.70	11.5	9.64	11.3	16.5	13.4	10.3	12.8	6.97
		HC	8.94	12.4	20.3	11.0	13.6	12.5	8.82	9.48	9.65
Minimum	BL	LC	41.9	39.7	38.5	50.4	48.8	40.1	52.8	53.6	53.9
		HC	41.2	41.0	49.4	50.4	49.5	50.4	51.1	63.3	55.3
	FU	LC	54.3	47.2	48.1	45.4	37.5	37.9	50.5	65.5	55.3
		HC	53.1	37.3	24.0	37.0	37.5	37.9	50.4	63.3	54.9
Maximum	BL	LC	68.5	78.9	76.7	75.6	75.4	76.0	77.0	89.7	81.2
		HC	70.2	93.0	77.2	88.4	75.5	88.0	77.3	93.9	81.7
	FU	LC	70.1	79.7	76.3	75.6	87.5	75.9	87.9	103	75.2
		HC	76.9	80.1	90.2	72.5	82.8	76.0	77.9	91.9	82.2
Shapiro-Wilk W	BL	LC	0.934	0.985	0.948	0.845	0.771	0.845	0.871	0.925	0.903
		HC	0.568	0.938	0.894	0.748	0.705	0.756	0.826	0.557	0.940
	FU	LC	0.769	0.941	0.921	0.912	0.915	0.888	0.734	0.629	0.910
		HC	0.906	0.866	0.952	0.919	0.923	0.902	0.878	0.592	0.822
Shapiro-Wilk p	BL	LC	0.550	0.983	0.694	0.086	0.014	0.085	0.154	0.471	0.310
		HC	< .001	0.588	0.253	0.008	0.003	0.010	0.054	< .001	0.610
	FU	LC	0.013	0.618	0.441	0.371	0.393	0.223	0.005	< .001	0.353
		HC	0.324	0.138	0.728	0.424	0.457	0.303	0.179	< .001	0.049

Table F-7: Spectralis OD Oblique (-Superior Temporal to +Inferior Nasal)

	Visit Type	Lens Only	M4	M3	M2	M1	0	1	2	3	4
N	BL	LC	8	8	8	8	8	8	8	8	8
		HC	8	8	8	8	8	8	8	8	8
	FU	LC	8	8	8	8	8	8	8	8	8
		HC	7	7	7	7	7	7	7	7	7

Missing	BL	LC	0	0	0	0	0	0	0	0	0	0
		HC	0	0	0	0	0	0	0	0	0	0
	FU	LC	0	0	0	0	0	0	0	0	0	0
		HC	1	1	1	1	1	1	1	1	1	1
Mean	BL	LC	70.7	70.7	62.3	61.0	60.6	61.6	63.5	70.4	65.5	
		HC	67.3	69.9	63.0	60.7	55.8	60.4	65.5	67.8	63.0	
	FU	LC	67.2	70.5	57.7	61.1	56.6	64.1	61.5	70.4	65.3	
		HC	65.2	63.7	63.3	64.7	60.4	65.1	69.6	71.0	72.3	
Median	BL	LC	68.5	70.5	64.0	62.9	62.2	63.0	64.8	68.6	62.9	
		HC	68.1	66.6	64.1	62.8	55.2	60.0	64.7	66.6	67.1	
	FU	LC	68.3	71.7	63.0	62.9	50.0	63.4	64.4	67.8	67.1	
		HC	67.8	66.1	64.7	63.1	62.5	63.6	65.4	67.6	71.3	
Standard deviation	BL	LC	9.94	10.6	4.14	12.2	7.31	7.77	13.6	7.75	11.2	
		HC	12.4	7.31	7.47	6.33	6.49	10.3	12.0	15.0	10.3	
	FU	LC	6.60	9.89	9.60	10.3	10.3	14.3	15.2	18.5	6.98	
		HC	10.9	4.99	2.82	8.73	8.82	8.56	12.0	11.7	11.5	
Minimum	BL	LC	55.1	50.7	52.7	37.4	50.0	50.5	39.2	56.4	54.6	
		HC	54.4	63.3	52.7	50.6	49.1	50.0	51.8	44.5	44.2	
	FU	LC	52.3	53.0	38.8	38.2	49.0	38.0	39.8	43.2	54.6	
		HC	54.2	53.0	57.6	50.3	50.0	51.0	53.0	55.7	55.3	
Maximum	BL	LC	85.8	82.5	65.3	75.9	71.9	75.5	84.1	79.4	82.5	
		HC	85.4	83.0	78.1	69.4	62.5	76.0	91.0	91.1	73.2	
	FU	LC	75.5	80.2	65.2	75.1	75.0	82.2	88.0	105	74.6	
		HC	82.8	67.5	65.2	75.9	75.8	76.0	91.0	91.2	84.9	
Shapiro-Wilk W	BL	LC	0.966	0.908	0.712	0.890	0.851	0.863	0.933	0.894	0.857	
		HC	0.861	0.740	0.891	0.870	0.737	0.880	0.838	0.937	0.869	
	FU	LC	0.748	0.873	0.793	0.744	0.757	0.933	0.832	0.947	0.945	
		HC	0.880	0.731	0.752	0.862	0.882	0.871	0.936	0.906	0.922	
Shapiro-Wilk p	BL	LC	0.868	0.338	0.003	0.232	0.099	0.128	0.545	0.256	0.112	
		HC	0.124	0.006	0.240	0.149	0.006	0.189	0.072	0.586	0.148	
	FU	LC	0.008	0.161	0.024	0.007	0.010	0.540	0.062	0.678	0.662	
		HC	0.226	0.008	0.013	0.157	0.233	0.189	0.602	0.371	0.486	

Table F-8: Spectralis OS Oblique (-Superior Temporal to +Inferior Nasal)

	Visit Type	Lens Only	M4	M3	M2	M1	0	1	2	3	4
N	BL	LC	8	8	8	8	8	8	8	8	8
		HC	8	8	8	8	8	8	8	8	8
	FU	LC	8	8	8	8	8	8	8	8	8
		HC	8	8	8	8	8	8	8	8	8
Missing	BL	LC	0	0	0	0	0	0	0	0	0
		HC	0	0	0	0	0	0	0	0	0
	FU	LC	0	0	0	0	0	0	0	0	0
		HC	0	0	0	0	0	0	0	0	0
Mean	BL	LC	68.8	71.9	67.8	64.4	59.8	63.1	66.4	72.6	68.1
		HC	68.2	70.6	63.1	58.0	56.8	63.8	61.4	67.8	68.7
	FU	LC	60.9	69.2	65.1	61.3	57.2	57.9	61.7	66.9	65.6
		HC	65.2	69.0	62.8	65.7	53.7	60.9	71.3	76.7	74.1
Median	BL	LC	68.7	66.7	71.3	68.6	60.4	63.5	64.8	75.4	69.7
		HC	68.0	65.9	64.1	56.3	50.5	62.1	64.7	67.0	69.7
	FU	LC	55.7	66.5	63.6	62.7	54.4	55.9	64.2	66.3	68.5
		HC	64.4	66.3	64.0	63.0	50.0	61.4	76.4	79.4	70.5
Standard deviation	BL	LC	8.87	9.43	11.0	13.9	9.90	12.2	10.7	9.30	13.1
		HC	12.3	16.4	6.19	13.6	14.1	11.7	8.19	6.94	9.58
	FU	LC	10.6	5.00	11.5	14.2	12.9	13.5	15.0	6.99	8.43
		HC	9.08	5.66	11.2	14.8	12.2	7.93	9.55	9.92	13.1
Minimum	BL	LC	55.0	65.7	52.1	38.0	49.0	36.2	52.1	54.3	54.1
		HC	54.5	52.2	52.2	38.2	37.2	50.6	51.7	54.9	54.6
	FU	LC	51.2	65.6	51.1	37.0	37.5	37.0	30.6	55.9	55.1
		HC	54.5	65.5	39.1	37.0	36.7	50.2	52.4	62.9	56.1
Maximum	BL	LC	83.3	92.7	77.3	75.6	75.5	76.1	78.5	81.3	92.5
		HC	83.9	98.8	73.6	76.0	78.1	84.9	74.3	79.1	82.2
	FU	LC	83.2	77.2	85.4	75.8	75.5	75.6	77.3	81.6	77.7
		HC	83.5	80.6	80.3	87.4	75.0	75.6	80.3	92.6	100

Shapiro-Wilk W	BL	LC	0.951	0.721	0.803	0.823	0.900	0.759	0.861	0.877	0.903
		HC	0.862	0.857	0.903	0.925	0.883	0.890	0.846	0.892	0.934
	FU	LC	0.806	0.697	0.901	0.898	0.940	0.928	0.852	0.778	0.887
		HC	0.924	0.675	0.760	0.909	0.828	0.882	0.826	0.941	0.922
Shapiro-Wilk p	BL	LC	0.718	0.004	0.031	0.050	0.286	0.010	0.124	0.177	0.306
		HC	0.126	0.113	0.304	0.471	0.200	0.232	0.087	0.246	0.557
	FU	LC	0.034	0.002	0.293	0.277	0.609	0.498	0.100	0.017	0.221
		HC	0.460	0.001	0.011	0.346	0.056	0.196	0.054	0.625	0.450

Appendix G

High and Low Contrast Visual Acuity

Table G-1: Best sphere over-refraction (BS O/R) and high contrast visual acuity results for participants 02-KC - 09-KC. Differences between follow-up and baseline for each lens and eye are in the column marked “FU-BL”.

Participant	Lens	Visit Type	Eye	BS O/R	Snellen Numerator	Snellen Denominator	Additional Optotypes	logMAR VA	FU-BL
02-KC	LC	BL	OD	+0.25	20	20	-1	0.02	0
02-KC	LC	FU	OD	+0.25	20	20	-1	0.02	
02-KC	LC	BL	OS	0.00	20	20	0	0	0.04
02-KC	LC	FU	OS	0.00	20	25	3	0.04	
02-KC	HC	BL	OD	+0.25	20	20	-1	0.02	0.02
02-KC	HC	FU	OD	+0.50	20	25	3	0.04	
02-KC	HC	BL	OS	-0.50	20	20	-3	0.06	-0.02
02-KC	HC	FU	OS	+0.50	20	20	-2	0.04	
04-KC	LC	BL	OD	-0.25	20	25	2	0.06	0
04-KC	LC	FU	OD	0.00	20	25	2	0.06	
04-KC	LC	BL	OS	0.00	20	30	2	0.14	-0.12
04-KC	LC	FU	OS	+0.25	20	20	-1	0.02	
04-KC	HC	BL	OD	0.00	20	20	-2	0.04	-0.04
04-KC	HC	FU	OD	0.00	20	20	0	0	
04-KC	HC	BL	OS	0.00	20	20	-1	0.02	0.02
04-KC	HC	FU	OS	+0.25	20	20	-2	0.04	
07-KC	LC	BL	OD	-0.25	20	25	2	0.06	-0.1
07-KC	LC	FU	OD	-0.25	20	20	2	-0.04	
07-KC	LC	BL	OS	+0.50	20	20	1	-0.02	0.06
07-KC	LC	FU	OS	0.00	20	20	-2	0.04	
07-KC	HC	BL	OD	-0.75	20	25	1	0.08	0
07-KC	HC	FU	OD	-0.75	20	25	1	0.08	
07-KC	HC	BL	OS	0.00	20	20	1	-0.02	0
07-KC	HC	FU	OS	0.00	20	20	1	-0.02	
09-KC	LC	BL	OD	0.00	20	30	2	0.14	0.02
09-KC	LC	FU	OD	-0.25	20	30	1	0.16	
09-KC	LC	BL	OS	0.00	20	20	2	-0.04	0.04
09-KC	LC	FU	OS	0.00	20	20	0	0	
09-KC	HC	BL	OD	0.00	20	30	2	0.14	0.18
09-KC	HC	FU	OD	0.00	20	40	-1	0.32	
09-KC	HC	BL	OS	0.00	20	15	-1	-0.1	0.06
09-KC	HC	FU	OS	0.00	20	20	2	-0.04	

Table G-2: Best sphere over-refraction (BS O/R) and high contrast visual acuity results for participants 11-KC - 15-KC. Differences between follow-up and baseline for each lens and eye are in the column marked “FU-BL”.

Participant	Lens	Visit Type	Eye	BS O/R	Snellen Numerator	Snellen Denominator	Additional Optotypes	logMAR VA	FU-BL
11-KC	LC	BL	OD	-0.50	20	20	2	-0.04	0
11-KC	LC	FU	OD	0.00	20	20	2	-0.04	
11-KC	LC	BL	OS	-0.25	20	30	2	0.14	-0.04
11-KC	LC	FU	OS	+0.50	20	25	0	0.1	
11-KC	HC	BL	OD	-0.50	20	20	2	-0.04	-0.04
11-KC	HC	FU	OD	-0.50	20	20	4	-0.08	
11-KC	HC	BL	OS	-0.25	20	30	2	0.14	-0.18
11-KC	HC	FU	OS	+0.75	20	20	2	-0.04	
13-KC	LC	BL	OD	0.00	20	15	-3	-0.06	0.06
13-KC	LC	FU	OD	0.00	20	20	0	0	
13-KC	LC	BL	OS	0.00	20	25	-3	0.16	-0.08
13-KC	LC	FU	OS	-0.25	20	25	1	0.08	
13-KC	HC	BL	OD	-0.25	20	25	-2	0.14	-0.08
13-KC	HC	FU	OD	-1.00	20	25	2	0.06	
13-KC	HC	BL	OS	0.00	20	30	1	0.16	-0.14
13-KC	HC	FU	OS	+1.50	20	20	-1	0.02	
14-KC	LC	BL	OD	0.00	20	40	-2	0.34	-0.06
14-KC	LC	FU	OD	0.00	20	40	1	0.28	
14-KC	LC	BL	OS	0.00	20	25	1	0.08	-0.02
14-KC	LC	FU	OS	0.00	20	25	2	0.06	
14-KC	HC	BL	OD	-0.50	20	40	2	0.26	0.08
14-KC	HC	FU	OD	0.00	20	40	-2	0.34	
14-KC	HC	BL	OS	0.00	20	20	-3	0.06	-0.04
14-KC	HC	FU	OS	-0.50	20	20	-1	0.02	
15-KC	LC	BL	OD	0.00	20	20	1	-0.02	0.06
15-KC	LC	FU	OD	+0.75	20	20	-2	0.04	
15-KC	LC	BL	OS	+0.25	20	20	-1	0.02	0.04
15-KC	LC	FU	OS	0.00	20	25	2	0.06	
15-KC	HC	BL	OD	+1.25	20	25	-1	0.12	0
15-KC	HC	FU	OD	0.00	20	25	-1	0.12	
15-KC	HC	BL	OS	0.00	20	25	-2	0.14	-0.08
15-KC	HC	FU	OS	+0.75	20	25	2	0.06	

Table G-3: Best sphere over-refraction (BS O/R) and low contrast visual acuity results for participants 02-KC - 09-KC. Differences between follow-up and baseline for each lens and eye are in the column marked “FU-BL”.

Participant	Lens	Visit Type	Eye	BS O/R	Snellen Numerator	Snellen Denominator	Additional Optotypes	logMAR VA	FU-BL
02-KC	LC	BL	OD	+0.25	20	60	-1	0.5	0.16
02-KC	LC	FU	OD	+0.25	20	100	2	0.66	
02-KC	LC	BL	OS	+0.25	20	50	-1	0.42	0.14
02-KC	LC	FU	OS	0.00	20	70	-1	0.56	
02-KC	HC	BL	OD	+0.25	20	70	-1	0.56	0
02-KC	HC	FU	OD	+0.50	20	70	-1	0.56	
02-KC	HC	BL	OS	-0.50	20	70	-2	0.58	-0.16
02-KC	HC	FU	OS	+0.50	20	50	-1	0.42	
04-KC	LC	BL	OD	-0.25	20	100	1	0.68	-0.24
04-KC	LC	FU	OD	0.00	20	60	2	0.44	
04-KC	LC	BL	OS	0.00	20	200	0	1	-0.6
04-KC	LC	FU	OS	+0.25	20	50	0	0.4	
04-KC	HC	BL	OD	0.00	20	50	-2	0.44	0.1
04-KC	HC	FU	OD	0.00	20	70	0	0.54	
04-KC	HC	BL	OS	0.00	20	60	-1	0.5	0.04
04-KC	HC	FU	OS	0.00	20	70	0	0.54	
07-KC	LC	BL	OD	-0.25	20	60	2	0.44	0.22
07-KC	LC	FU	OD	-0.25	20	100	2	0.66	
07-KC	LC	BL	OS	0.00	20	60	-2	0.52	0.16
07-KC	LC	FU	OS	0.00	20	100	1	0.68	
07-KC	HC	BL	OD	-0.75	20	60	1	0.46	0.18
07-KC	HC	FU	OD	-0.75	20	80	-2	0.64	
07-KC	HC	BL	OS	0.00	20	70	1	0.52	0.06
07-KC	HC	FU	OS	0.00	20	80	1	0.58	
09-KC	LC	BL	OD	0.00	20	200	0	1	-0.3
09-KC	LC	FU	OD	-0.25	20	100	0	0.7	
09-KC	LC	BL	OS	-0.50	20	70	-2	0.58	0.12
09-KC	LC	FU	OS	0.00	20	100	0	0.7	
09-KC	HC	BL	OD	0.00	20	80	0	0.6	0
09-KC	HC	FU	OD	0.00	20	80	0	0.6	
09-KC	HC	BL	OS	0.00	20	50	1	0.38	0.06
09-KC	HC	FU	OS	0.00	20	50	-2	0.44	

Table G-4: Best sphere over-refraction (BS O/R) and low contrast visual acuity results for participants 11-KC - 15-KC. Differences between follow-up and baseline for each lens and eye are in the column marked “FU-BL”.

Participant	Lens	Visit Type	Eye	BS O/R	Snellen Numerator	Snellen Denominator	Additional Optotypes	logMAR VA	FU-BL
11-KC	LC	BL	OD	-0.50	20	50	1	0.38	0.12
11-KC	LC	FU	OD	+0.25	20	60	-1	0.5	
11-KC	LC	BL	OS	-0.25	20	100	2	0.66	-0.14
11-KC	LC	FU	OS	0.00	20	60	-2	0.52	
11-KC	HC	BL	OD	-0.50	20	50	1	0.38	0.2
11-KC	HC	FU	OD	-0.50	20	80	1	0.58	
11-KC	HC	BL	OS	-0.25	20	100	2	0.66	0.04
11-KC	HC	FU	OS	+0.75	20	100	0	0.7	
13-KC	LC	BL	OD	0.00	20	60	-1	0.5	-0.06
13-KC	LC	FU	OD	0.00	20	50	-2	0.44	
13-KC	LC	BL	OS	0.00	20	200	0	1	-0.32
13-KC	LC	FU	OS	-0.25	20	100	1	0.68	
13-KC	HC	BL	OD	-0.25	20	60	-1	0.5	-0.08
13-KC	HC	FU	OD	-1.00	20	50	-1	0.42	
13-KC	HC	BL	OS	0.00	20	70	0	0.54	0.14
13-KC	HC	FU	OS	+1.50	20	100	1	0.68	
14-KC	LC	BL	OD	0.00	20	200	0	1	0.18
14-KC	LC	FU	OD	0.00	20	300	0	1.18	
14-KC	LC	BL	OS	0.00	20	100	1	0.68	-0.12
14-KC	LC	FU	OS	-0.25	20	70	-1	0.56	
14-KC	HC	BL	OD	-0.50	20	200	0	1	0
14-KC	HC	FU	OD	0.00	20	200	0	1	
14-KC	HC	BL	OS	0.00	20	70	1	0.52	-0.04
14-KC	HC	FU	OS	-0.50	20	70	3	0.48	
15-KC	LC	BL	OD	0.00	20	40	-2	0.34	0.34
15-KC	LC	FU	OD	+0.75	20	100	1	0.68	
15-KC	LC	BL	OS	0.00	20	70	0	0.54	0.14
15-KC	LC	FU	OS	0.00	20	100	1	0.68	
15-KC	HC	BL	OD	0.00	20	80	-1	0.62	-0.06
15-KC	HC	FU	OD	0.00	20	80	2	0.56	
15-KC	HC	BL	OS	+0.75	20	100	0	0.7	-0.02
15-KC	HC	FU	OS	+0.75	20	100	1	0.68	

Appendix H

Subjective Comfort Results

Table H-1: Subjective comfort results recorded at each visit for participants 02-KC - 09-KC. Each lens was given a clarity and comfort score from 0-100, with 0 being poor and 100 being excellent. Lens is indicated with LC or HC for low and high clearance, respectively. Visit type is abbreviated to BL (baseline) and FU (follow-up). For preferred lens, L1 refers to the first lens worn, and L2 to the second.

Participant	Lens	Visit Type	Eye	Comfort	Clarity	Preferred Lens	
						Chronological	By Clearance
02-KC	LC	BL	OD	90	100	L1	HC
02-KC	LC	FU	OD	90	95	L1	HC
02-KC	LC	BL	OS	95	100	L1	HC
02-KC	LC	FU	OS	90	95	L1	HC
02-KC	HC	BL	OD	95	80	-	-
02-KC	HC	FU	OD	95	100	-	-
02-KC	HC	BL	OS	95	80	-	-
02-KC	HC	FU	OS	95	100	-	-
04-KC	LC	BL	OD	65	95	L2	LC
04-KC	LC	FU	OD	75	85	L2	LC
04-KC	LC	BL	OS	65	95	L2	LC
04-KC	LC	FU	OS	65	85	L2	LC
04-KC	HC	BL	OD	65	65	-	-
04-KC	HC	FU	OD	30	20	-	-
04-KC	HC	BL	OS	50	55	-	-
04-KC	HC	FU	OS	20	10	-	-
07-KC	LC	BL	OD	95	100	L2	LC
07-KC	LC	FU	OD	100	100	L2	LC
07-KC	LC	BL	OS	95	100	L2	LC
07-KC	LC	FU	OS	100	100	L2	LC
07-KC	HC	BL	OD	70	100	-	-
07-KC	HC	FU	OD	90	70	-	-
07-KC	HC	BL	OS	90	100	-	-
07-KC	HC	FU	OS	95	70	-	-
09-KC	LC	BL	OD	95	90	L2	LC
09-KC	LC	FU	OD	90	90	L1=L2	LC=HC
09-KC	LC	BL	OS	90	85	L1=L2	LC=HC
09-KC	LC	FU	OS	90	85	L1=L2	LC=HC
09-KC	HC	BL	OD	90	85	-	-
09-KC	HC	FU	OD	90	90	-	-
09-KC	HC	BL	OS	85	90	-	-
09-KC	HC	FU	OS	90	85	-	-

Table H-2: Subjective comfort results recorded at each visit for participants 11-KC - 15-KC. Abbreviations and scores are as described in Table H-1.

Participant	Lens	Visit Type	Eye	Comfort	Clarity	Preferred Lens	
						Chronological	By Clearance
11-KC	LC	BL	OD	100	90	L2	LC
11-KC	LC	FU	OD	95	95	L2	LC
11-KC	LC	BL	OS	100	90	L2	LC
11-KC	LC	FU	OS	95	95	L2	LC
11-KC	HC	BL	OD	95	90	-	-
11-KC	HC	FU	OD	85	85	-	-
11-KC	HC	BL	OS	95	90	-	-
11-KC	HC	FU	OS	85	85	-	-
13-KC	LC	BL	OD	90	100	L2	LC
13-KC	LC	FU	OD	30	90	L1	HC
13-KC	LC	BL	OS	75	100	L1=L2	LC=HC
13-KC	LC	FU	OS	30	90	L1	HC
13-KC	HC	BL	OD	90	100	-	-
13-KC	HC	FU	OD	90	100	-	-
13-KC	HC	BL	OS	100	100	-	-
13-KC	HC	FU	OS	80	60	-	-
14-KC	LC	BL	OD	65	100	L1=L2	LC=HC
14-KC	LC	FU	OD	95	80	L2	LC
14-KC	LC	BL	OS	75	100	L1=L2	LC=HC
14-KC	LC	FU	OS	95	95	L2	LC
14-KC	HC	BL	OD	100	100	-	-
14-KC	HC	FU	OD	85	80	-	-
14-KC	HC	BL	OS	100	100	-	-
14-KC	HC	FU	OS	85	80	-	-
15-KC	LC	BL	OD	90	80	L2	HC
15-KC	LC	FU	OD	85	80	L1=L2	LC=HC
15-KC	LC	BL	OS	90	80	L2	HC
15-KC	LC	FU	OS	85	80	L1=L2	LC=HC
15-KC	HC	BL	OD	100	80	-	-
15-KC	HC	FU	OD	90	75	-	-
15-KC	HC	BL	OS	100	80	-	-
15-KC	HC	FU	OS	90	75	-	-

Appendix I

Assessment of Lens Centration

Table I-1: Description of lens decentration in the lateral and vertical plane for participants 02-KC – 09-KC. Negative values refer to the temporal and inferior direction, where positive values refer to superior and nasal. This assessment was qualitatively observed and graded on a scale from 0 (centred) to 2 (very decentred).

Participant	Lens	Visit Type	Eye	Lens Fit	
				Lateral (x)	Vertical (y)
02-KC	LC	BL	OD	0	-1
02-KC	LC	FU	OD	-1	-1
02-KC	LC	BL	OS	-1	-1
02-KC	LC	FU	OS	-1	-1
02-KC	HC	BL	OD	0	-2
02-KC	HC	FU	OD	-1	-1
02-KC	HC	BL	OS	0	-2
02-KC	HC	FU	OS	-1	-1.5
04-KC	LC	BL	OD	-1	-1
04-KC	LC	FU	OD	-0.5	-1
04-KC	LC	BL	OS	1	-1
04-KC	LC	FU	OS	1	-1
04-KC	HC	BL	OD	0	-1.5
04-KC	HC	FU	OD	-1	-2
04-KC	HC	BL	OS	-0.5	-1.5
04-KC	HC	FU	OS	-1	-2
07-KC	LC	BL	OD	0	-1
07-KC	LC	FU	OD	0	0
07-KC	LC	BL	OS	0	0
07-KC	LC	FU	OS	0	0
07-KC	HC	BL	OD	0	-1
07-KC	HC	FU	OD	0	0
07-KC	HC	BL	OS	-1	-1
07-KC	HC	FU	OS	0	0
09-KC	LC	BL	OD	0	-1
09-KC	LC	FU	OD	0	-1
09-KC	LC	BL	OS	0	-1
09-KC	LC	FU	OS	0	-1
09-KC	HC	BL	OD	-1	-1
09-KC	HC	FU	OD	-1	-1
09-KC	HC	BL	OS	0	-1
09-KC	HC	FU	OS	0	-1

Table I-2: Description of lens decentration in the lateral and vertical plane for participants 11-KC – 15-KC. Lens fit parameters are detailed as in Table I-1.

Participant	Lens	Visit Type	Eye	Lens Fit	
				Lateral (x)	Vertical (y)
11-KC	LC	BL	OD	-1	-1.5
11-KC	LC	FU	OD	-0.5	-1
11-KC	LC	BL	OS	-0.5	-1.5
11-KC	LC	FU	OS	-1	-1
11-KC	HC	BL	OD	-0.5	-1
11-KC	HC	FU	OD	0	0
11-KC	HC	BL	OS	0	-1
11-KC	HC	FU	OS	0	-1
13-KC	LC	BL	OD	0	0
13-KC	LC	FU	OD	0	0.5
13-KC	LC	BL	OS	-0.5	0
13-KC	LC	FU	OS	-1	0.5
13-KC	HC	BL	OD	0	0
13-KC	HC	FU	OD	0	0.5
13-KC	HC	BL	OS	0	-1
13-KC	HC	FU	OS	0	0
14-KC	LC	BL	OD	-1	-1
14-KC	LC	FU	OD	-0.5	-1.5
14-KC	LC	BL	OS	-1	-1
14-KC	LC	FU	OS	-1	-1.5
14-KC	HC	BL	OD	0	-1
14-KC	HC	FU	OD	0	-1.5
14-KC	HC	BL	OS	-1	-1
14-KC	HC	FU	OS	-1	-1
15-KC	LC	BL	OD	-1	-1
15-KC	LC	FU	OD	-1	-1.5
15-KC	LC	BL	OS	-1	-1
15-KC	LC	FU	OS	-1	-1.5
15-KC	HC	BL	OD	-1	0
15-KC	HC	FU	OD	-1	-1
15-KC	HC	BL	OS	-1	-1
15-KC	HC	FU	OS	-1	-1

Appendix J

Bulbar and Limbal Hyperemia Grading by Oculus K5®M

Table J-1: Hyperemia grading from 0-4 in 0.1 steps by the Oculus Keratograph 5®M JENVIS scale²⁵⁷ for participants 02-KC - 09-KC. Lens is indicated with LC or HC for low and high clearance, respectively. Visit type is abbreviated to BL (baseline) and FU (follow-up). Temporal scores are indicated with “T” and nasal with “N”.

Participant	Lens	Visit Type	Eye	Bulbar Hyperemia		Limbal Hyperemia		Analysed Area
				T	N	T	N	
02-KC	LC	BL	OD	1.1	1.1	0.6	0.9	19.5
02-KC	LC	FU	OD	0.9	0.8	0.5	0.6	20.8
02-KC	LC	BL	OS	1.2	1.5	0.8	0.9	23.4
02-KC	LC	FU	OS	1	0.8	0.5	0.4	23.5
02-KC	HC	BL	OD	1.2	1.1	0.7	0.9	21
02-KC	HC	FU	OD	1.2	0.6	0.3	0.4	19.7
02-KC	HC	BL	OS	1.2	1.8	0.8	1.1	23.9
02-KC	HC	FU	OS	1.1	1.3	0.4	0.3	26.2
04-KC	LC	BL	OD	0.7	0.6	0.4	0.5	22.5
04-KC	LC	FU	OD	1	0.9	0.3	0.3	21.2
04-KC	LC	BL	OS	0.7	0.8	0.5	0.3	27.1
04-KC	LC	FU	OS	1.1	1.1	0.3	0.1	24.9
04-KC	HC	BL	OD	0.8	0.7	0.4	0.5	24.4
04-KC	HC	FU	OD	0.8	1.3	0.4	0.3	25.9
04-KC	HC	BL	OS	0.7	1	0.5	0.3	26.2
04-KC	HC	FU	OS	1.1	1.1	0.5	0.3	26.3
07-KC	LC	BL	OD	0.7	0.8	0.2	0.2	18
07-KC	LC	FU	OD	1.2	1.4	0.4	0.3	20
07-KC	LC	BL	OS	0.9	1.2	0.6	0.4	17.5
07-KC	LC	FU	OS	1.7	2.5	0.6	0.5	20.5
07-KC	HC	BL	OD	0.4	0.7	0.1	0.2	11.3
07-KC	HC	FU	OD	0.9	1	0.4	0.3	17.6
07-KC	HC	BL	OS	0.6	0.7	0.2	0.4	12.2
07-KC	HC	FU	OS	2	2.1	0.7	0.4	14.8
09-KC	LC	BL	OD	1.1	1.3	0.7	0.8	11.7
09-KC	LC	FU	OD	0.8	1.2	0.5	1	10.8
09-KC	LC	BL	OS	0.9	1.3	0.6	0.9	13.7
09-KC	LC	FU	OS	0.8	1.7	0.8	1	12.8
09-KC	HC	BL	OD	0.8	1.1	0.6	0.7	14.4
09-KC	HC	FU	OD	0.8	1	0.7	0.8	13.1
09-KC	HC	BL	OS	0.7	1	0.4	0.6	17.3
09-KC	HC	FU	OS	0.9	1.4	0.9	1	13.4

Table J-2: Hyperemia grading for participants 11-KC - 15-KC, as detailed in Table J-1.

Participant	Lens	Visit Type	Eye	Bulbar Hyperemia		Limbal Hyperemia		Analysed Area
				T	N	T	N	
11-KC	LC	BL	OD	0.7	0.7	0.3	0.3	21.3
11-KC	LC	FU	OD	0.8	0.8	0.4	0.5	20.9
11-KC	LC	BL	OS	1	1.8	0.5	0.7	17
11-KC	LC	FU	OS	1.1	1.3	0.5	0.5	21.5
11-KC	HC	BL	OD	0.7	0.7	0.3	0.4	13
11-KC	HC	FU	OD	0.7	0.9	0.4	0.5	19.4
11-KC	HC	BL	OS	0.9	1.4	0.6	0.5	13.7
11-KC	HC	FU	OS	1	1.3	0.5	0.5	20.3
13-KC	LC	BL	OD	1.3	0.9	0.6	0.4	21.1
13-KC	LC	FU	OD	1.5	1.1	0.6	0.5	17.2
13-KC	LC	BL	OS	0.8	1.7	0.6	0.5	21.7
13-KC	LC	FU	OS	1.4	1.2	0.6	0.4	13
13-KC	HC	BL	OD	1	0.9	0.5	0.5	19.2
13-KC	HC	FU	OD	1.5	0.8	0.7	0.4	20.9
13-KC	HC	BL	OS	0.6	1.1	0.5	0.3	16.8
13-KC	HC	FU	OS	1.4	0.5	0.5	0.5	6.6
14-KC	LC	BL	OD	1	1	0.5	0.5	16.5
14-KC	LC	FU	OD	1.2	1.2	0.9	1.1	18.3
14-KC	LC	BL	OS	0.9	0.8	0.7	0.6	10.7
14-KC	LC	FU	OS	1.5	1	1	0.6	21.9
14-KC	HC	BL	OD	1.1	1.2	0.8	0.6	11.7
14-KC	HC	FU	OD	1	0.8	0.6	0.3	17.2
14-KC	HC	BL	OS	0.9	1.1	0.6	0.7	18.3
14-KC	HC	FU	OS	1.4	1.4	1	0.8	21.3
15-KC	LC	BL	OD	0.6	0.4	0.2	0.3	8.6
15-KC	LC	FU	OD	1.3	1.6	0.4	1.1	11.3
15-KC	LC	BL	OS	0.8	0.8	0.3	0.6	11.1
15-KC	LC	FU	OS	1.2	1.3	0.5	0.9	12.6
15-KC	HC	BL	OD	0.6	0.9	0.3	0.9	9.6
15-KC	HC	FU	OD	0.9	1.6	0.4	1	11.2
15-KC	HC	BL	OS	0.8	1.1	0.3	0.8	11.4
15-KC	HC	FU	OS	1	1.2	0.5	0.7	11.2

Appendix K

Corneal Fluorescein Staining Results

Table K-1: Corneal fluorescein staining for participants 02-KC - 09-KC by nature (positive vs negative), and if positive, the type graded from 0 (not present) to 4 (patch) and location according to the BHVI scale²⁸⁹. Location of negative staining is specified as C (central), S (superior), I (inferior), N (nasal), or T (temporal).

Participant	Lens	Visit Type	Eye	Positive Staining					Negative Staining	
				Central	Superior	Inferior	Temporal	Nasal	Presence	Location
02-KC	LC	BL	OD	1	1	1	1	1	-	-
02-KC	LC	FU	OD	1	3	1	1	1	-	-
02-KC	LC	BL	OS	1	1	1	1	1	-	-
02-KC	LC	FU	OS	1	1	1	1	1	-	-
02-KC	HC	BL	OD	0	1	1	0	0	-	-
02-KC	HC	FU	OD	1	1	1	3	3	-	-
02-KC	HC	BL	OS	1	1	1	0	1	-	-
02-KC	HC	FU	OS	1	1	1	0	1	-	-
04-KC	LC	BL	OD	0	1	1	0	0	+	C
04-KC	LC	FU	OD	0	1	1	0	0	-	-
04-KC	LC	BL	OS	0	1	0	0	0	+	C
04-KC	LC	FU	OS	0	1	1	0	0	-	-
04-KC	HC	BL	OD	0	1	0	0	0	+	C
04-KC	HC	FU	OD	0	1	1	0	2	-	-
04-KC	HC	BL	OS	0	1	1	0	0	-	-
04-KC	HC	FU	OS	0	1	1	0	1	-	-
07-KC	LC	BL	OD	0	0	1	1	1	+	C
07-KC	LC	FU	OD	0	1	1	1	1	-	-
07-KC	LC	BL	OS	1	1	1	1	0	+	C
07-KC	LC	FU	OS	1	1	2	2	1	-	-
07-KC	HC	BL	OD	0	2	0	0	0	+	C
07-KC	HC	FU	OD	1	1	1	1	1	+	C
07-KC	HC	BL	OS	0	1	0	0	0	-	-
07-KC	HC	FU	OS	1	1	1	1	1	+	C
09-KC	LC	BL	OD	1	1	1	1	0	-	-
09-KC	LC	FU	OD	1	1	1	2	1	-	-
09-KC	LC	BL	OS	1	1	1	0	1	-	-
09-KC	LC	FU	OS	1	1	2	1	1	-	-
09-KC	HC	BL	OD	0	1	1	0	1	-	-
09-KC	HC	FU	OD	1	1	1	1	1	-	-
09-KC	HC	BL	OS	1	2	1	0	0	-	-
09-KC	HC	FU	OS	0	1	2	0	0	-	-

Table K-2: Corneal fluorescein staining for participants 11-KC - 15-KC, as detailed in Table K-1.

Participant	LensOnly	Visit Type	Eye	Positive Staining					Negative Staining	
				Central	Superior	Inferior	Temporal	Nasal	Presence	Location
11-KC	LC	BL	OD	0	1	1	1	0	+	S, T
11-KC	LC	FU	OD	1	1	1	1	1	+	S, I, T
11-KC	LC	BL	OS	0	1	1	1	1	-	-
11-KC	LC	FU	OS	1	1	1	1	1	-	-
11-KC	HC	BL	OD	0	1	1	0	1	-	-
11-KC	HC	FU	OD	0	1	1	1	0	+	S, I, T
11-KC	HC	BL	OS	0	1	3	1	1	-	-
11-KC	HC	FU	OS	1	1	1	1	1	-	-
13-KC	LC	BL	OD	0	1	0	1	0	-	-
13-KC	LC	FU	OD	1	1	2	1	3	-	-
13-KC	LC	BL	OS	0	1	0	0	0	-	-
13-KC	LC	FU	OS	1	0	3	1	1	+	I
13-KC	HC	BL	OD	0	3	1	0	0	-	-
13-KC	HC	FU	OD	0	1	3	1	0	-	-
13-KC	HC	BL	OS	0	1	0	1	0	-	-
13-KC	HC	FU	OS	0	1	1	0	0	-	-
14-KC	LC	BL	OD	0	1	1	0	0	+	C
14-KC	LC	FU	OD	1	1	1	0	1	+	C
14-KC	LC	BL	OS	1	0	1	0	1	+	C
14-KC	LC	FU	OS	1	1	1	1	1	+	C
14-KC	HC	BL	OD	0	1	2	0	0	-	-
14-KC	HC	FU	OD	3	3	2	3	0	+	C, S, T
14-KC	HC	BL	OS	1	0	2	1	1	-	-
14-KC	HC	FU	OS	0	0	1	0	0	-	-
15-KC	LC	BL	OD	1	1	2	0	1	-	-
15-KC	LC	FU	OD	1	1	1	1	1	+	C
15-KC	LC	BL	OS	1	3	3	0	1	-	-
15-KC	LC	FU	OS	1	1	1	1	1	-	-
15-KC	HC	BL	OD	1	0	2	1	1	-	-
15-KC	HC	FU	OD	0	1	1	2	1	-	-
15-KC	HC	BL	OS	0	2	0	0	2	-	-
15-KC	HC	FU	OS	1	1	1	2	0	-	-

References

1. Kaufman PL, Alm A. *Adler's Physiology of the Eye*. 10th ed. St. Louis, Missouri: Mosby; 2003.
2. Dua HS, Faraj LA, Said DG, Gray T, Lowe J. Human corneal anatomy redefined: a novel pre-Descemet's layer (Dua's Layer). *Ophthalmology*. 2013;120(9):1778-1785. doi:10.1016/j.ophtha.2013.01.018
3. Dhanda, Kalevar. Applied Anatomy and Physiology of the Cornea. *Int Ophthalmol Clinics*. 1972;12(3):19-40.
4. McLaughlin BJ, Caldwell RB, Sasaki Y, Wood TO. Freeze-fracture quantitative comparison of rabbit corneal epithelial and endothelial membranes. *Curr Eye Res*. 1985;4(9):951-962. doi:10.3109/02713689509000002
5. Jentsch TJ, Keller SK, Wiederholt M. Ion transport mechanisms in cultured bovine corneal endothelial cells. *Curr Eye Res*. 1985;4(4):361-369. doi:10.3109/02713688509025149
6. Kuang K, Xu M, Koniarek JP, Fischbarg J. Effects of ambient bicarbonate, phosphate and carbonic anhydrase inhibitors on fluid transport across rabbit corneal endothelium. *Exp Eye Res*. 1990;50:487-493.
7. Stiemke MM, Roman RJ, Palmer ML, Edelhauser HF. Sodium activity in the aqueous humor and corneal stroma of the rabbit. *Exp Eye Res*. 1992;55:425-433.
8. Riley MV. Glucose and oxygen utilization by the rabbit cornea. *Exp Eye Res*. 1969;8:193-200.
9. Klyce SD. Stromal lactate accumulation can account for corneal oedema osmotically following epithelial hypoxia in the rabbit. *J Physiol*. 1981;321:49-64. doi:10.1113/jphysiol.1981.sp013971
10. Efron N. *Contact Lens Complications*. 3rd Ed. Elsevier Limited; 2012.
11. Smelser GK, Ozanics V. Importance of atmospheric oxygen for maintenance of the optical properties of the human cornea. *Science*. 1952;115(2980):140.
12. Hill R, Fatt I. How dependent is the cornea on the atmosphere? *J Am Optom Assoc*. 1964;35(873).

13. Mannis MJ, Zadnik K, Coral-Ghanem C, Kara-José N. *Contact Lenses in Ophthalmic Practice.*; 2004.
14. Fatt I, Freeman RD, Lin D. Oxygen tension distributions in the cornea: a re-examination. *Exp Eye Res.* 1974;18(4):357-365. doi:10.1016/0014-4835(74)90112-2
15. Fatt I, Bieber MT. The steady-state distribution of oxygen and carbon dioxide in the in vivo cornea. *Exp Eye Res.* 1968;7(1):103-112. doi:10.1016/s0014-4835(68)80032-6
16. Mandell RB, Polse KA, Fatt I. Corneal swelling caused by contact lens wear. *Arch Ophthalmol.* 1970;83(1):3-9. doi:10.1001/archopht.1970.00990030005003
17. Holden BA, Sweeney DF, Sanderson G. The minimum precorneal oxygen tension to avoid corneal edema. *Investig Ophthalmol Vis Sci.* 1984;25(4):476-480.
18. Holden BA, Mertz GW. Critical oxygen levels to avoid corneal edema for daily and extended wear contact lenses. *Investig Ophthalmol Vis Sci.* 1984;25(10):1161-1167.
19. Bonanno JA, Polse KA. Central and peripheral corneal swelling accompanying soft lens extended wear. *Am J Optom Physiol Opt.* 1985;62(2):74-81.
20. Efron N, Ang JHB. Corneal hypoxia and hypercapnia during contact lens wear. *Optom Vis Sci.* 1990;67(7):512-521.
21. Harvitt DM, Bonanno JA. Re-evaluation of the oxygen diffusion model for predicting minimum contact lens Dk/t values needed to avoid corneal anoxia. *Optom Vis Sci.* 1999;76(10):712-719. doi:10.1097/00006324-199910000-00023
22. Morgan PB, Brennan NA, Maldonado-Codina C, Quhill W, Rashid K, Efron N. Central and peripheral oxygen transmissibility thresholds to avoid corneal swelling during open eye soft contact lens wear. *J Biomed Mater Res Part B Appl Biomater.* 2010;92(2):361-365. doi:10.1002/jbm.b.31522
23. Bennett ES, Henry VA. *Clinical Manual of Contact Lenses.* 4th editio. Philadelphia, PA: Wolters Kluwer Health/Lippincott Williams & Wilkins; 2015. doi:10.1111/j.1444-0938.2009.00390.x
24. Holden BA, McNally JJ, Mertz GW, Swarbrick HA. Topographical corneal oedema. *Acta Ophthalmol.* 1985;63(6):684-691. doi:10.1111/j.1755-3768.1985.tb01581.x

25. Tsai J, Denniston A, Murray P, Huang J, Aldad T. *Oxford American Handbook of Ophthalmology*. New York, NY, USA: Oxford University Press; 2011.
26. Liesegang TJ. Physiologic changes of the cornea with contact lens wear. *CLAO J*. 2002;28(1):12-27.
27. Harris MG, Sarver MD, Brown LR. Corneal edema with hydrogel lenses and eye closure: Time course. *Am J Optom Physiol Opt*. 1981;58(1):18-20.
28. Moezzi AM, Fonn D, Simpson TL. Overnight corneal swelling with silicone hydrogel contact lenses with high oxygen transmissibility. *Eye Contact Lens*. 2006;32(6):277-280. doi:10.1097/01.icl.0000224529.14273.26
29. Wang J, Simpson TL, Fonn D. Objective measurements of corneal light-backscatter during corneal swelling, by optical coherence tomography. *Investig Ophthalmol Vis Sci*. 2004;45(10):3493-3498. doi:10.1167/iovs.04-0096
30. Hutchings N, Simpson TL, Hyun C, et al. Swelling of the human cornea revealed by high-speed, ultrahigh-resolution optical coherence tomography. *Investig Ophthalmol Vis Sci*. 2010;51(9):4579-4584. doi:10.1167/iovs.09-4676
31. Wang J, Fonn D, Simpson TL, Jones L. The measurement of corneal epithelial thickness in response to hypoxia using optical coherence tomography. *Am J Ophthalmol*. 2002;133(3):315-319. doi:10.1016/S0002-9394(01)01382-4
32. Wang J, Fonn D, Simpson TL. Topographical thickness of the epithelium and total cornea after hydrogel and PMMA contact lens wear with eye closure. *Investig Ophthalmol Vis Sci*. 2003;44(3):1070-1074. doi:10.1167/iovs.02-0343
33. Feng Y, Varikooty J, Simpson TL. Diurnal variation of corneal and corneal epithelial thickness measured using optical coherence tomography. *Cornea*. 2001;20(5):480-483. doi:10.1097/00003226-200107000-00008
34. Lu F, Tao A, Tao W, Zhuang X, Shen M. Thickness changes in the corneal epithelium and Bowman's layer after overnight wear of silicone hydrogel contact lenses. *BMC Ophthalmol*. 2018;18(1):1-7. doi:10.1186/s12886-018-0956-2
35. Erickson P, Comstock TL, Doughty MJ, Cullen AP. The cornea swells in the posterior direction under hydrogel contact lenses. *Ophthalmic Physiol Opt*. 1999;19(6):475-480.

doi:10.1046/j.1475-1313.1999.00470.x

36. Müller LJ, Pels E, Vrensen GFJM. The specific architecture of the anterior stroma accounts for maintenance of corneal curvature. *Br J Ophthalmol*. 2001;85(4):437-443.
doi:10.1136/bjo.85.4.437
37. Owens H, Watters G, Gamble G. Effect of SoftPerm lens wear on corneal thickness and topography: A comparison between keratoconic and normal corneae. *CLAO J*. 2002;28(2):83-87.
38. Holden BA, Sweeney DF, Vannas A, Nilsson KT, Efron N. Effects of long-term extended contact lens wear on the human cornea. *Investig Ophthalmol Vis Sci*. 1985;26(11):1489-1501.
39. Ren DH, Yamamoto K, Ladage PM, et al. Adaptive effects of 30-night wear of hyper-O2 transmissible contact lenses on bacterial binding and corneal epithelium: a 1-year clinical trial. *Ophthalmology*. 2002;109(1):27-39. doi:10.1016/S0161-6420(01)00867-3
40. Pérez JG, Méijome JMG, Jalbert I, Sweeney DF, Erickson P. Corneal epithelial thinning profile induced by long-term wear of hydrogel lenses. *Cornea*. 2003;22(4):304-307.
doi:10.1097/00003226-200305000-00005
41. Liu Z, Pflugfelder SC. The effects of long-term contact lens wear on corneal thickness, curvature, and surface regularity. *Ophthalmology*. 2000;107(1):105-111. doi:10.1016/S0161-6420(99)00027-5
42. Hamano H, Watanabe K, Hamano T, Mitsunaga S, Kotani S, Okada A. A study of the complications induced by conventional and disposable contact lenses. *Contact Lens Assoc Ophthalmol*. 1994;20(2):103-108.
43. Teranishi S, Kimura K, Kawamoto K, Nishida T. Protection of human corneal epithelial cells from hypoxia-induced disruption of barrier function by keratinocyte growth factor. *Investig Ophthalmol Vis Sci*. 2008;49(6):2432-2437. doi:10.1167/iovs.07-1464
44. Yanai R, Ko JA, Morishige N, Chikama T, Ichijima H, Nishida T. Disruption of zonula occludens-1 localization in the rabbit corneal epithelium by contact lens-induced hypoxia. *Investig Ophthalmol Vis Sci*. 2009;50(10):4605-4610. doi:10.1167/iovs.09-3407
45. Covey M, Sweeney DF, Terry R, Sankaridurg PR, Holden BA. Hypoxic effects on the anterior eye of high-Dk soft contact lens wearers are negligible. *Optom Vis Sci*. 2001;78(2):95-99.

doi:10.1097/00006324-200102000-00009

46. Papas EB. The role of hypoxia in the limbal vascular response to soft contact lens wear. *Eye Contact Lens*. 2003;29(1 Suppl):72-74. doi:10.1097/00140068-200301001-00020
47. Papas E. On the relationship between soft contact lens oxygen transmissibility and induced limbal hyperaemia. *Exp Eye Res*. 1998;67(2):125-131. doi:10.1006/exer.1998.0504
48. Maldonado-Codina C, Morgan PB, Schnider CM, Efron N. Short-term physiologic response in neophyte subjects fitted with hydrogel and silicone hydrogel contact lenses. *Optom Vis Sci*. 2004;81(12):911-921. doi:10.1097/01.OPX.0000147679.02577.4A
49. Papas EB, Vajdic CM, Austen R, Holden BA. High-oxygen-transmissibility soft contact lenses do not induce limbal hyperaemia. *Curr Eye Res*. 1997;16(9):942-948. doi:10.1076/ceyr.16.9.942.5049
50. Hamano H, Hori M, Hamano T, Kawabe H, Mikami M, Mitsunaga S. Effects of contact lens wear on mitosis of corneal epithelium and lactate content in aqueous humor of rabbit. *Jpn J Ophthalmol*. 1983;27(3):451-458.
51. Fadel D. Scleral lens issues and complications related to a non-optimal fitting relationship between the lens and ocular surface. *Eye Contact Lens*. 2019;45(3):152-163. doi:10.1097/ICL.0000000000000523
52. van der Worp E. *A Guide to Scleral Lens Fitting, Version 2.0 [Monograph Online]*. Forest Grove, OR: Pacific University; 2015. <http://commons.pacificu.edu/mono/10/>.
53. Fick AE, Letocha CF, Dabezies OH. A contact lens. *Arch Ophthalmol*. 1997;115(1):120-121.
54. Pearson RM. Karl Otto Himmler, manufacturer of the first contact lens. *Contact Lens Anterior Eye*. 2007;30(1):11-16. doi:10.1016/j.clae.2006.10.003
55. van der Worp E, Bornman D, Lopes Ferreira D, Faria-Ribeiro M, Garcia-Porta N, González-Meijome JM. Modern scleral contact lenses: a review. *Contact Lens Anterior Eye*. 2014;37(4):240-250. doi:10.1016/j.clae.2014.02.002
56. Michaud L, Lipson M, Kramer E, Walker M. The official guide to scleral lens terminology. *Contact Lens Anterior Eye*. 2020;43(6):529-534. doi:10.1016/j.clae.2019.09.006
57. Walker MK, Bergmanson JP, Miller WL, Marsack JD, Johnson LA. Complications and fitting

- challenges associated with scleral contact lenses: A review. *Contact Lens Anterior Eye*. 2016;39(2):88-96. doi:10.1016/j.clae.2015.08.003
58. Kim S, Lee JS, Park YK, et al. Fitting miniscleral contact lenses in Korean patients with keratoconus. *Clin Exp Optom*. 2017;100(4):375-379. doi:10.1111/cxo.12424
 59. Yeung D, Sorbara L. Scleral lens clearance assessment with biomicroscopy and anterior segment optical coherence tomography. *Optom Vis Sci*. 2018;95(1):13-20. doi:10.1097/OPX.0000000000001164
 60. Ko L, Maurice D, Ruben M. Fluid exchange under scleral contact lenses in relation to wearing time. *Br J Ophthalmol*. 1970;54(7):486-489. doi:10.1136/bjo.54.7.486
 61. Michaud L, van der Worp E, Brazeau D, Warde R, Giasson CJ. Predicting estimates of oxygen transmissibility for scleral lenses. *Contact Lens Anterior Eye*. 2012;35(6):266-271. doi:10.1016/j.clae.2012.07.004
 62. Korb DR, Finnemore VM, Herman JP. Apical changes and scarring in keratoconus as related to contact lens fitting techniques. *J Am Optom Assoc*. 1982;53(3):199-205.
 63. Barr JT, Wilson BS, Gordon MO, et al. Estimation of the incidence and factors predictive of corneal scarring in the Collaborative Longitudinal Evaluation of Keratoconus (CLEK) study. *Cornea*. 2006;25(1):16-25. doi:10.1097/01.ico.0000164831.87593.08
 64. Kauffman MJ, Gilmartin CA, Bennett ES, Bassi CJ. A comparison of the short-term settling of three scleral lens designs. *Optom Vis Sci*. 2014;91(12):1462-1466. doi:10.1097/OPX.0000000000000409
 65. Alonso-Caneiro D, Vincent SJ, Collins MJ. Morphological changes in the conjunctiva, episclera and sclera following short-term miniscleral contact lens wear in rigid lens neophytes. *Contact Lens Anterior Eye*. 2016;39(1):53-61. doi:10.1016/j.clae.2015.06.008
 66. Vincent SJ, Alonso-Caneiro D, Collins MJ. The temporal dynamics of miniscleral contact lenses: central corneal clearance and centration. *Contact Lens Anterior Eye*. 2018;41(2):162-168. doi:10.1016/j.clae.2017.07.002
 67. Otchere H, Jones L, Sorbara L. The impact of scleral contact lens vault on visual acuity and comfort. *Eye Contact Lens Sci Clin Pract*. 2018;44(6):S54-S59. doi:10.1097/ICL.0000000000000427

68. Vincent SJ, Alonso-Caneiro D, Collins MJ. Optical coherence tomography and scleral contact lenses: clinical and research applications. *Clin Exp Optom*. 2019;102(3):224-241. doi:10.1111/cxo.12814
69. Pullum KW, Whiting MA, Buckley RJ. Scleral contact lenses: The expanding role. *Cornea*. 2005;24(3):269-277. doi:10.1097/01.ico.0000148311.94180.6b
70. Pecego M, Barnett M, Mannis MJ, Durbin-Johnson B. Jupiter scleral lenses: the UC Davis Eye Center experience. *Eye Contact Lens*. 2012;38(3):179-182. doi:10.1097/ICL.0b013e31824daa5e
71. Rosenthal P, Croteau A. Fluid-ventilated, gas-permeable scleral contact lens is an effective option for managing severe ocular surface disease and many corneal disorders that would otherwise require penetrating keratoplasty. *Eye Contact Lens*. 2005;31(3):130-134. doi:10.1097/01.ICL.0000152492.98553.8D
72. Kok JHC, Visser R. Treatment of ocular surface disorders and dry eyes with high gas-permeable scleral lenses. *Cornea*. 1992;11(6):518-522. doi:10.1097/00003226-199211000-00006
73. Gobbe M, Guillon M. Corneal wavefront aberration measurements to detect keratoconus patients. *Contact Lens Anterior Eye*. 2005;28(2):57-66. doi:10.1016/j.clae.2004.12.001
74. Jinabhai A, O'Donnell C, Radhakrishnan H, Nourrit V. Forward light scatter and contrast sensitivity in keratoconic patients. *Contact Lens Anterior Eye*. 2012;35(1):22-27. doi:10.1016/j.clae.2011.07.001
75. Liduma S, Luguzis A, Krumina G. The impact of irregular corneal shape parameters on visual acuity and contrast sensitivity. *BMC Ophthalmol*. 2020;20(1):1-10. doi:10.1186/s12886-020-01737-x
76. Romero-Rangel T, Stavrou P, Cotter J, Rosenthal P, Baltatzis S, Foster CS. Gas-permeable scleral contact lens therapy in ocular surface disease. *Am J Ophthalmol*. 2000;130(1):25-32. doi:10.1016/S0002-9394(00)00378-0
77. Compăn V, Oliveira C, Aguilera-Arzo M, Mollá S, Peixoto-de-Matos SC, González-Méijome JM. Oxygen diffusion and edema with modern scleral rigid gas permeable contact lenses. *Investig Ophthalmol Vis Sci*. 2014;55(10):6421-6429. doi:10.1167/iovs.14-14038

78. Vincent SJ, Alonso-Caneiro D, Collins MJ. Corneal changes following short-term miniscleral contact lens wear. *Cont Lens Anterior Eye*. 2014;37(6):461-468.
doi:10.1016/j.clae.2014.08.002
79. Arlt C. *Clinical Effect of Tear Layer Thickness on Corneal Edema During Scleral Lens Wear (MSc Thesis)*. Aalen, Germany; 2015.
80. Kim YH, Tan B, Lin MC, Radke CJ. Central corneal edema with scleral-lens wear. *Curr Eye Res*. 2018;43(11):1305-1315. doi:10.1080/02713683.2018.1500610
81. Tan B, Zhou Y, Yuen TL, Lin K, Michaud L, Lin MC. Effects of scleral-lens tear clearance on corneal edema and post-lens tear dynamics: A pilot study. *Optom Vis Sci*. 2018;95(6):481-490.
doi:10.1097/OPX.0000000000001220
82. Lafosse E, Romín DM, Esteve-Taboada JJ, Wolffsohn JS, Talens-Estarellles C, García-Lázaro S. Comparison of the influence of corneo-scleral and scleral lenses on ocular surface and tear film metrics in a presbyopic population. *Contact Lens Anterior Eye*. 2018;41(1):122-127.
doi:10.1016/j.clae.2017.09.014
83. Vincent SJ, Alonso-Caneiro D, Collins MJ. The time course and nature of corneal oedema during sealed miniscleral contact lens wear. *Contact Lens Anterior Eye*. 2019;42(1):49-54.
doi:10.1016/j.clae.2018.03.001
84. Dhallu SK, Huarte ST, Bilkhu PS, Boychev N, Wolffsohn JS. Effect of scleral lens oxygen permeability on corneal physiology. *Optom Vis Sci*. 2020;97(9):669-675.
doi:10.1097/OPX.0000000000001557
85. Vincent SJ, Alonso-Caneiro D, Collins MJ, et al. Hypoxic corneal changes following eight hours of scleral contact lens wear. *Optom Vis Sci*. 2016;93(3):293-299.
doi:10.1097/OPX.0000000000000803
86. Giasson CJ, Rancourt J, Robillard J, Melillo M, Michaud L. Corneal endothelial blebs induced in scleral lens wearers. *Optom Vis Sci*. 2019;96(11):810-817.
doi:10.1097/OPX.0000000000001438
87. Dua HS, Azuara-Blanco A. Limbal stem cells of the corneal epithelium. *Surv Ophthalmol*. 2000;44(5):415-425. doi:10.1016/S0039-6257(00)00109-0
88. Hall LA, Hunt C, Young G, Wolffsohn J. Factors affecting corneoscleral topography. *Invest*

- Ophthalmol Vis Sci.* 2013;54(5):3691-3701. doi:10.1167/iovs.13-11657
89. Ritzmann M, Caroline PJ, Börret R, Korszen E. An analysis of anterior scleral shape and its role in the design and fitting of scleral contact lenses. *Contact Lens Anterior Eye.* 2018;41(2):205-213. doi:10.1016/j.clae.2017.10.010
 90. Visser ES, Visser R, Van Lier HJJ, Otten HM. Modern scleral lenses part II: Patient satisfaction. *Eye Contact Lens.* 2007;33(1):21-25. doi:10.1097/01.icl.0000228964.74647.25
 91. Fogt JS, Nau CB, Schornack M, Shorter E, Nau A, Harthan JS. Comparison of pneumatonometry and transpalpebral tonometry measurements of intraocular pressure during scleral lens wear. *Optom Vis Sci.* 2020;97(9):711-719. doi:10.1097/OPX.0000000000001574
 92. Davanger M, Evensen A. Role of the pericorneal papillary structure in renewal of corneal epithelium. *Nature.* 1971;229(5286):560-561.
 93. Bruce AS, Nguyen LM. Acute red eye (non-ulcerative keratitis) associated with mini-scleral contact lens wear for keratoconus. *Clin Exp Optom.* 2013;96(2):245-248. doi:10.1111/cxo.12033
 94. Krachmer JH, Feder RS, Belin MW. Keratoconus and related noninflammatory corneal thinning disorders. *Surv Ophthalmol.* 1984;28(4):293-322. doi:10.1016/0039-6257(84)90094-8
 95. Gomes JAP, Tan D, Rapuano CJ, et al. Global consensus on keratoconus and ectatic diseases. *Cornea.* 2015;34(4):359-369.
 96. Martínez-Abad A, Piñero DP. New perspectives on the detection and progression of keratoconus. *J Cataract Refract Surg.* 2017;43(9):1213-1227. doi:10.1016/j.jcrs.2017.07.021
 97. Mcmonnies CW. Inflammation and Keratoconus. *Optom Vis Sci.* 2015;92(2):35-41.
 98. Appelbaum A. Keratoconus. *Arch Ophthalmol.* 1936;15:900-921.
 99. Rabinowitz YS. Keratoconus. *Surv Ophthalmol.* 1998;42(4):297-319.
 100. Belin MW, Khachikian SS, Ambrósio R, Salomao M. Keratoconus/ectasia detection with the Oculus Pentacam: Belin/Ambrósio enhanced ectasia display. *Highlights Ophthalmol.* 2007;35(6):5-12.
 101. Rocha KM, Perez-Straziota CE, Perez-Straziota E, Stulting RD, Randleman JB. SD-OCT

- analysis of regional epithelial thickness profiles in keratoconus, postoperative corneal ectasia, and normal eyes. *J Refract Surg.* 2013;29(3):173-179. doi:10.3928/1081597X-20130129-08
102. Otchere H, Sorbara L. Repeatability of topographic corneal thickness in keratoconus comparing Visante™ OCT and Oculus Pentacam HR® topographer. *Contact Lens Anterior Eye.* 2017;40(4):217-223. doi:10.1016/j.clae.2017.05.002
103. Bizheva K, Tan B, Maclelan B, et al. Sub-micrometer axial resolution OCT for in-vivo imaging of the cellular structure of healthy and keratoconic human corneas. *Biomed Opt Express.* 2017;8(2):800-812. doi:10.1364/BOE.8.000800
104. Ihalainen A. Clinical and epidemiological features of keratoconus genetic and external factors in the pathogenesis of the disease. *Acta Ophthalmol.* 1986;178:1-64.
105. Kennedy RH, Bourne WM, Dyer JA. A 48-year clinical and epidemiologic study of keratoconus. *Am J Ophthalmol.* 1986;101(3):267-273. doi:10.1016/0002-9394(86)90817-2
106. Hofstetter HW. A keratoscopic survey of 13,395 eyes. *Am J Optom Am Acad Optom.* 1959;36(1):3-11. doi:10.1097/00006324-195901000-00002
107. Pearson AR, Soneji B, Sarvananthan N, Sandford-Smith JH. Does ethnic origin influence the incidence or severity of keratoconus ? *Eye (Lond).* 2000;14:625-628.
108. Godefrooij DA, de Wit GA, Uiterwaal CS, Imhof SM, Wisse RPL. Age-specific Incidence and Prevalence of Keratoconus: A Nationwide Registration Study. *Am J Ophthalmol.* 2017;175:169-172. doi:10.1016/j.ajo.2016.12.015
109. Georgiou T, Funnell C, Cassels-Brown A, O’Conor R. Influence of ethnic origin on the incidence of keratoconus and associated atopic disease in Asians and white patients. 2004;18:379-383. doi:10.1038/sj.eye.6700652
110. Cozma I, Atherley C, James N. Influence of ethnic origin on the incidence of keratoconus and associated atopic disease in Asian and white patients. *Eye (Lond).* 2005;19:924-925. doi:10.1038/sj.eye.6701674
111. Owens H, Gamble G. A profile of keratoconus in New Zealand. *Cornea.* 2003;22(2):122-125. doi:10.1097/00003226-200303000-00008
112. Wagner H, Barr JT, Zadnik K. Collaborative Longitudinal Evaluation of Keratoconus (CLEK) Study: Methods and findings to date. *Contact Lens Anterior Eye.* 2007;30(4):223-232.

doi:10.1016/j.clae.2007.03.001

113. Mathew JH, Goosey JD, Bergmanson JPG. Quantified histopathology of the keratoconic cornea. *Optom Vis Sci.* 2011;88(8):988-997. doi:10.1097/OPX.0b013e31821ffbd4
114. Naderan M, Jahanrad A, Balali S. Histopathologic findings of keratoconus corneas underwent penetrating keratoplasty according to topographic measurements and keratoconus severity. *Int J Ophthalmol.* 2017;10(11):1640-1646. doi:10.18240/ijo.2017.11.02
115. Iwamoto T, Devoe AG. Particulate structures in keratoconus. *Arch Ophthalmol Rev Gen Ophthalmol.* 1975;35(1):65-72.
116. Tsubota K, Mashima Y, Murata H, Sato N, Ogata T. Corneal epithelium in keratoconus. *Cornea.* 1995;14(1):77-83.
117. Somodi S, Hahnel C, Slowik C, Richter A, Weiss D, Guthoff R. Confocal in vivo microscopy and confocal laser-scanning fluorescence microscopy in keratoconus. *Ger J Ophthalmol.* 1997;5(6):518-525.
118. Sherwin T, Brookes NH. Morphological changes in keratoconus: pathology or pathogenesis. *Clin Exp Ophthalmol.* 2004;32:211-217.
119. Hollingsworth JG, Bonshek RE, Efron N. Correlation of the appearance of the keratoconic cornea in vivo by confocal microscopy and in vitro by light microscopy. *Cornea.* 2005;24(4):397-405. doi:10.1097/01.icc.0000151548.46231.27
120. Efron N, Hollingsworth JG. New perspectives on keratoconus as revealed by corneal confocal microscopy. *Clin Exp Optom.* 2008;91(1):34-55. doi:10.1111/j.1444-0938.2007.00195.x
121. Hollingsworth JG, Efron N, Tullo AB. In vivo corneal confocal microscopy in keratoconus. *Ophthalmic Physiol Opt.* 2005;25(3):254-260. doi:10.1111/j.1475-1313.2005.00278.x
122. Uçakhan ÖÖ, Kanpolat A, Yılmaz N, Özkan M. In vivo confocal microscopy findings in keratoconus. *Eye Contact Lens.* 2006;32(4):183-191. doi:10.1097/01.icl.0000189038.74139.4a
123. Hollingsworth J, Perez-Gomez I, Mutalib HA, Efron N. A population study of the normal cornea using an in vivo, slit-scanning confocal microscope. *Optom Vis Sci.* 2001;78(10):706-711. doi:10.1097/00006324-200110000-00010
124. Sorbara L, Lopez JCL, Gorbet M, et al. Impact of contact lens wear on epithelial alterations in

- keratoconus. *J Optom.* 2020. doi:10.1016/j.optom.2020.02.005
125. Fernandes BF, Logan P, Zajdenweber ME, Santos LN, Cheema DP, Burnier MN. Histopathological study of 49 cases of keratoconus. *Pathology.* 2008;40(6):623-626. doi:10.1080/00313020802320648
 126. Kenney MC, Nesburn AB, Burgeson RE, Butkowski RJ, Ljubimov AV. Abnormalities of the extracellular matrix in keratoconus corneas. *Cornea.* 1997;16(3):345-351.
 127. Sherwin T, Brookes NH, Loh I-P, Poole CA, Clover GM. Cellular incursion into Bowman's membrane in the peripheral cone of the keratoconic cornea. *Exp Eye Res.* 2002;74:473-482. doi:10.1006/exer.2001.1157
 128. Takahashi A, Nakayasu K, Okisaka S, Kanai A. Quantitative analysis of collagen fiber in keratoconus. *Acta Soc Ophthalmol Jap.* 1990;94(11):1068-1073.
 129. Fullwood NJ, Tuft SJ, Malik NS, Meek KM, Ridgway AEA, Harrison RJ. Synchrotron x-ray diffraction studies of keratoconus corneal stroma. *Invest Ophthalmol Vis Sci.* 1992;33(5):1734-1741.
 130. Akhtar S, Bron AJ, Salvi SM, Hawksworth NR, Tuft SJ, Meek KM. Ultrastructural analysis of collagen fibrils and proteoglycans in keratoconus. *Acta Ophthalmol.* 2008;86(7):764-772. doi:10.1111/j.1755-3768.2007.01142.x
 131. Yue BYJT, Sugar J, Benveniste K. Heterogeneity in keratoconus: possible biochemical basis. *Proc Soc Exp Biol Med.* 1984;175:336-341.
 132. Critchfield JW, Calandra AJ, Nesburn AB, Kenney MC. Keratoconus: I. Biochemical studies. *Exp Eye Res.* 1988;48:953-963.
 133. Radda TM, Menzel EJ, Freyler H, Gnad HD. Collagen types in keratoconus. *Graefe's Arch Clin Exp Ophthalmol.* 1982;218:262-264.
 134. Newsome DA, Foidart J-M, Hassell JR, Krachmer JH, Rodrigues MM, Katz SI. Detection of specific collagen types in normal and keratoconus corneas. *Invest Ophthalmol Vis Sci.* 1981;20(6):738-750.
 135. Zimmermann DR, Fischer RW, Winterhalter KH, Witmer R, Vaughan L. Comparative studies of collagens in normal and keratoconus corneas. *Exp Eye Res.* 1988;46:431-442.

136. Yue BYJT, Sugar J, Schrode K. Histochemical studies of keratoconus. *Curr Eye Res.* 1988;7(1):81-86. doi:10.3109/02713688809047024
137. Erie JC, Patel S V., McLaren JW, Nau CB, Hodge DO, Bourne WM. Keratocyte density in keratoconus. A confocal microscopy study. *Am J Ophthalmol.* 2002;134(5):689-695.
138. Funderburgh JL, Funderburgh ML, Rodrigues MM, Krachmer JH, Conrad GW. Altered antigenicity of keratan sulfate proteoglycan in selected corneal diseases. *Investig Ophthalmol Vis Sci.* 1990;31(3):418-428.
139. Teng CC. Electron microscope study of the pathology of keratoconus: Part I. *Am J Ophthalmol.* 1963;5:19-47. doi:10.4324/9780429468674-4
140. Stone DL, Kenyon KR, Stark WJ. Ultrastructure of keratoconus with healed hydrops. *Americ.* 1976;82:450-458.
141. Jongebloed WL, Dijk F, Worst JGF. Keratoconus morphology and cell dystrophy: A SEM study. *Doc Ophthalmol.* 1989;72(3-4):403-409. doi:10.1007/BF00153510
142. Buxton JN. Contact lenses in keratoconus. *Contact Intraocul Lens Med J.* 1978;4(3):74-85.
143. Perry HD, Buxton JN, Fine BS. Round and oval cones in keratoconus. *Ophthalmology.* 1980;87(9):905-909. doi:10.1016/S0161-6420(80)35145-2
144. Carney LG. Contact lens correction of visual loss in keratoconus. *Acta Ophthalmol.* 1982;60(5):795-802. doi:10.1111/j.1755-3768.1982.tb06741.x
145. Zadnik K. An analysis of contrast sensitivity in identical twins with keratoconus. *Cornea.* 1984;3(2):99-104.
146. Barr JT, Yackels T. Corneal scarring in keratoconus - measurements and influence on visual acuity. *Int Contact Lens Clin.* 1995;22:173-175.
147. Barr JT, Schechtman KB, Fink BA, et al. Corneal scarring in the collaborative longitudinal evaluation of keratoconus (CLEK) study: baseline prevalence and repeatability of detection. *Cornea.* 1999;18(1):34-46.
148. Zadnik K, Barr JT, Edrington TB, et al. Corneal scarring and vision in keratoconus: a baseline report from the collaborative longitudinal evaluation of keratoconus (CLEK) study. *Cornea.* 2000;19(6):804-812. doi:10.1097/00003226-200011000-00009

149. Amsler M. Kératocône classique et kératocône fruste; arguments unitaires. *Ophthalmol.* 1946;111(2-3):96-101.
150. Lee LR, Hirst LW, Readshaw G. Clinical detection of unilateral keratoconus. *Aust N Z J Ophthalmol.* 1995;23(2):129-133. doi:10.1111/j.1442-9071.1995.tb00141.x
151. Barraquer-Somers E, Chan CC, Green WR. Corneal epithelial iron deposition. *Ophthalmology.* 1983;90(6):729-734. doi:10.1016/S0161-6420(83)34519-X
152. Ambekar R, Toussaint KC, Wagoner Johnson A. The effect of keratoconus on the structural, mechanical, and optical properties of the cornea. *J Mech Behav Biomed Mater.* 2011;4(3):223-236. doi:10.1016/j.jmbbm.2010.09.014
153. Choi JA, Kim MS. Progression of keratoconus by longitudinal assessment with corneal topography. *Investig Ophthalmol Vis Sci.* 2012;53(2):927-935. doi:10.1167/iovs.11-8118
154. Carney LG. Visual Loss in Keratoconus. *Arch Ophthalmol.* 1982;100(8):1282-1285. doi:10.1001/archophth.1982.01030040260012
155. Amsler M. Le kératocône fruste au Javal. *Ophthalmologica.* 1938;96(2):77-83.
156. Duncan JK, Belin MW, Borgstrom M. Assessing progression of keratoconus: novel tomographic determinants. *Eye Vis.* 2016;3(6):1-9. doi:10.1186/s40662-016-0038-6
157. Jones LW, Srinivasan S, Ng A, Schulze M. Diagnostic Instruments. In: Efron N, ed. *Contact Lens Practice.* Elsevier Ltd; 2018:327-345.
158. OCULUS Optikgeräte GmbH. OCULUS Pentacam ® and Pentacam ® HR Interpretation Guide. 2021:212.
159. OCULUS Optikgeräte GmbH. Technical data by Pentacam® model.
160. Huang D, Swanson EA, Lin CP, et al. Optical coherence tomography. *Science.* 1991;254(5035):1178-1181.
161. Heidelberg Engineering. Spectralis Anterior Segment Module User Guide. 2010;(18):23.
162. Maeda N, Klyce SD, Smolek MK, Thompson HW. Automated keratoconus screening with corneal topography analysis. *Invest Ophthalmol Vis Sci.* 1994;35(6):2749-2757.
163. Rabinowitz YS, Rasheed K. KISA % index: a quantitative videokeratography algorithm embodying minimal topographic criteria for diagnosing keratoconus. *J Cataract Refract Surg.*

- 1999;25(10):1327-1335.
164. Li X, Yang H, Rabinowitz YS. Keratoconus: classification scheme based on videokeratography and clinical signs. *J Cat Refract Surg.* 2009;35(9):1597-1603. doi:10.1016/j.jcrs.2009.03.050
165. Mahmoud AM, Roberts CJ, Lembach RG, et al. CLMI: the cone location and magnitude index. *Cornea.* 2008;27(4):480-487.
166. Alió JL, Shabayek MH. Corneal higher order aberrations: A method to grade keratoconus. *J Refract Surg.* 2006;22(6):539-545.
167. Kamiya K, Ishii R, Shimizu K, Igarashi A. Evaluation of corneal elevation, pachymetry and keratometry in keratoconic eyes with respect to the stage of Amsler-Krumeich classification. *Br J Ophthalmol.* 2014;98(4):459-463. doi:10.1136/bjophthalmol-2013-304132
168. Kanellopoulos AJ, Asimellis G. Revisiting keratoconus diagnosis and progression classification based on evaluation of corneal asymmetry indices, derived from Scheimpflug imaging in keratoconic and suspect cases. *Clin Ophthalmol.* 2013;7:1539-1548. doi:10.2147/OPHTH.S44741
169. Maguire LJ, Klyce SD, McDonald MB, Kaufman HE. Corneal topography of pellucid marginal degeneration. *Ophthalmology.* 1987;94(5):519-524.
170. Spadea L, Maraone G, Verboschi F, Vingolo EM, Tognetto D. Effect of corneal light scatter on vision: A review of the literature. *Int J Ophthalmol.* 2016;9(3):459-464. doi:10.18240/ijo.2016.03.24
171. Krumeich JH, Daniel J, Knülle A. Live-epikeratophakia for keratoconus. *J Cataract Refract Surg.* 1998;24(4):456-463. doi:10.1016/S0886-3350(98)80284-8
172. McMahon TT, Szczotka-Flynn L, Barr JT, et al. A new method for grading the severity of keratoconus: the keratoconus severity score (KSS). *Cornea.* 2006;25(7):794-800.
173. Sandali O, Sanharawi M El, Temstet C, et al. Fourier-domain optical coherence tomography imaging in keratoconus: a corneal structural classification. *Ophthalmology.* 2013;120(12):2403-2412. doi:10.1016/j.ophtha.2013.05.027
174. Zadnik K, Barr JT, Gordon MO, Edrington TB, Group CS. Biomicroscopic signs and disease severity in keratoconus. *Cornea.* 1996;15(2):139-146.

175. Greenstein SA, Shah VP, Fry KL, Hersh PS. Corneal thickness changes after corneal collagen crosslinking for keratoconus and corneal ectasia: One-year results. *J Cataract Refract Surg.* 2011;37(4):691-700. doi:10.1016/j.jcrs.2010.10.052
176. Avedro Inc. *Study to Evaluate the Safety and Efficacy of Epi-on Corneal Cross-Linking in Eyes with Progressive Keratoconus.* Bethesda, MD; 2021.
<https://clinicaltrials.gov/ct2/show/study/NCT03442751>.
177. O'Brart DPS, Chan E, Samaras K, Patel P, Shah SP. A randomised, prospective study to investigate the efficacy of riboflavin/ultraviolet A (370 nm) corneal collagen cross-linkage to halt the progression of keratoconus. *Br J Ophthalmol.* 2011;95(11):1519-1524.
doi:10.1136/bjo.2010.196493
178. Li X, Rabinowitz YS, Rasheed K, Yang H. Longitudinal study of the normal eyes in unilateral keratoconus patients. *Ophthalmology.* 2004;111(3):440-446.
doi:10.1016/j.ophtha.2003.06.020
179. Belin MW, Kundu G, Shetty N, Gupta K, Mullick R, Thakur P. ABCD: A new classification for keratoconus. *Indian J Ophthalmol.* 2020;68(12):2831-2834. doi:10.4103/ijo.IJO_2078_20
180. Meyer JJ, Gokul A, Vellara HR, Prime Z, McGhee CNJ. Repeatability and agreement of Orbscan II, Pentacam HR, and Galilei tomography systems in corneas with keratoconus. *Am J Ophthalmol.* 2017;175:122-128. doi:10.1016/j.ajo.2016.12.003
181. Cohen EJ, Parlato CJ. Fitting polycon lenses in keratoconus. *Int Ophthalmol Clin.* 1986;26(1):111-117. doi:10.1097/00004397-198602610-00015
182. Smiddy WE, Hamburg TR, Kracher GP, Stark WJ. Keratoconus: contact Lens or keratoplasty? *Ophthalmology.* 1988;95(4):487-492. doi:10.1016/S0161-6420(88)33161-1
183. Mandell RB. Contemporary management of keratoconus. *Int Contact Lens Clin.* 1997;24(2):43-58.
184. Davis LJ. Keratoconus current understanding of diagnosis and management. *Clin Eye Vis Care.* 1997;9(1):13-22.
185. Crews MJ, Driebe WT, Stern GA. The clinical management of keratoconus: A 6 year retrospective study. *Contact Lens Assoc Ophthalmol.* 1994;20(3):194-197.
186. Jinabhai A, Radhakrishnan H, Tromans C, O'Donnell C. Visual performance and optical

- quality with soft lenses in keratoconus patients. *Ophthalmic Physiol Opt.* 2012;32(2):100-116. doi:10.1111/j.1475-1313.2011.00889.x
187. Zadnik K, Barr JT, Edrington TB, et al. Baseline findings in the collaborative longitudinal evaluation of keratoconus (CLEK) study. *Investig Ophthalmol Vis Sci.* 1998;39(13):2537-2546.
188. Mannis MJ, Zadnik K. Contact lens fitting in keratoconus. *Contact Lens Assoc Ophthalmol.* 1989;15(4):282-289.
189. Koliopoulos J, Tragakis M. Visual correction of keratoconus with soft contact lenses. *Ann Ophthalmol.* 1981;13(7):835-837.
190. Griffiths M, Zahner K, Collins M, Carney L. Masking of irregular corneal topography with contact lenses. *Contact Lens Assoc Ophthalmol.* 1998;24(2):76-81.
191. Leung KK. RGP fitting philosophies for keratoconus. *Clin Exp Optom.* 1999;82(6):230-235.
192. Barnett M, Mannis MJ. Contact lenses in the management of keratoconus. *Cornea.* 2011;30(12):1510-1516. doi:10.1097/ICO.0b013e318211401f
193. Weissman BA, Ye P. Calculated tear oxygen tension under contact lenses offering resistance in series: Piggyback and scleral lenses. *Contact Lens Anterior Eye.* 2006;29(5):231-237. doi:10.1016/j.clae.2006.09.001
194. Fernandez-Velazquez FJ. Severe epithelial edema in Clearkone Synergeyes contact lens wear for keratoconus. *Eye Contact Lens.* 2011;37(6):381-385. doi:10.1097/ICL.0b013e31822a33a6
195. Yamazaki ES, Silva VCB da, Morimitsu V, Sobrinho M, Fukushima N, Lipener C. Adaptação de lente de contato gelatinosa especial para ceratocone. *Arq Bras Oftalmol.* 2006;69(4):557-560. doi:10.1590/s0004-27492006000400018
196. Shimazaki J, Ishii N, Shinzawa M, Yamaguchi T, Shimazaki-Den S, Satake Y. How much progress has been made in corneal transplantation? *Cornea.* 2015;34(11):S105-S111. doi:10.1097/ICO.0000000000000604
197. Pramanik S, Musch DC, Sutphin JE, Farjo AA. Extended long-term outcomes of penetrating keratoplasty for keratoconus. *Ophthalmology.* 2006;113(9):1633-1638. doi:10.1016/j.opthta.2006.02.058

198. Javadi MA, Feizi S, Yazdani S, Mirbabae F. Deep anterior lamellar keratoplasty versus penetrating keratoplasty for keratoconus: A clinical trial. *Cornea*. 2010;29(4):365-371. doi:10.1002/14651858.CD009700.pub2
199. Coster DJ, Lowe MT, Keane MC, Williams KA. A comparison of lamellar and penetrating keratoplasty outcomes: A registry study. *Ophthalmology*. 2014;121(5):979-987. doi:10.1016/j.ophttha.2013.12.017
200. Anwar M, Teichmann KD. Big-bubble technique to bare Descemet's membrane in anterior lamellar keratoplasty. *J Cataract Refract Surg*. 2002;28(3):398-403. doi:10.1016/S0886-3350(01)01181-6
201. Sarnicola V, Toro P, Sarnicola C, Sarnicola E, Ruggiero A. Long-term graft survival in deep anterior lamellar keratoplasty. *Cornea*. 2012;31(6):621-626. doi:10.1097/ICO.0b013e31823d0412
202. Colin J, Cochener B, Savary G, Malet F. Correcting keratoconus with intracorneal rings. *J Cataract Refract Surg*. 2000;26(8):1117-1122. doi:10.1016/S0886-3350(00)00451-X
203. Kanellopoulos AJ, Pe LH, Perry HD, Donnenfeld ED. Modified intracorneal ring segment implantations (INTACS) for the management of moderate to advanced keratoconus: Efficacy and complications. *Cornea*. 2006;25(1):29-33. doi:10.1097/01.ico.0000167883.63266.60
204. Ertan A, Kamburoğlu G. Intacs implantation using a femtosecond laser for management of keratoconus: Comparison of 306 cases in different stages. *J Cataract Refract Surg*. 2008;34(9):1521-1526. doi:10.1016/j.jcrs.2008.05.028
205. Alió JL, Shabayek MH, Belda JI, Correas P, Feijoo ED. Analysis of results related to good and bad outcomes of Intacs implantation for keratoconus correction. *J Cataract Refract Surg*. 2006;32(5):756-761. doi:10.1016/j.jcrs.2006.02.012
206. Spoerl E, Huhle M, Seiler T. Induction of cross-links in corneal tissue. *Exp Eye Res*. 1998;66(1):97-103. doi:10.1006/exer.1997.0410
207. Wollensak G, Spoerl E, Seiler T. Riboflavin/ultraviolet-A-induced collagen crosslinking for the treatment of keratoconus. *Am J Ophthalmol*. 2003;135(5):620-627. doi:10.1016/S0002-9394(02)02220-1
208. Kymionis GD, Portaliou DM, Bouzoukis DI, et al. Herpetic keratitis with iritis after corneal

- crosslinking with riboflavin and ultraviolet A for keratoconus. *J Cataract Refract Surg.* 2007;33(11):1982-1984. doi:10.1016/j.jcrs.2007.06.036
209. Abad JC, Panesso JL. Corneal collagen cross-linking induced by UVA and riboflavin (CXL). *Tech Ophthalmol.* 2008;6(1):8-12. doi:10.1097/ITO.0b013e31816a17c3
210. Dahl BJ, Spotts E, Truong JQ. Corneal collagen cross-linking: An introduction and literature review. *Optometry.* 2012;83(1):33-42. doi:10.1016/j.optm.2011.09.011
211. Meek KM, Hayes S. Corneal cross-linking - a review. *Ophthalmic Physiol Opt.* 2013;33(2):78-93. doi:10.1111/opo.12032
212. De Bernardo M, Capasso L, Lanza M, et al. Long-term results of corneal collagen crosslinking for progressive keratoconus. *J Optom.* 2015;8(3):180-186. doi:10.1016/j.optom.2014.05.006
213. Bochner Eye Institute. Corneal Collagen Crosslinking (C3R) – Co-Management Guidelines. <https://www.bochner.com/eyecare-professionals-forms/>. Published 2021. Accessed April 21, 2021.
214. Sykakis E, Karim R, Evans JR, et al. *Corneal Collagen Cross-Linking for Treating Keratoconus.*; 2015. doi:10.1002/14651858.CD010621
215. Porcar E, Montalt JC, España-Gregori E, Peris-Martínez C. Impact of corneoscleral contact lens usage on corneal biomechanical parameters in keratoconic eyes. *Eye Contact Lens.* 2019;45(5):318-323. doi:10.1097/ICL.0000000000000579
216. Luce DA. Determining in vivo biomechanical properties of the cornea with an ocular response analyzer. *J Cataract Refract Surg.* 2005;31(1):156-162. doi:10.1016/j.jcrs.2004.10.044
217. Pinero DP, Nieto J, Lopez-Miguel A. Characterisation of corneal structure in keratoconus. *J Cataract Refract Surg.* 2012;38:2167-2183.
218. Ortiz D, Piñero D, Shabayek MH, Arnalich-Montiel F, Alió JL. Corneal biomechanical properties in normal, post-laser in situ keratomileusis, and keratoconic eyes. *J Cataract Refract Surg.* 2007;33(8):1371-1375. doi:10.1016/j.jcrs.2007.04.021
219. Vellara HR, Patel D V. Biomechanical properties of the keratoconic cornea: a review. *Clin Exp Optom.* 2015;98(1):31-38. doi:10.1111/cxo.12211
220. Daxer A, Fratzl P. Collagen fibril diameter in the human corneal stroma and its implication in

- keratoconus. *Investig Ophthalmol Vis Sci.* 1997;38(1):121-129.
221. Cannon DJ, Foster CS. Collagen crosslinking in keratoconus. *Investig Ophthalmol Vis Sci.* 1978;17(1):63-65.
222. Mannion LS, Tromans C, O'Donnell C. Reduction in corneal volume with severity of keratoconus. *Curr Eye Res.* 2011;36(6):522-527. doi:10.3109/02713683.2011.553306
223. Dawson DG, Grossniklaus HE, McCarey BE, Edelhauser HF. Biomechanical and wound healing characteristics of corneas after excimer laser keratorefractive surgery: is there a difference between advanced surface ablation and sub-Bowman's keratomileusis? *J Refract Surg.* 2008;24(1):S90-96.
224. Weissman BA. Ring corneal clouding in keratoconus. *Optom Vis Sci.* 1994;71(6):392-396.
225. Tuft SJ, Gartry DS, Rawe IM, Meek KM. Photorefractive keratectomy: Implications of corneal wound Healing. *Br J Ophthalmol.* 1993;77(4):243-247. doi:10.1136/bjo.77.4.243
226. Wilson SL, El Haj AJ, Yang Y. Control of Scar Tissue Formation in the Cornea: Strategies in Clinical and Corneal Tissue Engineering. *J Funct Biomater.* 2012;3(3):642-687. doi:10.3390/jfb3030642
227. Vinciguerra P, Albè E, Mahmoud AM, Trazza S, Hafezi F, Roberts CJ. Intra- and postoperative variation in ocular response analyzer parameters in keratoconic eyes after corneal cross-linking. *J Refract Surg.* 2010;26(9):669-676. doi:10.3928/1081597X-20100331-01
228. Mikielewicz M, Kotliar K, Barraquer RI, Michael R. Air-pulse corneal applanation signal curve parameters for the characterisation of keratoconus. *Br J Ophthalmol.* 2011;95(6):793-798. doi:10.1136/bjo.2010.188300
229. Greenstein SA, Fry KL, Hersh PS. In vivo biomechanical changes after corneal collagen cross-linking for keratoconus and corneal ectasia: 1-Year analysis of a randomized, controlled, clinical trial. *Cornea.* 2012;31(1):21-25. doi:10.1097/ICO.0b013e31821eea66
230. Küçümen RB, Şahan B, Yıldırım CA, Çiftçi F. Evaluation of corneal biomechanical changes after collagen crosslinking in patients with progressive keratoconus by ocular response analyzer. *Turkish J Ophthalmol.* 2018;48(4):160-165. doi:10.4274/tjo.56750
231. Pullum KW, Hobley AJ, Parker JH. Hypoxic corneal changes following sealed gas permeable

- impression scleral lens wear. *J Br Contact Lens Assoc.* 1990;13(1):83-87.
232. Pullum KW, Hopley AJ, Davison C. 100+ Dk: does thickness make much difference? *J Br Contact Lens Assoc.* 1991;14(1):17-19. doi:10.1016/0141-7037(91)80057-S
233. Bleshoy H, Pullum KW. Corneal response to gas-permeable impression scleral lenses. *J Br Contact Lens Assoc.* 1988;11(2):31-34. doi:10.1016/S0141-7037(88)80006-5
234. Mountford J, Carkeet N, Carney L. Corneal thickness changes during scleral lens wear: Effect of gas permeability. *Int Contact Lens Clin.* 1994;21(1-2):19-22. doi:10.1016/0892-8967(94)90036-1
235. Lu H, Wang MR, Wang J, Shen M. Tear film measurement by optical reflectometry technique. *J Biomed Opt.* 2014;19(2):027001-1-027007-027008. doi:10.1117/1.jbo.19.2.027001
236. Wang J, Fonn D, Simpson TL, Jones L. Precorneal and pre- and postlens tear film thickness measured indirectly with optical coherence tomography. *Investig Ophthalmol Vis Sci.* 2003;44(6):2524-2528. doi:10.1167/iovs.02-0731
237. Fatt I. Oxygen-transmissibility considerations for a hard-soft contact-lens combination. *Am J Optom Physiol Opt.* 1977;54(10):666-672.
238. Jaynes JM, Edrington TB, Weissman BA. Predicting scleral GP lens entrapped tear layer oxygen tensions. *Contact Lens Anterior Eye.* 2015;38(1):44-47. doi:10.1016/j.clae.2014.09.008
239. Compan V, Aguilera-Arzo M, Edrington TB, Weissman BA. Modeling corneal oxygen with scleral gas permeable lens wear. *Optom Vis Sci.* 2016;93(11):1339-1348.
240. Frisani M, Beltramo I, Grec M. Changes in corneal thickness by miniscleral contact lenses. In: *Contact Lens and Anterior Eye.* Vol 38. British Contact Lens Association; 2015:e38-e39. doi:10.1016/j.clae.2014.11.064
241. Giasson CJ, Morency J, Melillo M, Michaud L. Oxygen tension beneath scleral lenses of different clearances. *Optom Vis Sci.* 2017;94(4):466-475. doi:10.1097/OPX.0000000000001038
242. Mertz GW. Overnight swelling of the living human cornea. *J Am Optom Assoc.* 1980;51(3):211-213.

243. Soeters N, Visser ES, Imhof SM, Tahzib NG. Scleral lens influence on corneal curvature and pachymetry in keratoconus patients. *Contact Lens Anterior Eye*. 2015;38(4):294-297. doi:10.1016/j.clae.2015.03.006
244. Esen F, Toker E. Influence of apical clearance on mini-scleral lens settling, clinical performance, and corneal thickness changes. *Eye Contact Lens*. 2017;43(4):230-235. doi:10.1097/ICL.0000000000000266
245. Serramito M, Carpena-Torres C, Carballo J, Piñero D, Lipson M, Carracedo G. Posterior cornea and thickness changes after scleral lens wear in keratoconus patients. *Contact Lens Anterior Eye*. 2019;42(1):85-91. doi:10.1016/j.clae.2018.04.200
246. Yeung D, Murphy PJ, Sorbara L. Objective and subjective evaluation of clinical performance of scleral lens with varying limbal clearance in keratoconus. *Optom Vis Sci*. 2020;97(9):703-710. doi:10.1097/OPX.0000000000001561
247. Hall L. What you need to know about sagittal height and scleral lenses. *Contact Lens Spectrum*. <https://www.clspectrum.com/issues/2015/may-2015/what-you-need-to-know-about-sagittal-height-and-sc>. Published 2015.
248. Yeung D, Sorbara L. A survey of scleral lens prescribing trends and complications. In: *Global Specialty Lens Symposium*. Las Vegas, Nevada; 2017.
249. Hall LA, Young G, Wolffsohn JS, Riley C. The influence of corneoscleral topography on soft contact lens fit. *Investig Ophthalmol Vis Sci*. 2011;52(9):6801-6806. doi:10.1167/iovs.11-7177
250. Achong-Coan R, Caroline PJ, Kinoshita B. How do normal and keratoconic eyes differ in shape? In: *Global Specialty Lens Symposium*. Las Vegas, Nevada; 2012.
251. Sorbara L, Maram J, Mueller K. Use of the Visante™ OCT to measure the sagittal depth and scleral shape of keratoconus compared to normal corneae: Pilot study. *J Optom*. 2013;6(3):141-146. doi:10.1016/j.optom.2013.02.002
252. Bausch + Lomb Specialty Vision Products, Alden Optical. Zenlens™ Brochure. 2018. <http://www.aldenoptical.com/docs/zenlens/Zenlens-brochure.pdf>.
253. OCULUS. Pentacam® Optional Software Modules: New CSP Report. <https://www.pentacam.com/int/ophthalmologist-diagnostic-without-pentacam/models/pentacamr/optional-software.html>. Published 2020. Accessed May 5, 2020.

254. Sorbara L, Maram J, Fonn D, Woods C, Simpson T. Metrics of the normal cornea: Anterior segment imaging with the Visante OCT. *Clin Exp Optom*. 2010;93(3):150-156. doi:10.1111/j.1444-0938.2010.00472.x
255. Izatt JA, Hee MR, Swanson EA, et al. Micrometer-scale resolution imaging of the anterior eye in vivo with optical coherence tomography. *Arch Ophthalmol*. 1994;112(12):1584-1589. doi:10.1001/archophth.1994.01090240090031
256. Maram J, Sorbara L, Simpson T. Accuracy of Visante and Zeiss-Humphrey optical coherence tomographers and their cross calibration with optical pachymetry and physical references. *J Optom*. 2011;4(4):147-155. doi:10.1016/S1888-4296(11)70057-7
257. OCULUS Optikgeräte GmbH. User Guide - Oculus Keratograph 5M. 2020.
258. Wu S, Hong J, Tian L, Cui X, Sun X, Xu J. Assessment of bulbar redness with a newly developed Keratograph. *Optom Vis Sci*. 2015;92(8):892-899. doi:10.1097/OPX.0000000000000643
259. Sickenberger W, Oehring D. Validation of a novel morphing software to classify different slit lamp findings. *Contact Lens Anterior Eye*. 2012;35(2012):e20-e21. doi:10.1016/j.clae.2012.08.065
260. OCULUS, Alden Optical. Pentacam® CSP Report Scleral Lens Fitting Guide for Zenlens or Zen RC. 2019.
261. International Organization for Standardization. *ISO 11980:2012(EN) Ophthalmic Optics—Contact Lenses and Contact Lens Care Products—Guidance for Clinical Investigations*. Geneva, Switzerland; 2012.
262. Gemoules G. A novel method of fitting scleral lenses using high resolution optical coherence tomography. *Eye Contact Lens*. 2008;34(2):80-83. doi:10.1097/ICL.0b013e318166394d
263. Carter K, Sorbara L. A starting point for scleral lens fitting: ocular sagittal height measured with OCT and Scheimpflug CSP software in keratoconic and healthy eyes: a pilot study. *Contact Lens Anterior Eye*. 2021;44(1):e1-e2. doi:10.1016/j.clae.2020.12.008
264. Schindelin J, Arganda-Carreras I, Frise E, et al. Fiji: an open-source platform for biological-image analysis. *Nat Methods*. 2012;9(7):676-682.
265. Schindelin J. Align Image by line ROI. 2021. <https://imagej.net/plugins/align-image-by-line-312>

roi.

266. Joachim, Carter K. Degradation of image quality after running Align Image by line ROI plugin (.tif files). Community Partners. <https://forum.image.sc/t/degradation-of-image-quality-after-running-align-image-by-line-roi-plugin-tif-files/44545>. Published 2020. Accessed October 27, 2020.
267. Podoleanu A, Charalambous I, Plesea L, Dogariu A, Rosen R. Correction of distortions in optical coherence tomography imaging of the eye. *Phys Med Biol*. 2004;49:1277-1294. doi:10.1088/0031-9155/49/7/015
268. Read SA, Alonso-Caneiro D, Vincent SJ, et al. Anterior eye tissue morphology: scleral and conjunctival thickness in children and young adults. *Sci Rep*. 2016;6(September):1-10. doi:10.1038/srep33796
269. Ramasubramanian V, Glasser A. Distortion correction of Visante optical coherence tomography cornea images. *Optom Vis Sci*. 2015;92(12):1170-1181. doi:10.1097/OPX.0000000000000725
270. Vincent SJ, Alonso-Caneiro D, Kricancic H, Collins MJ. Scleral contact lens thickness profiles: The relationship between average and centre lens thickness. *Contact Lens Anterior Eye*. 2019;42(1):55-62. doi:10.1016/j.clae.2018.03.002
271. Bausch + Lomb. Boston XO. <http://www.bausch.com/ecp/our-products/contact-lenses/gp-lens-materials/boston-xo>. Published 2017. Accessed May 6, 2021.
272. Craig JP, Simmons PA, Patel S, Tomlinson A. Refractive index and osmolality of human tears. *Optom Vis Sci*. 1995;72(10):718-724.
273. Standardization IO for. *ISO 18369-2:2017(EN) Ophthalmic Optics–Contact Lenses–Part 2: Tolerances*. Geneva, Switzerland; 2017.
274. Jamovi. The jamovi project. 2021. <https://www.jamovi.org>. Accessed June 1, 2021.
275. R Core Team. R: A language and environment for statistical computing. 2021:(R packages retrieved from MRAN snapshot 2021-04-0. doi:10.1002/wics.1212
276. Holm S. A simple sequentially rejective multiple test procedure. *Scand J Stat*. 1979;6(2):65-70.
<http://www.jstor.org/stable/4615733%0Ahttp://www.jstor.org/page/info/about/policies/terms.j>

sp%0Ahttp://www.jstor.org.

277. Morey RD, Rouder JN. BayesFactor: Computation of Bayes Factors for Common Designs. 2018. <https://cran.r-project.org/package=BayesFactor>.
278. Rouder JN, Speckman PL, Sun D, Morey RD, Iverson G. Bayesian t tests for accepting and rejecting the null hypothesis. *Psychon Bull Rev.* 2009;16(2):225-237. doi:10.3758/PBR.16.2.225
279. Singmann H. afex: Analysis of Factorial Experiments. 2018. <https://cran.r-project.org/package=afex>.
280. Pohlert T. PMCMR: Calculate Pairwise Multiple Comparisons of Mean Rank Sums. 2018. <https://cran.r-project.org/package=PMCMR>.
281. Lenth R. emmeans: Estimated Marginal Means, aka Least-Squares Means. 2020. doi:10.1080/00031305.1980.10483031>. Version
282. Team Rs. RStudio: Integrated Development Environment for R. 2021. <http://www.rstudio.com/>.
283. R Core Team. R: A language and environment for statistical computing. 2020. <https://www.r-project.org/>.
284. Wickham H, Averick M, Bryan J, et al. Welcome to the tidyverse. *J Open Source Softw.* 2019;4(43):1686. doi:10.21105/joss.01686
285. Wilke CO. cowplot: Streamlined Plot Theme and Plot Annotations for “ggplot2.” 2020. <https://cran.r-project.org/package=cowplot>.
286. Wickham H. stringr: Simple, Consistent Wrappers for Common String Operations. 2019. <https://cran.r-project.org/package=stringr>.
287. Kassambara A. ggpubr: “ggplot2” Based Publication Ready Plots. 2020. <https://cran.r-project.org/package=ggpubr>.
288. Tiew S, Lim C, Sivagnanasithiyar T. Using an excel spreadsheet to convert Snellen visual acuity to LogMAR visual acuity. *Eye.* 2020;34(11):2148-2149. doi:10.1038/s41433-020-0783-6
289. Brien Holden Vision Institute (BHVI). Grading Scales.

<https://brienholdenfoundation.org/international-program/learning-resources/>. Published 2017. Accessed June 24, 2021.

290. Carter K, Sorbara L. Changes in corneal thickness associated with variation of central corneal clearance of scleral lenses. *Contact Lens Anterior Eye*. 2019;42(6):e7. doi:10.1016/j.clae.2019.10.026
291. Sorbara L, Gorbet M, Bizheva KK, et al. Impact of contact lens wear on epithelial alterations in keratoconus. *Investig Ophthalmol Vis Sci*. 2019;60(9):932.
292. Otchere H, Jones LW, Sorbara L. Effect of time on scleral lens settling and change in corneal clearance. *Optom Vis Sci*. 2017;94(9):908-913. doi:10.1097/OPX.0000000000001111
293. Schulze M-M, Ng A, Yang M, et al. Bulbar redness and dry eye disease. *Optom Vis Sci*. 2021;Publish Ah(00):18-23. doi:10.1097/opx.0000000000001638
294. Downie LE, Keller PR, Vingrys AJ. Assessing ocular bulbar redness: A comparison of methods. *Ophthalmic Physiol Opt*. 2016;36(2):132-139. doi:10.1111/opo.12245